Paddock Scale Nitrous Oxide Emissions from Intensively Grazed Pasture:

Quantification and Mitigation

A thesis

submitted in fulfilment

of the requirements for the degree

of

Doctor of Philosophy in Earth Sciences

at

The University of Waikato

by

Anne Roswitha Wecking

THE UNIVERSITY OF
WAIKATO
Te Whare Wānanga o Waikato

2021

…

Presented by:

Anne Roswitha Wecking

Master of Science, Leibniz University Hanover

Born 24-12-1990

Citizen of Germany

…

Supervised by:

Prof. Dr Louis A. Schipper
Assoc. Prof. Dr David I. Campbell
Dr Jiafa Luo
Dr Lìyǐn L. Liáng

Examined by:

Dr Roberta Gentile
Dr Lutz Merbold

…

2021

…

Humankind

this thesis is dedicated to all your optimists

in the face of a great challenge

…

…

"Ka ora te whenua, ka ora te tangata."

When the land is well, the people will be well

Māori proverb

…

Abstract

Agricultural soils are the main contributor to global emissions of the potent greenhouse gas nitrous oxide (N_2O) to the atmosphere. Nitrous oxide can absorb and transform radiative energy emitted from the sun to earth into heat. The ability of N_2O to absorb energy is part of the greenhouse effect and naturally contributes to habitable temperature conditions for life on earth. Atmospheric concentrations of N_2O have never before increased as rapidly as observed since the onset of industrialisation. High N_2O concentrations enhance the greenhouse effect and, at present, add to a warming atmosphere and a changing climate. A major pathway for N_2O production is from soils that receive large surpluses of reactive nitrogen, e.g., in the form of animal excreta or fertiliser. Once available in the soil, microbes can access and transform this nitrogen into different compounds: N_2O, for example. The current contribution of agricultural soils to global N_2O emissions is about 60% but higher in New Zealand, where soils are responsible for 94% of national N_2O emissions. However, robust quantifications are not straightforward and challenging for science to overcome. This thesis is sited at the interface of this challenge and aimed at measuring the exchange of N_2O over an intensively grazed dairy pasture in New Zealand. The core of the work was based on eddy covariance (EC), a technique that allows measuring the N_2O exchange between the soil and the atmosphere at ten times per second. Since EC measurements of N_2O over dairy grazed land are rare, main objectives of this work were: to 1) compare EC to traditional measurement approaches, i.e. static chambers, 2) quantify annual N_2O emission budgets and 3) determine the effect of farm management including pasture renewal on N_2O emissions. The findings of this thesis show that EC provided a realistic picture of the N_2O exchange at paddock scales. This means EC data identified cattle grazing, land history, farm management, soil moisture and temperature as the main factors controlling N_2O exchange throughout the year. Interestingly, using one EC system for measurements across adjacent but differently managed paddocks also allowed to compare the effect of different pasture management scenarios on N_2O emissions. This will help researchers to test different mitigation options more easily in the future, ideally, to reduce N_2O emissions and avoid further atmospheric warming. This thesis advances our understanding of the N_2O exchange process from intensively grazed land as well as it shows how limited this knowledge still is. Micrometeorological N_2O flux measurements will have to be used more frequently in the future to provide researchers with answers in the face of a rapidly changing climate on earth.

Whakarāpopoto

Ko ngā oneone ahuwhenua te tino kaitāpae ki ngā tuhanga haurehu ao whānui o te kati mahana kikino nei, arā, o te hauota-rua ōkai e whakaputaina ana ki te kōhauhau. He haurehu moroiti ā-kōhauhau te hauota-rua ōkai (N_2O). Ā, e taea ana te miti me te whakawhiti ngā pūngao hihi, e ahu mai ana i te rā ki te whenua, hei pōkākā. Nā te āhei o te N_2O ki te miti pūngao i ahu mai ai te *kati mahana*, ā, nā reira e taea nei te noho heipū i tētahi tītaranga mahanatanga pai mō te noho ora i te whenua. Heoi anō, kāore anō i kitea pēnetia te tere whanake o te kukū mai o te N_2O i te kōhauhau, nō mai anō i te kunenga o te ahumahitanga. Nā te nui o te kukū o te N_2O i te kōhauhau e tūperepere nei te *kati mahana*, ā, i tēnei wā, e āpiti ana ki te mahana haeretanga o te kōhauhau me te rerekē haeretanga o te āhuarangi. Ko tētahi huarahi tāpua mō te waihanga N_2O, kei roto i ngā oneone e nui nei te whai hauota hohe tuhene, hei tauira, kei roto i ngā tukuparatanga a ngā kararehe, i ngā hauota whakahaumako, i ngā koiora whakamau hauota rānei. Ka āhei ana ēnei i te oneone, ka taea te hauota e ngā moroiti oneone, ā, ka panonihia hei pūhui rerekē: hei tauira, hei N_2O. I tēnei wā, ko te tāpaetanga o te oneone ahuwhenua ki ngā tuhanga N_2O o te ao whānui kei tōna 60%. Engari, he nui atu i Aotearoa, kei te 94% kē te tāpaetanga o te oneone ahuwhenua ki te tuhanga tahua N_2O ā-motu. Ahakoa te uekaha o te tatau, e uaua tonu ana, nā te āhua taurangi o te mokowā me te wāhi i roto i te tukanga whakawhiti o te N_2O.

I tēnei tuhinga whakapae, ka inea te whakawhitinga o te N_2O i tētahi pito whenua ā-ohu miraka e tītongitia āwaitia ana i Aotearoa, mā te whakamahi i te inenga mātai huarere iti i ētahi tau maha, me ētahi whakahaerenga pito whenua ā-ohu miraka rerekē. Whakamahia ai te rautaki *eddy convariance* (EC), hei ine i te whakawhitinga N_2O i te whenua ki te kōhauhau, i te tekau inenga ā-hēkona. I te mea, me uaua kē ka whakamahi i te rautaki EC hei ine i te N_2O i tētahi pito whenua e tītongitia āwaitia ana, ko ngā whāinga o te tuhinga whakapae nei he whakatatū i: 1) ngā tauritenga ine o te rautaki EC me ngā rautaki riterite mā te matakikī; 2) ngā tahua tuhanga N_2O ā-tau, me; 3) ngā pānga o ngā whakahaerenga pāmu i ngā karawhitinga N_2O. E ai ki ō mātou kitenga, mā ngā ingenga EC e whakaahua tūturu ngā whakawhitinga N_2O i ngā āwhata pātiki. Ko ngā āhuatanga pūmau ko: ngā whakaurunga hauota nā te tītongi a ngā kararehe, te hītori o te whenua, te whakahaerenga pāmu, te mākūtanga o te oneone, me te pāmahanatanga o te oneone. Nā te rautaki *eddy covariance* i āhei ai ngā whakatauritenga o ngā pānga i waenganui i pātiki e noho piritaha, ko tētahi pātahi i whakahoutia, ko tētahi i waiho me te tupu o te karaehe rai.

Hei whakarāpopoto ake, ko ngā kitenga o tēnei tuhinga whakapae hei tāpaetanga, hei whanaketanga anō hoki mō tō tātou mōhio ki ngā tukanga whakawhiti N_2O i ngā oneone mahi whenua. Ka mutu, hei whakaatu e whāiti tonu ana te puna mātauranga. E whakakīhia ai ēnei whārua mātauranga, me riterite kē atu te whakamahia o ngā inenga mātai huarere iti karawhitinga N_2O e ngā kairangahau o rā ngā e tū mai nei. Mā te whakamahi i ngā momo rautaki pēnei i te EC, e uruparetia ai te wawe o ngā rerekē haeretanga o te āhuarangi me te noho ora i te whenua. Ko te mariu, mā ngā raraunga me ngā puna mātauranga mō te ine haurehu kati mahana N_2O, hei āwhina te tangata ki te whakamauru i te mahana haeretanga tonutanga o te kōhauhau.

Zusammenfassung

Landwirtschaftlich genutzte Böden sind globale Hauptemittenten des klimawirksamen Treibhausgases Distickstoffmonoxid (N_2O), auch bekannt als Lachgas. In der Atmosphäre besitzt Lachgas die Fähigkeit, die kurzwellige Einstrahlung der Sonne zu absorbieren und in Wärmeenergie umzuwandeln. Dieser Prozess wird als Treibhauseffekt bezeichnet und trägt auf natürliche Weise zu einem ausgeglichenen Wärmehaushalt auf der Erde bei. Seit der Industrialisierung hat sich die N_2O-Konzentration allerdings so stark erhöht, dass der Treibhauseffekt seitdem nicht mehr nur zu ansteigenden Temperaturen in der Atmosphäre führt, sondern auch den Wandel des Weltklimas beschleunigt. Seinen Ursprung hat N_2O überall dort, wo Böden reaktiven Stickstoffverbindungen ausgesetzt sind, z.B. von Tierexkrementen oder Düngern. Den Stickstoff dieser Einträge können Kleinstlebewesen im Boden zu verschiedenen chemischen Verbindungen umbauen: N_2O, zum Beispiel. Derzeit tragen landwirtschaftlich genutzte Böden so geschätzt zu 60% zum globalen N_2O-Emissionsbudget bei. In manchen Fällen, wie in Neuseeland (94%), liegt der Anteil höher. Eine Herausforderung für Wissenschaftler, Emissionsbudgets wie diese zu erstellen, ist derzeit die Messung der Emissionen selbst. Die vorliegende Doktorarbeit war daher der Aufgabe gewidmet, zu erforschen, wie sich der Austausch von N_2O zwischen Boden und Atmosphäre besser erfassen lässt. Der Kern der Arbeit beruht auf der eddy covariance (EC) Technik, einer meteorologischen Messmethode, welche zehn Messwerte pro Sekunde generiert und dabei, je nach Windrichtung, bis zu einige Hektar Messfläche abdecken kann. Wichtige Forschungsanliegen waren 1) EC mit traditionellen Ansätzen (Messkammern) zu vergleichen, 2) Emissionsbudgets zu erstellen, und 3) den Einfluss von Managementmaßnahmen (Weideumbruch) auf die N_2O-Flüsse des Bodens zu untersuchen. Die Ergebnisse dieser Arbeit zeigen, dass EC-Messungen praktisch gut geeignet waren, um die Interaktion verschiedener Faktoren (z.B. Bodenwassergehalt, Stickstoffinput) auf den Fluss von N_2O zu erfassen. Die EC-Technik ermöglichte es sogar, simultane Messungen auf angrenzenden, aber unterschiedlich gemanagten Weiden durchzuführen und dabei das Analysegerät des Messsystems (einen Quantumkaskadenlaser) nicht nur für EC, sondern auch für die Analyse von Proben aus Kammermessungen zu verwenden. Eine robuste Quantifizierung von N_2O-Emissionen ist unabdingbar, um aussagekräftige Treibhausgasinventare berechnen und die Wirkung von Maßnahmen zur Schadstoffminderung erfassen zu können.[1]

[1] Eine wissenschaftliche Zusammenfassung der Ergebnisse ist im Anhang zu finden (siehe A1).

Scientific Abstract

Agricultural soils are the main contributor to global emissions of the potent greenhouse gas nitrous oxide (N_2O). This applies in particular to soils under intensively grazed land that receive large surpluses of reactive nitrogen (N_r) in the form of animal excreta, nitrogen fertiliser and/or biologically fixed nitrogen compounds. The contribution of agricultural soils to global N_2O emissions is estimated to be around 60% and is in some cases even higher, i.e. in New Zealand, where agricultural soils contribute 94% to total N_2O emissions. The exchange process of N_2O from soil to the atmosphere is controlled by a range of factors (e.g., soil microbial activity, environmental conditions, and farm management) and highly variable in both space and time. Measuring soil N_2O fluxes has, therefore, remained challenging and uncertainties associated with the measurement and quantification of N_2O emissions are generally high. However, robust quantifications are not only essential for understanding the multitude of factors and processes that trigger N_2O emission from the soil but also to compute comprehensive inventories and to ultimately develop effective mitigation strategies. Recent advances in gas analyser technology have now overcome some of this uncertainty by allowing continuous N_2O flux measurements, e.g. eddy covariance (EC), at field scales. Despite this advance, knowledge about the spatio-temporal dynamics of N_2O emissions at field and farm scales has remained rudimentary as micrometeorological N_2O flux measurements have not yet been determined for a range of different soil types, land uses, farm management practices and mitigation scenarios. Uncertainty currently also exists about how results from these micrometeorological measurements would link to traditional emission factor (EF) approaches based on chamber measurements, and vice versa. Emission factors are the foundation for most greenhouse gas inventories and yet aligning both measurement techniques could be important as a field scale verification.

This study aimed at overcoming a few of the above knowledge-gaps by using EC measurements of N_2O fluxes from an intensively grazed dairy pasture in New Zealand. Measurements were conducted on a commercially operating farm across multiple years and under different pasture management scenarios. The pasture sward in the footprint of the EC system initially comprised traditional perennial ryegrass (*Lolium perenne*) and white clover (*Trifolium repens*). After one and a half year, one paddock of the EC footprint underwent renovation (i.e. pasture renewal via chemical killing) before re-establishing a diverse sward containing plantain (*Plantago lanceolata*) in addition to

perennial ryegrass, white and red clover (*Trifolium pratense*) species. At two points of time, static chambers were installed to determine pasture N_2O fluxes in conjunction with the EC measurements, 1) to help understanding differences of methodology and scale on resulting N_2O fluxes, and 2) to develop a field-based approach allowing the immediate injection of N_2O samples derived from static chambers into the quantum cascade laser absorption spectrometer (QCL) of the EC system.

Results showed that commonly used static chamber techniques might lead to underestimations of annual N_2O emissions. When using a site-specific EF approach, annual N_2O emissions were quantified at 3.82 kg N_2O-N ha^{-1} yr^{-1} whereas cumulative and gap-filled data from EC resulted in 7.30 kg N_2O-N ha^{-1} yr^{-1}. The difference between the two budgets was explained by the EF approach not taking into account the effect of additional factors such as supplementary feed, seasonal variability and background N_2O emissions. Eddy covariance data, in contrast, already included these due to the micrometeorological nature, temporal frequency and continuity of the method itself. In future, computing annual N_2O emissions based on static chambers and EFs will demand a more careful consideration that reaches beyond the effect of individual treatments on resulting N_2O emissions and the simple upscaling to annual budgets.

The second objective of this work was to assess the effect of a no-till, direct-drill pasture renewal technique paired with a rapid reseeding approach on N_2O emissions for the first 66 days after management intervention. Flux measurements were made in a split-footprint across a control and renewal site using a single EC system. Results demonstrated that pulsed N_2O emissions from the renewed paddock were strikingly short and limited to a two weeks' window. The difference between N_2O emissions from the renewed and control paddock was 1.22 kg N_2O-N ha^{-1}; 93.4% of which were emitted shortly after intervention. Rapid reseeding and establishment of the new sward, therefore, were found a suitable mitigation strategy to likely prevent the prolonged loss of N_2O after pasture renewal. Besides, findings also showed that the chosen gap-filling technique allowed for robust quantification of emission budgets and comparison of treatment effects on two adjacent paddocks using a single EC system. Gap-filling of micrometeorological N_2O flux data has previously been a major constraint in producing defensible greenhouse gas budgets, and when assessing the effect of N_2O mitigation strategies at paddock scales. As demonstrated in this thesis, using a suitable gap-filling approach can realistically overcome this challenge.

Thirdly, using static chamber measurements parallel to EC might, in some cases, be very beneficial offering to complement N_2O flux measurements at different scales while isolating the effect of individual treatments. This thesis demonstrated that N_2O samples taken from static chambers can be analysed by the QCL absorption spectrometer in the field alternatively to standard gas chromatography (GC) in the laboratory. Quantum cascade lasers have previously been coupled to EC systems or auto-chambers, but here we found that a QCL could be used equally well for the analysis of N_2O samples derived from static chambers. A comparison between the two analytic methods (QCL and GC) showed that resulting N_2O fluxes were for all intents and purposes the same, i.e. equivalent. Using the QCL analyser for the above purpose and near-concurrent to EC was highly cost-efficient and provided immediate data outputs while avoiding further laboratory work.

Finally, to contextualise our contribution to the field of greenhouse gas research: This thesis demonstrated and advanced our knowledge about how robust EC measurements of N_2O fluxes can be conducted in an intensively grazed farming environment that receives high and dynamic inputs of N_r. Findings served to 1) verify site EC and EF emission budgets, 2) demonstrate that a single EC system can be used to distinguish treatment effects on adjacent paddocks, and 3) invent a novel technique that allowed immediate, field-based injections of chamber derived gas samples into the QCL of the EC system.

Acknowledgements

Mein innigster Dank gebührt meiner *Familie* – meinen Großeltern, Eltern, Paten und meinen zwei Brüdern. Großgezogen habt ihr mich in der behüteten Umgebung kleinstädtischer Idylle. Durch eure strikte, liebevolle und inspirierende Erziehung habt ihr einen Geist geformt, der nun, freiheitlich und global denkend, durch die Welt zieht. Erkundet. Gestaltet. Kreiert. Diese Promotionsarbeit ist entstanden auch Dank eurer Unterstützung, ein halbes Mal um die Welt – und zurück. Einmal habt ihr zu mir gesagt:

"Solange die Kinder klein sind, gib ihnen Wurzeln,
wenn sie älter geworden sind, gib ihnen Flügel!"

(Aus Indien, Khalil Gibran)

Wie wahr!

Great achievements are rarely accomplished individually but result from the spirit, power and creativity of a team. Please, let me highlight the potpourri of people behind the scenes: the supervisors, scientists, brains and thinkers, the team players and the individualists, the care-takers and compassionate, the rationalists and officials, the communicators and creative, the challenging, the collaborators and friends. Each one of them has contributed to the success of this work and, ultimately, its final realisation.

I would like to thank:

Louis Schipper – for his overall guidance and support throughout the journey
David Campbell – for his technical know-how and letting me play with QCLs
Aaron Wall – for his brilliance of mind, honest opinion and MatLab support
Jordan Goodrich – for filling the 'gaps' and reviewing my manuscripts
Lìyǐn Liáng – for introducing me to EC and being my email back-up
Chris Morcom – for his muscles in the fields and some good jokes
The WaiBER team – for providing cakes, resources and research environment
Sci-Admin & SGR – for getting the administrative nitty-gritty right
Student health – Michelle, Chris, Carine and Steve thank you from all my heart
Whetū Taukamo – for helping me acknowledge the Māori heritage of Aotearoa
Cheryl Ward – for her contagious joy and support when formatting this thesis
David Lowe – for his soil passion and convening the WaiBoP conference
Megan Balks & Tanya O'Neill – for your mentoring at the NZSSS competition
Femke Rambags, Mahdiyeh Salmanzadeh, Joss Ratcliffe & Seb Hoepker – for being my companions on the way, offering advice, motivation and lots of life philosophy

Jiafa Luo – for his off-site support and inspiring discussions at lunch time
Dave Houlbrooke – for adopting me at AgResearch and a calm leadership
Stuart Lindsey – for collecting and talking cow 'shit' together, plus ice cream!
Moira Dexter, Bridget Wise, Bill Carlston – for your helping hands and smiles
Vanessa Cave – for her great, friendly, and so efficient statistical advice
Nick Smith – for sharing an office with me and for all those pancakes
Amanda Judge – for your cheering during the Covid-19 lock-down

The University of Waikato – for funding and support
New Zealand Agricultural Greenhouse Gas Research Centre – for funding
DairyNZ – for a three years' scholarship
AgResearch Ruakura – for providing staff, research and technical resources

Georg Guggenberger – for being an enduring mentor and inspiration
Susanne Woche – for loving the pedosphere as much as I do
Thomas Caspari – for letting me expand my mind and write about soils
Emily Huang – for all those N_2O standards and introducing me to GC
Alec Mackay – for initially breaking my leg and making me return to NZ
Troughton Family – for providing the research site and farm management data
Aerodyne Research Inc. – for technical support and email communication

Kati Hewitt – for your all-embracing presence as a dear GeWi friend
Jess Roeger – for your creativity, amazing food, and mindfulness
Megan Clemance – for your warm heart and those swims in Raglan waters
Jonathan Arkley – for making me feel welcome in NZ and a lovely home
Florian Gehring – for your revisions and, more importantly, the train tales
Christchurch friends & Eilidh Hilson – for sharing South Island beauty
German friends & Iris Anneser, Sophia Sachs, Stefan Diebäcker – for sparkling like stars in the distance afar always staying connected in spirit and thoughts

…

Tom.
My partner in crime. Thank you for your loving support and sharing this journey with me. You might agree, the past years have been an extraordinary voyage leading us through both, calm waters and stormy seas. Let us now hoist our sails towards new endeavours and keep smiling at the future ahead.

Preface

1096 days, 26 304 hours, and 1 578 240 minutes.

…

Dear reader, this is my attempt to quantify what has remained difficult to grasp – the amount of time that the past three of my years comprised. Perhaps you might have just concluded the same numbers, and I agree: Time is equitable. It does not distinguish between a person's gender, intelligence, origin or skin colour. Each one of us has been provided with an equal budget – a lifetime – and the only, but important, difference is how we decide to spend this time. With the decision made to write a doctoral thesis, I invested the majority of days and hours of my most recent lifetime in one undertaking. Results at hand, I now entertain the thought that this was time spent worthwhile. I assume you, dear reader, might be eager to explore the research part of this thesis. But before let me borrow a few minutes of your time – on a personal note.

…

Climate change research is a challenging and sometimes even precarious undertaking. As scientists, we have to deal with findings that feel like a prophecy of doom. And the overall trend seems clear: ice sheets are melting, weather extremes are increasing and the global biodiversity is in decline. Researchers around the world strive to put climate change into words and numbers. However, the extent to which climate phenomena affect life on earth often remains difficult to comprehend – even for us. Atmospheric warming is a rapidly proceeding real-time challenge. Its speed is intimidating, especially when everyday life for others seems to spin on, just so, as if the hard facts did not exist. It is complicated, of course: The impacts of a changing climate and environment have not spread equally across the globe. Geographical discrepancies prevent individuals, regions and countries from experiencing climate change the same and, consequently, challenge united action against it.

Wandering on the path of climate science myself, I became familiar with the facts and the further I went, the more I noticed that the impacts of climate and environmental change are not only related but indispensably connected also to the level of equality of human interaction and cohabitation. Climate change and gender equality, for example, share a strong interconnection and the resulting consequences will be severe for human development. Meaning that the impacts of a changing climate are likely to shift power relations and gender rights throughout the world with women being disproportionately more affected than men. To date, women are already confronted by greater limitations:

access to education, knowledge, resources, their participation in policy development, decision making, voice and accountability, … Just recently, I discovered a thought-provoking initiative: *gender cc*, a global network of organisations, experts and activists that work for climate justice and gender rights. Information on the gender cc website are plentiful and not only explain why climate change affects women differently than men but also pointing out how this inequality and discrepancy can be overcome.

Dear reader, I like to encourage you – take a look and be inspired. There is hope and yet no reason to loose optimism. The functional blindness that makes us fear to 'change' can be overcome. We have to realise that change is as powerful as it is painful and ultimately inescapable. Moving towards a sustainable future will include stepping back from luxurious, resource-inefficient lifestyle choices and policy decision making – worldwide. We will have to let go and redefine our norms and habits in various, if not all, areas of life. Probably, even our life philosophy! I often imagine what would happen if humanity just realised its greater power for the good. If every single one of us would contribute to this important realisation. I wished we would be encouraged more to use our skills, sense of fairness, creative, intellectual and financial resources to empower sustainability and defeat (gender) injustice. And even if there was nothing else to add, at least, to stay optimistic and be responsible, mindful and kind to the world around us. Whatever we do and wherever we might go.

Table of Contents

List of Figures

List of Tables

List of Abbreviations

AMO	Ammonia monooxygenase
AN	Ammonium nitrate fertiliser
ANOVA	Analysis of variance
ATP	Adenosine triphosphate
BNE	Background nitrous oxide emission
BNF	Biological nitrogen fixation
C	Carbon
°C	Degrees Celsius
CH_4	Methane
Cl^-	Chloride
cm	Centimetre
C_{N2O}	Nitrous oxide concentration
C_{N2O_GC}	Nitrous oxide concentration based on GC analysis
C_{N2O_QCL}	Nitrous oxide concentration based on QCL analysis
CO_2	Carbon dioxide
d	Day
DM	Dry matter
DMI	Dry matter intake
DON	Dissolved organic nitrogen
EC	Eddy covariance
EF / EFs	Emission factor/emission factors
F	Flux / Fertiliser (in the context of Chapter 3)
$F_{chamber}$	Nitrous oxide flux from static chambers
$F_{pad,chamber}$	Nitrous oxide flux from static chambers, paddock scale
F_{EC}	Nitrous oxide flux from eddy covariance
F_{N2O_F}	Nitrous oxide flux based on filtered EC data
F_{N2O_CF}	Nitrous oxide flux based on filtered EC data, control site
F_{N2O_RF}	Nitrous oxide flux based on filtered EC data, renewed site
F_{N2O_G}	Nitrous oxide flux based on gap-filled EC data
F_{N2O_CG}	Nitrous oxide flux based on gap-filled EC data, control site
F_{N2O_RG}	Nitrous oxide flux based on gap-filled EC data, renewed site
F_{N2O_GC}	Nitrous oxide flux from static chambers analysed by GC
F_{N2O_QCL}	Nitrous oxide flux from static chambers analysed by QCL
g	Gram
GC	Gas chromatograph / gas chromatography
Gg	Gigagram
GWC	Gravimetric water content
GWP	Global warming potential
H	Hydrogen
ha	Hectare
HO	Hydroxide
H_2O	Water
IPCC	Intergovernmental Panel on Climate Change
IR	Infrared
K_2SO_4	Potassium sulphate
kg	Kilogram
kNN	k-nearest neighbour
kt	Kiloton
L	Litre
m	Metre

min	minute
mm	Millimetre
μmol	Micromole (10^{-6} moles)
mL	Millilitre
N	Nitrogen
N_r	Reactive nitrogen
N_2	Dinitrogen
NEE	Net ecosystem exchange
NEP	Net ecosystem productivity
NH_2OH	Hydroxylamine
NH_3	Ammonia
NH_4^+	Ammonium
NIS	Nitrification-inhibiting substances
N_{min}	Mineralised nitrogen
nmol	Nanomole (10^{-9} moles)
NN	Neural network
NO	Nitric oxide
NO_2^- / NO_2	Nitrite / nitrogen dioxide
NO_3^-	Nitrate
N_2O	Nitrous oxide
Nor	Nitric oxide reductase
NTP	Network time protocol
NZ	New Zealand
NZD	New Zealand dollars
NZDT	New Zealand daylight time
NZ-NCNM	New Zealand National Centre for N_2O Measurements
O	Oxygen (the element)
O_2	Dioxygen
O_3	Ozone
ODP	Ozone depletion potential
P	Paddock
pH	Measure of the concentration of protons (H^+) in a solution
PLS	Partial least squares
ppb	Parts per billion
PPFD	Photosynthetic photon flux density
ppm	Parts per million
ppt	Parts per trillion
PTFE	Polytetrafluoroethylene
s, sec	Second
S	Supplementary feed
SD	Standard deviation
SEM	Standard error of the mean
SOC	Soil organic carbon
SOM	Soil organic matter
QCL	Quantum cascade laser absorption spectrometer
TDL	Tunable diode laser
Tg	Teragram
VWC	Volumetric water content
W	Watt
WFPS	Water-filled pore space
yr	Year
°	Degrees

Chapter One

Introduction

1.1 Nitrous oxide emissions and the climate change challenge

Livestock production and the application of nitrogen fertilisers are the main catalysts of higher than natural nitrous oxide (N_2O) emissions from agricultural soils (Galloway et al., 2013). Nitrous oxide is a long-lived atmospheric trace gas that has a global warming potential 265–298 times greater than carbon dioxide and efficiently promotes radiative forcing but also depletes stratospheric ozone (Ravishankara et al., 2009; IPCC, 2013). For most of the Holocene, the atmospheric mixing ration of N_2O was below 265 parts per billion (ppb) (Flückiger et al., 2002; MacFarling Meure et al., 2006). The natural nitrogen cycle, i.e. the equilibrium between N_2O production in soils and its biochemical transformation to more inert nitrogen compounds in the atmosphere, has only recently been altered by a surplus of reactive nitrogen (N_r) added to agricultural land through anthropogenic activity (Kroeze et al., 1999; Syakila and Kroeze, 2011). Since the onset of industrialisation, the increase in atmospheric N_2O concentrations has been persistent and at rates greater than the chemical removal of N_2O (MacFarling Meure et al., 2006; Schilt et al., 2013). From 2009 onwards, Thompson et al. (2019) found that the increase in global N_2O emissions occurred at even faster rates than initially estimated by the Intergovernmental Panel on Climate Change (IPCC). Overall, global N_2O emissions were projected to increase by 29% from 2000 to the year 2050 (Bouwman et al., 2013; Cai and Akiyama, 2016). The mean annual growth rate of the atmospheric N_2O mixing ratio is currently at 0.2–0.3% but might soon be exceeded with N_2O mixing ratios in future well beyond present-day 330 ppb (Signor and Cerri, 2013; WMO, 2018).

Limiting N_2O emissions in future will, therefore, greatly depend on strategies to prevent and optimise the addition of excess N_r to agricultural soil, adoption of appropriate land management strategies and the state of the soil itself. Presently, soils are estimated to contribute 56–70% to global N_2O emissions, particularly when utilised for livestock agriculture (Forster et al., 2007; Syakila and Kroeze, 2011; Ussiri and Rattan, 2012). Ruminants and other grazing animals require large amounts of feed but only retain 10–25% of the original feed nitrogen with the remainder of this nitrogen being excreted (Whitehead, 2000; Jones et al., 2017). Deposited in relatively small urine

and dung patches, excreta nitrogen often exceeds plant demand and, thereby, becomes a substrate for a wealth of microbial metabolic pathways that can produce (or consume) N_2O (Butterbach-Bahl et al., 2013; Luo et al., 2017). Whether net N_2O production occurs is defined by differences in the availability and distribution of N_r, climate factors, soil properties and the soil microbiome (Firestone and Davidson, 1989). Strongly interlinked with each other, these factors form a heterogeneous environment in which spatial and temporal variabilities make the quantification, understanding and mitigation of N_2O emissions challenging to determine (Voglmeier et al., 2019). Nitrous oxide emission data from intensively managed and grazed land, therefore, still comprise the highest uncertainty among all grassland types to date (Flechard et al., 2007; Gibbs, 2018b; van der Weerden et al., 2020). Measurements using static and automated incubation chambers enforced the understanding of the N_2O emission process at point scales but continuous N_2O flux (F_{N2O}) datasets beyond the chamber scale have yet remained sparse (Fuchs et al., 2018; Liáng et al., 2018; Voglmeier, 2018). However, reliable long-term datasets will be crucial when quantifying greenhouse gas emissions from pastoral high-flux ecosystems, not only to establish comprehensive emission inventories, but also to enable mitigation strategies that decelerate and ultimately prevent the radiative forcing effect of N_2O on the global climate at present and in the future (Kelliher et al., 2017).

1.2 Nitrous oxide emissions from New Zealand dairy pastures

Intensively managed, grazed pastures are of global importance for the exchange of carbon dioxide (CO_2), methane (CH_4) and nitrous oxide (N_2O) greenhouse gases (Jones et al., 2017). Emissions of these gases are inherently interlinked with the utilisation of grasslands to sustain most of the world's grazing animal herd and to satisfy the human demand for animal-based proteins, i.e. primarily milk and meat (de Klein et al., 2010; Mottet et al., 2017). Managed grasslands cover 26% of the terrestrial land surface globally and as non-native *exotic grassland* around 40% (or 10,675,261 ha) of New Zealand (Suttie et al., 2005; MfE, 2012; FAO, 2020). The predominance of exotic grassland in New Zealand originates from forest and land clearance in the early days of European settlement history. Livestock farming in New Zealand is thus pasture-based with beef and dairy cattle as well as most other animals (e.g., sheep, deer, horses) grazing on outdoor paddocks year-round. The pasture sward is generally dominated by perennial ryegrass (*Lolium perenne*) and white clover (*Trifolium repens*) to promote biological nitrogen fixation and N_2O emissions commonly range between 0.2 and 15.9 kg N_2O-N ha^{-1} yr^{-1} (Luo et al., 2008a; de Klein et al., 2010; Luo et al., 2017).

For the past three decades, a large number of New Zealand case studies have identified and discussed the effect of animal excreta, nitrogen fertiliser, environmental variables and farm management strategies on N_2O emissions creating knowledge for national policies (Gibbs, 2018b; MfE, 2019, 2020). For instance, the New Zealand 1990–2017 greenhouse gas inventory distinguished N_2O emissions from ruminant excreta deposited onto pastoral soil into a urine and dung component equal to an emission factor (EF) of 1% and 0.25%, respectively (Carran et al., 1995; Mueller et al., 1995; de Klein et al., 2003; Luo et al., 2009). Note that these urine and dung EFs have been amended in the latest version (1990–2018) of the New Zealand inventory to 0.98% and 0.33% for N_2O emissions from cattle urine depending on slope, and 0.12% for cattle dung (MfE, 2020; van der Weerden et al., 2020). Better accounting for N_2O emissions from pastoral soils and understanding the underlying controls and drivers led to the insight that N_2O emissions in New Zealand are currently increasing (Lassaletta et al., 2014). In 2018, for example, agricultural soils were a major contributor of domestic N_2O emissions with levels 56.7% (2,543 kt CO_2-equivalent) above 1990 and a contribution to national gross greenhouse gas emission of an estimated 8.9% (7,026 kt CO_2-equivalent) (MfE, 2020).

Domestic research focuses on finding new approaches and mitigation strategies to this enduring challenge, i.e. the country's increasing N_2O emissions. For instance, Gardiner et al. (2016) reviewed possible effects of increasing the percentage of plantain (*Plantago lanceolata*) in the cattle diet and the pasture sward likewise on mitigating urine derived N_2O emissions. First results suggested that plantain reduces urinary nitrogen excretion and potentially also inhibits microbial nitrification in the soil (Bowatte et al., 2015; Gardiner et al., 2018; Simon et al., 2019). However, whether findings like this or other mitigation strategies will suit whole-farm systems is yet to be evaluated (de Klein et al., 2010). Because often the scale of testing the effect of new mitigation strategies on N_2O emission has remained limited by methodological constraints.

At present, chambers are the most commonly used technique for determining the flux of N_2O with 95% of all field studies referring to this technique (Rochette and Bertrand, 2007; Rochette, 2011; Lammirato et al., 2018). Chambers are relatively easy to deploy, cost-efficient and follow standardised guidelines but operate over areas less than 1 m^2 and offer limited temporal coverage (Rochette and Eriksen-Hamel, 2008; Jones et al., 2011; de Klein et al., 2015). However, the disconnect between point scale chamber measurements and environmental processes that occur at farm system scales (~100 ha) has only been overcome in the last decade promoted by the development of fast and

field-applicable N_2O analysers. When coupled to micrometeorological eddy covariance (EC), these "new" analysers provide continuous measurements of F_{N2O} at paddock scales (Rapson and Dacres, 2014; Rannik et al., 2015) and provide robust results e.g., based on continuous wave quantum cascade laser absorption spectrometry (QCL) (Fuchs et al., 2018; Tallec et al., 2019; Cowan et al., 2020). Presently, there are three QCL EC systems operating in New Zealand and the measurement data from one of these three sites form a major component of this thesis.

To date, only a few studies have used QCL EC for flux measurements of N_2O and this might explain why our understanding of paddock scale to whole farm emission processes has remained underdeveloped. Further research is needed to compare micrometeorological measurements with the existing (chamber) techniques and the role of these new approaches in the field of N_2O research has to be discussed.

1.3 The Troughton farm research site

Data used for this thesis originate from greenhouse gas research conducted on Troughton Farm (37.77°S, 175.8°E, 54 m a.s.l.), a commercial dairy farm in the Waikato region, North Island, Aotearoa New Zealand. The farm was located in the Hauraki Plains, a graben filled with volcanic deposits and alluvial sediments of an ancient river system (McLeod, 1992). Under a temperate-oceanic and moderate climate, mean annual temperature and precipitation were 13.3°C and 1249 mm (1981-2010) according to the nearest climate station 13 km to the south-west of the farm (NIWA, 2018). Extended dry periods occurred in late summer and early autumn, and frosts only on a few days in winter (NIWA, 2018). Precipitation was generally received as rainfall. Soils on the old alluvial surface were characterised by variations in sedimentation and drainage, and often contained rhyolitic volcanic ash. Described by New Zealand soil taxonomy, a Mottled Orthic Allophanic soil (Te Puninga silt loam) was the dominant soil type of the study area with a clay content of up to 20% in the topsoil and a mean soil organic carbon (SOC) content of 9% (Hewitt, 2010).

Troughton farm had been managed for dairy production for at least 80 years. The total area of the farm was 207 ha (199 effective ha) with paddocks sized between 2.5 to 3.5 ha and rotationally grazed year-round (Rutledge et al., 2017a; Wall et al., 2020b). Most of the pasture sward comprised a traditional mix of perennial ryegrass and white clover. More recently, diverse swards (e.g., red clover, lucerne, sunflowers, chicory, prairie grass), maize forage and plantain have been established on some paddocks of the farm. In spring, when the dry matter (DM) production rate reached 70 kg DM

ha^{-1} d^{-1} grazing rotation could be as short as 21 days, whereas in winter when DM production was around 15–20 kg DM ha^{-1} d^{-1} grazing rotation could extend for up to 90 days (Pronger et al., 2016). Cattle received supplementary feed during times of lower pasture production from imported and on-site sources that were mostly provided in the form of hay, grass or maize silage either on a feed pad or on the paddocks before or during grazing. The total number of cows decreased with time from 701 Jersey cows in 2012 (3.5 cows ha^{-1}) to 437 cows in 2018 (2.2 cows ha^{-1}) (Wall et al., 2020b). Greenhouse gas emissions had been monitored on the farm for multiple years using different EC systems, one of which was also equipped with a QCL for measuring F_{N2O} (Table 1-1). The QCL EC site system (Fluxnet code NZ-Tr3.) was established in November 2016 and since then has provided this work with continuous F_{N2O} measurement data. The first year of F_{N2O} data was reported by Liáng et al. (2018).

Table 1-1 Site-specific publications from research conducted at Troughton farm.

Author (year)	Title of publication
Pronger et al. (2016)	Low spatial and inter-annual variability of evaporation from a year-round intensively grazed temperate pasture system
Sparling et al. (2016)	Estimates of annual leaching losses of dissolved organic carbon from pastures on Allophanic Soils grazed by dairy cattle, Waikato, New Zealand
Rutledge et al. (2017a)	The carbon balance of temperate grasslands part I: The impact of increased species diversity
Rutledge et al. (2017b)	The carbon balance of temperate grasslands part II: The impact of pasture renewal via direct drilling
Liáng et al. (2018)	Nitrous oxide fluxes determined by continuous eddy covariance measurements from intensively grazed pastures: Temporal patterns and environmental controls
Pronger et al. (2019)	Toward optimisation of water use efficiency in dryland pastures using carbon isotope discrimination as a tool to select plant species mixtures
Wall et al. (2019)	Carbon budget of an intensively grazed temperate grassland with large quantities of imported supplemental feed
Liáng et al. (2020)	Modelling the effects of pasture renewal on the carbon balance of grazed pastures
Wall et al. (2020a)	Quantifying carbon losses from periodic maize silage cropping of permanent temperate pastures
Wall et al. (2020b)	Temperate grazed grassland carbon balances for two adjacent paddocks determined separately from one eddy covariance system
Wecking et al. (2020a)	A novel injection technique: using a field-based quantum cascade laser for the analysis of gas samples derived from static chambers
Wecking et al. (2020b)	Reconciling annual nitrous oxide emissions of an intensively grazed dairy pasture determined by eddy covariance and emission factors
Goodrich et al. (2021)	Improved gap-filling approach and uncertainty estimation for eddy covariance N_2O fluxes
Pronger et al. (unpublished)	Short pasture renewal period minimises soil carbon losses, but poor pasture establishment leads to annual scale soil carbon losses

1.4 Research objectives and outline

Despite an increasing number of studies using EC for the measurement of N_2O continuous datasets determined over multiple years for agricultural, but in particular intensively grazed systems, have remained sparse. A comprehensive understanding of the soil nitrogen cycle, soil flux dynamics at different temporal and spatial scales, and superimposed impacts of day-to-day farm management decisions on the exchange of N_2O in these systems are still lacking; both in the short- and long-term. At present, greenhouse gas inventories and N_2O mitigation strategies are affected by great uncertainties, which make reliable assessments difficult.

This thesis used the EC technique to measure N_2O fluxes (F_{N2O}) from an intensively grazed grassland that received high inputs of reactive nitrogen. The aim was to quantify the exchange of N_2O across different spatio-temporal scales and, specifically, to determine the effect of farm management on resulting F_{N2O} via the following objectives:

i. To study the factors contributing to differences in paddock scale annual N_2O emission budgets, this thesis compared EC with static chamber measurements and estimates derived from emission factors (EFs).

ii. To investigate the effect of farm management on paddock F_{N2O}, this thesis compared N_2O emissions of two adjacent paddocks, one of which underwent pasture renewal (chemical spray, direct-drill). The other paddock was a control.

iii. To further explore the capability of QCL EC, this work tested whether a field-based QCL analyser could be used for the injection and analysis of N_2O samples captured by chambers nearby the EC station.

A literature review was conducted to support the experimental approach of this work and provide thorough background information (Chapter 2). To address the above objectives, three field-based experiments were conducted in the time between 2017 and 2019. In the first part, EC and static chamber measurements were used to determine and compare annual N_2O emission budgets (Chapter 3). In March 2018, one paddock of the EC footprint underwent pasture renewal. Eddy covariance measurements were used to assess the effects of the renewal event on N_2O exchange (Chapter 4). In September 2019, a new method was tested to allow manual injections of static chamber derived N_2O samples into the QCL of the EC system (Chapter 5). Overall findings and implications were brought to conclusion at the end of this thesis in Chapter 6 (Fig. 1-1).

It is to note that Chapters 3, 4 and 5 were developed as independent manuscripts and might include repetitions regarding the introduction, site details and methodological descriptions. Format and style of Chapters 3 and Chapter 5 follow the guidelines of the journals they have been published in, i.e.:

- **Chapter 3:**

  Wecking, A. R., Wall, A. M., Liáng, L. L., Lindsey, S. B., Luo, J., Campbell, D. I., and Schipper, L. A.: Reconciling annual nitrous oxide emissions of an intensively grazed dairy pasture determined by eddy covariance and emission factors, Agriculture, Ecosystems & Environment, 287, 1-14, 2020.

- **Chapter 4:**

  Results presented in Chapter 4 will be published in future work, which is aimed at quantifying a multiple-year, full greenhouse gas budget for the EC research site at Troughton farm. The data processing was based on the work from Goodrich et al. (2021) and Wall et al. (2020).

- **Chapter 5:**

  Wecking, A. R., Cave, V. M., Liáng, L. L., Wall, A. M., Luo, J., Campbell, D. I., and Schipper, L. A.: A novel injection technique: using a field-based quantum cascade laser for the analysis of gas samples derived from static chambers, Atmos. Meas. Tech. Discuss., 13, 5763-5777, 2020.

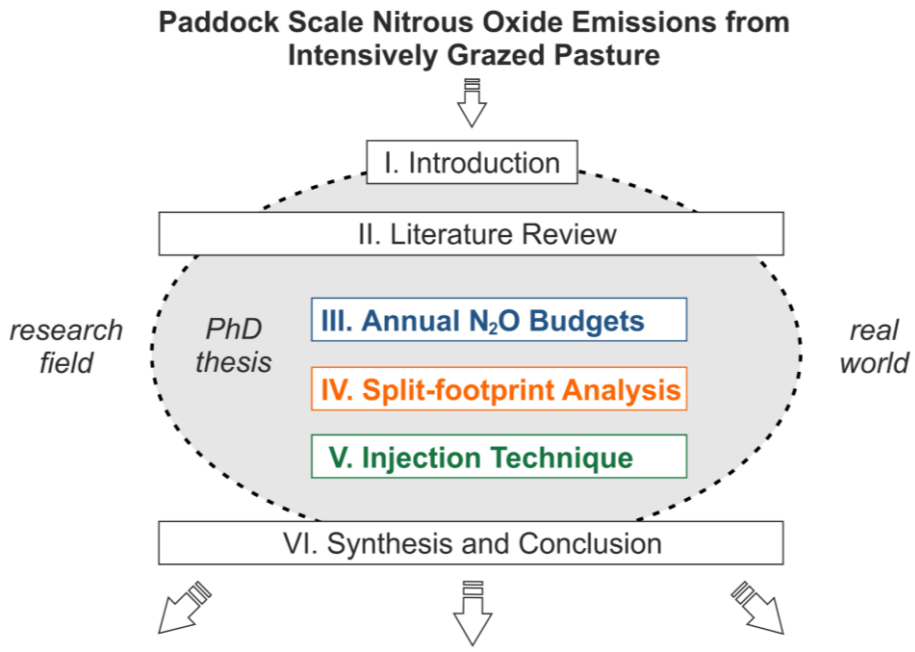

Figure 1-1 Structure of this PhD work with the thesis itself forming an open system (dashed ellipse) right at the interface between research objectives and the broader field of greenhouse gas research (real world). Introduction and literature review reach across the thesis boundary by introducing the reader to the general problem (Chapter 1) and summarising the current state of knowledge (Chapter 2) with respect to the research topic (headline). Chapter 3, 4 and 5 form the body of the thesis and investigate individual objectives based on how to measure N_2O in a real farm environment. Chapter findings are summarised and discussed at the end of the thesis (Chapter 6) with implications reaching from the thesis scale back out to the research field and eventually including real world applications (arrows).

Chapter Two

Literature Review

2.1 Nitrogen cycling in terrestrial grasslands

The discovery of nitrogen and its species dates to the 18th century. In 1744, Joseph Priestley discovered N_2O and ammonia (NH_3) gas, just two years after Daniel Rutherford had isolated the nitrogen element (Austin, 1788). However, the scientific understanding of the soil nitrogen cycle and the overall importance of N_2O emissions concerning global climate change have taken another around 250 years to advance. Even at present, understanding the biogeochemical complexity of nitrogen cycling in soils still poses an intellectual challenge (Sylvia et al., 2005; Butterbach-Bahl et al., 2013).

2.1.1 Natural functioning

Nitrogen is a limiting resource in unperturbed terrestrial ecosystems, where the bioavailability of plant accessible reactive nitrogen (N_r) compounds is a factor that controls net primary ecosystem production (Vitousek and Howarth, 1991). Most of the nitrogen in the soil is bound to soil organic matter (SOM) and in the soil flora and fauna. Bound in these complex organic forms, nitrogen is an essential building block of e.g., amino acids, proteins, enzymes, antibiotics, chlorophyll, vitamins and metabolic intermediates (Blume et al., 2009). The cycling of nitrogen through biosphere and pedosphere, therefore, is considered one of the main biogeochemical cycles in terrestrial ecosystems (Butterbach-Bahl et al., 2011).

The two processes that enable inert dinitrogen (N_2) from the atmosphere to enter the terrestrial nitrogen cycle naturally are biological nitrogen fixation (BNF) and wet or dry atmospheric nitrogen deposition (Galloway et al., 2003; Hertel et al., 2011; Vitousek et al., 2013). Biological nitrogen fixation is promoted by specialised prokaryotes (e.g., symbiotic *Rhizobium* bacteria in the root nodules of legume plants) that can catalyse the conversion of atmospheric N_2 to plant-accessible NH_3. Nitrogen fixation rates from symbiotic bacteria can be as high as 200 kg N ha^{-1} yr^{-1}; or as low as 1–5 kg N ha^{-1} yr^{-1} when associated with heterotrophic nitrogen fixation during the decomposition of SOM (Pihlatie, 2007; Butterbach-Bahl et al., 2011). An overview on nitrogen-fixing symbioses and organisms is provided by Herridge et al. (2008) and furthermore, it has to be considered that the nitrogen cycle can also be closely linked to other elemental cycles e.g., the carbon, iron and manganese cycles (Kuypers et al., 2018).

Per se, the terrestrial nitrogen cycle is coupled to a variety of different biochemical processes in the plant-soil system that transform, mobilise or immobilise organic and inorganic N_r compounds (Fig. 2-1). The main drivers for these processes are litter production from plants and the decomposition of SOM (Blume et al., 2009). Once incorporated into the soil and bound to its reactive surfaces (e.g. SOM), soil nitrogen can remain immobilised until subsequent mineralisation takes place. The residence time of soil nitrogen in natural grasslands reaches from decades to centuries, which is mainly due to slow SOM mineralisation. The potential of internal nitrogen retention and the accumulation in grassland ecosystems is, consequently, generally high (Epstein et al., 2001; Galloway et al., 2003). With time, some of the nitrogen bound to SOM mineralises and transforms from large polymers back to bio-available organic monomers, which are accessible to plants and microbes (Blume et al., 2009). Alternatively, soil nitrogen can also remain in simple organic forms (such as amino acids), particularly, when the SOM turnover is governed by accessibility, instead of recalcitrance (Dungait et al., 2012). Soil microbes then mineralise these simple organic monomers to form inorganic ammonium (NH_4^+) or organic nitrogen (N_{org}) (Butterbach-Bahl et al., 2011). From there, NH_4^+ and N_{org} can be nitrified, i.e. oxidised, to nitrate (NO_3^-) (Stüeken et al., 2016). Any subsequent reduction via denitrifying processes from NO_3^- back to inert N_2 depends on the properties and redox-state of the soil but generally includes the formation of gaseous intermediates, i.e. nitrogen oxides and N_2O, which are emitted to the atmosphere (Fenchel et al., 2012; Stüeken et al., 2016). Other potential pathways that lead to N_r losses from soils are plant uptake, NH_3 volatilisation, leaching, soil erosion and fire (Galloway et al., 2003).

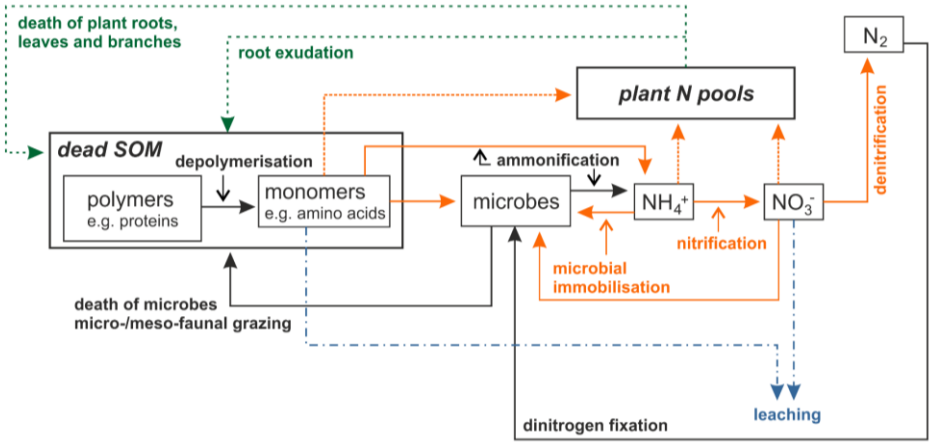

Figure 2-1 Scheme of major ecosystem processes in the nitrogen cycle including some internal retention pathways, shown are: plant processes (dashed lines), microbial processes (solid lines), competitive processes between plants (orange dashed line) and microorganisms (orange solid lines), hydrological transport pathways (long dotted-dashed blue lines) and soil organic matter (SOM). Modified from Rennenberg et al. (2009) and Butterbach-Bahl et al. (2011).

2.1.2 Anthropogenic modification

Agricultural ecosystems are extremes of high biomass production that require a constant input of plant-available nitrogen to sustain productivity (Pihlatie, 2007). The amount of N_r added from anthropogenic sources to terrestrial and, in particular, agricultural soils has increased since industrialisation from 15 Tg N yr^{-1} in 1890 and 156 Tg N yr^{-1} in 1990 to 210 Tg N yr^{-1} in the early 21st century (Galloway et al., 2004; Fowler et al., 2013). With the invention of the Haber-Bosch process to synthesise NH_3 from atmospheric N_2, former boundaries of the natural nitrogen cycle have been overcome (Haber, 2002). Using the Haber-Bosch process, inorganic nitrogen fertiliser can be produced at large scale and, apart from its benefits for nourishing about half of the global population, contributes to the omnipresence of excess N_r in present-day agroecosystems (Erisman et al., 2008; Erisman et al., 2013).

The majority of additional N_r in intensively used grassland soils originates from the application of synthetic nitrogen fertiliser and excreta nitrogen from grazing animals (Davidson, 2009; Paustian et al., 2016). In 2010, fertiliser application added approximately 14–15 Tg N yr^{-1} to pastoral soils equal to 14–15% of the total global nitrogen fertiliser budget (IFA, 2011). For the same year, the amount of N_r from animal excreta was estimated as large as, or even larger than, the total global consumption of nitrogen fertiliser which for the given year was 103 Tg N yr^{-1} (IFA, 2011; Saggar et al., 2013). Key drivers for increased N_r deposition in New Zealand's pastoral soils (1990–2018) were the growth of national dairy herd (86%) and increases in the application of synthetic nitrogen fertiliser (673%), both of which were consistent with the global trend (MfE, 2020). Earlier work from Parfitt et al. (2012) had confirmed this finding and quantified the annual input of N_r to New Zealand pasture soil as 689 Gg N in 1990 and 951 Gg N in 2010. The main sources for this increase in excess N_r were fertilisation and imported feed whereas total BNF from pasture legumes (40 kg N ha^{-1}) decreased from 495 to 420 Gg N (Heggie and Savage, 2009; Parfitt et al., 2012).

The nitrogen cycle accelerates if stimulated by excess N_r and, once stimulated, includes the rapid cycling of nitrogen within, through and out of the plant-soil system (Paustian et al., 2016). The supply of nitrogen in the soil can locally exceed plant demands and this becomes particularly apparent in cow urine patches, where nitrogen loading rates are equivalent to 500–700 kg N ha^{-1} (but sometimes as high as 2000 kg N ha^{-1}) (Selbie et al., 2015). Soils, microorganisms and plants can experience nitrogen saturation when exposed to high nitrogen loads and might fail to assimilate or retain nitrogen and significant amounts of N_r might be lost via nitrogen leaching and/or gaseous emissions

(Saggar et al., 2011; Saggar et al., 2013; Cai and Akiyama, 2016). At the global scale, Van Drecht et al. (2003) reported total nitrogen leaching losses from agroecosystems to the groundwater of 55 Tg N yr^{-1}. In contrast, gaseous losses of N_2O, nitric oxide (NO) and NH_3 were estimated 4.1 Tg N_2O-N yr^{-1}, 3.7 Tg NO-N yr^{-1} and 30.4 Tg NH_3-N yr^{-1}; i.e. equivalent to respective contributions of 60%, 10% and 76% to their global emission budgets (IPCC, 2013).

Agricultural practices can have substantial impacts on soil nitrogen cycling as these practices define the amount of N_r that is added to and ultimately lost from the soil (Firestone and Davidson, 1989; de Klein et al., 2010; Rees et al., 2013). In pastoral systems, anthropogenic modifications are most commonly associated with animal grazing (e.g., animal species, grazing frequency, choice of forage) and the application of nitrogen fertiliser (Henry and Eckard, 2009; Saggar et al., 2013). Management practices may also include tillage during pasture renewal (Davies et al., 2001; Cowan et al., 2016; Drewer et al., 2016), manure application (Amon et al., 2006; Sonthi, 2010) or irrigation (Luo et al., 2008c); all of which contribute to the loss of soil N_r. Also, it was found that grazed pastures tend to experience higher nitrogen losses from leaching and via gaseous emission than cut and ungrazed pastures, which is likely due to higher additional inputs of N_r through animal excreta (Jones et al., 2017). However, whether a grassland acts as a net sink or source of nitrogen depends on the previous land use and specific site characteristics such as underlying soil and climate conditions (Firestone et al., 1980; Firestone and Davidson, 1989). For instance, Jones et al. (2017) found that soil from permanent pasture stored up to 9.4 ± 4.14 g N m^{-2} yr^{-1} across seven years, whereas Schipper et al. (2007) reported that some soils from managed grasslands in New Zealand were a net source of nitrogen with 9.1 g N m^{-2} yr^{-1} lost over 20 years. For the latter case, there was clear evidence that the sink strength of New Zealand grassland soils was limited due to increased nitrogen saturation of SOM and decreased net nitrogen immobilisation (Schipper et al., 2004; Schipper et al., 2014).

Changes in soil nitrogen stocks do not only depend on changes in nitrogen inputs and outputs, but can also be tightly interlinked with the cycling and the availability of soil organic carbon (SOC) (Schipper et al., 2004; Piñeiro et al., 2009). In grasslands, the coupling between carbon (C) and nitrogen (N) cycles is strong with the rate and strength at which the coupling occurs defined by the stoichiometry of soil-vegetation C/N ratios; and by processes that contribute to or vary this ratio (e.g. mineralisation-immobilisation turnover) (Bol et al., 2011; Soussana and Lemaire, 2014).

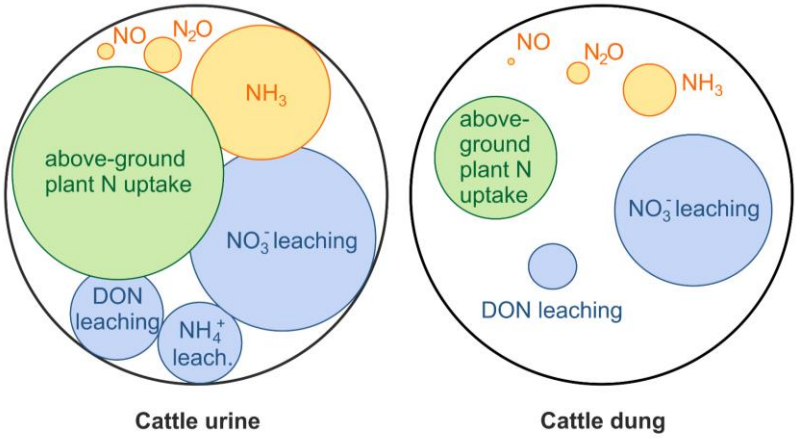

Figure 2-2 Fate of nitrogen losses from cattle urine and dung patches distinguished into a leaching (blue), gaseous (orange) and plant uptake (green) component. DON stands for dissolved organic nitrogen. The size of the circles, i.e. individual components, can be put into perspective compared to the two large black circles that reference a patch nitrogen load of 1000 g. Figure adapted from Cai and Akiyama (2016).

Animal production in this regard uncouples the natural equilibrium between carbon and nitrogen cycles in soils by releasing digestible carbon as CO_2 and CH_4 gas (respiration), and by returning N_r at high concentrations to the soil (excreta) (Soussana and Lemaire, 2014; Jones et al., 2017). This means that grassland soils that act as a nitrogen source can sometimes outbalance the carbon sink strength of a pasture (Niu et al., 2010; Jones et al., 2017; Zhou et al., 2017). Consequently, all carbon and nitrogen import-export processes must be assessed first before identifying the true greenhouse gas source-sink potential of an intensively managed grassland becomes possible. At present, only a few studies have quantified combined carbon and nitrogen budgets for intensively managed grasslands (Soussana et al., 2007; Ammann et al., 2009); and yet research that determined the response of net ecosystem exchange and carbon sequestration to nitrogen enrichment in grassland soils remained inconsistent: showing positive (Xia et al., 2009) as well as no significant responses (Harpole et al., 2007).

2.2 Nitrous oxide

2.2.1 Atmospheric warming potential of nitrous oxide

Nitrous oxide is a linear molecule and next to N_2 is the most abundant nitrogen species in the atmosphere (Li et al., 2013b). The chemical formula N_2O is referred to as nitrous oxide or dinitrogen monoxide. Three fundamental vibrational modes, *v1* (wave number 1285 cm^{-1}, 7.78 μm), *v2* (2224 cm^{-1}, 4.50 μm), and *v3* (589 cm^{-1}, 16.98 μm) enable N_2O molecules to absorb electromagnetic energy (Li et al., 2013b). The atmospheric N_2O concentration peaks in the mid-stratosphere, where N_2O molecules capture longwave radiation re-radiated from the earth's surface with the effect of

transforming electromagnetic energy to heat energy (Wayne, 2000; Schimel and Holland, 2005; Portmann et al., 2012). Due to its ability to outlive chemical destruction in the troposphere and lower stratosphere, N_2O is commonly referred to as a long-lived greenhouse gas (Wayne, 2000). The atmospheric lifetime of N_2O, described as the burden (in Tg) divided by the mean global sink (Tg yr^{-1}) for a gas in steady-state (Bolin and Rodhe, 1973; Ehhalt et al., 2001), is around 114 years before chemical break down via photolysis takes place (Forster et al., 2007).

At around 30 km altitude, the chemical transformation of surface-emitted N_2O strongly interacts with the depletion of ozone (Portmann et al., 2012). This process is relatively efficient although only ~10% of N_2O gas in the atmosphere is converted to short-lived but reactive and ozone-depleting NO_x species such as nitric oxide (NO) and nitrogen dioxide (NO_2) (Seinfeld, 2006; Ravishankara et al., 2009; Portmann et al., 2012). As described in the early work from Crutzen (1970) and Johnston (1971), ozone destruction is triggered by the catalytic potential of N_2O and NO_x. Without removal mechanisms in the lower troposphere, N_2O is transported to the stratosphere, where it eventually reacts with excited oxygen $O(^1D)$ atoms to form NO (Bolan et al., 2004):

$$N_2O + O(^1D) \rightarrow 2NO \qquad \text{(Eq. 2-1)}$$

The presence of NO subsequently catalyses the destruction of ozone (O_3):

$$\begin{aligned} NO + O_3 &\rightarrow NO_2 + O_2 \\ O + NO_2 &\rightarrow NO + O_2 \\ \text{Net: } O + O_3 &\rightarrow 2O_2 \end{aligned} \qquad \text{(Eq. 2-2)}$$

The overall ozone depletion potential (ODP) of N_2O under current atmospheric conditions is 0.017 with ODP defined as the relative capability of a unit mass of any chemical released into the atmosphere to destroy ozone compared with chlorofluorocarbons (Ravishankara et al., 2009). Similarly, the ODP of reactive NO_x is relatively high and one *x* (here NO, HO or Cl species) can remove 10^3–10^5 ozone molecules before any chemical transformation to less-reactive forms takes place (Lary, 1997; Portmann et al., 2012).

Furthermore, the increase of global N_2O concentration has a strong impact on the temperature in the stratosphere, where N_2O molecules act as radiative agents capable of emitting heat energy (0.17 ± 0.03 W m^{-2}) (Forster et al., 2007; Portmann et al., 2012; Ming et al., 2016). Nitrous oxide, therefore, has been identified as a climate forcing agent that disturbs the equilibrium between the amount of solar energy absorbed and the amount of solar energy emitted to space from the earth's surface or the atmosphere

(Shine et al., 1990). The global warming potential (GWP)[2] of N_2O over 100 years (i.e. the radiative efficiency in W m^{-2} ppb^{-1}) is ~265 times higher than that of CO_2, and together with the long atmospheric lifetime of the N_2O molecule contributes to atmospheric warming (Seinfeld, 2006; Forster et al., 2007; IPCC, 2013).

In 1998, the atmospheric concentration of N_2O was 314 ppb or, expressed as the global burden, 1,510 Tg N yr^{-1} (Ehhalt et al., 2001; Forster et al., 2007). In 2017, the N_2O mixing-ratio had reached 330 ppb with the increase being strongly linked to the availability of excess N_r in soils (WMO, 2018). Predictions exist that the human demand for animal- and plant-based proteins in combination with population growth are likely to increase in the future and, hence, are going to alter atmospheric N_2O concentrations even further (Ravishankara et al., 2009). Even if the most stringent mitigation strategies were applied, N_2O levels would be unlikely to decrease below present-day levels and are far from pre-industrial 270 ppb (Section 2.5) (Ravishankara et al., 2009; Li et al., 2013b). Based on the IPCC A1B-scenario, Nakicenovic and Swart (2000) estimated the N_2O mixing-ratio to reach 372 ppb by the end of the 21st century.

2.2.2 Main biochemical pathways of nitrous oxide production in soil

Autotrophic nitrification and heterotrophic denitrification are the key microbial pathways of N_r transformation in soil and contribute about 70% to the annual global N_2O emission budget (Tiedje, 1988; Butterbach-Bahl et al., 2013). Nitrification and denitrification are predominantly performed by soil microbes to meet intrinsic energy demands with N_2O being a by-product (nitrification) and intermediate (denitrification) of these processes (Oenema et al., 1997; Burgin et al., 2011; Ussiri and Rattan, 2012). Under aerobic conditions, nitrifying microbes oxidise NH_3 and NH_4^+ via the intermediate nitrite (NO_2^-) to nitrate (NO_3^-). In this oxidised state, NO_2^- and NO_3^- may subsequently be reduced, i.e. denitrified, under more anaerobic conditions in the soil. The product of complete denitrification is inert N_2. However, the denitrification process can be incomplete, then including the production of intermediate by-products. One of which is N_2O (Ussiri and Rattan, 2012).

The process of nitrification was first described by Schloesing and Muentz in 1877 (McCosh, 1984; Elmerich and Newton, 2007). Nine years later, in 1886, Gayon and Dupetit discovered denitrification (Payne, 1986; Elmerich and Newton, 2007). An overarching framework capturing the production and consumption of N_2O and NO

[2] By IPCC (1990) definition, the GWP describes the ratio of the time-integrated radiative forcing from an instantaneous release of 1 kg trace substance or gas relative to that of 1 kg reference gas, i.e. CO_2 (Shine et al., 1990).

by nitrification and denitrification within a conceptual model was published by Firestone and Davidson (1989) and has been acknowledged as the 'hole in the pipe model'. However, recent research suggests that a range of other biotic and abiotic pathways might also lead to the emission of N_2O e.g., heterotrophic nitrification, nitrifier denitrification, chemodenitrification, coupled nitrification-denitrification, co-denitrification, and anaerobic NH_3 oxidation (anammox) (Conrad, 1996; Braker and Conrad, 2011; Butterbach-Bahl et al., 2013) – apart from potential other yet still undiscovered processes in the nitrogen-cycling network (Kuypers et al., 2018).

Irrespective of the underlying process, most nitrification and denitrification pathways in soil lead to the net emission of N_2O (Myrold, 2005). Only under certain conditions denitrifier activity, and to some extent that of nitrifiers, stimulate the uptake of atmospheric N_2O (Casciotti and Ward, 2001; Schmidt et al., 2004). Soils are more likely to act as a sink for N_2O when the soil mineral nitrogen is low and when high soil moisture or other factors prevent microbial access to alternative oxygen (O_2) sources (Nömmik, 1956; Cicerone, 1989; Chapuis-Lardy et al., 2007; Philippot et al., 2009). Individual negative N_2O fluxes have been relatively frequently reported in the literature (Neftel et al., 2010; Cowan et al., 2014b; Liáng et al., 2018). However, the sink strength of soils to consume N_2O has not yet been fully examined and is often dismissed as experimental noise (Verchot et al., 1999; Chapuis-Lardy et al., 2007). Syakila et al. (2010) showed that the global uptake of N_2O at the earth's surface would not likely exceed 0.1 Tg N yr^{-1} and this is very small compared with a global nitrogen surplus of 17 Tg N yr^{-1} (Syakila and Kroeze, 2011; Ussiri and Rattan, 2012; Thompson et al., 2014).

2.2.2.1 Nitrification

Autotrophic nitrification in soils is a highly specialised process, particularly, when compared with the wide range of potential pathways for denitrification (Butterbach-Bahl et al., 2013). Under aerobic conditions, nitrification forms a two-step oxidation comprising (1) ammonium oxidation (NH_4^+ to NO_2^-) and (2) nitrite oxidation (NO_2^- to NO_3^-) (Signor and Cerri, 2013).

$$2\ NH_4^+ + 3\ O_2 \rightarrow 2\ NO_2^- + 2\ H_2O + 4H^+ + \text{energy} \qquad \text{(Eq. 2-3)}$$

$$2\ NO_2^- + O_2 \rightarrow 2\ NO_3^- + \text{energy} \qquad \text{(Eq. 2-4)}$$

Ammonium and nitrite oxidation in soils generally occur at a water-filled pore space (WFPS) of less than 60% as the optimum for chemoautotrophic bacteria of '*Nitroso-*' and '*Nitro-*' genera to perform nitrification strictly depends on the presence of free O_2 (Davidson, 1991; Sylvia et al., 2005). Under natural conditions, 3×10^5 nitrifiers per

gram soil are capable of processing 1 mg N d^{-1} (Stevenson, 1982; Myrold, 2005). A prerequisite for NH_4^+ oxidation at such rate is readily available N_r either in organic or inorganic form (Firestone and Davidson, 1989). Microbial mineralisation via aminisation and ammonification can transform organic nitrogen (N_{org}) to inorganic NH_4^+. Mineralised NH_4^+ may be nitrified but, alternatively, can also be immobilised on charged soil interfaces, up-taken by plants or volatilised as NH_3 (Bolan et al., 2004).

The gaseous release of NO and N_2O is a by-product of NH_4^+ oxidation with emission occurring mainly during the initial mineralisation of hydroxylamine (NH_2OH). The amount of N_2O emitted via nitrification is generally of several magnitudes smaller than the formation of NO_2^-, and N_2O contributions from nitrification sum up to totals less than 1% of all NH_4^+ oxidised (Arp and Stein, 2003; Sylvia et al., 2005). Generally, the emission of N_2O during the nitrification process is triggered by nitrite reductase enzymes. The activity of reductase enzymes increases under O_2 limiting conditions and lower pH-values at which autotrophic NH_4^+ oxidisers use NO_2^- as an electron acceptor to conserve O_2 for the oxidation of NH_4^+ (Poth and Focht, 1985; Ussiri and Rattan, 2012).

The majority of energy produced during nitrification benefits the Calvin cycle of microorganisms to metabolise CO_2 and adenosine triphosphate (ATP) (Ussiri and Rattan, 2012). With 35 mol of NH_4^+ and 100 mol of NO_2^- oxidised per one mol CO_2 fixed, nitrification is a low-yield energy source even under optimum conditions and within a suitable temperature range (2–40°C) (Wood, 1986). Due to the low energy yield, large amounts of NO_2^- are unlikely to accumulate in soils. Increases or decreases in N_2O production remain difficult to predict since O_2 partial pressure, NH_4^+ and NH_3^+ concentrations, as well as soil pH-value, rarely reach equilibrium. Fluctuations of these factors are common and control the spatio-temporal variability of N_2O production in soils (Tiedje, 1988; Firestone and Davidson, 1989).

Microbial nitrification consumes molecular O_2 and produces protons (H^+) acidifying the soil. Ultimately, nitrification generates oxidised NO_3^-, which once it has become available to denitrifier communities can be used for further microbial respiration following the reduction pathway to N_2 (Erisman et al., 2007). Nitrification and denitrification determine the overall form of N_r cycling in the soil and both these microbial processes are not only tightly interlinked but likewise capable of driving soil N_2O exchange dynamics whilst also controlling the absorption, utilisation and dispersal of soil N_r to the environment (Ussiri and Rattan, 2012).

2.2.2.2 Denitrification

In contrast to nitrification, denitrification is conducted by a wide array of soil microbes (Groffman et al., 2006; Groffman et al., 2009; Butterbach-Bahl et al., 2013). In soils, 0.1–5% of the total bacteria population can adapt its metabolism to facultative anaerobic pathways (Tiedje, 1988; Henry et al., 2004; Burgin et al., 2011). Denitrification is mediated mostly by heterotrophic microbes, and respective enzymes, and describes a stepwise dissimilatory reduction of NO_3^- to N_2 under anaerobic conditions:

$$2\ NO_3^- + 5\ H_2 + 2\ H^+ \rightarrow N_2 + 6\ H_2O \qquad \text{(Eq. 2-5)}$$

Respiratory denitrifiers gain energy by coupling NO_3^- reduction to electron transport phosphorylation. The reduction reaction from NO_3^- to N_2 is accompanied by a change in oxidation state from +5 to 0 (Firestone and Davidson, 1989; Zumft, 1997). Possible secondary pathways in the denitrification process are e.g., assimilatory NO_3^- reduction and chemodenitrification but these will not be further described at this point (Sylvia et al., 2005; Butterbach-Bahl et al., 2013). Simplified, N_2O emissions can be a product of various denitrification processes in soils, all of which are potent to release different forms of N_r into the environment (Otte et al., 2019).

As determined in numerous field and laboratory studies (Groffman et al., 2006; Seitzinger et al., 2006; Balaine et al., 2013; Ball, 2013), denitrification depends on the availability of O_2 in the soil which is strongly linked to enzyme activity. The synthesis of nitrate-, nitrite- and nitric oxide reductase enzymes is favoured only under increasing anaerobic conditions with nitric oxide reductase (Nor) being the most sensitive to O_2 (Sylvia et al., 2005). Heterotrophic denitrifiers use NO_3^- as an alternative terminal electron acceptor substituting O_2 under anaerobic conditions, i.e. at a WFPS greater than 60% (Davidson, 1991; Ussiri and Rattan, 2012). At very high WFPS and very low O_2 partial pressure in the soil, denitrification may fully reduce NO_3^- to terminal N_2 (high N_2O:N_2 ratio) (Seitzinger et al., 2006; Philippot et al., 2009; Fowler et al., 2013).

Denitrification is often favoured in anaerobic microsites where short-term changes in soil conditions are common and may change for more than a 100-times within a few days (Sylvia et al., 2005). In contrast to nitrification, N_2O and NO are obligatory intermediates in the denitrification process (Fig. 2-3) (Firestone and Davidson, 1989). Under some soil conditions, N_2O might even be the end product of an incomplete denitrification process that transformed a greater proportion of soil NO_3^- to N_2O than to N_2 gas (Cofman Anderson and Levine, 1986). Incomplete denitrification is

particularly likely when the availability of oxidants exceeds the availability of reductants (i.e. SOM) (Firestone and Davidson, 1989; Mosier et al., 1996; Ussiri and Rattan, 2012). Global estimations suggest that about 124 Tg N yr^{-1} are denitrified in terrestrial soil equal to around 40% of the terrestrial nitrogen pool (Seitzinger et al., 2006).

2.2.3 Drivers and controls of nitrous oxide production in soil

Nitrification and denitrification processes are driven by a complex interplay of controls reaching from cellular to environmental scales. Introduced by Tiedje (1988) and Robertson (1989), drivers of N_2O production that affect the immediate environment of the bacterial cell are commonly referred to as 'proximal'. Factors that are driven by environmental regulators are termed 'distal'. The cellular level of soil N_2O production is generally regulated by proximal controls: 1) the level of soil O_2 availability, 2) the availability of N_r substrate, and 3) the presence of electron donors, particularly SOM (Robertson, 1989; Sylvia et al., 2005; Ussiri and Rattan, 2012). Distal controls are linked to climate conditions, inherent soil properties and anthropogenic changes and often determine the overall rate of soil N_2O and NO production and consumption. Proximal and distal factors are in a constant interplay with each other and thereby lead to highly variable conditions in the soil and diverse spatio-temporal patterns of associated trace gas emissions difficult to predict (Barnard et al., 2005; Butterbach-Bahl et al., 2011).

The regulatory effect of microbial and environmental drivers on nitrogen trace gas production has been described in the 'hole-in-the-pipe' model by Firestone and Davidson (1989). In this conceptual model, production and consumption of gaseous N_2O and NO are imagined as a 'leaky pipe' (Fig. 2-3). The trace gas production within the pipe broadly depends on two levels of control: 1) the flow of N_r through the pipes, which is equal to the total rate of nitrification and denitrification, and 2) the size of the holes, which relates to the proportion of trace gases released. The rate at which N_r flows through the pipes is controlled at the proximal scale and can be either low or high; whilst distal drivers determine the portion (i.e. the size of the holes) at which N_2O and NO are finally emitted (Firestone and Davidson, 1989; Sylvia et al., 2005).

Despite the pioneering work of Firestone and Davidson (1989), understanding the effect of environmental drivers and, in particular, anthropogenic modifications on N_2O emissions has remained challenging (Parkin, 1993; Groffman et al., 2009; Imer et al., 2013). Linn and Doran (1984), for instance, found that fluctuations in WFPS had a distinct effect on the activity of soil microbes and, therefore, were the most important control for N_2O emissions. When close to a WFPS of 60–80%, soil conditions support

simultaneous nitrification and denitrification with both these processes leading to higher yields in final N_2O production (Ruser et al., 2006; Butterbach-Bahl et al., 2013). An overall 74–86% of the variations in N_2O/NO production and emission might be explained by the variation of moisture, aeration and temperature in soil (Schindlbacher et al., 2004). For instance, the release of N_2O is favoured by temperatures at an optimum of 37°C with Q_{10}-values ranging between 1.7–9.3 (Abdalla et al., 2009).

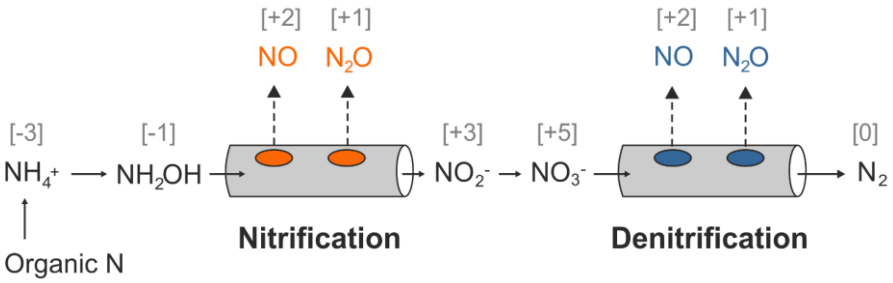

Figure 2-3 The microbial nitrogen cycle described and simplified by the 'hole-in-the-pipe' model based on the work from Firestone and Davidson (1989). Parentheses indicate the oxidation state of nitrogen.

When decoupling the effects of different drivers and controls on N_2O emission, it is important to consider syntrophic linkages between different biogeochemical cycles in soil, i.e. the nitrogen and carbon cycle, and the consequent effects of these linkages on microbial interactions (Burgin et al., 2011; van Groenigen et al., 2011). Nitrogen mineralisation rates can increase if carbon sources are not limited. Following Gundersen et al. (2012), N_2O emissions were negatively correlated at C/N-ratios > 30 but showed a positive correlation at C/N-ratios of ~11 when the coupling between nitrogen and carbon cycles was tight (Gundersen et al., 2012). High SOM contents and nitrogen mineralisation rates are likely to increase the rate of soil respiration and, thus, include potential not only to enhance net ecosystem carbon exchange but also to trigger the emission of N_2O (Niu et al., 2010).

2.2.4 Nitrous oxide emissions from intensively grazed pastures

Intensively grazed pastures are agricultural systems with a wide range of environmental and management conditions that can result in the emission of N_2O. Interestingly, a large proportion of total farm N_2O emissions in grazing systems often occurs from relatively small areas, i.e. hotspots (Groffman et al., 2009; Cai and Akiyama, 2016; Luo et al., 2017). These hotspots can be located in areas where animals congregate (feeding bins, water troughs and gateways), occur after additional irrigation or result from soil compaction due to trampling and in the soil underneath excreta patches (Saarijarvi and Virkajarvi, 2009; Aguirre-Villegas et al., 2017; Mumford et al., 2019).

Ruminants are overall poor nitrogen converters, meaning that only 5–30% of ingested nitrogen are uptaken by the animal and the remaining 70–95% are excreted in form of urine and dung (Jarvis et al., 2001; Oenema et al., 2005). Nitrogen loads in animal urine and dung patches, therefore, often exceed plant demands and are vulnerable to losses via gaseous emissions and leaching (Selbie et al., 2015). Barrow and Lambourne (1962), and Jarvis et al. (1995) found that the proportion of nitrogen in animal urine increased with increasing nitrogen intake; while it remained relatively constant in dung. Selbie et al. (2015), in turn, described ruminant urine patches as the "engine room" of nitrogen cycling in intensively grazed pastoral systems but also laid out that high urinary nitrogen loads might not necessarily result in high N_2O emissions.

More generally, the magnitude of N_2O emissions depends on the interplay between prevailing soil microclimate, microbial activity, plant composition, biomass, and excreta composition, which again is defined by animal type and feed intake. All these factors can alter the spatial heterogeneity of soil respiration and, hence, cause impact also on resulting N_2O emissions (van der Weerden et al., 2011; Luo et al., 2015; Shi et al., 2019). A meta-analysis by López-Aizpún et al. (2019) showed that it was important to account for differences in animal diet, gender and breed genetics when reporting urine derived N_2O emissions, in addition to urine composition and nitrogen loads. The urine patch characteristics of different animal species have been thoroughly discussed by Haynes and Williams (1993) and Selbie et al. (2015) where it was pointed out that mean urinary nitrogen concentrations from sheep, goats or deer (1.4–17.8 g N L^{-1}) are not necessarily lower than those from dairy cattle (3.0–13.3 g N L^{-1}). The similarity of urinary nitrogen contents between different animal types might explain why excreta EFs are often not further distinguished in national N_2O inventories (Section 2.4.1).

Mean annual N_2O emissions from intensively grazed pastoral soil in New Zealand were quantified equivalent to 8 kg N_2O-N ha^{-1} yr^{-1} (de Klein et al., 2006a). However, true N_2O emissions are likely to include a far greater range in dependence on the variability of soil and site characteristics. Luo et al. (2017), for instance, found that N_2O emissions from a single cattle urine and dung application can be as high as 16.8 kg N_2O-N ha^{-1} yr^{-1} and 5.57 kg N_2O-N ha^{-1} yr^{-1}, respectively (equivalents). Above that, Velthof and Oenema (1995) demonstrated that N_2O losses were 1.5–2.5 times greater from grazed than from cut or harvested pasture, especially during the wet season, and annual N_2O emissions from pastoral soils in Ireland were higher from frequently (8.6–12.5 kg N_2O-N ha^{-1} yr^{-1}) than less frequently (2.0–4.3 kg N_2O-N ha^{-1} yr^{-1}) grazed sites (Rafique et al., 2011). Farm management adds to the effect of site characteristics and climate

variability on N_2O emission and, therefore, has to be considered an equally important control (Rees et al., 2013).

2.2.5 Emission management and mitigation potential

Estimates based on the IPCC A1B-scenario predict the global mean atmospheric N_2O concentration to reach 372 ppb at the end of the 21st century (Nakicenovic and Swart, 2000) with the agricultural sector already contributing 84% to global anthropogenic N_2O emissions (Smith et al., 2008). Agricultural greenhouse gas dynamics are complex and to prevent further atmospheric warming stringent mitigation strategies for N_2O and other greenhouse gases are required (Cai et al., 2017a; Cai et al., 2017b). Strategies to mitigate N_2O emissions from pastoral land comprise two levels: 1) to manage the sources of nitrogen uptake at the animal level, and 2) to control N_2O production in situ through soil and grazing management (Oenema et al., 1997; de Klein et al., 2010).

Referring to 1), livestock management can be achieved by improving feeding practices, including dietary additives, and increasing animal productivity and nitrogen efficiency per kilogram of animal product through breeding and genetic manipulation (Castillo et al., 2001; Smith et al., 2008; Gregorini et al., 2010). Alternative pasture species such as plantain (*Plantago lanceolata*) were recently shown to offer the potential to decrease nitrogen concentration in dairy cow urine as well as to act as a biological denitrification inhibitor in the soil (de Klein et al., 2010; Box et al., 2018; Gardiner et al., 2018). First trials have demonstrated that cattle urinary nitrogen concentration decreased from initial 5.4 g N L^{-1} to 3.6 g N L^{-1} and 2.4 g N L^{-1} when fed on a 0%, 50% or a 100% plantain sward, respectively (Box et al., 2017). Moreover, plantain did not only act as a diuretic lowering the amount of urinary nitrogen but increased urination volumes from 47 L d^{-1} cow^{-1} to 74 L d^{-1} cow^{-1} (dilution effect) (Box et al., 2017). Lower urinary nitrogen contents were likely caused by secondary metabolites of the plantain plant that acted as nitrification-inhibiting substances (NIS) in the rumen (Subbarao et al., 2006). Once excreted to the soil, NIS were found to suppress the first step of NH_3 oxidation, i.e. reducing the activity of ammonia (AMO) monooxygenase. Identified as responsible for this inhibition were plantain-specific allelochemicals, mainly polyphenol verbascosids and iridoid glycosides (aucubin and catapol) which inactivated the AMO enzymatic reactions in the soil (Wichtl, 2004; Dietz et al., 2013).

Referring to 2), mitigation strategies addressed at soil and grazing management are manifold and e.g., include managing the intensity and timing of grazing events (de Klein et al., 2006b; Watson et al., 2007; van der Weerden et al., 2018), increasing

pasture productivity and soil carbon storage (Allard et al., 2007; Johnson et al., 2007; Whitehead et al., 2018), and advanced nutrient, fertiliser, and manure management (Davidson, 2009; Glassey et al., 2013; Kim and Giltrap, 2017). A popular farm management and mitigation strategy in New Zealand is controlled grazing, where cattle spend time on stand-off pads during the wet season (van der Weerden et al., 2017a). Removing animals from pasture areas can reduce treading damage, prevent leaching and gaseous losses of N_r, and thus preserve soil conditions (de Klein et al., 2006b; Šimek, 2008; Luo et al., 2013b). However, negative side effects of stand-off pads can be the accumulation of manure and cost-inefficiency, both of which might outweigh the desired mitigation benefits. van der Weerden et al. (2017a) showed that controlled grazing was beneficial on poorly drained soils where it contributed to reducing N_2O emissions, whereas the approach was not suitable on imperfectly-drained pasture.

Past research shows that there are promising strategies available for mitigating greenhouse gas emissions from pastoral and agricultural land, but also that mitigation potentials have not yet been fully realised (de Klein and Eckard, 2008; Smith et al., 2008; Decock et al., 2015). Beukes et al. (2010) determined that appropriate measures (e.g., animal genetics, reduction nitrogen fertilisation, grazing management) applied to one dairy farm in the Waikato region, New Zealand, had the potential to decrease greenhouse gas emissions from pasture-based systems by 27–32%. Future mitigation should ideally be focused on finding combined strategies that avoid any offsetting effect of the desired mitigation benefits and also help to improve the efficiency of nitrogen cycling through the soil-plant-animal system while, at the same time, preventing excess emissions (Schils et al., 2005; Stewart et al., 2009; Cai et al., 2017b).

2.3 Direct ways to quantify nitrous oxide emissions from soil

Despite the abundance of studies conducted on intensively grazed pastures, measuring F_{N2O} has remained defined (and limited) by the strengths and weaknesses of the associated measurement techniques. Rochette and Bertrand (2003) reported that more than 95% of all published field data used chamber methods that were mostly based on non-flow-through, non-steady-state designs. Alternative measurement approaches to using these static chambers (or dynamic chambers) are micrometeorological methods. Analytical techniques coupled to either chamber or micrometeorological equipment are broadly distinguished into three groups: 1) chromatographic, 2) optical and 3) amperometric (Rapson and Dacres, 2014).

This PhD study used analytical techniques of group 1) point scale static chambers and gas chromatography and group 2) micrometeorological eddy covariance (EC) coupled to a continuous-wave quantum cascade laser absorption spectrometer (QCL). Both methods were reviewed below. An introduction to alternative other approaches can be found in Rapson and Dacres (2014) and Rannik et al. (2015).

2.3.1 Static chambers

The principle of static chamber measurements is to determine the flux of N_2O, or any other trace gas of interest, from the change in chamber headspace gas concentration with time (Pumpanen et al., 2004). Using a syringe, air samples are taken periodically from the chamber headspace, are injected into pre-evacuated septum-sealed glass exetainers and stored until subsequent analysis commonly conducted in the laboratory. The resulting N_2O flux ($F_{chamber}$) in units mg N_2O-N m^{-2} h^{-1} can then be calculated:

$$F_{chamber} = \frac{\Delta N_2O}{\Delta T} \times \frac{M}{V_m} \times \frac{V}{A} \quad \text{(Eq. 2-6)}$$

where ΔN_2O is the increase or decrease in headspace N_2O concentration (μL L^{-1}) with time, ΔT is the enclosure period (h); $\Delta N_2O/\Delta T$ is the slope from the regression between N_2O concentrations and measured time; M is the molar weight of N_2O-N; Vm is the mol volume of the gas (L mol^{-1}) at the headspace air temperature recorded at each sampling occasion; V is the headspace volume (m^3); and A is the soil area (m^2) covered by the chamber base (van der Weerden et al., 2011).

Static chambers are easy to deploy, cost-efficient and provide valuable information for comparisons between different treatments by following standardised guidelines (Parkin and Venetera, 2010; de Klein et al., 2015; Pavelka et al., 2018; de Klein et al., 2020). Results from static chamber measurements are most commonly used to derive N_2O emission factors (EFs) that are the foundation of national greenhouse gas inventories, both in New Zealand and elsewhere (Section 2.4.1) (Rochette and Bertrand, 2007; Rochette, 2011; MfE, 2019). However, due to the low spatial and temporal resolution of chamber measurements, uncertainties of associated EFs can be as high as 50% (Smith and Dobbie, 2001; Zheng et al., 2004; Flechard et al., 2007). In 2016, for instance, the New Zealand-specific uncertainty range of chamber derived EF estimates was ± 55.4% (Kelliher et al., 2017; MfE, 2018).

Further disadvantages associated with chamber measurements include the alteration of the immediate soil environment after insertion of chambers or chamber collars into the ground that eventually lead to a modification in the resulting fluxes (de Klein et al., 2015). Likewise, pressure differences caused by removing air from the chamber

headspace and overall insufficient mixing in the headspace can interfere with natural gas diffusion (Rochette, 2011). This means that a higher gas concentration building up in chamber headspace and the soil pores reduces the diffusive flux from the soil to the surface and, thus, can result in non-linear gas concentration versus time data (Hutchinson and Mosier, 1981; Livingston and Hutchinson, 1995; Parkin et al., 2012). Consequently, the assumption of a linear increase or decrease (Eq. 2-6) in chamber gas concentration is not always applicable and can lead to underestimations in the true F_{N2O} before chamber deployment (Rochette and Bertrand, 2007; Venterea and Baker, 2008; Venterea, 2010). Misleading flux calculations are particularly apparent at close to ambient N_2O concentrations when sampling and analytical variability can result in apparent positive or negative flux values, although the true N_2O concentration in the chamber headspace does not change with time (Parkin et al., 2012). Adjusting the sampling rate and applying non-linear flux calculation methods have been suggested to reduce the limitations of static chambers (Kroon et al., 2008; Levy et al., 2011; Hüppi et al., 2018).

Upscaling F_{N2O} from the microbial to field and landscape scales has become increasingly important and so, perhaps, the most relevant drawback of static chambers is their inability to adequately capture the spatio-temporal variation of these F_{N2O}. Chamber measurements determine F_{N2O} typically over spatial areas much less than 1 m^2 and are often measured only once-daily (Rochette and Eriksen-Hamel, 2008; Jones et al., 2011). The continuous exchange of N_2O between the soil and the atmosphere may, therefore, not be consistently captured, particularly, from intensively managed pastoral land where cattle urine and dung patches form spatially variable and dynamic emission hotspots (Section 2.2.4) (Luo et al., 2017). However, N_2O emissions from these hotspots and, in some cases, hot moments that occur under favourable environmental conditions might significantly contribute to total annual N_2O budgets. Using micrometeorological EC measurements, e.g. Liáng et al. (2018), determined distinctive seasonal and diurnal patterns of F_{N2O} with soil moisture and soil temperature as dominant controls. Alternative approaches to static chambers, such as EC, can help to integrate flux measurements across greater spatio-temporal scales and understand the complicated ensemble of controlling factors on F_{N2O} in pastoral systems (Fig. 2-4).

Figure 2-4 Photos illustrate the two different methods used in this work: static chambers and micrometeorological eddy covariance with (a) showing the experimental set-up of a static chamber trial and (b) a close-up of an individual chamber; (c) shows the eddy covariance system used with the quantum cascade laser housed in the white box, and a close-up of the sample air inlet and sonic anemometer in (d).

2.3.2 Eddy covariance

Micrometeorological EC measurements determine gas exchange fluxes in the near-surface atmosphere at scales relevant to the ecosystem and provide a near-continuous data record under ideal conditions (Voglmeier, 2018). In the past three decades, EC has been the most commonly used technique for measuring the gaseous exchange of CO_2 and CH_4 (Baldocchi, 2014) and, more recently, EC flux measurements of N_2O have become possible through technological advance and the availability of fast and highly precise analysers (Nicolini et al., 2013; Eugster and Merbold, 2015; Nemitz et al., 2018). This development might explain why the EC method for F_{N2O} measurements is receiving increasing attention and its use has now become appealing to environmental scientists for complementing traditional chamber methods (Table 2-1).

2.3.2.1 Basic concept, strengths and limitations

Eddy covariance measurements calculate the covariance between the turbulent upward and downward movement of air (vertical wind speed) in the near-surface atmosphere and a scalar concentration (gas) within those air parcels (eddies) (Baldocchi et al., 1988;

Aubinet et al., 2012; Baldocchi, 2014). Eddy covariance measurements have to be conducted fast and long enough to determine the average flux density of the gaseous exchange between the soil-plant canopy and the atmosphere (Baldocchi, 2014). Required are measurement frequencies of at least 10 Hz and averaging intervals of 30 minutes or longer (Loescher et al., 2006). Rapid measurements above the plant canopy are generally achieved by mounting wind velocity and gas concentration sensors to a tower located within the ecosystem. This includes the advantage of minimising disturbances at the ground surface whilst also providing a direct measure of flux densities across an area (i.e. footprint) of paddock to ecosystem scale (Schuepp et al., 1990; Horst and Weil, 1994; Schmid, 1994). In practice, EC measurements are based on a statistical analysis of the instantaneous vertical mass flux density F (commonly in units nmol N_2O m^{-2} s^{-1}) expressed as the covariance between the fluctuation in gas mixing ratio c ($c = \rho_c/\rho_a$ with ρ_a being the density of dry air and ρ_c the density of N_2O) and vertical wind velocity (w). (Baldocchi, 2003; Rapson and Dacres, 2014):

$$F = \overline{\rho_a} \times \overline{w'c'} \qquad \text{(Eq. 2-7)}$$

The overbar in the equations denotes time averages (as the instantaneous deviation from the mean of the half-hourly values) and primes indicate fluctuations from the mean (Aubinet et al., 2012). To yield F, the results from Eq. 2-7 have to be integrated from the soil surface to EC tower height (Eugster and Merbold, 2015). Positive results would then represent a net gas transfer (upward flux) from the soil to the atmosphere, and negative F values show the reverse (Baldocchi, 2003). For a more comprehensive description of the EC technique see e.g., Baldocchi (2003), Aubinet et al. (2012), and Eugster and Merbold (2015).

Also, there are some limitations to the EC technique that must be considered when analysing and interpreting flux data, i.e.:

- Using EC measurements requires a well-mixed, turbulent atmospheric regime and does not account for fluxes under low turbulence conditions, at least not without additional measurement efforts (Massman and Lee, 2002). The boundary of a well-mixed atmosphere under stable conditions is commonly defined by applying a threshold (the friction velocity, u_*) to the data set (Goulden et al., 1996; Aubinet et al., 1999). Fluxes below the u_* threshold (e.g. 0.11 m s^{-1}) have to be excluded from subsequent analysis, but the associated systematic underestimation of night-time fluxes at less turbulent conditions is generally less pronounced for the measurement of N_2O than for CO_2 (Goulden et al., 1996; Liáng et al., 2018; Nemitz et al., 2018).

- The EC technique for measuring F_{N2O} partially differs from approaches used for CO_2. Atmospheric N_2O concentrations are of magnitudes smaller than CO_2 and, therefore, are more affected by instrument noise and the choice of the analytic set-up (Nemitz et al., 2018).
- Closed-path gas analysers, such as quantum cascade lasers (QCL), require mains power to operate and to transfer sample air drawn by a pump through long tubes to the sensor (Cowan et al., 2020). Biasing might result from tube attenuation of the signal or time lags up to tens of seconds between wind components and gas concentrations measured by the analytic device, especially, when not corrected (Leuning and Moncrieff, 1990; Liáng et al., 2018; Nemitz et al., 2018).
- Most gas concentration analysers demand housing in a temperature-stable environment or continuous cooling (Zahniser et al., 1995; Nelson et al., 2004).
- Eddy covariance measurements remain challenging in complex terrain and require the measurement of additional environmental variables such as soil moisture profiles, stocking density and other farm management data to allow for a process-based understanding of the underlying exchange dynamics (Nemitz et al., 2018).
- Finally, EC measures the net F_{N2O} integrated over large areas and does not differentiate between different source areas or treatments (urine, dung, fertiliser) from where these F_{N2O} ultimately originated (Molodovskaya et al., 2011; Dumortier et al., 2019).

In contrast, EC measurements offer distinct advantages: (1) EC allows manipulative experiments in different parts of the EC footprint (Wall et al., 2017; Baldocchi, 2019); and (2) provides ongoing flux measurements, which can be very useful for long-term climate observations (e.g. flux networks) (Baldocchi et al., 2001; Baldocchi, 2014; Eugster and Merbold, 2015). Voglmeier et al. (2019), for instance, showed that EC flux measurements made during one grazing season were capable to distinguish the effect of two different pasture management scenarios on N_2O emissions. On the other hand, Fuchs et al. (2020) applied four years of long-term F_{N2O} data measured by EC to different process-based biogeochemical models with results compared to Swiss greenhouse gas inventory data. Thus, if set-up wisely, EC can be a powerful tool for the measurement of F_{N2O} (Baldocchi, 2019; Merbold et al., 2020).

2.3.2.2 Quantum cascade laser absorption spectrometry

Applying EC successfully depends on the use of fast-response analysers that deliver measurements at sufficient temporal frequencies and are as well capable to operate reliably in field environments. In recent years, the application of N_2O analysers based on spectroscopic techniques has become particularly prominent when coupled to EC,

with tunable diode lasers (TDL) and QCL spectrometers as the main representatives (Rannik et al., 2015). The TDL and some other analysers have been reviewed by e.g., Allan et al. (2006), Rannik et al. (2015) and Lebegue et al. (2016) but here the focus is on introducing the basic principles of QCL as the preferred analytic technique for the work of this thesis.

Quantum cascade lasers generate a spectrometric light source that efficiently operates as a continuous wave over the mid-infrared spectrum (3.5 μm to 25 μm) (Faist et al., 1995; Curl et al., 2010). The light emission of a QCL is based on electron transition in between quantum well levels and comprises high output radiation triggered by the emission of multiple photons cascading through nanometre-thin layers of semi-conductors (Curl et al., 2010; Bidaux et al., 2016). The principles of QCL differ fundamentally from other conventional semiconductor lasers. This means that with QCL development, light emission has become independent of the material bandgap, which had previously defined the emission wavelength of the laser, and now solely depends on the layer properties of the semi-conductors chosen (Li et al., 2013b). Using a QCL, therefore, allows the measurement of various absorption bands of many different molecules (e.g., CO, CH_4, NO, N_2O, NH_3) of atmospheric interest and can be utilised also for isotope analysis (Li et al., 2013a; Li et al., 2013b; Chen et al., 2016).

Modern QCLs comprise a high sensitivity at ppb or even ppt (parts per trillion) levels of trace gas concentration (Faist et al., 1994; Curl et al., 2010). This high sensitivity is necessary when measuring trace gases, such as N_2O, which occur only at very low atmospheric concentrations (Curl et al., 2010). Operating a QCL at room temperature without cryogenic cooling is one of the main advantages of the technique and enables the application of QCL coupled to EC and/or chambers in field environments (Beck et al., 2002; Joly et al., 2008; Li et al., 2012). Eugster et al. (2007), Kroon et al. (2007), and Neftel et al. (2010) were among the first using QCL based EC systems in the field. The development of the QCL technique itself reaches back to the early nineties (Faist et al., 1994; Faist et al., 1995). Recent studies using QCL EC for campaign-based flux measurements of N_2O were conducted on intensively grazed pasture (Liáng et al., 2018) and cropland (Lognoul et al., 2019; Tallec et al., 2019) and add to a growing pool of research (see references in Brümmer et al. 2017). However, long-term F_{N2O} measurements using QCL EC across multiple years have remained scarce with F_{N2O} measurements from intensively grazed pastures being no exception. Utilising the QCL EC technique has only lately become a more commonly used routine (Table 2-1) (Fuchs et al., 2018; Cowan et al., 2020; Merbold et al., 2020).

2.3.2.3 Published nitrous oxide data from managed grasslands

The first studies reporting EC measured F_{N2O} from intensively managed grasslands have confirmed that these fluxes are highly site-specific and greatly dependent on the underlying management of the land (Neftel et al., 2010; Liáng et al., 2018). Management interventions such as tillage, fertilisation, grass cutting, and animal grazing were often associated with a high variability in resulting F_{N2O}, particularly when effects of these interventions overlapped (Fuchs et al., 2018; Merbold et al., 2020).

From the published studies, emission could be as low as < 1 kg N_2O-N ha^{-1} yr^{-1} (Hörtnagl and Wohlfahrt, 2014) when measured on a managed hay meadow or as high as 29 kg N_2O-N ha^{-1} yr^{-1} after restoration and fertilisation (Merbold et al., 2014). In comparison, EC measured emissions from intensively grazed dairy pastures in New Zealand were found to be 6.5 kg N_2O-N ha^{-1} yr^{-1} (Liáng et al., 2018). Grazing animals were not always a strong predictor for increased emissions and, based on differences in grazing intensity and overall farm practices, N_2O emissions can be lower with grazing, e.g. 1.5 kg N_2O-N ha^{-1} (nine months) from an extensively grazed Swiss pasture (Voglmeier et al., 2019) or at least similar to N_2O emissions from ungrazed but intensively managed soils (Kroon et al., 2010a; Fuchs et al., 2018). However, comparisons between F_{N2O} data collected from different sites using the EC technique have remained difficult. Multi-annual flux measurements are extremely scarce even if considering data from EC systems coupled to other fast-response analysers (e.g. tunable diode lasers) or large scale measurements based on other techniques (e.g. flux gradient), (Scanlon and Kiely, 2003; Phillips et al., 2007; Teh et al., 2011).

At present, EC data mainly originate from Europe and New Zealand and, as yet, these datasets hardly allow for comparisons between daily, seasonal and annual N_2O emissions from different farm management systems. Another reason for the inability of drawing thorough comparisons are persisting differences in measurement protocols, data processing, gap-filling, and reporting procedures when using EC for F_{N2O} measurements (Goodrich et al., 2021). Some standardised guidelines were discussed by Nemitz et al. (2018) and Giltrap et al. (2020), but more comprehensive work is needed to enable robust comparisons. Eddy covariance measurements presented in contribute to the understanding of N_2O exchange from intensively grazed pastures with results now allowing future comparisons to other northern and southern hemisphere pastoral systems (Makowski, 2019).

Table 2-1 Published studies using the eddy covariance technique coupled to a quantum cascade laser for the measurement of N_2O from intensively managed grasslands. The table distinguishes location, land use and management, duration of the research, average and range of measured N_2O fluxes (F_{N2O}), best quality data after filtering, mean annual air temperature (Temp.) and precipitation (Prec.). Suffix symbols are explained at the bottom of the table, † points at studies that included measurements of F_{N2O} from cattle-grazed land. The table adds to the reviews published by Nicolini et al. (2013) and Nemitz et al. (2018).

Reference	**Location** country	**Land use/ land management**	**Duration of study** [year, month, days]	**F_{N2O}** **min | max** total [kg N_2O-N ha^{-1}]	 half-hourly [nmol N_2O-N m^{-2} s^{-1}]	**Best quality data** [%]	**Temp.** [°C]	**Prec.** [mm]
Cowan et al., 2016	Scotland	**grassland**, managed: tilled, fertilised	2012, APR-SEP, 175	2.1_{PT} tilled 1.7_{PT} untilled	0.0 | 8.8	24 | 34	--	1191_{PM}
Cowan et al., 2020	United Kingdom	**grassland**, managed: sheep, urea ammonium nitrate (AN) fertilisation	2012, APR-SEP, 175 2016-18, APR-AUG, 632	0.6_{PM} urea 0.8_{PM} AN	<1.0 | 40.0	35	--	1191_{PM} 754_{PM}
Fuchs et al., 2018	Switzerland	**grassland**, managed: different swards, fertilised, forage production and harvested	2015, JAN-DEC, 365 2016, JAN-DEC, 366 2013-14, JAN-DEC, 365 preliminary measurements	4.1_{AT} control 1.9_{AT} clover 6.3_{AT}control 3.8_{AT} clover	>0.2 | $0.7_{PM, G}$	24 27 22 22	10.3_{AM} 9.7_{AM}	1029_{AM} 1202_{AM}
Hörtnagl et al., 2014 & 2018	Austria	**hay meadow**, managed	2010-12, 22 months	$0.7_{PT, G}$	-0.4 | 1.0_{G}	39	531_{PM}	6.6_{PM}
Kroon et al., 2007	Netherlands	**grassland**, managed: fertilised, harvesting	2006, AUG-NOV, 74	1.9_{PT}	-3.6 | 14.3	87	10.3_{PM}	870_{PM}
Kroon et al., 2010	Netherlands	**grassland**, managed: fertilised with manure and artificial, harvesting	2006, FEB, 7 2006-08, APR-OCT, 945	24.0_{AT}	--	48	11.1 11.1 10.6	767 1087 736
Liang et al., 2018 †	New Zealand	**grassland**, managed: fertilised, cattle grazed	2016-17, DEC-NOV, 365	6.5_{AT}	-1.9 | 11.3	37	16.2_{PM}	1758_{PM}
Merbold et al., 2014	Switzerland	**grassland**, managed: slurry, harvest, restoration	2012, JAN-DEC, 366	29.1_{AT}	-- | 70.0	--	9.56_{PM}	1023.5_{PM}

Merbold et al., 2020	Switzerland	**grassland**, managed: slurry, harvest, restoration	2012-2014	2-8–27.7$_{AT}$	normal 4–8, higher after restoration	62.07$_{G}$	9.1$_{AM}$	1151$_{AM}$
Neftel et al., 2007	Switzerland	**grassland**, managed: fertilised, AN and slurry application	2005, AUG-SEP, 61	--	-0.9|1.2$_{G}$	--	9$_{AM}$	1200$_{AM}$
Neftel et al., 2010	Switzerland	**grassland**, managed: tillage, fertilised, forage production and harvested	2008, JUN-SEP, 122	1.5$_{PT, G}$	-2.0|20.0$_{G}$	42	9$_{AM}$	1200$_{AM}$
Rannik et al., 2015 Shurpali et al., 2016	Finland	**grassland**, bioenergy: reed canary grass, fertilised	2011, APR-NOV, 215	2.8	0.07|0.8$_{PM}$	61.9	3.2$_{AM}$	612$_{AM}$
Voglmeier et al., 2019 †	Switzerland	**grassland**, managed: fertilised, cattle grazed, occasionally cut	2016, MAR-NOV, 198	1.5$_{PT}$	-1.5|28.8$_{G}$	31|36	8.7$_{AM}$	1075$_{AM}$
Wecking et al., 2020 †	New Zealand	**grassland**, managed: fertilised, cattle grazed	2017-18, MAR-FEB, 365	7.3$_{AT}$	-1.0|15.0	49	14.3$_{PM}$	1875$_{PM}$
Wolf et al., 2015 (isotopic characterisation)	Switzerland	**grassland**, managed: cattle and sheep grazed, mowing, slurry application	2013, MAY-SEP, 153	--	-1.0|5.0$_{PM}$	--	9.1$_{AM}$	1151$_{AM}$

Legend:

G	graphical extrapolation or calculation and unit conversion from known values
AM	annual mean
AT	annual cumulative total
PM	period mean
PT	period cumulative total
†	studies on grazed grassland

2.4 Indirect ways to quantify nitrous oxide emissions from soil

The upscaling of N_2O emissions from direct flux measurements to regional, national or even global scale estimates is useful for assessing the impact of changing farm management practices, climate and policies on yields and overall greenhouse gas emissions (Fuchs et al., 2020). Large scale estimates of N_2O emissions are determined either from 'bottom-up' inventories, with data commonly based on field measurements (i.e. chamber techniques) and derived emission factors (EFs), or 'top-down' modelling using atmospheric measurements and inversion models (Davidson and Kanter, 2014). A quantification of N_2O and other greenhouse gas emissions at the national scale is compulsory for many countries to meet international climate conventions and to develop robust mitigation strategies (Reay et al., 2012; Sutton et al., 2013). However, estimates based on the above approaches often still include relatively high uncertainties and therefore, can lead to confusion among policy decision makers and the general public with regard to the 'true' contribution of livestock farming to global N_2O emissions and radiative forcing (Herrero et al., 2011; Reisinger and Clark, 2018).

2.4.1 Bottom-up national inventories

Bottom-up inventories are based on the quantification of the relationship between known inputs of N_r and the associated increase or decrease in N_2O emissions, which is commonly referred to by emission factors (EFs) (Kelliher et al., 2014b). Emission factors are widely applied to quantify N_2O emission budgets and build the foundation for emission reporting at national and international scales (Reay et al., 2012). The methodology of using EFs in national inventories was introduced by the IPCC and broadly distinguishes three sub-categories: 1) Tier 1 universal EFs that can be combined with country-specific activity data (if available); 2) Tier 2 EFs that are derived from country-specific measurements and activity data; and 3) Tier 3 originating from direct measurements and process-based models (IPCC, 2006a). For agricultural soils, N_2O emissions and associated EFs are distinguished further into their source of origin: i.e. direct emissions, emissions from animal waste management systems, and indirect emissions from N_r exported from agricultural land through e.g., volatilisation or leaching (Nevison, 2000).

Most national and sub-national inventories employ Tier 1 and/or Tier 2 inventory approaches for estimating agricultural N_2O emissions whereas Tier 3 is rarely used (Reay et al., 2012). Testing a Tier 3 approach, Fuchs et al. (2020) recently reported that using a multi-model ensemble could reduce the error in estimated annual N_2O

emissions from a Swiss pasture by 41% compared to estimates derived from other national IPCC methods. More generally, Reay et al. (2012) found that uncertainties associated with estimated or modelled emissions were often related to insufficient measurements while using an adequate data foundation, in contrast, resulted in reasonably consistent estimates even at increasing scales (Del Grosso et al., 2008).

The IPCC Tier 1 and Tier 2 approaches for direct and indirect N_2O emissions from managed grassland soils differentiate five EFs that can be used either as default values (i.e. brackets below, units describe the percentage contribution of soil or applied nitrogen emitted as N_2O) or need to be defined by country-specific data (IPCC, 2019):

- EF_1 (1.0%) for N_2O emitted from synthetic fertiliser application, organic amendments, crop residues, and nitrogen mineralised due to the loss of SOC.
- EF_2 (1.6–9.5%) for N_2O emitted from drained organic soils. The range of EF_2 is wide depending on climate characteristics and vegetation zone (IPCC, 2013, 2014)
- $EF_{3,PRP}$ (0.4%) and $EF_{3,PRP,SO}$ (0.3%) for N_2O emitted from animal urine and dung deposited on pasture, range, and paddock land. Both EFs are distinguished by animal type: cattle/poultry/pigs ($EF_{3,PRP}$) and sheep/other animals ($EF_{3,PRP,SO}$).
- EF_4 (1.0%) for N_2O indirectly emitted from volatilisation and re-deposition.
- EF_5 (1.1%) for N_2O indirectly emitted from leaching and runoff.

The latest revision of IPCC inventory Tier 1 $EF_{3,PRP}$ for animal excreta nitrogen was announced in May 2019 with default $EF_{3,PRP}$ that were not only lower than in previous years (IPCC, 1996, 2006b) but disaggregated for wet (0.6%) and dry climates (0.2%) (IPCC, 2019). However, most comparisons between Tier 1 and Tier 2 EFs found that Tier 1 estimates were generally insufficient; while country-specific Tier 2 EFs allowed national inventories to better account for the variability of controlling factors on N_2O emissions (Lesschen et al., 2011; Cai and Akiyama, 2016; Krol et al., 2016a). Chadwick et al. (2018), for instance, reported a significantly lower combined $EF_{3,PRP}$ for urine and dung from grazing cattle (< 25%) than provided by the 2006 IPCC default values. Similarly, large site-specific differences between cattle urine (1.12%) and dung (0.16%) $EF_{3,PRP}$ were determined by Voglmeier et al. (2019), who proposed that including $EF_{3,PRP}$ disaggregated by excreta type might be useful to advance the Swiss greenhouse gas inventory.

The New Zealand greenhouse gas inventory for N_2O emissions from agricultural soils has adopted the differentiation of $EF_{3,PRP}$, in fact not only by applying disaggregated EFs for cattle urine and cattle dung but by favouring a combined approach of Tier 2 and Tier 1 default EFs (if country-specific data are not available) (Giltrap and Godfrey,

2016; MfE, 2019). Since signing the Kyoto Protocol in 1997, New Zealand has undertaken considerable efforts to define a country-specific emission profile for N_2O (de Klein et al., 2002; de Klein et al., 2003; Luo et al., 2007; van der Weerden et al., 2011; Luo et al., 2013a; Giltrap et al., 2014; Kelliher et al., 2014a; Kelliher et al., 2017; van der Weerden et al., 2020). Resulting from these research efforts, country-specific $EF_{3,PRP}$ were estimated to be 1.0% for cattle urine (Carran et al., 1995; Muller et al., 1995; de Klein et al., 2003), 0.25% for cattle dung (Luo et al., 2009) and an EF_1 of 0.59% for urea fertiliser (van der Weerden et al., 2016).

Lately, Luo et al. (2019) and van der Weerden et al. (2020) recommended to further distinguish these EFs by land topography and animal type with the refinements being adopted in the most recent inventory (MfE, 2020)[3]. Based on the 1990–2018 version of the New Zealand inventory, N_2O from agricultural soils contributed 8.9% to overall gross emissions (7,026.3 kt CO_2-equivalents), 18.6% to agricultural emissions and 92.5% to emissions from the agricultural soil category. This means that agricultural soils were the major contributor of domestic N_2O emissions in 2018 with emissions from animal excreta alone increasing by 30.7% (897.4 kt CO_2-equivalents) when compared with the reference year, i.e. 1990 (MfE, 2020). Key drivers for this increase were the growth of national dairy herd size and the accelerated application of synthetic nitrogen fertilisers, both of which were consistent with global trends (MfE, 2019). However, the uncertainty range of the above emission estimates was high, i.e. ± 55.3% (Kelliher et al., 2017; MfE, 2020).

An additional drawback of national N_2O inventories is that these do not currently account for background N_2O emissions (BNE); or only apply a single, but not compulsory, default value of 1 kg N_2O-N ha^{-1} yr^{-1} (Bouwman, 1996). Per se, BNE are defined as positive F_{N2O} from soils that received no external nitrogen inputs and soil management; but BNE are likely altered for agricultural and pastoral land (Bouwman, 1996; Kim et al., 2012). In intensively managed soils, BNE can result from the reactivation (i.e. mineralisation) of residual nitrogen accumulated in the soil after grazing, fertilisation or biologically fixed in plant residues. Any subsequent mineralisation of these residual nitrogen stocks can contribute to and result in BNE higher than in natural or less disturbed systems (Neftel et al., 2007; Gu et al., 2009; Aliyu et al., 2018). A meta-analysis by Kim et al. (2013) quantified global mean BNE

[3] Note: Results presented in thesis chapter 3 were based on the 1990–2017 New Zealand inventory guidelines. Revised $EF_{3,PRP}$ in the 1990–2018 version are 0.98% ($EF_{3,PRP-FLAT}$) and 0.33% ($EF_{3,PRP-STEEP}$) both for direct N_2O emissions from cattle urine, 0.12% ($EF_{3,DUNG}$), 1% (EF_1), and 0.59% (EF_{1-UREA}).

for agricultural land at 1.52 kg N_2O-N ha^{-1} yr^{-1} and, specifically, 1.8 kg N_2O-N ha^{-1} yr^{-1} for pastures. Testing different management scenarios on grazed pastures in Ireland, Rafique et al. (2011) found that about 61% of total N_2O emissions could be attributed to BNE. Past research also indicated the effect of soil type (mineral vs. organic) on BNE (Velthof and Oenema, 1997) alongside potential other influences e.g., sward composition, nitrogen fertiliser inputs and overall farm management (Ledgard et al., 2009; Fuchs et al., 2018).

2.4.2 Top-down global budgets

Based on atmospheric measurements and inversion models (Daniel et al., 2007; Syakila and Kroeze, 2011; Prather et al., 2012), top-down techniques are widely used to estimate greenhouse gas emissions at continental to global scales (Hirsch et al., 2006; Huang et al., 2008; Thompson et al., 2014). The top-down approach is recognised as an independent verification of bottom-up inventories and acknowledged by the IPCC (IPCC, 2006a, 2019). When applied at very large scales, top-down approaches can quantify reasonably realistic estimates of global emissions (Bergamaschi et al., 2014). However, the comparability between top-down and bottom-up estimates remains debated (Crutzen et al., 2008; Vuuren et al., 2011; Makowski, 2019).

Top-down EF for N_2O from agricultural land can range between 0.02 (2%) and 0.05 (5%) kg N_2O-N/kg N (Crutzen et al., 2008; Davidson, 2009; Smith et al., 2012). Estimates based on global atmospheric inversion frameworks determined a global N_2O EF of 2.3% ± 0.6% for the period 1998 to 2016 (Thompson et al., 2019). This EF was noticeably larger than a global EF (1.375%) defined by IPCC Tier 1 approach, suggesting that the relationship between N_2O emissions and high nitrogen inputs might be non-linear (Thompson et al., 2019). The non-linear response in this relationship likely related to the sporadic nature of the N_2O emission process and its high spatio-temporal variability. Field studies previously showed that a nonlinearity between N_2O emissions and high inputs of nitrogen can occur, whereas EFs are based on the assumption of a linear relationship (Rafique et al., 2011; Shcherbak et al., 2014). As a result, EFs might underestimate the actual increases in global N_2O emissions, particularly when nitrogen surpluses are not constant but change with time. The extent to which the discrepancy between top-down and bottom-up estimates might become relevant at large scales is therefore currently unknown (Thompson et al., 2019). A useful comparison of bottom-up and top-down global N_2O budgets was provided by Tian et al. (2016) and Tian et al. (2020) including a discussion about the strengths and weaknesses of the two approaches.

Finally, top-down estimates indicate that anthropogenic activities have doubled the amount of N_r available to the terrestrial biosphere since industrialisation, which led to increasing emissions from 10–12 Tg N_2O-N yr^{-1} before 1750 to ~17 Tg N_2O-N yr^{-1} in the last decade (Syakila and Kroeze, 2011; Ussiri and Rattan, 2012; Thompson et al., 2014). Following these top-down estimates, the change in the global N_2O budget was mainly associated with emissions from agricultural soils, i. e. 0.3-1.0 Tg N yr^{-1} in 1850 compared to 3.9-5.3 Tg N yr^{-1} in 2010 (Syakila and Kroeze, 2011; Tian et al., 2019). In contrast, the atmospheric sink-strength to remove surplus N_2O via photolytic reactions was determined 12.3 ± 2.5 Tg N yr^{-1} indicating that global N_2O emissions, at present, clearly outbalance the former equilibrium state between emission and atmospheric removal (Kroeze et al., 1999).

Chapter Three

Reconciling Annual Nitrous Oxide Emissions of an Intensively Grazed Dairy Pasture Determined by Eddy Covariance and Emission Factors

3.1 Abstract

Estimates of regional and national nitrous oxide (N_2O) emissions rely on emission factors (EFs) commonly derived from measurements using static chambers. These measurements can include high uncertainties and might obscure the quantification of N_2O fluxes (F_{N2O}). Advances in micrometeorological eddy covariance technique (EC) now allow direct measurements of F_{N2O} at the field scale. Here, we compared N_2O emissions calculated from site-specific EFs with F_{N2O} data derived from year-round EC measurements on an intensively grazed dairy pasture in the Waikato region, NZ. Annual N_2O emissions of 7.30 kg N_2O-N ha^{-1} yr^{-1} determined using gap-filled EC flux data were greater than N_2O estimates of 3.82 kg N_2O-N ha^{-1} yr^{-1} based on site-specific EFs for cattle urine (1.53%), cattle dung (0.24%) and urea fertiliser (0.16%). Likely reasons for this difference were that the EF approach did not take into account the seasonal variability of EFs, the effect of supplementary feed on cattle nitrogen (N) excretion and background N_2O emissions (BNE). Including calculated emissions from supplementary feed N (0.92 kg N_2O-N ha^{-1} yr^{-1}) and BNE (1.09 kg N_2O-N ha^{-1} yr^{-1}) increased annual EF-based emissions to 5.83 kg N_2O-N ha^{-1} yr^{-1}. The site-specific EFs were established in spring 2017 and may not have adequately represented summer, winter and particularly autumn N_2O emissions. The EF approach, therefore, did not fully account for the seasonal variability of F_{N2O} as measured by EC but, if quantified, could have led to further agreement between measurements. Using EC measurements to complement static chambers and EF approaches altered annual N_2O emissions estimates from intensively grazed pastoral land. Hence, we conclude that N_2O budgets derived from EFs need to better capture the effect of seasonal variability, supplementary feed and BNE.

3.2 Introduction

Nitrous oxide (N_2O) is a long-lived atmospheric trace gas with a global warming potential 265 times higher than carbon dioxide (CO_2) over a 100-year horizon (IPCC, 2013). Also, N_2O has been considered the primary ozone-depleting substance in the 21st century (Ravishankara et al., 2009). The concentration of N_2O in the atmosphere has steadily increased from a pre-industrial level of 270 ppb in 1750 to 329 ppb in 2017 (WMO, 2017). Globally, anthropogenic activities add 210 Tg of reactive nitrogen (N_r) per year to the terrestrial environment, promoting the emission of N_2O (Galloway et al., 2013). In pastoral agriculture, excess N_r enters the soil mainly through the application of synthetic N fertilisers and animal excreta. Both are important substrates for soil microbes that produce N_2O through either nitrification and/or denitrification (Luo et al., 2017). Soils under agricultural and pastoral land are considered the most dominant anthropogenic source of N_2O and have been estimated to contribute 3.8–6.8 Tg N_2O-N yr^{-1} to the total global N_2O emission budget (i.e. 18.0 Tg N_2O-N yr^{-1}) (Kroeze et al., 1999; Aliyu et al., 2018). International climate conventions require the reporting of national N_2O emissions in annual budgets that depend on a reliable quantification at large scale. However, the upscaling of N_2O emissions to regional and national scales or in other words, understanding the discrepancy between microbial-driven N_2O production in soils and measurements that capture the enormous range of spatiotemporal conditions under which N_2O is emitted, has remained challenging (Butterbach-Bahl et al., 2013). At the national scale, N_2O budgets commonly use emission factors (EFs) to quantify the amount of gaseous N_2O-N lost as a fraction of N inputs excluding background N_2O emissions (BNE) (De Klein et al., 2010; Kim et al., 2013). National EFs can be either default values recommended by the IPCC or are based on country-specific data (Giltrap and Godfrey, 2016). Research in New Zealand advanced the use of EFs from default to country-specific disaggregated values that distinguish different forms of N input, e.g., cattle urine and cattle dung, and were tested under different management practices, climates and soils (Luo and Kelliher, 2014). In 2017, N_2O emissions from the agricultural soil category contributed 10.6% (8,566 kt CO_2-equivalent) to the New Zealand gross emission profile. Agricultural soils were the major contributor of domestic N_2O emissions, with levels 28.1% (1,877 kt CO_2-equivalent) above the year 1990 (MfE, 2019). Key drivers for increasing N_2O emissions in New Zealand since 1990 were the growth of national dairy herd size by 89.6% and the accelerated application of synthetic N fertilisers (650%), which are consistent with global trends (MfE, 2019).

To date, static chamber measurements are most commonly used to derive EFs for N_2O and determine national greenhouse gas inventories both in New Zealand and elsewhere, with chamber making up more than 95% of all field N_2O flux (F_{N2O}) measurements (Rochette and Bertrand, 2008; Rochette, 2011; Lammirato et al., 2018). Static chambers are relatively easy to deploy, cost-efficient and provide valuable information for comparisons between different treatments by following standardised guidelines (Velthof et al., 1996; Jones et al., 2007; De Klein et al., 2015). Nonetheless, studies using static chambers measure F_{N2O} typically over a spatial area less than 1 m^2 per chamber and offer limited coverage with time (Rochette and Eriksen-Hamel, 2008; Jones et al., 2011). The continuous flux of soil N_2O to the atmosphere, therefore, is often not consistently captured, particularly in soils under highly intensified pastoral land where cattle urine and dung patches form spatially variable and dynamic emission hotspots (Luo et al., 2017). Chamber measurements also alter the soil environment once installed into the ground, introducing additional uncertainties in measured F_{N2O} (De Klein et al., 2015). Insufficient mixing in the chamber headspace, pressure differences that interfere with natural gas diffusion, and the assumption of a linear increase in headspace gas concentration during the sampling period are all potential sources of error that can lead to uncertainties in chamber derived EF estimates (Denmead, 2008; Christiansen et al., 2011; Chadwick et al., 2014). Due to the generally low spatial and temporal resolution of chamber measurements, these uncertainties can be as high as 50% (Smith and Dobbie, 2001; Zheng et al., 2004; Flechard et al., 2007). In 2016, the country-specific uncertainty range of EF estimates in New Zealand was ± 55.4% (Kelliher et al., 2017; MfE, 2018).

In the last two decades, eddy covariance (EC) has been the most commonly used technique to quantify the gaseous exchange of CO_2 and methane (CH_4) between soil and the atmosphere at ecosystem scales (i.e. 0.1–1 km^2) (Wang et al., 2013b). Only lately, measurements of N_2O using EC systems have become possible through the availability of fast and highly precise absorption spectrometers, such as continuous-wave quantum cascade lasers (QCL). This new generation of laser absorption spectrometers does not require liquid N cooling or frequent calibration, which previously limited the long-term deployment of other N_2O detectors (e.g. tunable diode lasers) in outdoor environments (Cowan et al., 2014a, 2015). The number of studies measuring F_{N2O} and indeed those of other N-species using QCL is currently increasing (Nicolini et al., 2013; Nemitz et al., 2018). Individual studies have been conducted e.g., over agricultural crops such as corn (Huang et al., 2014; Bureau et al.,

2017), maize (Tallec et al., 2019), cotton (Wang et al., 2013b), drained peatland (Zöll et al., 2016), managed grassland (Fuchs et al., 2018; Liáng et al., 2018; Voglmeier et al., 2019), and hay and fen meadows (Kroon et al., 2010; Hörtnagl and Wohlfahrt, 2014).

In this study, we aimed to compare annual N_2O emissions measured by EC to those estimated by default EFs and those derived from site-specific EFs based on measurements with static chambers. Due to resource constraints, we were only able to determine site-specific EFs during one season. Other studies have initially investigated the technical differences between the chamber and EC method (Jones et al., 2011; Wang et al., 2013b; Lucas-Moffat et al., 2018), but to our knowledge, a point to field scale comparison of N_2O emissions from intensively grazed land has only been conducted by Voglmeier et al. (2019) using a "fast-box" approach and QCL EC. Objectives of our study were to, therefore, 1) determine site-specific EFs for cattle urine, cattle dung and urea fertiliser; 2) calculate annual N_2O emissions using EC QCL; 3) investigate differences between the two methods and compare results from EC with emission estimates based on site-specific EFs for N_2O aligned to New Zealand greenhouse gas inventory methods.

3.3 Methods

3.3.1 Site and experiment description

This study was conducted on a commercially operating 199 ha dairy farm in the Waikato region, North Island, Aotearoa New Zealand. The experimental site had been under long-term dairy grazing for at least 80 years and was located on Troughton Farm, 3 km east of Waharoa (37.78 °S, 175.80 °E, 54 m a.s.l.). From 1981 to 2010, a climate station 13 km to the south-west of the farm recorded mean annual temperature and precipitation of 13.3°C and 1249 mm including occasional winter frosts (NIWA, 2015). The field site covered three paddocks (P51, P53 and P54) in the north of the farm that were relatively similar in size, previously described by Rutledge et al. (2017a) as 'NewRye' (Fig. 3-1). The 'NewRye' site underwent pasture renewal in 2013. Measurements made in autumn 2016 found the sward composition to be 65% perennial ryegrass (*Lolium perenne*) and 16% white clover (*Trifolium repens*) with the remainder comprising a mixture of herbs, weeds or bare ground (Rutledge et al., 2017a, 2017b). Drainage classes varied across soil types, all of which formed in rhyolitic and andesitic volcanic ash and rhyolitic alluvium (McLeod, 1992). A Mottled Orthic Allophanic soil (Te Puninga silt loam) was the dominant soil type containing a clay content of up to 20% in the topsoil and a soil carbon content of 9.3% (Hewitt, 2010).

The EC system monitoring F_{N2O} was located in the centre of P53 comprising a footprint of about 6–8 ha which was equal to the combined area of P51, P53 and P54. The prevailing wind direction varied throughout the year with a slight predominance of westerlies. In addition to flux measurements, a suite of soil and meteorological data had been continuously recorded since 2012. In this study, static chamber measurements were conducted from 4 October 2017 to 6 January 2018. Chamber plots were located to the west of the EC system in P54 (Fig. 3-1). Eddy covariance measurements covered twelve months, 1 March 2017 to 28 February 2018. The EC system operated continuously (except 5–30 July 2017 due to equipment failure) over these twelve months. The day of treatment application to the chamber plots on 4 October 2017 was synchronised with cattle grazing on P54 to allow later comparison between the chamber and EC fluxes measurements for the first 16 days after nitrogen application to the chamber plots.

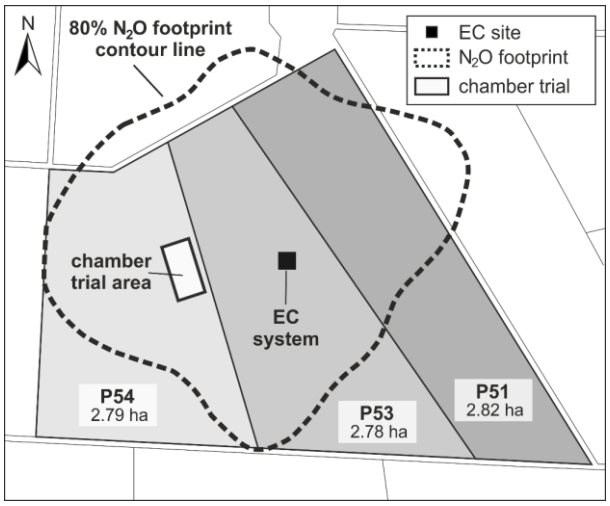

Figure 3-1 Map showing paddock 51, 53 and 54 at Troughton farm with the eddy covariance (EC) system (black square) located in the centre and the chamber trial (rectangle) to the west. The dashed line indicates the 80% contour of the EC fetch.

3.3.2 Farm management

The farm was rotationally grazed throughout the year. In the 2017–2018 milking season (June 2017 to May 2018) the farm was grazed by 478 Jersey cows with two milking herds. The overall stocking density averaged 2.4 cows ha^{-1} with cattle feeding on paddocks ranging in size from 2.5 to 3.5 ha. Supplementary feed from both imported and on-site sources was available year-round and was provided to the animals either on the feed pad or the research paddocks prior to or during grazing. Additional feed from outside the farm boundary accounted for 7% of cattle dry matter (DM) intake including dried distiller grains, grass silage, maize silage, hay and straw bales. Forage produced on-farm was provided in the form of pasture, grass silage and maize

silage. From 1 March 2017 to 28 February 2018, each paddock under the EC footprint experienced 14 grazing events equal to 11–13.5 grazing days. The instantaneous stocking density averaged 89 cows ha^{-1} but ranged from 65.7 cows ha^{-1} to as high as 407 cows ha^{-1} during short-term grazing of selective areas. Fertiliser was applied on five occasions: on 9 March 2017 (22 kg N ha^{-1}), 29 April 2017 (9 kg N ha^{-1}), 12 June 2017 (3 kg N ha^{-1}), 3 August 2017 (3 kg N ha^{-1}) and 1 December 2017 (3 kg N ha^{-1}). By using site-specific data of pasture and supplementary DM and N intake, the calculated total N load of cattle urine and dung was 284 kg N ha^{-1} yr^{-1} and 140 kg N ha^{-1} yr^{-1}, respectively. The farm management applied was considered typical for the Waikato region, with day to day management decisions made by the farmer.

Table 3-1 Chronology of static chamber measurements to derive site-specific N_2O EFs.

Date	Activity
4-Sep-17	Fencing-off
15-Sep-17	Mowing
21-Sep-17	Implementation of chamber collars into the soil
28-Sep-17	Gas and soil sampling – day 0
2-Oct-17	Urine collection at morning milking, 5-8 AM
3-Oct-17	Dung collection from P54
	Mowing
4-Oct-17	Treatment application to chamber and soil plots
	Gas and soil sampling – day 1
	Grazing on P54
5-Oct-17	Gas and soil sampling – day 2
7-Oct-17	Gas and soil sampling – day 3
9-Oct-17	Gas and soil sampling – day 4
11-Oct-17	Gas and soil sampling – day 5
13-Oct-17	Gas and soil sampling – day 6
17-Oct-17	Gas and soil sampling – day 7
20-Oct-17	Gas and soil sampling – day 8
24-Oct-17	Gas and soil sampling – day 9
27-Oct-17	Gas and soil sampling – day 10
30-Oct-17	Gas and soil sampling – day 11
	Mowing
2-Nov-17	Gas and soil sampling – day 12
9-Nov-17	Gas and soil sampling – day 13
15-Nov-17	Gas and soil sampling – day 14
21-Nov-17	Gas and soil sampling – day 15
	Mowing
30-Nov-17	Gas and soil sampling – day 16
13-Dec-17	Gas and soil sampling – day 17
6-Jan-18	Gas and soil sampling – day 18
24-Jan-18	Trial finished

3.3.3 Static chamber measurements

3.3.3.1 Flux measurement and calculation

The chamber trial for measuring F_{N2O} comprised a randomised block design where urine, dung and urea fertiliser treatments were applied to circular plots, i.e. the chamber base, and replicated five times. Adjacent to the circular chamber plots, a separate area (1 m × 1 m) was established to collect soil samples for subsequent laboratory analyses of soil moisture and soil mineral N contents. Chamber and associated soil plots experienced the same treatment application, i.e. the N loading of the soil plots did not differ from that applied to the chamber bases. Compared with the chamber bases, however, soil plots received a mixture of real and artificial cow urine to the ratio of 1:2.28. The treatment application followed procedures described by Luo et al. (2008b). All cattle excreta used in the chamber experiment originated from the study farm. Real dairy cow urine was collected during morning milking whereas dairy cow dung was collected from P54. Excreta were stored at 4°C overnight (Haynes and Williams, 1993) and applied to the chamber plots at actual N loading rates of 540 kg N ha^{-1} (urine) and 1,133 kg N ha^{-1} (dung) on 4 October 2017. Urea fertiliser was applied at 50 kg N ha^{-1} which compared well with the fertilisation practices of the farm. Control plots did not receive any applied N or other additions.

Nitrous oxide flux measurements were made by using a standardised chamber technique (De Klein et al., 2003, 2015). Gas sampling was carried out between 10 AM and 12 PM (NZDT) to obtain representative F_{N2O} for each sampling occasion (van der Weerden et al., 2013). Chamber sampling took place on 19 days during a three months measurement period (Table 3-1). The trial area had been excluded from cattle grazing one month prior to sampling. Bases for each chamber were inserted 50–100 mm into the soil one week before treatment application.

During sampling, PVC lids were fitted to water-filled base channels to provide a gas-tight seal over a 10 L headspace volume. Gas samples were taken from the chamber headspace during 60 min at four times t_0, t_{20}, t_{40} and t_{60} on all sampling days except sampling days 16 and 17 (t_0 and t_{60} only). Headspace samples were extracted through a sampling port by using a 50 mL plastic syringe (Terumo Corp., Tokyo, Japan) with 15 mL of each sample being injected into a pre-evacuated, septum-sealed, screw-capped 5.6 mL glass vial (Exetainer, Labco Ltd., High Wycombe, UK). Glass vials were over-pressurised to maintain sample integrity until the gas samples were analysed for N_2O concentration by automated gas chromatography (GC) at the National Centre

for Nitrous Oxide Measurement, Lincoln University, NZ. Sample analysis was performed with a SRI 8610 GC (SRI Instruments, Torrance, CA, USA) and a Shimadzu GC-17a (Shimadzu Corp., Kyoto, Japan) equipped with a ^{63}Ni-electron capture detector and oxygen-free N as the carrier gas at a detection limit of 0.1 μL L^{-1} (De Klein et al., 2003; Luo et al., 2008b). As linearity was confirmed, the hourly flux in mg N_2O-N m^{-2} h^{-1} ($F_{chamber}$) was calculated using linear regression from the increase in chamber headspace N_2O concentration between time t_0 and time t_{60} (van der Weerden et al., 2011):

$$F_{chamber} = \frac{\Delta N_2O}{\Delta T} \times \frac{M}{Vm} \times \frac{V}{A} \qquad \text{(Eq. 3-1)}$$

where ΔN_2O is the increase in headspace N_2O concentration (μL L^{-1}) over time, ΔT is the enclosure period (h); M is the molar weight of nitrogen in N_2O; Vm is the molar volume of gas (L mol^{-1}) at the sampling temperature recorded at each occasion; V is the headspace volume (m^3) and A is the area (m^2) covered by the chamber base.

3.3.3.2 Calculation of emission factors

The hourly $F_{chamber}$ values from Eq. 3-1 were integrated over three months to quantify the total amount of N_2O-N emitted from each treatment. Subsequently, the corresponding N_2O EFs were calculated by dividing treatment-induced emissions by the total amount of treatment N applied to each chamber:

$$EF = \frac{N_2O\text{-}N\ total\ (treatment) - N_2O\text{-}N\ total\ (control)}{N\ applied\ (treatment)} \qquad \text{(Eq. 3-2)}$$

where EF is the emission factor for N_2O-N emitted in kg per kg N ha^{-1} applied (expressed as a percentage, i.e. EF * 100); $N_2O\text{-}N\ total\ (treatment)$ and $N_2O\text{-}N\ total\ (control)$ are the cumulative N_2O emissions from a specified treatment (kg N ha^{-1}) and the control (kg N ha^{-1}); and $N\ applied$ (treatment) refers to the initial amount of N applied to each specified treatment (kg N ha^{-1}).

3.3.3.3 Upscaling of chamber treatment fluxes to paddock scale fluxes

A direct comparison between static chamber ($F_{chamber}$) and EC (F_{EC}) flux measurements was possible for the first 16 days of the chamber trial, as grazing of the experimental paddocks (grazing event 8) occurred concurrently with the application of the chamber treatments. To enable this comparison, the fluxes derived from static chamber measurements needed to be upscaled to the paddock scale by taking into account the area of urine and dung deposition in the grazed paddocks. Upscaled and area-weighted chamber fluxes ($F_{pad,chamber}$) were calculated following:

$$\begin{aligned} F_{pad,chamber} = {} & Area_{urine} \times F_{chamber,urine} + \\ & Area_{dung} \times F_{chamber,dung} + \\ & Area_{remain} \times F_{chamber,control} \end{aligned} \quad \text{(Eq. 3-3)}$$

where $Area_{urine}$ was the proportion of the paddock covered by urine; $Area_{dung}$ was the proportion of the paddock covered by dung; and $Area_{remain}$ was the remaining proportion of the paddock without urine or dung deposition (i.e. $1 - (Area_{urine} + Area_{dung})$). As previously calculated (Eq. 3-1), $F_{chamber,urine}$, $F_{chamber,dung}$, and $F_{chamber,control}$ were the individual, chamber derived N_2O fluxes for urine and dung treatments and the control, respectively. $Area_{urine}$ and $Area_{dung}$ were quantified using the generic equation:

$$Area_x = \frac{Event_x \times Herd\ size \times Area_{patch,x} \times Grazing\ duration}{Area_{paddock}} \quad \text{(Eq. 3-4)}$$

where x relates to either urine or dung patches. $Event_x$ was the number of urine or dung deposition events per cow specified for Jersey cows at 8.7 urinations and 10.9 defecations per grazing day (White et al., 2001); *Herd size* quantified the number of cows grazing; $Area_{patch,x}$ was the wetted surface area of each deposition event with 0.20 m^2 for urine (Haynes and Williams, 1993) and 0.12 m^2 for dung (Wilkinson and Lowrey, 1973). *Grazing duration* described the time cattle spent on the paddock grazing (in days), and $Area_{paddock}$ was the area of the paddocks grazed. Finally, to compare $F_{pad,chamber}$ to F_{EC}, units were converted from mg N_2O-N m^{-2} h^{-1} to nmol N_2O m^{-2} s^{-1}. Fertilisation effects on $F_{pad,chamber}$ were not considered since the experimental paddocks did not receive N fertiliser during the grazing event of interest.

3.3.4 Additional measurements at chamber site

On each day of chamber sampling, soil cores (75 mm depth, 25 mm diameter) were taken from all soil plots to determine soil moisture and soil mineral nitrogen (N_{min}) contents, i.e. NH_4^+ and NO_3^-. Soil samples were replicated three times per plot and sampling day. Field-moist soil samples were sieved to 4 mm and extracted in 0.5 M K_2SO_4 (ratio 1:5 of field-moist soil to K_2SO_4) for 1 h within the first 24 h post sampling. Subsequently, soil solutions were filtered (Whatman No. 42 filter paper) and filtrates were frozen until NH_4^+ and NO_3^- analysis after Mulvaney (1996) was conducted using a Skalar SAN++ segmented flow analyser (Skalar Analytical B.V., Breda, Netherlands). Aliquots of all soil samples were dried at 105°C for 24 h to determine the soil's gravimetric water content (GWC). The site-specific bulk density of the soil measured at the chamber site was 0.73 g cm^{-3} and used to calculate the volumetric water content of the soil (VWC). The soil particle density was 2.65 g cm^{-3} (Danielson and Sutherland, 1986). The water-filled pore space (WFPS) of the soil was calculated by dividing VWC

by total porosity (Linn and Doran, 1984). Further analysis included the measurement of soil and air temperature in the chamber headspace at each sampling occasion. Additionally, the N content of the pasture sward was analysed (Eurofins, NZ).

3.3.5 Emission budgeting

The estimation of total annual N_2O emissions from chamber data was conducted in two steps: 1) site-specific data of N retained in cattle feed, cattle milk and cattle excreta were obtained either from direct measurements (biomass growth, feed and milk N content) or indirectly calculated using a mass balance approach; 2) the N input data were fed into equations based on the greenhouse gas inventory for N_2O in New Zealand (Gibbs, 2018). All calculations were based on the paddock area comprised in the EC footprint (i.e. P51, P53, P54) and included the use of site-specific EFs to quantify the total N_2O emitted. Finally, results using site-specific EFs were compared to emissions calculated from national EFs following the recommendations of the IPCC (De Klein et al., 2006; Gibbs, 2018).

For each paddock, the amount of urine and dung excreted was defined as N_{ex} and calculated for each grazing event as:

$$N_{ex} = N_i - (N_{rm} + N_{lwg}) \quad \text{(Eq. 3-5)}$$

where N_{ex} is the total amount of N excreted (kg N) and N_i the N intake (kg N) calculated as the product of total DM intake (kg N) and feed N content of either pasture sward or supplementary feed. N_{rm}, the amount of N secreted in milk (kg N), was calculated as the product of daily milking yield (kg N) and N content of the milk. N_{lwg} was the N retained in livestock weight gain (kg N), here assumed zero since the weight of dairy cattle was expected to remain relatively constant for twelve months.

Following Luo and Kelliher (2014), the amount of N excreted (N_{ex}) was further partitioned into urine and dung components:

$$N_u = \left(10.5 \times \frac{Feed_N}{100} + 0.34\right) \times N_{ex} \quad \text{(Eq. 3-6)}$$

where N_u is the amount of N excreted in urine (kg N) and $Feed_N$ the N content of feed consumed by the animals expressed as a percentage of total DM intake from pasture and supplementary feed. N_{ex} was the N excretion calculated from Eq. 3-5 in kg N per grazing event. The N excretion in faeces (N_f), i.e. dung, was derived from subtracting N_u from N_{ex}. Subsequently, the final amount of direct N_2O emitted (kg N_2O) was calculated from using the excreta data partitioned in N_u and N_f following:

$$N_2O\ direct_N = \frac{44}{28} \times N \times EF \quad \text{(Eq. 3-7)}$$

where N is the amount of N applied to the soil (kg N) in form of either urine (N_u), dung (N_f) or urea fertiliser, EF is the emission factor described by site-specific or IPCC default values for each of urine, dung or urea fertiliser in kg N_2O-N per kg N applied, and $\frac{44}{28}$ is the molecular factor to convert kg N to kg N_2O.

In contrast to the New Zealand N_2O inventory guidelines, we accounted for the effect of supplementary feed on cattle diet and cattle excretion in the above equations by considering feed specific nitrogen intake data (Table 3-2). The inventory considers supplementary feed intake only indirectly, i.e. by acknowledging the metabolic energy requirements of dairy cattle, which are exclusively based on the intake of a pasture ryegrass-clover diet (Gibbs, 2018).

Table 3-2 Averaged stocking densities and total dry matter (DM) and nitrogen (N) intake per ha from pasture (P) and supplementary feed (S) for each grazing cycle across the EC footprint, i.e. paddock 51, 53 and 54. Grazing of individual paddocks took place over multiple days. 'S N waste' describes the amount of supplementary feed not ingested by cattle and, therefore, excluded from subsequent calculations. All data provided below based on site and farm specific measurements and records. The asterisk indicates the start of the static chamber trial.

graz. event [no.]	**start date**	**end date**	stocking density [cows ha^{-1}]	**P** DM eaten [kg ha^{-1}]	**S** DM eaten [kg ha^{-1}]	**P** N eaten [kg ha^{-1}]	**S** N eaten [kg ha^{-1}]	**S** N waste [kg ha^{-1}]
1	1-Mar-17	4-Mar-17	78.3	1,378	499	41	17	-
2	26-Mar-17	30-Mar-17	80.1	1,138	225	41	6	-
3	17-Apr-17	19-Apr-17	78.0	957	249	35	4	-
4	19-May-17	21-May-17	73.7	796	582	29	11	0.3
5	27-Jun-17	5-Jul-17	61.0	1,460	1,018	53	19	0.6
6	13-Aug-17	17-Aug-17	109.2	903	773	33	18	0.3
7	8-Sep-17	12-Sep-17	78.0	882	525	32	11	-
*8	2-Oct-17	4-Oct-17	76.0	958	346	35	7	-
9	23-Oct-17	25-Oct-17	82.6	1,023	349	37	6	-
10	15-Nov-17	17-Nov-17	65.2	796	204	29	2	-
11	7-Dec-17	9-Dec-17	73.5	1,389	224	50	3	-
12	30-Dec-17	1-Jan-18	87.8	967	296	35	5	-
13	15-Jan-18	17-Jan-18	58.4	702	464	25	8	0.5
14	19-Feb-18	21-Feb-18	112.7	2,358	826	85	19	-
				15,466	**6,579**	**559**	**134**	**1.6**

In our study, the intake of supplementary forages was included in addition to pasture and quantified in variable Ni (Eq. 3-5). Once N_2O emissions were calculated for each grazing event (n = 14), the sum was then used to obtain annual totals. All calculations were adjusted to the actual time dairy cattle spent on the paddocks of interest (P51, P53, P54) to avoid overestimation of N excretion or incorporation of N_2O emissions

that originated from faeces deposited on areas outside the experimental site. Background N_2O emissions (BNE) were measured at the untreated control sites of the chamber trial and were upscaled to an annual total by multiplying the flux average of 3.0 g N_2O-N ha^{-1} d^{-1} by 365 days. However, BNE determined at chamber control sites were not directly comparable to those measured by EC. The EC footprint regularly experienced new inputs of N_r through cattle excretion and fertilisation, which likely increased BNE, whereas chamber sites did not receive multiple N applications. Due to resource constraints, site-specific EFs were only determined for the spring season 2017 with the term 'season' referring to calendar seasons of the Southern Hemisphere.

3.3.6 Eddy covariance flux measurement and data collection

A detailed description of the experimental set-up at Troughton farm site was provided by Liáng et al. (2018). In brief, the EC system comprised a 3D sonic anemometer (CSAT3B; Campbell Scientific Instruments (CSI), Logan, UT, USA) and a continuous-wave quantum cascade laser absorption spectrometer (CW-QCLAS; Aerodyne Research Inc., Billerica, MA, USA). Measurements of atmospheric N_2O, CH_4 and water vapour were made at 2 m height and 10 Hz frequency. The airflow from the sampling inlet was controlled by a dry scroll vacuum pump (XDS35i, Edwards, West Sussex, UK), run through a heated, 6.1 m long sampling line at a normal flow rate of 15 L min^{-1} into an insulated enclosure box. The QCL operated at a stable temperature inside the enclosure of either 30°C in winter and 32°C in summertime ± 0.1°C. Routine maintenance of the EC system was conducted monthly, including standard gas check-ups and replacement of the 0.45 μm PTFE membrane filter (ThermoFisher Scientific, NZ) positioned near the air inlet of the sampling line. Before further processing, raw QCL data were automatically stored on the internal QCL computer. To avoid time lags, data logger clocks and QCL times were synchronised every half hour and aligned with a local network time protocol server (NTP, 1.nz.pool.ntp.org) (Felber et al., 2015; Liáng et al., 2018). Environmental parameters at the EC site were measured by various sensors recording air temperature and relative humidity (HMP155; Vaisala, Helsinki, Finland), wind velocity, soil temperature, soil VWC at 5 cm depth (CR6 CSAT3B, CS107 and CS616; CSI, Logan, UT, USA) and rainfall (TB5; Hydrological Services). Data loggers (CR3000 and CR1000; CSI, Logan, UT, USA) kept a continuous record with data stored in 30-min intervals. The soil WFPS was calculated as previously described from VWC and soil porosity (Section 3.3.4) (Liáng et al., 2018).

3.3.7 Processing of flux data

The 30-min ecosystem flux of N_2O (F_{EC}) was determined using the EC method (Baldocchi et al., 1988; Eugster and Merbold, 2015). The processing of F_{EC} data followed standardised guidelines provided by Nemitz et al. (2018). Clock drifts between wind components recorded from the CSAT3B and any N_2O mixing ratio measured by QCL were identified, and raw data of wind velocities and trace gas concentrations were re-aligned before F_{EC} calculation using MatLab R2017a (The MathWorks Inc., Natick, MA, USA). The flux processing was executed in EddyPro 6.2.2 (LI-COR Inc., Lincoln, NE, USA), with raw data screened for spikes, drop-outs, values above or below absolute limits, and insufficient amplitude resolution, skewness and kurtosis, discontinuities, and steadiness of horizontal wind (Vickers and Mahrt, 1997). Block averaging was used to detrend the data, and time lags between the vertical wind speed and N_2O concentration were determined using covariance maximisation with limits determined from the automated time lag optimisation routine within EddyPro. Spectral corrections used the Moncrieff et al. (1997) fully analytical approach for high-pass filtering, and the Fratini et al. (2012) in-situ/analytic method for low-pass filtering. However, the raw N_2O signal included considerable noise levels and, thus, only 30-min F_{EC} with high signal-to-noise ratios were used to determine cut-off frequencies. Finally, spectral losses caused by instrument separation were corrected following Horst and Lenschow (2009).

A four-step quality control protocol antedated the post-processing of the 30-min F_{EC} data: 1) out-of-range values greater than 20 nmol N_2O m^{-2} s^{-1} and smaller than -1.0 nmol N_2O m^{-2} s^{-1} were rejected (Neftel et al., 2010; Liáng et al., 2018); 2) a 0-1-2 flag system following Mauder and Foken (2006) was used and only fluxes in the flag 0 (best quality fluxes) and flag 1 (fluxes suitable for annual budgets) category were considered; 3) a u_* threshold of 0.11 m s^{-1} of the standard deviation of vertical wind speed was applied to remove measurements under low turbulence conditions (Acevedo et al., 2009; Hunt et al., 2016; Rutledge et al., 2017a); and 4) flux measurements during periods of instrument maintenance were discarded as well as those sourced from the lee side of the EC tower. After filtering, 49% of all 30-min F_{EC} remained as best quality data including 43 individual negative 30-min F_{EC}. There was no strong reason for rejecting these fluxes and, hence, negative F_{EC} were retained in the data set (Chapuis-Lardy et al., 2007; Cowan et al., 2014b).

The calculation of flux cumulative sums used gap-filled F_{EC} data. Several gap-filling methods were applied, and for gap-filling only, the data were separated into two

subsets – (1) pulse F_{EC} during emission events, and (2) F_{EC} of lower magnitude in the background of pulse emissions. Firstly, gaps in the pulse F_{EC} subset were filled by linear interpolation. Gap-filling of the background F_{EC} data set was a several step process: (i) linear interpolation was used for F_{EC} where the gaps were three hours or less duration; (ii) gaps from greater two hours to three days were filled using mean diurnal variation that comprised a standard window length of three days; (iii) during the long gap from 5 to 30 July 2017 (instrument failure) F_{EC} were extrapolated from multiple linear regression between F_{EC}, soil temperature and WFPS (Taylor et al., 2017; Liáng et al., 2018); (iv), where possible remaining gaps were filled using daily means; and (v) any remaining gaps utilised linear interpolation (Nemitz et al., 2018).

3.4 Results

3.4.1 Environmental conditions

The daily mean of the minimum and maximum air temperature ranged from 2.0°C to 23.5°C. The mean air temperature of 14.3°C during the measurement period was higher than the 30-year annual average (13.3°C) measured at a nearby weather station from 1981 to 2010 (NIWA, 2015).

The total precipitation was 1875 mm with nearly half of the amount (871 mm) accumulating during autumn. Other seasons during the time of interest received relatively equal amounts of rainfall ranging from 310 to 340 mm season^{-1}. The lowest monthly cumulative rainfall was measured in December 2017 of just 13.7 mm. However, the amount of annual rainfall received was overall 50% higher than the long-term average (1249 mm yr^{-1}) (NIWA, 2015). Seasonal changes in precipitation corresponded well with the WFPS of the soil, which was particularly dynamic in autumn (Fig. 3-2a). Chamber measurements took place in the seasonal transition from moist spring to dry summer, 28 September 2017 to 6 January 2018. The mean daily air temperature during this time increased from 11.5°C to 21°C whereas the soil WFPS dropped from an initial > 80% to < 40%.

3.4.2 Chamber measurements

3.4.2.1 Soil variables

The application of urine, dung and urea fertiliser treatments to the soil had an immediate effect on soil NH_4^+ levels. Soil NH_4^+ for urine and fertiliser treatments peaked on the day of treatment application at 317 kg NH_4^+ ha^{-1} and 45 kg NH_4^+ ha^{-1}, respectively.

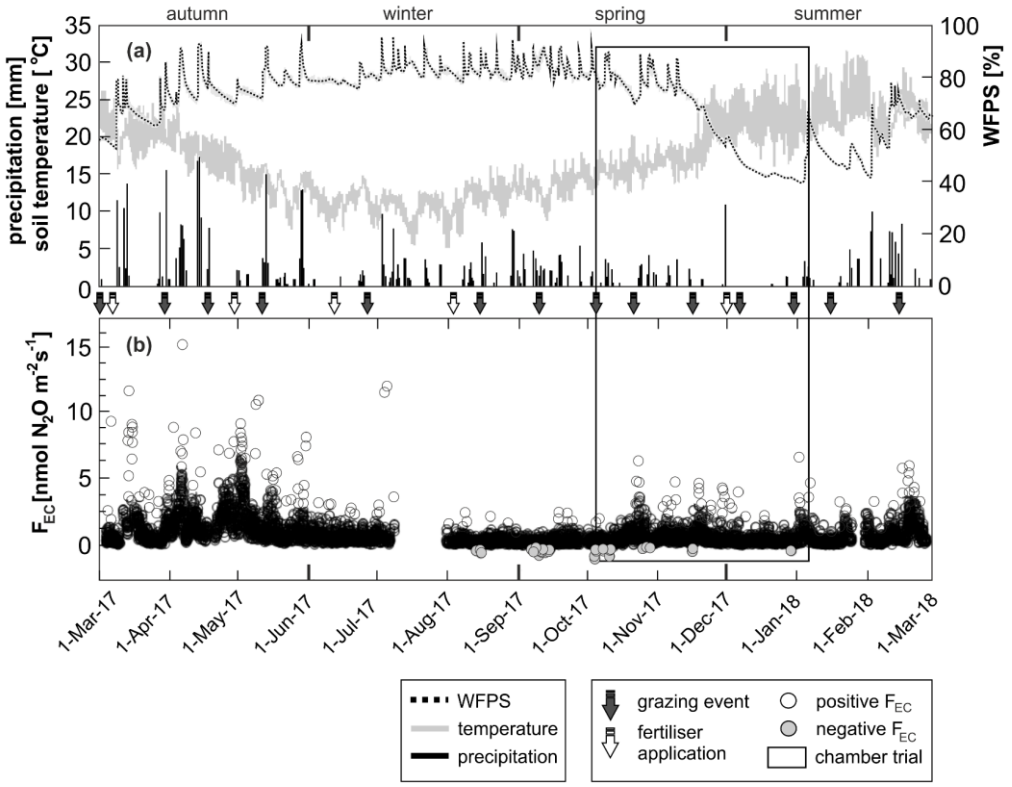

Figure 3-2 Environmental data (panel a) and associated eddy covariance N_2O fluxes (F_{EC}) (panel b) measured from 1 March 2017 to 28 February 2018. Illustrated are the soil temperature in 5 cm depth (grey line), precipitation (black bars) and soil WFPS (dotted line). Averaged 30-min values for positive F_{EC} are depicted as white circles whereas negative F_{EC} are represented as grey circles. Arrows indicate the addition of N originating either from cattle grazing (dark arrows) or fertiliser application (white arrows). The frame overlapping panel (a) and (b) highlights the time during which static chamber measurements were conducted.

Dung NH_4^+ generally remained lower reaching 9.6 kg NH_4^+ ha^{-1}, 13 days after application. Ammonium returned to background levels (4.1 kg NH_4^+ ha^{-1}) on day 16 for dung and fertiliser treatments and day 29 after application of cattle urine. Soil NO_3^- did not increase until 13 days after treatment application. However, a peak of NO_3^- in plots treated with urine occurred on 20 October (79.5 kg NO_3^- ha^{-1}). Soil NO_3^- stayed elevated for up to two months after urine and dung application. Apart from an initial increase of NH_4^+ on the day of application (45.3 kg NH_4^+ ha^{-1}), urea fertiliser did not noticeably affect soil NH_4^+ and NO_3^- which remained similar to control levels averaging at 4.1 kg NH_4^+ ha^{-1} and 2.5 kg NO_3^- ha^{-1}. The soil WFPS was relatively constant determined at values of around 80% or slightly below for the first two weeks after treatment application.

On 20 October, the WFPS dropped initially to 70% before showing a short, subsequent increase. Drier conditions led the WFPS of the soil to decrease at the end of November 2017. The lowest WFPS of 23% and 34.4% for sites treated with urine and dung, respectively, was measured in mid-December 2017 (Fig. 3-3b).

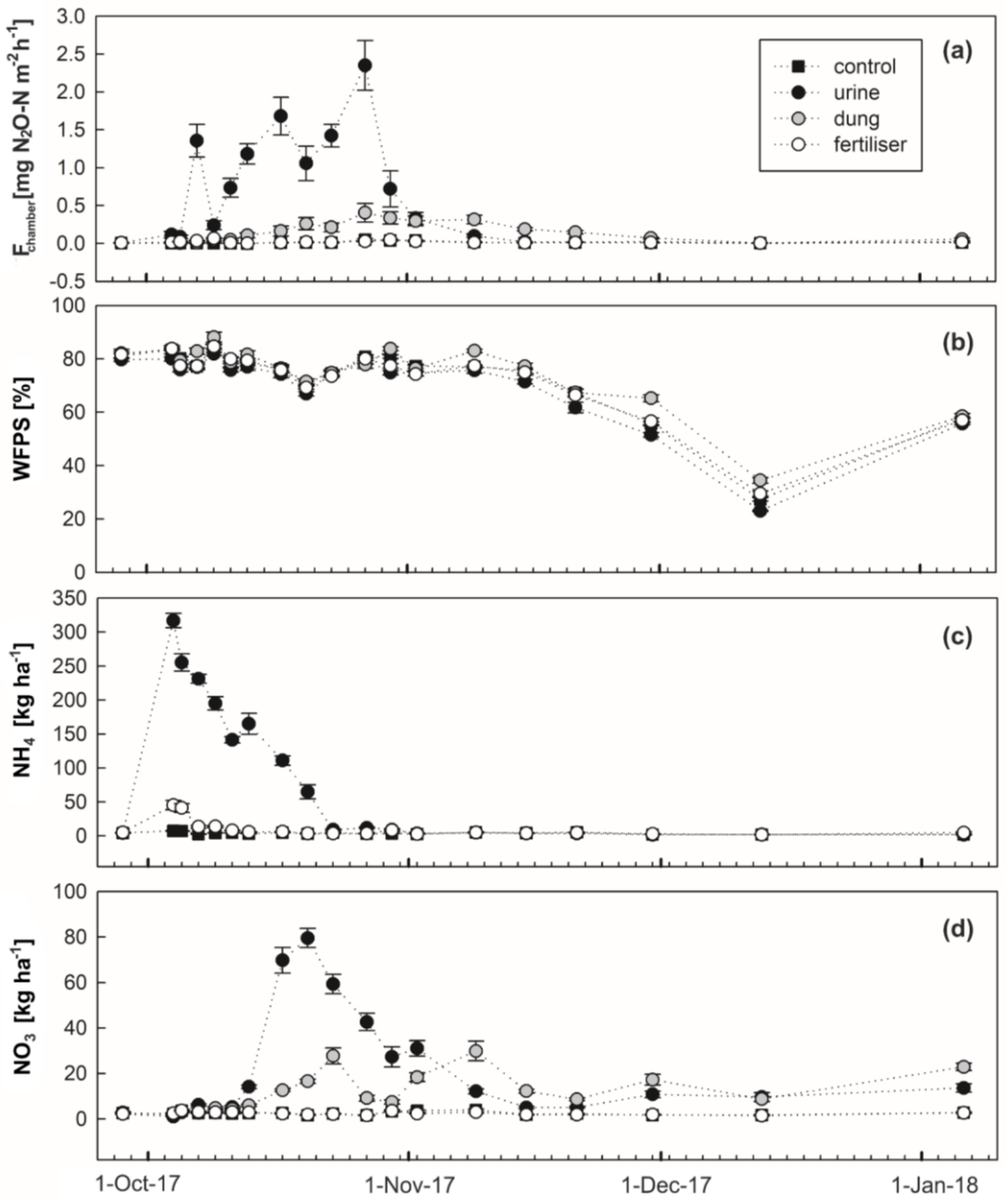

Figure 3-3 Data received from measurements at static chamber and soil plots (4 October 2017 and 6 January 2018) for (a) flux N_2O (Fchamber), (b) soil WFPS, (c) soil NH_4^+ and (d) soil NO_3^-. Results from measurements undertaken before treatment application on 29 September 2017 were included in the panels as a reference. Error bars illustrate the standard error of the mean (SEM) across replicates. Symbols distinguish control (black square), urine (black circle), dung (grey circle) and urea fertiliser (white circle) treatments.

3.4.2.2 Nitrous oxide fluxes from static chambers

$F_{chamber}$ determined by static chambers corresponded closely with soil moisture conditions and the type of treatment applied. Maximum pulse $F_{chamber}$ were measured on 27 October, 23 days after treatment application, from both urine (563.7 g N_2O-N ha^{-1} d^{-1}) and dung (97.1 g N_2O-N ha^{-1} d^{-1}) plots. On this day, $F_{chamber}$ coincided with elevated soil NO_3^- but were also associated with a rain event of 31.6 mm which triggered control sites to emit around four times more N_2O than the mean background N_2O emissions (BNE) quantified at 3.0 g N_2O-N ha^{-1} d^{-1}. Depending on underlying environmental factors, $F_{chamber}$ measured at the chamber control sites generally ranged from 0.1–11.8 g N_2O-N ha^{-1} d^{-1}. Urea fertilisation showed an immediate but very low $F_{chamber}$ response of 16.3 g N_2O-N ha^{-1} d^{-1} five days after treatment application. With the ongoing transformation from urine-N to readily available forms of NH_4^+ and NO_3^-, urine plots emitted two further $F_{chamber}$ pulses (7 and 17 October) before $F_{chamber}$ eventually returned to control levels. Cattle dung applied to the soil caused a delayed response of positive $F_{chamber}$ that decreased to initial levels at the end of the measurement period (Fig. 3-3a).

3.4.2.3 Site-specific emission factors

Static chamber measurements with N application in spring 2017 resulted in site-specific EFs of 1.53% ± 0.18 for urine (mean ± SEM), 0.24% ± 0.10 for dung and 0.16% ± 0.13 for urea fertiliser (Table 3-3). Daily $F_{chamber}$ measured across replicates of the same treatment were highly variable including a noticeable SEM (Fig. 3-3a).

Table 3-3 Total N_2O-N emitted in kg per ha^{-1} from static chambers over three months, 4 October 2017 to 6 January 2018. The arithmetic mean and standard error of the mean (SEM) are shown for each of the specified treatments and the control. Emission factors (EF) derived from chamber measurements and associated SEM are provided at the bottom of the table.

	N_2O emitted in kg N ha^{-1}			
rep.	control	urine	dung	fertiliser
1	0.26	9.91	1.84	0.43
2	0.31	11.00	3.79	0.56
3	0.43	5.90	1.37	0.29
4	0.25	6.71	0.92	0.33
5	0.17	9.36	6.98	0.23
mean	0.28	8.57	2.98	0.37
SEM	0.04	0.87	1.00	0.05
EF (%)	-	**1.53**	**0.24**	**0.16**
EF SEM	-	**0.18**	**0.10**	**0.13**

3.4.3 Eddy covariance measurements

Eddy covariance measurements showed a clear seasonal pattern. Distinct short-term F_{EC} pulses occurred mainly under warm and dry conditions coinciding with rainfall after grazing in the summer months or over multiple days, i.e. in autumn and spring, when the interplay of underlying soil conditions, WFPS and N_r inputs favoured high positive F_{EC} (Fig. 3-2b). Pulse F_{EC} often remained discrete from more regularly occurring F_{EC} of lower magnitude ≤ 0.6 nmol N_2O m^{-2} s^{-1} as defined by Liáng et al. (2018). The transition from F_{EC} pulses to F_{EC} of lower magnitude was less distinguishable in autumn and spring, and large pulses of F_{EC} did not occur in the winter season. Generally, the accumulative rate of F_{EC} was around three times greater in autumn (40.2 g N_2O-N ha^{-1} d^{-1}), than in spring (15.0 g N_2O-N ha^{-1} d^{-1}) and the F_{EC} was lowest in winter when the soil was generally water-saturated with a WFPS > 80%. During these wet months, the cumulative F_{EC} was 13.5 g N_2O-N ha^{-1} d^{-1} despite consistent grazing and the associated input of N_r throughout the year. The highest 30-min average F_{EC} were measured during the autumn season, reaching up to 15.0 nmol m^{-2} s^{-1}. There was, however, no observable increase in F_{EC} after N fertilisation and unlike F_{EC} that appeared in bursts, F_{EC} of lower magnitude occurred consistently throughout the year accounting for 76% of total annual N_2O emissions measured by EC. Overall, annual nitrous oxide emissions derived from EC measurements totalled 7.3 kg N_2O-N ha^{-1} yr^{-1}, negative F_{EC} included.

3.4.4 Nitrous oxide budgets

Nitrous oxide fluxes and total N_2O emissions (in kg N_2O-N ha^{-1}) were calculated and compared for three periods of time using site-specific as well as New Zealand default EFs and flux data measured by EC. The selected periods included: 1) the first 16 days (4 to 20 October 2017) after treatment application (T_1) to the chamber plots, which corresponded with one grazing in the EC footprint; 2) the period of chamber measurements T_2 (4 October 2017 to 6 January 2018) that comprised five grazing events (8–12) in the EC footprint; and 3) twelve months (T_3) from 1 March 2017 to 28 February 2018. Comparisons made over T_2 and T_3 also accounted for the effect of supplementary feed and BNE on N_2O emissions (Table 3-4).

During T_1, $F_{pad,chamber}$ was directly comparable to F_{EC} with both N_2O fluxes measured at the same time of the day, 10 AM–12 PM. Extrapolating $F_{chamber}$ to the paddock scale and subsequent comparison to EC became possible by choosing an area-weighted approach resulting in $F_{pad,chamber}$ as described in Section 3.3.3.3.

Table 3-4 Nitrous oxide budgets using site-specific EFs are depicted for each grazing event (1 to 14) and are distinguished by individual contributions from pasture intake and excretion (P); supplementary feed intake and excretion (S), N fertiliser (F) and the combined sum of PSF+BNE. The dashed frame indicates the months during which chamber measurements were conducted. Resulting emissions for each grazing event were quantified in kg N_2O-N ha^{-1}. Annual totals are provided at the bottom of the table for both site-specific and default EFs and are compared with N_2O emissions measured by EC at the right-hand side.

			P			**S**			**F**		**PSF + BNE**	**EC**
graz. event	**start date**	**end date**	urine N_{ex} [kg ha^{-1}]	dung N_{ex} [kg ha^{-1}]	**emission N_2O-N** [kg ha^{-1}]	urine N_{ex} [kg ha^{-1}]	dung N_{ex} [kg ha^{-1}]	**emission N_2O-N** [kg ha^{-1}]	fertiliser N [kg ha^{-1}]	**emission N_2O-N** [kg ha^{-1}]	**emission N_2O-N** [kg ha^{-1}]	**emission N_2O-N** [kg ha^{-1}]
1	1-Mar-2017	4-Mar-2017	16.4	6.7	0.27	6.7	2.7	0.11	22.2	0.036	0.49	0.87
2	26-Mar-2017	30-Mar-2017	22.1	9.4	0.36	3.0	1.3	0.05	-	-	0.49	0.72
3	17-Apr-2017	19-Apr-2017	20.1	9.7	0.33	2.2	1.1	0.04	8.6	0.014	0.46	1.53
4	19-May-2017	21-May-2017	16.4	9.1	0.27	6.0	3.4	0.10	3.1	0.005	0.46	0.75
5	27-Jun-2017	5-Jul-2017	24.3	13.4	0.40	8.2	4.6	0.14	3.1	0.005	0.62	0.59
6	13-Aug-2017	17-Aug-2017	13.8	7.2	0.23	7.9	4.1	0.13	-	-	0.44	0.18
7	8-Sep-2017	12-Sep-2017	13.9	7.1	0.23	5.5	2.9	0.09	-	-	0.40	0.23
8	2-Oct-2017	4-Oct-2017	17.9	8.8	0.30	3.5	1.7	0.06	-	-	0.43	0.26
9	23-Oct-2017	25-Oct-2017	14.5	7.2	0.24	2.4	1.2	0.04	-	-	0.36	0.43
10	15-Nov-2017	17-Nov-2017	17.1	8.6	0.28	1.4	0.7	0.02	2.7	0.004	0.39	0.41
11	7-Dec-2017	9-Dec-2017	16.3	7.5	0.27	0.8	0.4	0.01	-	-	0.36	0.23
12	30-Dec-2017	1-Jan-2018	12.0	5.8	0.20	1.8	0.9	0.03	-	-	0.31	0.25
13	15-Jan-2018	17-Jan-2018	9.6	5.3	0.16	3.1	1.8	0.05	-	-	0.29	0.52
14	19-Feb-2018	21-Feb-2018	13.7	6.4	0.22	3.0	1.4	0.05	-	-	0.35	0.34
			228.0	112.1	**3.76**	55.6	28.2	**0.92**	39.8	**0.06**	**5.83**	**7.30**
*using NZ default EFs					*2.56			*0.63		*0.23		

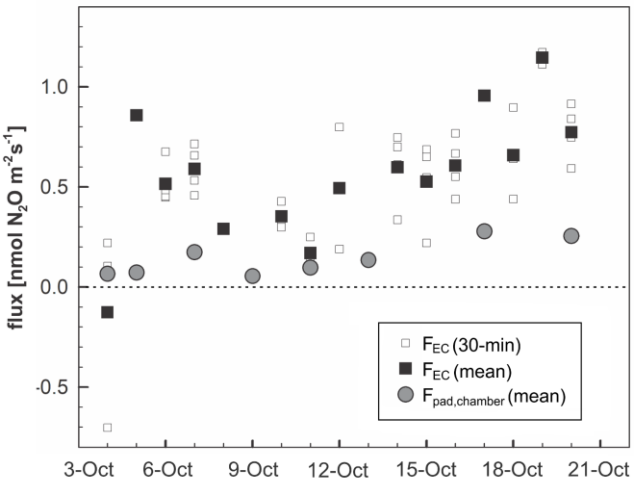

Figure 3-4 Comparison of $F_{pad,chamber}$ and F_{EC} for the first 16 days after treatment application. The date of treatment application (4 October 2017) to the chamber plots was timed to the simultaneous input of excreta N through cattle grazing in the EC footprint. Quality-controlled (filtered but no gap-filled) F_{EC} depict 10 AM to 12 PM fluxes only, i.e. the time of the day during which chamber measurements were conducted. F_{EC} are distinguished into 10 AM to 12 PM means (black squares) and individual 30-min F_{EC} (white squares) within this time. $F_{pad,chamber}$ (grey circles) were unit-transformed and are illustrated as the sum of area-weighted urine, dung and control fluxes. Fluxes from fertiliser treatments were excluded from this sum since the EC footprint did not receive fertiliser N during the time of comparison.

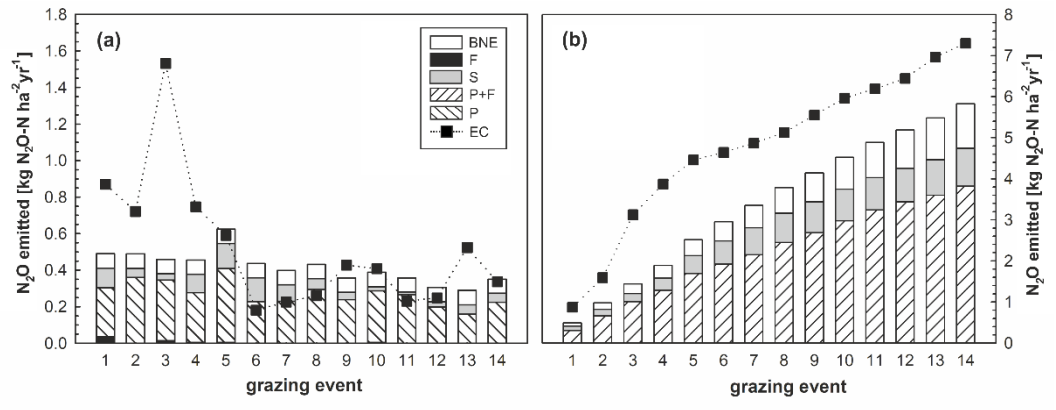

Figure 3-5 Comparison of N_2O-N budgets in kg ha^{-1} for each grazing event on paddock P51, P53 and P54 calculated from site-specific EF estimates and EC measurements. Bars show EF-based N_2O estimates by taking into account the contribution of fertiliser (F, black), pasture intake (P, diagonal pattern), supplementary feed intake (S, grey) and background N_2O emissions (BNE, white). The black squares present gap-filled N_2O flux data measured by EC. Panel (a) illustrates the sums of EF and EC budgets for each grazing event whereas panel (b) shows cumulative sums for both budgets.

Overall, $F_{pad,chamber}$ and F_{EC} responded similarly to underlying natural and anthropogenic controls, i.e. the input of N_r via grazing and the change of soil WFPS in particular. Nonetheless, during T_1 the upscaled $F_{pad,chamber}$ remained lower than F_{EC} (Fig. 3-4). The agreement between $F_{pad,chamber}$ and F_{EC} did not become as apparent when using calculated site-specific EFs over T_1, instead of the immediate $F_{pad,chamber}$. In this case, the EF-based budget of 0.43 kg N_2O-N ha^{-1} yr^{-1} (including supplementary feed and

BNE) was greater than that from EC measured as 0.26 kg N_2O-N ha^{-1} yr^{-1} (grazing event 8, Table 3-4). It is noteworthy that the effect of fertilisation was excluded from the above considerations since N fertiliser was not applied to the EC footprint for T_1. Also, a detailed comparison expanding on differences or similarities of $F_{pad,chamber}$ and F_{EC} on a sub-daily to hourly basis was outside the scope of this study, as this would have required chamber measurements of higher sampling frequency and spatial replication (Nicolini et al., 2013; Wang et al., 2013a; Voglmeier et al., 2019). The closest agreement in EF and EC derived N_2O budgets was found for T_2. The use of site-specific EFs applied to the intake and subsequent excretion of pasture N (P), supplementary feed N (S) and BNE resulted in the emission of 1.28 kg N_2O-N ha^{-1}, 0.16 kg N_2O-N ha^{-1} and 0.36 kg N_2O-N ha^{-1}, respectively, whereas emissions from urea fertiliser (F) remained negligible (Fig. 3-5). In comparison, measurements from EC resulted in total T_2 emissions of 1.57 kg N_2O-N ha^{-1}. Accordingly, total emissions measured by EC were 13% below the EF T_2 budget of 1.81 kg N_2O-N ha^{-1} including P, S, F, and BNE.

At the annual scale (T_3), chamber derived EF estimates and EC measurements differed by a factor of two when excluding the effect of supplements and BNE. Annual emissions based on site-specific EFs applied to pasture intake and fertilisation only scaled to 3.82 kg N_2O-N ha^{-1} yr^{-1} whilst EC quantified annual N_2O emissions at 7.30 kg N_2O-N ha^{-1} yr^{-1}. Emission estimates from EFs showed the greatest deviation from the EC budget in autumn when the daily rate of F_{EC} was higher than in any other season. Consequently, emissions based on site-specific EFs were around 45–75% lower for grazing events 1 and 3 for instance than those quantified in the EC budget of 0.87 and 1.53 kg N_2O-N ha^{-1}, respectively (Table 3-4). Seasonal patterns observed in the F_{EC} data did not necessarily match to EFs estimates, particularly not for grazing events in late summer, autumn and winter (Fig. 3-5a). This was likely due to site-specific EFs being established exclusively in spring 2017.

Accounting for supplementary feed and BNE in T_3 increased the annual N_2O budget derived from site-specific EFs from 3.82 to 5.83 kg N_2O-N ha^{-1} yr^{-1}, including emissions from N fertiliser (0.06 kg N_2O-N ha^{-1} yr^{-1}). Nitrous oxide emissions resulting from cattle excretion of supplementary feed N contributed 0.92 kg N_2O-N ha^{-1} yr^{-1}. Considering BNE added a further 1.09 kg N_2O-N ha^{-1} yr^{-1} to the annual N_2O budget (Fig. 3-5b). Using New Zealand default EFs for cattle urine (1.00%), cattle dung (0.25%) and urea fertiliser (0.59%), instead of site-specific EFs, summed annual emissions to 2.77 kg N_2O-N ha^{-1} yr^{-1} excluding S and BNE and 3.42 kg N_2O-N ha^{-1}

yr^{-1} including these factors (Table 3-4). The calculated EF for N_2O measured by EC was 1.57%. Calculations for the EC derived EF took into account the cumulative sum of 7.30 kg N_2O-N ha^{-1} yr^{-1} emitted over T_3 and the total N input of 463.61 kg N ha^{-1} but excluded contributions from biologically fixed or other sources of residual soil N.

3.5 Discussion

Recent developments in the EC technique for measuring F_{N2O} provide an opportunity to directly compare N_2O estimates based on chamber measurements and associated EFs with those from continuous micrometeorological datasets. Using both EF calculations and EC quantification methods over one year resulted in a difference of 3.48 kg N_2O-N ha^{-1} yr^{-1} in the total annual N_2O budget of an intensively grazed New Zealand dairy pasture. Following the site-specific EF approach, annual N_2O emissions were calculated as 3.82 kg N_2O-N ha^{-1} yr^{-1} compared with 7.30 kg N_2O-N ha^{-1} yr^{-1} measured by EC (Fig. 3-6). The difference between the two budgets reduced when EFs accounted for supplementary feed intake and BNE. The remaining disparity was likely related to not adequately accounting for seasonal variabilities and the two different measurement techniques operating over different soils and at different spatio-temporal scales (Molodovskaya et al., 2011; Kutsch et al., 2013; Wang et al., 2013a).

3.5.1 Seasonal variability

Annual N_2O emissions in New Zealand are calculated using country-specific, default EFs for cattle urine (1.00%), cattle dung (0.25%) and urea fertiliser (0.59%) that do not change with season (Gibbs, 2018). However, most research has shown that N_2O fluxes are highly variable in space and time (Rowlings et al., 2015; Selbie et al., 2015; Luo et al., 2017). Positive pulse fluxes of N_2O depend on N_r input after grazing or fertilisation but also respond to seasonal variations in soil temperature and WFPS (Rowlings et al., 2015; Rabot et al., 2016). Similarly, we demonstrated that site-specific spring EFs deviated from EC-based data particularly in autumn when the daily rate of F_{EC} (53.65 g N_2O-N ha^{-1} d^{-1}) was three to five times higher than in any other season. This was also observed by Liáng et al. (2018) who acknowledged that F_{EC} at the same site were much higher in autumn. In contrast, late summer and autumn emissions based on EF estimates were 45–75% lower than suggested by EC, even when including P, S, F and BNE (Table 3-4). Eddy covariance and EF N_2O budgets agreed more closely during spring and in early summer (i.e. grazing events 8–12) when EF derived emissions exceeded the cumulative from EC by 15%.

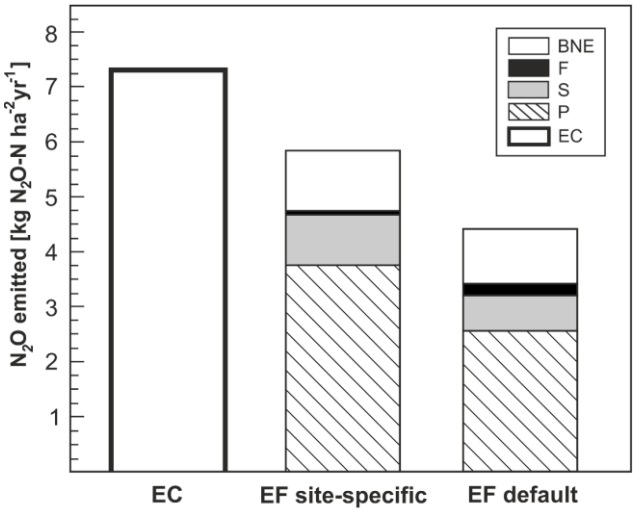

Figure 3-6 Breakdown of annual N_2O budgets measured by EC and estimated by using site-specific and New Zealand default EFs. Annual budgets calculated from using these EFs are further distinguished into different variables that contributed to the emission of N_2O in these budgets. Variables are: cattle intake and excretion of ryegrass-clover pasture (P, diagonal pattern), intake and excretion of supplementary feed (S, grey), N fertilisation (F, black) of the soil and background N_2O emissions (BNE, white).

Eddy covariance measurements at our site resulted in a clear seasonal pattern of F_{EC} with a strong interrelationship between soil moisture and soil temperature (Fig. 3-2). As previously shown by Liáng et al. (2018), at a soil temperature of 25°C this correlation was negative when < 70% WFPS and positive when > 70% WFPS. Elevated positive F_{EC} were measured during times of high cumulative rainfall (871 mm) in autumn 2017 when the soil WFPS fluctuated between 60–80%, i.e. was in the zone of optimal soil N_2O production from microbial nitrification and denitrification (Butterbach-Bahl et al., 2013; van der Weerden et al., 2014). The constant fluctuation in the zone of ideal N_2O production likely favoured soil nitrification at lower WFPS and increased aerobic condition whereas denitrification seemed to have accelerated at higher soil moisture contents (Firestone and Davidson, 1989; Selbie et al., 2015). Also, a decrease in pasture and biomass growth along with reduced plant N uptake and biological N fixation during the autumn months might have further promoted soil N_2O production (Ledgard et al., 1998; Cai and Akiyama, 2016). In winter, a relatively high WFPS of > 80% constrained microbial nitrification thereby decreasing the availability of NO_3^- for soil denitrifiers (Liáng et al., 2018). Consequently, winter F_{EC} rarely exceeded 1 nmol N_2O m^{-2} s^{-1} with no pulse F_{EC} observed after grazing. In summer, F_{EC} pulses only occurred after grazing and rainfall, i.e. when anaerobic microsites allowed denitrifying microbes to utilise NO_3^- that had accumulated previously under drier conditions.

The seasonal pattern present in EC measurements was not well described when applying site-specific EFs determined during spring to the input of N_r in other seasons (Fig. 3-5). This finding agrees with studies from Schaufler et al. (2010), van der Weerden et al. (2017) and De Klein et al. (2003) who found the flux of N_2O varied seasonally depending on WFPS, soil temperature, soil type, livestock species and farming system. Krol et al. (2016) showed that EFs calculated from urine application across three Irish grassland sites with contrasting soil types were higher in autumn (1.56%) than in summer (0.71%) or spring (0.67%). Also, Rafique et al. (2011) demonstrated that application of N in early spring and autumn increased the emission of N_2O while De Klein et al. (2003) determined EFs for dairy cow urine ranged from 0.03–3.70% following a single urine application on different New Zealand pastures in autumn. Generally, the seasonal variation of N_2O fluxes was found to correlate with variability in daily rainfall irrespective of measurement technique (Rowlings et al., 2015; Uchida and Clough, 2015; Petrakis et al., 2017). Using spring-specific EFs for calculating an annual N_2O budget in our study resulted in relatively similar amounts of N_2O emitted across all seasons, with 0.96 kg N_2O-N ha^{-1} emitted in autumn, 0.90 kg N_2O-N ha^{-1} in winter, 1.05 kg N_2O-N ha^{-1} in spring and 0.85 kg N_2O-N ha^{-1} in summer, excluding supplementary feed (S) and BNE (Fig. 3-5a). Therefore, we could not draw firm conclusions on how and to what extent the use of different seasonal EFs would have affected the annual N_2O emission budget at our site; and whether the application of urine, dung and urea fertiliser in other seasons than spring would have resulted in larger or smaller EFs than described in the above studies (Chadwick et al., 2018).

3.5.2 Role of supplementary feed

Traditionally, dairy farming in New Zealand has been pasture-based with non-pasture supplements comprising only a small percentage of the dairy cattle diet, e.g., 4% in 1990/1991 (MPI, 2016). In more recent years, the use of supplementary feed increased triggered by intensified dairy production. On average, supplementary feed now makes up to nearly 20% of the dairy cattle diet, with maize, silage, palm kernel extract and winter crops used as common supplements (MPI, 2016; Ma et al., 2019). However, the EF approach for calculating N_2O emissions in New Zealand has not yet directly included cattle intake of supplementary feed N, its effect on excretion and likely N_2O emissions due to a lack of activity data. Current reporting only accounts for the intake of supplementary feed by considering the animals' metabolic energy requirements but does not consider feed specific N excretion other than ryegrass-clover pasture (Gibbs, 2018). In other words, supplementary feed N is only indirectly included in the New

Zealand inventory but classified as pasture and thus may eventually even overestimate annual N_2O emissions, particularly if the supplementary forage comprises a lower N content than pasture. Closing the gap between N_2O emissions estimated by site-specific EFs and measured by EC, therefore, might require the estimation of N_2O emissions attributable to supplementary feed.

During our study, 29.3% of the cattle diet originated from supplementary feed rather than from ryegrass-clover pasture. For the experimental area, an estimated total of 559 kg N ha^{-1} yr^{-1} was ingested from pasture and 132 kg N ha^{-1} yr^{-1} from supplements resulting in a total N intake of 691 kg N ha^{-1} yr^{-1} (Table 3-2). Around 61.5% of this N intake was subsequently excreted and eventually a proportion emitted as N_2O. Supplements such as maize silage generally contain lower N contents than traditional perennial ryegrass-white clover pasture. Expected to improve cattle N utilisation, the intake of supplements likely leads to reductions in the excretion of urinary N while still meeting the animals' metabolic requirements (Luo et al., 2008c; Dijkstra et al., 2011; Gregorini et al., 2016). In this study, maize silage, dried distiller grains, grass and hay silage were the main supplements with measured N contents of 1.2%, 3.4%, 1.5% and 1.6%. In comparison, the mean pasture N content was 3.6%. Distinguishing diet-specific N contents allowed us to quantify the amount of N excreted from pasture and supplementary feed while also differentiating N_2O emissions into a supplementary feed (0.92 kg N_2O-N ha^{-1} yr^{-1}) and a pasture component (3.76 kg N_2O-N ha^{-1} yr^{-1}) (Fig. 3-6). We hypothesised that supplement intake would reduce excreta N loads and this was confirmed when manipulating Eq. 3-6 by substituting feed-specific N contents ($Feed_N$) with pasture N (3.6%), i.e. resulting in feed related N_2O emissions of 4.71 kg instead of 4.68 kg N_2O-N ha^{-1} yr^{-1} (P + S, Table 3-4).

3.5.3 Background nitrous oxide emissions

The quantification of EFs following IPCC guidelines does not consider F_{N2O} from untreated control sites, i.e. BNE (Kim et al., 2013; Aliyu et al., 2018). Instead, the use of a single default value of approximately 1 kg N_2O-N ha^{-1} yr^{-1} is suggested, but not compulsory, for all non-natural, anthropogenically triggered BNE that occur alongside direct F_{N2O} pulses caused by specified treatment application of e.g., urine, dung and fertiliser (Bouwman, 1996). The literature defines background N_2O emissions (BNE) as positive F_{N2O} from soils that received no N fertiliser and soil management (e.g., Bouwman, 1996; Gu et al., 2009; Kim et al., 2012). For agricultural and pastoral land, BNE might be altered by previous fertilisation, N fixation by clover, soil management or other sources of N such as grazing and inflow during flooding that lead N to

accumulate in the soil and BNE to subsequently increase (Bouwman, 1996; Neftel et al., 2007; Gu et al., 2009; Aliyu et al., 2018). A recent meta-analysis by Kim et al. (2013) quantified the global mean of BNE for agricultural land as 1.52 kg N_2O-N ha^{-1} yr^{-1} and, more specifically, as 1.8 kg N_2O-N ha^{-1} yr^{-1} for pasture.

Measurements at our site highlighted the significance that F_{N2O} of lower magnitude can play in annual N_2O budgets apart from those fluxes that are emitted in pulses associated with the input of N_r. The mean $F_{chamber}$ measured at our chamber control sites (i.e. where there was no treatment applied) scaled up to 1.09 kg N_2O-N ha^{-1} yr^{-1} and compared well with Bouwman (1996). Also, only 24% of the F_{EC} measured by EC appeared in short bursts (1–2 days) after grazing or management intervention and subsequent rainfall; while 76% of F_{EC} occurred at low magnitude continuously throughout the year. These low magnitude F_{N2O} are not the same as BNE derived from chamber measurements but contributed overall 5.4 kg N_2O-N ha^{-1} yr^{-1} to the annual EC budget. Recently discussed by Liáng et al. (2018) and Voglmeier et al. (2019), EC measurements are capable to continuously operate over space and time capturing the full range of F_{N2O} no matter the sources of N_2O emitted. In other words, EC measurements already include the contribution of BNE to annual totals, which might explain why fluxes of lower magnitude dominated the annual N_2O budget rather than flux pulses.

Furthermore, the relevance of low magnitude F_{EC} identified in our study agrees with the literature. For instance, Wang et al. (2013b) used chamber and TDL-EC measurements on fertilised cotton fields in China, with 52% of the chamber and 59% of the EC fluxes occurring during periods of low N_2O emissions. Wang et al. (2013b) determined that cumulative N_2O emissions from EC were 44% higher than those measured by static chambers and that F_{N2O} from EC were 147% higher during periods of otherwise low N_2O emissions. Chamber-based methods are prone to larger absolute errors in the quantification of EFs and N balances than EC, particularly when used in high N exchange regimes, such as intensively grazed pastures (Jones et al., 2011; Brümmer et al., 2017). This, in turn, might mean chamber measurements tend to underestimate F_{N2O} caused by the reactivation of residual N accumulated in the soil after cattle grazing, fertilisation or biologically fixed in plant residues but not yet mineralised (Huang et al., 2004; Miller et al., 2008; Gu et al., 2009).

In our study, we did not specifically determine how biologically fixed N contributed to the emission of N_2O. However, Fuchs et al. (2018) have shown that N_2O emissions from an unfertilised, up to 44% clover-containing pasture resulted in emissions of up

to 3.8 kg N_2O-N ha^{-1} yr^{-1}. Findings included that biological N fixation (BNF) and clover residual decomposition did not enhance N_2O emissions, nonetheless, contributed to annual N_2O totals (Li et al., 2011). Hence, by only considering treatment derived N_2O emissions, current EF estimates may not accurately account for low magnitude fluxes of N_2O from agricultural land (Aliyu et al., 2018). In our study, we recognised BNE as F_{N2O} of lower magnitude that can be promoted by soil compaction through animal treading and trampling or may even result from the reactivation of residual soil N over time (Voglmeier et al., 2019). Background N_2O emissions measured at the chamber control sites added 1.09 kg N_2O-N ha^{-1} yr^{-1} to the EF derived budget irrespective of seasonal effects; whereas EC already included the contribution of low F_{EC} in the annual total as well as across seasons (Fig. 3-5) (Section 3.5.1). Despite our findings, BNE have remain disregarded in annual emission budgets and national inventories that often do not account for BNE and its variation with climate and multiple other factors associated with farm and soil management (Kim et al., 2013; Aliyu et al., 2018).

3.5.4 Annual nitrous oxide budget

The annual N_2O budget of this study was calculated using 1) an EF approach following the New Zealand inventory guidelines for N_2O, and 2) using gap-filled F_{N2O} data measured by EC. The EF-based budget excluded the effect of seasonal variability but included supplementary feed and BNE on total annual N_2O emissions. Using site-specific EFs that excluded the effect of the aforementioned factors, N_2O emissions upscaled to a total of 3.82 kg N_2O-N ha^{-1} yr^{-1}. Including the effect of supplementary feed (0.92 kg N_2O-N ha^{-1} yr^{-1}) and BNE (1.09 kg N_2O-N ha^{-1} yr^{-1}) resulted in the emission of 5.83 kg N_2O-N ha^{-1} yr^{-1} (Fig. 3-6). Eddy covariance measurements determined totals of 7.30 kg N_2O-N ha^{-1} yr^{-1} emitted over the same twelve-month period. Both chamber derived EFs and EC budgets were within the commonly reported range of N_2O emissions from intensively grazed dairy pastures in New Zealand ranging from 0.2–15.9 kg N_2O-N ha^{-1} yr^{-1} (Luo et al., 2008a; De Klein et al., 2010; Luo et al., 2017) but were slightly below the global IPCC default value of 8 kg N_2O-N ha^{-1} yr^{-1} for grazed pastoral land (De Klein et al., 2006). The lower annual N_2O emissions calculated from the EF approach also mirrored the results observed in the first 16 days of the chamber experiment, where the alignment of grazing allowed for comparison of $F_{pad,chamber}$ and F_{EC} (Fig. 3-4). During this period, the upscaled $F_{pad,chamber}$ were lower than F_{EC}. This was, however, not unexpected due to three possible reasons. Firstly, other studies (Moir et al., 2011; Selbie et al., 2015) reported urine patch sizes

might be larger than the most commonly cited 0.20 m^2 (Haynes and Williams, 1993) chosen here for $Area_{patch,x}$ (Eq. 3-4). Had $Area_{patch,x}$ been greater than this value, $F_{pad,chamber}$ would have been closer to F_{EC}. Secondly, excluding the chamber site from N_r inputs one month prior to treatment application likely decreased the contribution of BNE and thus lowered $F_{pad,chamber}$ whereas the EC footprint continued to receive N_r through grazing (one event). We, therefore, hypothesise that the lack of N_r inputs during the pre-treatment period of the chamber trial led to lower $F_{chamber}$ measured at the chamber control plots. Thirdly, the extent to which urine and dung patches remained spatially heterogeneous across the experimental paddocks was not determined.

Other studies have shown that areas, where cattle congregate, can form potential emission hotspots e.g., close to water troughs, feeding bins, gateways and stock campsites (Matthews et al., 2010; Luo et al., 2017). In our study, the experimental paddocks were grazed only over short periods (< 24 h) with animals foraging and excreting more or less evenly across the paddock area (Felber et al., 2015). The heterogeneous distribution of excreta patches was, therefore, not considered a major factor for explaining why annual emission estimate based on EF remained lower than that suggested by EC. Site-specific EFs for direct N_2O emissions from soil were established at 1.53% for cattle urine, 0.24% for cattle dung and 0.16% for urea fertiliser. For cattle urine, our EF was 50% higher than suggested by the New Zealand Tier 2 inventory (1.00%). The EF for cattle dung was similar to the default (0.25%) whereas the EF for urea fertiliser was 27% lower than the inventory EF (0.59%) (MfE, 2019).

In comparison to EFs, EC measurements did not generally distinguish between treatment effects on F_{EC} but integrated F_{N2O} over space and time (Fig. 3-6) (Neftel et al., 2010; Brümmer et al., 2017; Fuchs et al., 2018). Hörtnagl et al. (2018), for instance, synthesised F_{N2O} data from 14 grassland sites in Central Europe, one of which included measurements of F_{N2O} using QCL-CW EC over an intensively managed, but only extensively grazed, Swiss grassland. Over the course of different EC measurement campaigns and years, Hörtnagl et al. (2018) quantified annual N_2O emissions of 5.22 kg N_2O-N ha^{-1} yr^{-1} (2010/2011), 7.89 kg N_2O-N ha^{-1} yr^{-1} (2010/2011), and 2.55 kg N_2O-N ha^{-1} yr^{-1} (2013), which were also expressed as EFs (2.70%, 3.60%, and 1.10%). This put into perspective, the EF calculated from EC measurements at our site (1.57%) was within by Hörtnagl et al. (2018) determined range. That the EC-EF at our experimental site was at the lower end of this range remained interesting, particularly, based on the repetitive and high inputs of N_r that paddock soils received via grazing.

3.6 Conclusion

The quantification of N_2O fluxes (F_{N2O}) from intensively grazed pastoral ecosystems is challenged by highly variable inputs of N_r, dynamic changes in environmental conditions and variable farm management. Static chamber measurements and derived EFs are established methods to measure and to calculate the emission of N_2O originating from these environments. However, EF-based estimates include a relatively high uncertainty which often limits the ability to reliably quantify N_2O emissions at larger scales with sufficient temporal frequency. In this study, the cumulative sum of gap-filled EC N_2O flux data (7.30 kg N_2O-N ha^{-1} yr^{-1}) exceeded the N_2O budget of 3.82 kg N_2O-N ha^{-1} yr^{-1} based on site-specific EFs. The difference between EC and EF budgets decreased to 1.47 kg N_2O-N ha^{-1} yr^{-1} when accounting for the intake of supplementary feed (0.92 kg N_2O-N ha^{-1} yr^{-1}) and BNE (1.09 kg N_2O-N ha^{-1} yr^{-1}). Including these factors increased the EF-based emissions to 5.83 kg N_2O-N ha^{-1} yr^{-1}. Site-specific EFs established in spring were not adequate to fully reflect the seasonal variability of F_{N2O}. Nonetheless, static chamber and EC fluxes matched considerably well when compared on a sub-daily basis, i.e. during a 16-day period after treatment application to the chamber trial.

In anticipation of ongoing climate change and increased atmospheric N_2O concentrations, the reliable quantification of annual N_2O emissions is crucial. The intensification of agroecosystems and farm management strategies ask for a more improved validation of the effect of additional factors, such as supplementary feed and BNE, on the emission of N_2O. To date, static chamber methods deliver treatment-dependent F_{N2O} measurements at point scales whereas EC allows F_{N2O} measurements under real-world conditions. By complementing static chamber methods, EC measurements therefore facilitate to overcome the discrepancy between microbial-driven N_2O production in soils and the enormous range of spatio-temporal conditions under which N_2O is emitted. Eddy covariance offers a promising opportunity to add to our current understanding of flux dynamics and also to advance the quantification of N_2O emissions in future.

3.7 Acknowledgements

This research (project 17-CAN9.3.4) was supported by the New Zealand Agricultural Greenhouse Gas Research, AgResearch Ruakura and DairyNZ. The authors like to acknowledge the cooperation with the farm owners, Sarah and Ben Troughton, for providing the research site as well as detailed management and farm activity data. Fieldwork was kindly supported by Chris Morcom, Bridget Wise, Esther Peerlings, Jarrod Hall and Jack Pronger. Moira Dexter is thanked for her introduction to the laboratory at AgResearch Ruakura. The continuous support by Aerodyne Research to maintain the QCL EC site was appreciated at all times as was the input by Gerardo Fratini from Li-COR assisting with flux processing methods in EddyPro. We would further like to thank Jordan Goodrich, Dorisel Torres-Rojas, Florian Gehring, Kati Hewitt, Tom Moore and two anonymous reviewers for thoroughly revising the manuscript.

3.8 Author contributions

Author names: Anne R. Wecking (ARW), Stuart B. Lindsey (SL), Jiafa Luo (JL), Louis A. Schipper (LS), Lìyǐn L. Liáng (LL), Aaron M. Wall (AW), David I. Campbell (DC).

ARW, SL, JL and LS designed the experiment. ARW and SL conducted the fieldwork with contributions from LL. Soil and gas samples were prepared for collection and analysis by ARW with occasional contributions from SL. AW, LL, DC provided MatLab scripts and advice in data processing. ARW performed the result analysis, wrote and revised the manuscript with inputs from AW, LL, SL, JL, DC and LS.

Chapter Four

The Effect of Pasture Renewal on Short-term Nitrous Oxide Fluxes: an Eddy Covariance Study

4.1 Abstract

Pasture renewal is a common management practice used to enhance plant productivity and yield in intensively grazed farm systems. However, pastures that undergo renewal can have an increased risk of nutrient losses due to disruptions of the soil carbon and nitrogen cycling. This study used eddy covariance (EC) measurements to determine the effect of a no-till, direct-drill pasture renewal followed by rapid reseeding on nitrous oxide (N_2O) exchange for 66 days after management intervention in autumn. Flux measurements were made using a single EC system coupled to a quantum cascade laser absorption spectrometer (QCL) sited at the boundary of two adjacent paddocks, P54, which was renewed, and P53, the control. Data processing involved an analysis of source area contributions (footprint-splitting) and gap-filling of the measured N_2O fluxes (F_{N2O}) using a machine learning tool. The approach provided robust F_{N2O} data at high temporal resolution and accounted for the renewal effect on F_{N2O} more comprehensively than using filtered but not gap-filled F_{N2O}. Pulses of F_{N2O} on the renewed P54 were strikingly short, i.e. limited to a two weeks' window with individual half-hourly F_{N2O} as high as 13.0 nmol N_2O m^{-2} s^{-1} 15 days after herbicide application to P54 on 10 March 2018. The difference in total emissions between P54 (2.61 kg N_2O-N ha^{-1}) and P53 (1.39 kg N_2O-N ha^{-1}) was 1.22 kg N_2O-N ha^{-1}, 93.4% of which arose in only 14 days of the overall 66-day measurement period. Cumulative N_2O emissions from P53 and P54 were similar for the remaining days when environmental drivers controlled pasture N_2O exchange (soil moisture and temperature) rather than only after-effects from pasture renewal intervention (e.g., decreased plant nitrogen uptake, enhanced soil organic matter mineralisation). Rapid reseeding seemed to have prevented the prolonged loss of N_2O after pasture renewal and our findings also showed that the applied data processing approach allowed for the quantification of treatment effects on F_{N2O} from two adjacent paddocks while using a single EC system.

4.2 Introduction

Extensive grasslands and permanent pastures cover an estimated 26% of the global terrestrial land surface area; which is more than twice the total area of croplands (FAO, 2020). Under intensive management, these grasslands can produce forage high in biomass that provides energy, protein, and structural carbohydrates for feeding livestock but yield and nutritive values often decline with time if not managed appropriately (Hopkins et al., 1995; Kayser et al., 2018; Gawel and Grzelak, 2020). Consequently, occasional renewal of the pasture sward is carried out to maintain and improve productivity (Reinsch, 2014; Krol et al., 2016b). Pasture renewal (also termed: reseeding, renovation, restoration) is an accepted practice for intensively managed harvested and grazed temperate grasslands, where it is commonly conducted every five to 15 years (Hopkins et al., 1990; Velthof et al., 2010; Thomas et al., 2014; Rutledge et al., 2017b).

Grassland soils have relatively high soil organic carbon (SOC) contents due to plant coverage year-round and the absence of repetitive disturbances as in cropping agriculture (Conant et al., 2001; Tate et al., 2005; Johnston et al., 2009; Reinsch et al., 2018a). Conversely, grassland soils can lose some of this SOC along with reactive nitrogen (N_r) after renewal-related disturbances because soil organic matter (SOM) mineralisation rates accelerate and plant nitrogen uptake is temporarily limited (Davies et al., 2001; Poeplau et al., 2011). In turn, the risk of N_r leaching and N_2O emissions can increase (Whitehead et al., 1990; Shepherd et al., 2001; Dennis, 2009; Helfrich et al., 2020). This is important not only since nitrogen is a limiting nutrient for agricultural production but also because of its reactive forms (N_r) contributing to environmental pollution and atmospheric warming. Nitrous oxide, for instance, has a global warming potential 265 times higher than carbon dioxide (CO_2) over a 100-year time horizon and is an ozone-depleting substance with a current atmospheric mixing ratio of 329 ppb (2017) compared to pre-industrial 270 ppb (1750) (Ravishankara et al., 2009; Portmann et al., 2012; IPCC, 2013; WMO, 2017a).

Relatively high emissions of 29.1 kg N_2O-N ha^{-1} were observed by EC measurements after ploughing of an intensively managed Swiss grassland with almost 15% of the total nitrogen applied lost and emitted during the following six months (Merbold et al., 2014). Other studies have noted similar effects on N_2O emissions (Baggs et al., 2000; Yamulki and Jarvis, 2002; Cowan et al., 2016) and also demonstrated that the available inorganic nitrogen content in the topsoil increased considerably in the first year after ploughing (100–400 kg N ha^{-1}) (Vertes et al., 2007; Necpálová et al., 2013; Mori, 2020).

The amount of N_r available for the mineralisation and subsequent emission post-renewal is controlled by nitrogen input rate and the amount of residual nitrogen present in the soil before management intervention with sward age as the associated indicator of the N_r mineralisation potential (Whitehead et al., 1990; Davies et al., 2001; Eriksen and Jensen, 2001). However, the interplay of the various controls on N_2O emissions and pasture renewal is not fully understood. Reinsch et al. (2018b) reported average emissions of 8.35 kg N ha^{-1} yr^{-1} from pastures in northern Germany after mouldboard ploughing and slurry application (240 kg N ha^{-1} yr^{-1}). In contrast, Velthof et al. (2010) and MacDonald et al. (2011) showed that pasture renewal without ploughing caused up to 2.5 kg N ha^{-1} higher total N_2O emissions than with ploughing, particularly when coinciding with precipitation in spring, and resulted in overall lower coverage of perennial ryegrass in the new pasture sward (60–84% versus 90%). More generally, the effects of using no-till renewal (e.g., sward improvement, herbicide application, reseeding via over- or undersowing) as a strategy to mitigate N_2O emissions have remained inconclusive and in contrast to the well-understood effects that soil moisture and temperature have on microbial nitrification and denitrification (Firestone and Davidson, 1989; Vertes et al., 2007; Buchen et al., 2017). This means that emissions of N_2O resulting from pasture renewal are not always proportional to the initial degree of soil disturbance and less invasive renewal techniques therefore might not necessarily lead to reductions in N_2O emissions (Kong et al., 2009; Velthof et al., 2010; Kayser et al., 2018).

Most of our current understanding regarding the emission of N_2O after management intervention comes from short-term studies with the majority using chamber techniques for N_2O flux (F_{N2O}) measurements (Krol et al., 2016b; Buchen, 2017; Reinsch et al., 2018b). The lack of high temporal resolution in these datasets is one of the main reasons for limited knowledge on the N_2O exchange process during and after renewal intervention and constrains the quantification of paddock to farm scale N_2O budgets (Merbold et al., 2014). Eddy covariance, coupled to a quantum cascade laser (QCL), can overcome some of the drawbacks associated with chamber techniques (e.g., spatio-temporal discontinuity, alteration of the soil environment after installation, biased flux calculation) (Rochette and Eriksen-Hamel, 2008; Jones et al., 2011), and enables compilation of flux datasets with high temporal resolution (Jones et al., 2011; Lammirato et al., 2018). Measurements using QCL EC over intensively managed pastures have provided promising insights in recent years, which has helped to further disentangle the spatio-temporal heterogeneity associated with the exchange of N_2O

from pastoral soils (Fuchs et al., 2018; Voglmeier et al., 2019; Wecking et al., 2020b). For instance, Liáng et al. (2018) was the first to use EC for F_{N2O} measurements at our study site to document the dependence of pulse and background F_{N2O} on environmental drivers and cattle grazing. To date, there are only a few other studies that have used EC to measure F_{N2O} following pasture renewal (Merbold et al., 2014; Cowan et al., 2016; Fuchs et al., 2018; Merbold et al., 2020), but none of these studies was conducted on intensively grazed land. Another EC study by Lognoul et al. (2019) determined the effects of topsoil disturbance on F_{N2O} under a sugar beet crop.

The challenge of using the EC technique in farming systems is that the expense of the QCL analyser often precludes the deployment of multiple towers at the same site and time (Goodrich et al., 2021). Therefore, in the absence of more than one EC system, measurement of different treatment effects can only become possible when isolating and assigning the F_{N2O} data to a specific source area in the EC footprint (footprint-splitting) as demonstrated by Wall et al. (2020b) for carbon dioxide (CO_2) fluxes and Merbold et al. (2020) for N_2O. One disadvantage of footprint-splitting is that the data coverage is reduced by more than half of the original full footprint time series, depending on footprint contribution thresholds and wind direction (Wall et al., 2020b; Goodrich et al., 2021). Procedures to fill the gaps in the resulting time series have remained under debate and, as yet, are not standardised (Mishurov and Kiely, 2011; Fuchs et al., 2018; Liáng et al., 2018; Nemitz et al., 2018; Lognoul et al., 2019; Cowan et al., 2020).

Our study aims to address these knowledge gaps by (1) quantifying F_{N2O} resulting from pasture renewal using a no-till renewal technique including herbicide application and direct-drilling; (2) discussing the effect of rapid reseeding as a mitigation strategy for N_2O emissions; and (3) using a split-footprint and associated gap-filling approach developed by Wall et al. (2020b) and Goodrich et al. (2021) to allow a direct comparison of F_{N2O} data from a renewed pasture with an adjacent intact control site using a single EC system.

4.3 Methods

4.3.1 Site description and farm management

The experimental site was located on Troughton Farm, a 199 ha commercial dairy farm 3 km east of Waharoa (37.78 °S, 175.80 °E, 54 m a.s.l.) in the Waikato Region, North Island, Aotearoa New Zealand. The site has a reasonably long history of EC flux measurements of CO_2 (2012) which, since November 2016, also included N_2O. The

experimental site of this study was named *'New Rye'* in previous work and described in detail by Liáng et al. (2018) and Rutledge et al. (2017b). In brief, the experimental site had been under long-term grazing for at least 80 years with a climate station 13 km to the south-west of the farm recording mean annual temperature and precipitation (1981-2010) of 13.3°C and 1249 mm, respectively (NIWA, 2018). Soils formed in rhyolitic and andesitic volcanic ash and rhyolitic alluvium. A Mottled Orthic Allophanic soil was identified as the dominant soil type based on the New Zealand soil taxonomy (Hewitt, 2010). In the June 2017 to May 2018 milking season, the farm was rotationally grazed by 478 Jersey cows split into two milking herds. The overall stocking density averaged 2.4 cows ha^{-1} with cattle feeding on pasture and from supplementary feed produced on-site and imported. The initial sward of the experimental site was ryegrass-clover (*Lolium perenne, Trifolium repens*) last renewed in 2013 (Rutledge et al., 2017b). With the most recent pasture renewal in 2018, two (P53, P54) of the former three experimental paddocks (P51, P53, P54) were re-fenced on 5 March 2018 in an approximate east-west orientation (65°-245°) with the new fence line parallel to the prevailing direction of the wind approaching from the south west to west. The EC tower was located at the boundary of two paddocks to equally detect F_{N2O} derived from either side of the footprint, i.e. from paddock P54 that had undergone renewal (F_{N2O_R}) and from the control P53 (F_{N2O_C}) that remained unaltered and under normal management (Fig. 4-1).

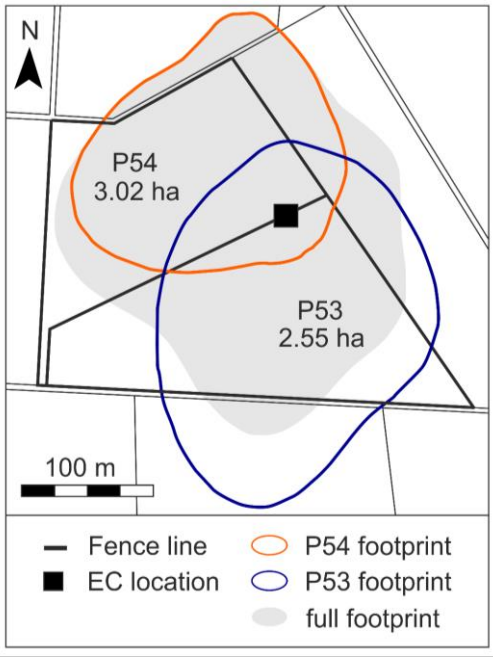

Figure 4-1 Layout of the eddy covariance (EC) flux measurement site. The full EC footprint mainly comprised two experimental paddocks: P53 (control) and P54 (renewed) for which the 80% flux footprint contour lines are indicated in blue (P53) and orange (P54) as well as the flux footprint as a whole (grey area). The EC tower (black square) was located at the boundary of P53 and P54.

4.3.2 Pasture renewal measures

Pasture renewal took place on 10 March 2018 with Weedmaster TS5440 (540 g L^{-1} glyphosate) and Pulse penetrant (800 g L^{-1} organo-modified polydimethylsiloxane) sprayed on paddock P54 to kill the existing ryegrass-clover sward. Direct-drilling of seed was conducted on 14 March using a Duncan triple-disc seeder. Sowing rates of the new seeds were: 7 kg ha^{-1} plantain (*Plantago lanceolata*), 3 kg ha^{-1} One50 AR37 and 3 kg ha^{-1} Samson AR37 Perennial ryegrass (*Lolium perenne*), 2 kg ha^{-1} Relish Red clover (*Trifolium pratense*), and 1 kg ha^{-1} Tribute white clover (*Trifolium repens*). A targeted herbicide (Broadstar, 480 g L^{-1} bentazone) was applied post seedling emergence on 7 April to control the simultaneous germination of weeds in the new sward. The control paddock P53 was grazed on 17 April whereas the renewed P54 experienced its first grazing post-renewal on 15 May. Note, that both paddocks were also grazed on the days (6–8 March) before spraying. To exclude any direct effects from cattle grazing on immediate F_{N2O} measurements on the renewed paddock (P54), the start date of our study was chosen to be 10 March and the end date 14 May 2018 (Fig. A2-1). However, the choice of time period did not exclude that reactive nitrogen (N_r) originating from grazing prior to renewal might have accumulated in the soil and, subsequently, been mineralised and eventually lost as N_2O. Data for the days prior to renewal intervention were illustrated for completeness in Figure 4-2 (6 March to 14 May 2018).

4.3.3 Eddy covariance measurements

4.3.3.1 Instrumentation

In brief, EC measurements consisted of a continuous-wave quantum cascade laser absorption spectrometer (CW-QCLAS, Aerodyne Research Inc., Billerica, MA, USA) and a 3-D sonic anemometer (mounted at 2 m height, orientated to 270°; CSAT3B, Campbell Scientific Inc., CSI, Logan, UT, USA). Both instruments operated at 10 Hz recording the dry mole fraction of the trace gases N_2O and CH_4 (QCL), and wind variables (CSAT3B). A dry scroll vacuum pump (XDS35i, Edwards, West Sussex, UK) directed the airflow from the sampling inlet into the QCL with the sample air being drawn at a flow rate of 15 L min^{-1} through a heated, 6.1 m long insulated tube. The QCL was housed in an insulated weatherproof enclosure ,where it operated at a stable temperature of 28°C in winter and 32°C in the summertime, ± 0.1°C. Monthly maintenance of the EC system included replacement of the 0.45 μm PTFE membrane filter (ThermoFisher Scientific, NZ) attached to the air inlet of the sampling line and standard gas check-ups. Raw data from the QCL were automatically stored on the

internal QCL computer and an external hard drive. Data logger clocks and QCL times were synchronised every half hour and aligned with a local network time protocol server (NTP, 1.nz.pool.ntp.org). See details on the EC set-up in Liáng et al. (2018).

Additional micrometeorological and soil measurements included air temperature, relative humidity, rainfall and, at 5 cm depth, soil temperature and soil volumetric water content (Wall et al., 2020b; Wecking et al., 2020b). The latter was used to calculate the water-filled pore space of the soil (WFPS) (Liáng et al., 2018; Wecking et al., 2020b). All auxiliary measurements were conducted in a fenced-off enclosure around the EC tower with results representing both paddocks. The net ecosystem productivity (NEP) used for comparison made in the result section based on measurements of the net ecosystem exchange (NEE) of CO_2 using a CO_2/H_2O gas analyser (LI-7200, LI-COR); see Wall et al. (2020b) and Pronger et al. (unpublished) for details regarding the instrument set-up, footprint-splitting, gap-filling, and carbon balance calculations. Following Woodwell and Whittaker (1968), NEP is the difference between gross primary production and total ecosystem respiration, equal in magnitude but opposite in sign to NEE.

4.3.3.2 Data processing

Resulting F_{N2O} data were processed following the standardised guidelines by Nemitz et al. (2018) and as described by Wecking et al. (2020b). After filtering of 66 days (10 March to 15 May 2018) worth of half-hourly F_{N2O} data (n = 3168), 52.6 % (n = 1665) of these F_{N2O} remained at best quality flag 0 with no negative F_{N2O} determined. In the following, filtered F_{N2O} that met the flag 0 quality control criterium were denoted by F_{N2O_F} (filtered, full-footprint), F_{N2O_CF} (control), and F_{N2O_RF} (renewal) when distinguished by source-area after footprint-splitting.

4.3.3.3 Split-footprint approach

Previous research at Troughton farm (Wall et al., 2020b; Goodrich et al., 2021) and elsewhere (Fuchs et al., 2018) has shown that a split-footprint approach can be used experimentally to study the effect of spatially different treatments but measured by only a single EC system (Baldocchi, 2019). We utilised the analytical footprint model of Kormann and Meixner (2001) and at first calculated the contribution (footprint fraction) of the measured half-hourly F_{N2O} from each paddock of interest which resulted in a data set of two times 1655 contribution values (i.e. one for each paddock). In a second step, calculated footprint fractions from the investigated source areas (P53, P54) were used in conjunction with a footprint fraction rejection threshold. The

rejection threshold served as an additional selection criterion to determine whether F_{N2O_CF} and F_{N2O_RF} were representatives of the measurement area. The rejection threshold in this study was 70% for day time F_{N2O_F} (photosynthetic photon flux density, PPFD ≥ 20 μmol m^{-2} s^{-1}) and 60% for night time F_{N2O_F} (PPFD < 20 μmol m^{-2} s^{-1}) based on Wall et al. (2020b). This means, half-hourly F_{N2O_F} were only considered to have originated from either the renewal or the control site when at least 70% (or 60% at night) of the averaged half-hourly F_{N2O_F} originated from P53 (F_{N2O_CF}) or P54 (F_{N2O_RF}). The rejection threshold of 70% during the day and 60% at night was the best compromise between data quantity (lower rejection threshold) and certainty of the source area (higher rejection threshold) (Wall et al., 2017). Increasing the rejection threshold would have severely reduced the number of data available for gap-filling whereas lowering the rejection threshold would have led to an unsatisfactory certainty about F_{N2O} source areas. The chosen rejection thresholds provided the best compromise and best-possible certainty that F_{N2O} were sourced from P53 and P54. Other F_{N2O} from outside the paddock boundaries held only a small natural share.

4.3.3.4 Gap-filling

We used a recently developed gap-filling approach by Goodrich et al. (2021), which was based on partial least squares (PLS) decomposition (Wold et al., 1987) rather than other gap-filling techniques e.g., 30-day running medians (Merbold et al., 2020), linear interpolation (Liáng et al., 2018) and general additive models (Cowan et al., 2020). Input variables for the training sets were derived from a suite of meteorological and ancillary environmental data measured at the EC site. Additionally, cross-products between these parameters and all possible combinations were computed including running maximums and 30-day running medians calculated from filtered F_{N2O_F} data.

To estimate missing F_{N2O} values, PLS loadings were used as input to a k-nearest neighbour (kNN) locally-weighted regression and a three-layer artificial neural network (ANN) with error back-propagation. Both these algorithms were trained repetitively (n = 50 runs) using different training sets for each run, ultimately, feeding into the PLS. The kNN algorithm resulted in the lowest bias and best accounted for variance in the observed validation data compared to ANN. The gap-filled fluxes (F_{N2O_G}) presented in the following sections originated from the kNN approach and, when distinguished by source area, were denoted as F_{N2O_CG} (control) and F_{N2O_RG} (renewed). Finally, total N_2O emissions were derived from individual cumulative sums of gap-filled F_{N2O_CG} and F_{N2O_RG}, and converted to kg N_2O-N ha^{-1}. Instead, filtered F_{N2O_F}, F_{N2O_CF} and F_{N2O_RF} were used when cumulative totals were not required.

4.4 Results

4.4.1 Environmental conditions

The pasture renewal was undertaken in the New Zealand (Southern Hemisphere) autumn season, March to May 2018, and all 66 days of the study period lay within this season. Half-hourly air temperatures ranged between 1.6°C and 24.6°C. The daily mean air temperature across the measurement period was 15.2°C. Rainfall totalled 241 mm during the study period. More than half of this amount occurred in April, i.e. during a few days in mid-April (54.5 mm) and at the end of the month (87.5 mm) (Fig. 4-2a). Precipitation occurred on 37 of 66 days. The first rain event (28.6 mm) was received on the third day after herbicide application, 12 March. Consecutive rainfall was recorded daily during the last 13 days of March, albeit of smaller magnitude ≤ 10 mm, and on the last four days of the measurement period (33 mm). The mean water-filled pore space (WFPS) of the soil was 71%, and the half-hourly maximum and minimum WFPS were 91% and 62%, respectively (Fig. 4-2a). The wind direction varied with a slight predominance (41.8%) from south to west (175–285°).

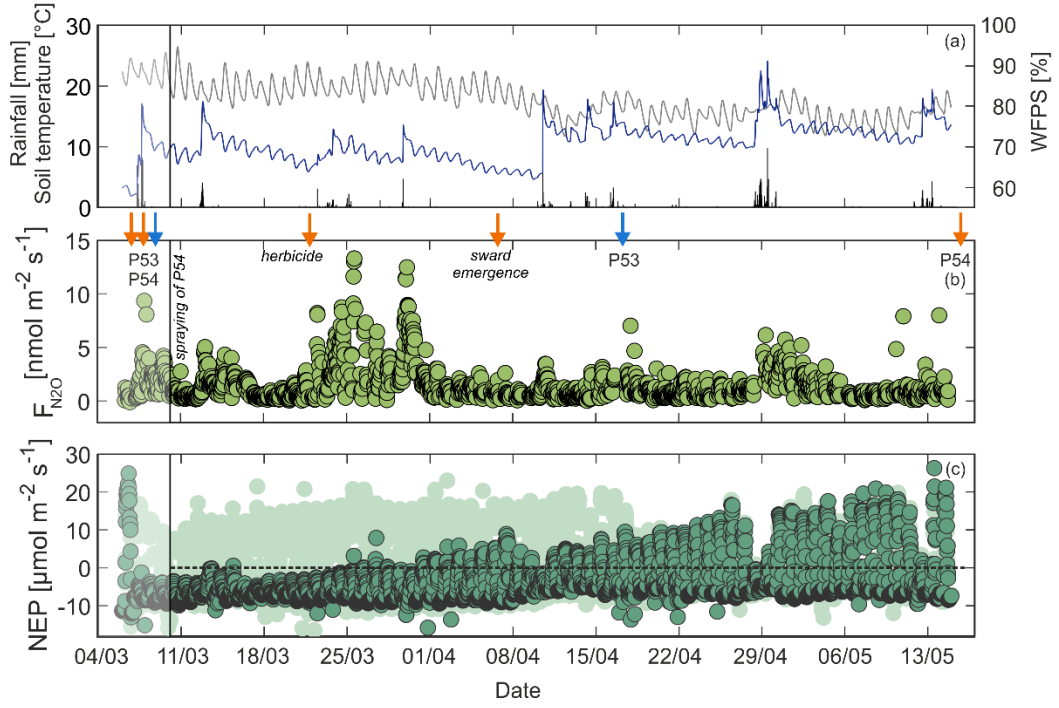

Figure 4-2 Environmental variables, filtered half-hourly fluxes (F_{N2O}), and net ecosystem production (NEP) for the first 66 days after renewal. Panel (a) shows site precipitation (black bars), soil water-filled pore space (WFPS, blue line), and soil temperature (grey line) both at 5 cm soil depth; (b) depicts filtered (green circles) F_{N2O}, arrows indicate farm management interventions including grazing on P53 (orange) and P54 (blue); (c) presents the NEP of the pasture sward at the renewed paddock P54 (turquoise circles) and the control P53 (light turquoise circles).

4.4.2 Net ecosystem productivity

On 10 March, the daily NEP was -1.0 g C m^{-2} for P53 (control) and -6.0 g C m^{-2} for P54 (renewal) implying that both paddocks were a source of CO_2 (Fig. 4-2). Both paddocks had been grazed immediately prior (6–8 March) to herbicide application on P54 and so the amount of available plant biomass in the EC footprint had already been decreased. Negative values of daily NEP were measured from the beginning of the measurement period for both paddocks comprising the first 27 consecutive days on P53 and 49 days on P54, respectively. The difference in daily NEP between P53 and P54 became most apparent from 10 March to 8 April, i.e. the time when the difference between daily paddock NEP was consistently ≥ -2.0 g C m^{-2} d^{-1}. Within this period, the greatest difference between P53 and P54 daily NEP (-6.2 g C m^{-2}) was observed on 21 March. This difference decreased slowly, but steadily, with time and was found near-zero from 14 April to the end of the measurement period. On the same day (14 April), cattle grazing was recorded on P53, but this did not affect the difference in daily NEP between P53 and P54 which remained at near-zero.

4.4.3 Nitrous oxide fluxes

The total number of measured half-hourly F_{N2O} was 3168, 52.6 % of which were in the flag 0 category (high quality). After filtering and footprint-splitting, 10.8% (n = 342) and 16.6% (n = 525) of these F_{N2O_F} remained at best quality for paddocks P53 and P54, respectively. Large pulse fluxes on P54 were evident in both these F_{N2O_F} and the F_{N2O_G} data retrieved from the gap-filling approach. After gap-filling, 6.5% of all F_{N2O_CG} and 24.2% of all F_{N2O_RG} were > 2.0 nmol N_2O m^{-2} s^{-1}. Furthermore, 5.7% of all F_{N2O_RG} were > 5.0 nmol N_2O m^{-2} s^{-1} while only less than 0.1% (n = 4) of all half-hourly F_{N2O_CG} were identified as pulse fluxes of this magnitude (Table 4-1). The greatest half-hourly F_{N2O_F} was 13.0 nmol N_2O m^{-2} s^{-1} measured on P54 on 25 March, the day with the greatest difference of daily mean F_{N2O_G} between the renewed and the control paddock (i.e. 6.5 nmol N_2O m^{-2} s^{-1}) (Fig. 4-3a).

The divergence of F_{N2O_RG} from F_{N2O_CG} became most apparent between 18 March and 1 April when the daily mean flux from P54 was consistently 1.5 nmol N_2O m^{-2} s^{-1} greater than on P53 and half-hourly F_{N2O_RG} exceeded low magnitude fluxes by far. Control F_{N2O_CG} remained at around low magnitude for most of this time (Fig. 4-3) and pulsed fluxes before renewal intervention were only observed for the first six days after grazing on P53 and in the days around 29 April following animal grazing in mid-April. The latter grazing event caused mean daily F_{N2O_CG} to increase and exceed F_{N2O_RG} on

the subsequent days of measurements (except 9–11 May). At the end of the measurement period, total N_2O emissions were 2.61 kg N_2O-N ha^{-1} for P54 and 1.39 kg N_2O-N ha^{-1} for P53 (Fig. 4-4). More than half of the total N_2O emissions from P54 occurred in March (1.59 kg N_2O-N ha^{-1}), i.e. which was 1.14 kg N_2O-N ha^{-1} more than emitted from P53 at the same time. In April and May, the difference in N_2O emissions between the control and the renewed paddock was near-equal and only slightly greater for P54 in April (+0.07 kg N_2O-N ha^{-1}) and P53 in May (+0.06 kg N_2O-N ha^{-1}).

Further, it was found that F_{N2O_F} were interdependent on environmental drivers, i.e. soil temperature but particularly rainfall and the associated subsequent increase in WFPS (Fig. 4-5). The large pulsed F_{N2O_FR} observed on P54 in March were likely favoured by small but consecutive rainfall events and a WFPS varying between 60–80% that triggered, if not promoted, the transformation of soil N_r to N_2O. More generally, the dependency between precipitation, variability of WFPS in the ideal zone of soil N_2O production, and occurring F_{N2O} appeared ubiquitous and was observed on both paddocks across the 66-day measurement period (Fig. 4-2a).

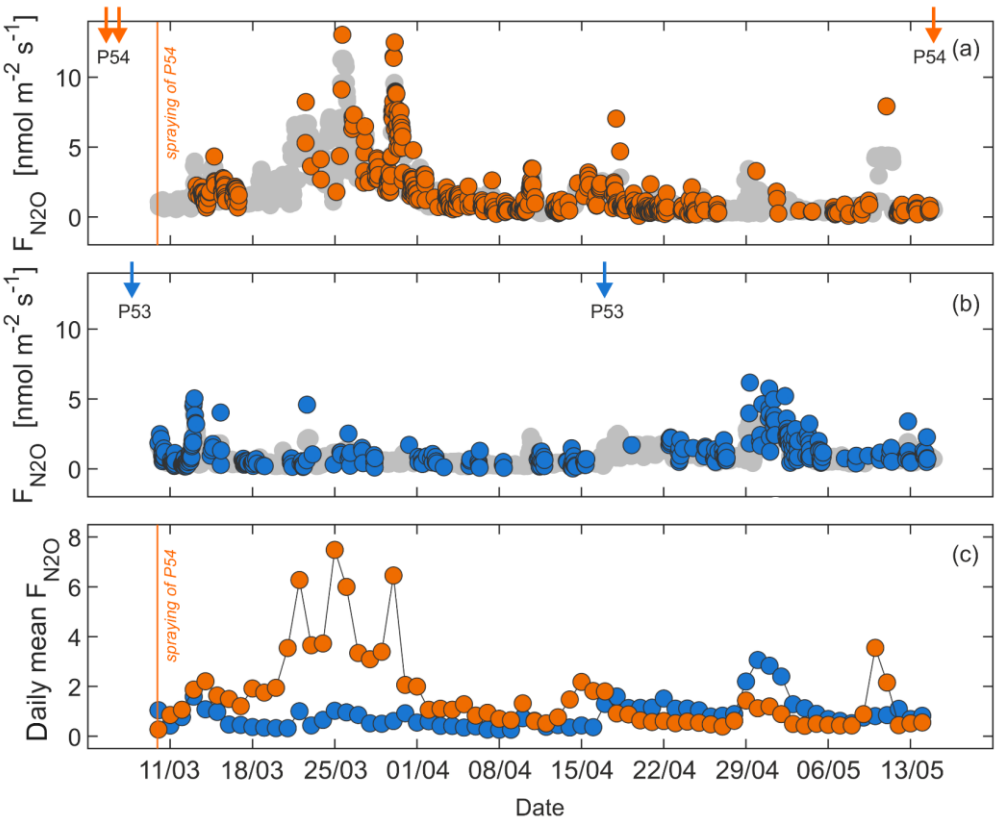

Figure 4-3 Half-hourly F_{N2O} distinguished in filtered (coloured circles) and gap-filled (grey circles) data with (a) depicting filtered (F_{N2O_RF}) and gap-filled (F_{N2O_RG}) fluxes at P54, and (b) filtered (F_{N2O_CF}) and gap-filled (F_{N2O_CG}) fluxes at P53. Panel (c) shows mean daily F_{N2O_RG} (orange circles) and F_{N2O_CG} (blue circles). Arrows indicate grazing events and the dashed vertical line refers to the date of spraying on P54, 10 March 2018.

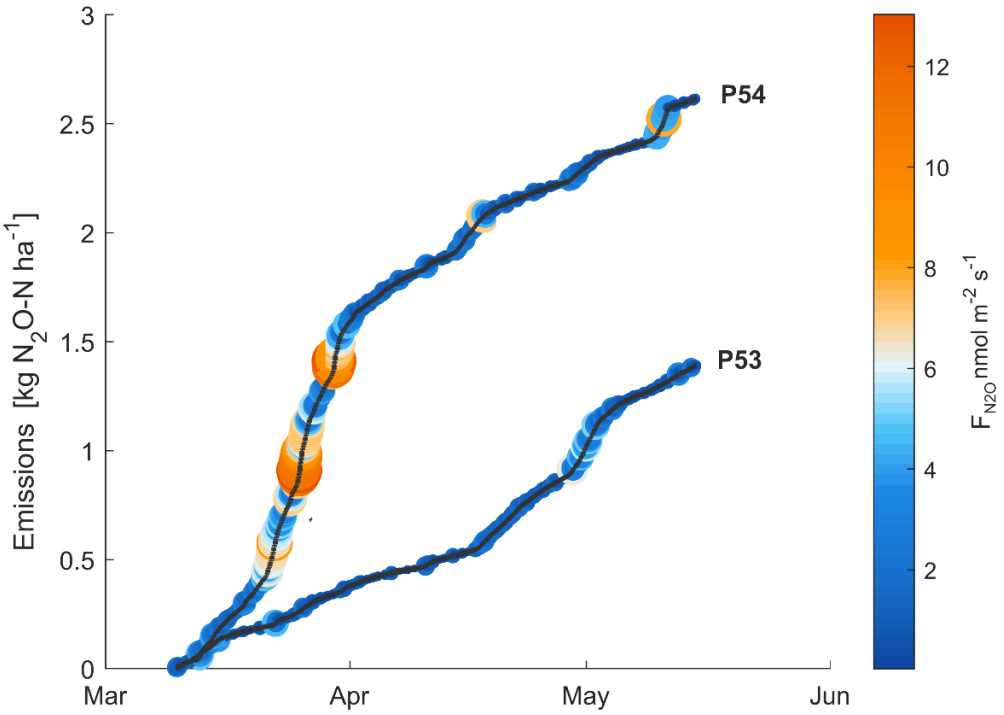

Figure 4-4 Cumulative sums of gap-filled F_{N2O} (kg N_2O-N ha^{-1}) for the 66-day study period. Contributions are distinguished by paddock, i.e. P53 (control) and P54 (renewed). Circle size and colour scheme change with flux magnitude (see scale at the right-hand side).

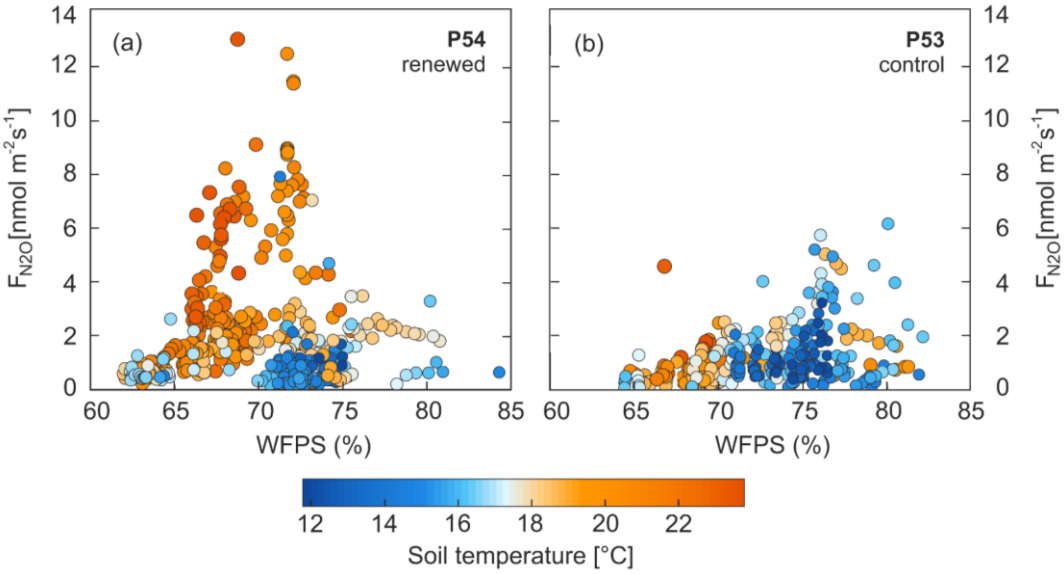

Figure 4-5 Relationship between water-filled pore space (WFPS) of the soil, soil temperature and filtered half-hourly N_2O fluxes (F_{N2O_F}) distinguished by paddock. Panel (a) shows the effect of soil water-filled pore space (WFPS) and soil temperature (colour bar) on F_{N2O_F} on the renewed P54 and (b) depicts the same for the control, P53.

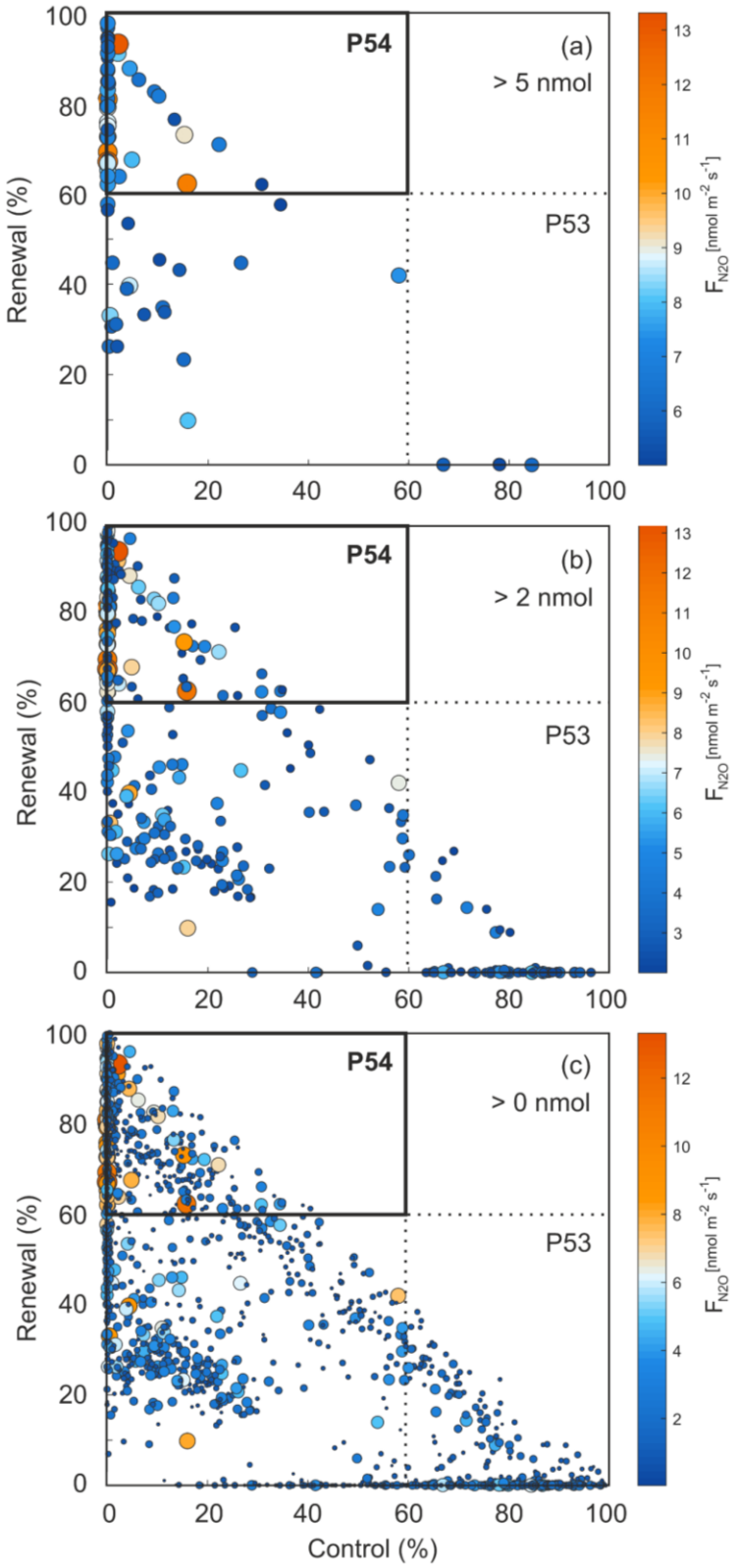

Figure 4-6 Percentage contribution of filtered half-hourly N_2O fluxes (F_{N2O_F}) from the control (P53) and renewed paddock (P54). The contribution of each F_{N2O_F} is presented as a percentage (%) value that indicates which F_{N2O_F} originated from P53 and which from P54. Note that circle size and colour scheme change with flux magnitude. Circles above and to the right of the dotted 60% contribution line show F_{N2O_F} that were attributable to either P53 or P54. All other fluxes (i.e. those below the horizontal 60% line and to the left of the vertical 60% line) shared a contribution across the footprint area of both paddocks or originated partly from outside the paddocks' boundary. Panel (a) shows pulsed $F_{N2O\_F} \geq 5$ nmol N_2O m^{-2} s^{-1}, panel (b) pulsed $F_{N2O\_F} \geq 2$ nmol N_2O m^{-2} s^{-1}, and panel (c) all measured best quality F_{N2O_F}.

4.4.4 The renewal effect

To add further confidence to the gap-filling approach, we were interested in whether a renewal effect would have also been observed if F_{N2O_G} data had not been used and the analysis had been solely based on filtered F_{N2O_F} and footprint-splitting. For this purpose, we assorted all best quality F_{N2O_F} (n = 1665, flag 0) by their percentage paddock contribution derived from the footprint-splitting analysis explained in Section 4.3.3.3 (Fig. 4-6). We then examined the number of individual half-hourly F_{N2O_F} from each paddock that fell above or below an established 60% contribution threshold. After applying this threshold, 387 half-hourly F_{N2O_F} were assorted by their origin to P53 and 623 F_{N2O_F} to the renewed site, P54 (Table 4-1). The remaining half-hourly F_{N2O_F} (n = 655) were not spatially assigned to one of the two paddocks sites, i.e. shared a contribution across P53 and P54 or even originated from outside the paddocks' boundary.

Building on the findings from Section 4.4.3, we found that pulsed F_{N2O_F} often remained discrete from more regularly occurring F_{N2O_F} of lower magnitude. To distinguish these pulsed F_{N2O_F} from F_{N2O_F} of lower magnitude, we classified all F_{N2O_F} ≤ 0.6 nmol N_2O m^{-2} s^{-1} as background fluxes following Liang et al. (2018). Using this differentiation, our results then showed that 15.5% and 1% from F_{N2O_CF} on P53 were determined pulsed fluxes > 2 nmol N_2O m^{-2} s^{-1} (n = 60) and > 5 nmol N_2O m^{-2} s^{-1} (n = 4), respectively (Fig. 4-6). In contrast, the contribution from pulsed F_{N2O_RF} observed on P54 was higher, i.e. 26.2% for fluxes > 2 nmol N_2O m^{-2} s^{-1} (n = 163), and 7.9% for those at a magnitude > 5 nmol N_2O m^{-2} s^{-1} (n = 49). Higher contribution of F_{N2O_RF} indicated that the majority of pulsed F_{N2O_F} originated from P54, not P53. Plotting F_{N2O_F} by flux magnitude and associated wind direction supported this finding with high pulsed F_{N2O_F} similarly and predominately sourced from P54 (Fig. 4-7).

Table 4-1 Number of N_2O fluxes (F_{N2O}) differentiated by magnitude in the left-hand side column of the table and distinguished into filtered (F_{N2O_F}) and gap-filled (F_{N2O_G}) data by paddock contribution (P53, P54) on the right-hand side. Gap-filling substantially increased the number of half-hourly F_{N2O} available for subsequent data analysis.

F_{N2O}	**F_{N2O_F}**				**F_{N2O_G}**			
nmol N_2O m^{-2} s^{-1}	P53		P54		P53		P54	
	[n]	[%]	[n]	[%]	[n]	[%]	[n]	[%]
F_{N2O} > 0	387	100.0	623	100.0	3168	100.0	3168	100.0
F_{N2O} > 2	60	15.5	163	26.6	206	6.5	768	24.2
F_{N2O} > 5	4	1.0	49	7.9	4	0.1	182	5.7

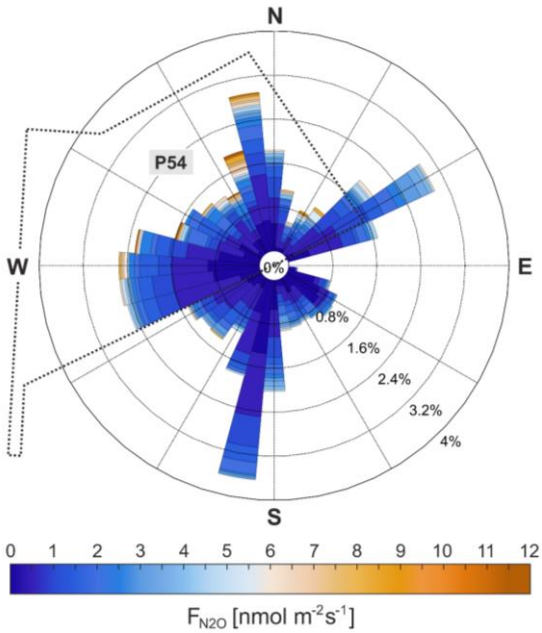

Figure 4-7 Windrose showing the prevailing direction of the wind (orientation of the bars) in the EC footprint and the percentage contribution of filtered half-hourly fluxes (F_{N2O_F}) (length of the bars) associated with each wind direction. The magnitude of F_{N2O_F} in nmol N_2O m^{-2} s^{-1} is highlighted by the colour gradient of each bar and refers to the legend at the bottom. The location of the renewed paddock is referenced by the dotted line, but not drawn to scale.

4.5 Discussion

4.5.1 Short-term effect of pasture renewal on nitrous oxide fluxes

Renewal alters the carbon and nitrogen cycling of pasture soils and can lead to nutrient losses both in short- and long-term (Kayser et al., 2018). As shown by several studies, losses of N_r in the form of gaseous N_2O are relatively short-lived with the majority often occurring immediately in the first months after renewal intervention (Davies et al., 2001; Mori and Hojito, 2007; Velthof et al., 2010; MacDonald et al., 2011; Cowan et al., 2016; Krol et al., 2016b; Buchen, 2017). At our site, the majority of pulsed F_{N2O_R} were measured between 18 March and 1 April 2018 when cumulative F_{N2O_G} from the renewed P54 exceeded those from the control site by 1.14 kg N_2O-N ha^{-1}. This means that 93.4% of the difference (1.22 kg N_2O-N ha^{-1}) between P53 and P54 emissions occurred in only two weeks of the overall 66-day study period (Fig. 4-4). For the remaining 52 days, there was no distinct difference in paddock N_2O emissions determined apart from some F_{N2O_C} that were associated with grazing on P53, 17 April, and coincided with rainfall. The short-term nature of the observed pulsed F_{N2O_R} shortly after renewal intervention on P54 was somewhat surprising. Conducting EC measurements in a high N_r regime, we initially thought that the renewal effect would have extended over greater temporal scales e.g., as caused by prolonged mineralisation of soil N_r, and might not have been as distinct in magnitude due to potential

superordinate effects of environmental drivers on the soil N_2O exchange. Instead, the immediate renewal effect on F_{N2O_R} from P54 appeared only temporary but included relatively high half-hourly (max. 13.03 nmol N_2O m^{-2} s^{-1}), daily mean F_{N2O_R} (7.50 nmol N_2O m^{-2} s^{-1}) and cumulative emissions (1.59 kg N_2O-N ha^{-1} in March), especially, when considering the use of a no-till renewal technique and the short two weeks' period within which these pulsed F_{N2O_R} occurred. Likewise using EC measurements, Cowan et al. (2016) reported that tillage of a managed pasture in Scotland contributed an additional 0.85 ± 0.11 kg N_2O-N ha^{-1} to the emission budget of the first two months post-renewal. Other research on grasslands based on chamber measurements has shown that short-term losses of N_2O can range between 0–3.30 kg N_2O-N ha^{-1} in the first months after conversion (Davies et al., 2001; Skiba et al., 2002; Pinto et al., 2004; Grandy and Robertson, 2006). Nitrous oxide emissions associated with pasture renewal at our site were not as high as reported by some of these other studies.

Merbold et al. (2020), for instance, observed F_{N2O} peaks for almost seven continuous months after ploughing conversion of a Swiss grassland with annual pasture N_2O emissions 13.5-times higher than in non-renewal years (chosen as the control). In contrast, N_2O emissions on P54 were only 1.8-times higher than those of control P53, which was likely related to the initial, but very short-termed nature, of the emission pulse. The difference in magnitude compared well with findings from Velthof et al. (2010), who showed that pasture renewal increased N_2O emissions by a factor of 1.8–3.0 when compared to an undisturbed control. However, unlike Velthof et al. (2010) we did not further determine the effect of different renewal techniques on N_2O emissions and opposing to Merbold et al. (2020), our study was limited to 66 days. The increase in N_2O emissions can be, but is not always, associated with increasing sward and soil disturbance, i.e. the conversion technique chosen (Buchen et al., 2017; Helfrich et al., 2020).

From pasture renewal events conducted on the same research site in previous years, we know that chemical killing and direct drilling, instead of ploughing, did not result in lower daily rates of respiratory CO_2 losses (Rutledge et al., 2017b). Since the grassland carbon and nitrogen cycles are closely interlinked, the same might have been the case for N_2O, meaning that a change of pasture renewal technique would not have led to any major difference in the amount of N_2O lost. Nonetheless, it might have been likely that choosing a different renewal technique could have led to different responses in sward re-establishment and long-term yields (Powell et al., 2007; Kayser et al., 2018; Gaweł and Grzelak, 2020).

4.5.2 Potential drivers of nitrous oxide emissions

Emissions of N_2O after grassland renewal have been acknowledged to be driven by the increase in net soil nitrogen mineralisation due to the accelerated decomposition of plant litter (Reinsch et al., 2018b; Helfrich et al., 2020). Although changes in soil mineralised nitrogen (N_{min}) were not measured at our site, we believe that this effect contributed to the observed pulsed F_{N2O_R} on P54. Firstly, after the death of the old sward there was little to no nitrogen uptake by plants and, secondly, net mineralisation of plant residues and SOM were possibly enhanced providing readily-available N_r to microbes in the topsoil (Grandy and Robertson, 2006; Velthof et al., 2010; Kayser et al., 2018). Buchen et al. (2017), for instance, found that the amount of N_{min} in the upper 0–30 cm of a pasture soil increased by 48% for the first two months after herbicide application and direct-drilling.

Similar findings were reported by Davies et al. (2001), Vertes et al. (2007), and Velthof et al. (2010) – showing that using a no-till conversion technique led to the decomposition and mineralisation of plant residues and roots almost entirely on the soil surface and in the upper topsoil (Groffman, 1985; Helfrich et al., 2020). An immediate protection and complete incorporation of freshly formed particulate organic matter into new soil aggregates, as observed in tilled soils, was, therefore, more unlikely at our site (Tisdall and Oades, 1982; Balesdent et al., 2000). Instead, the net mineralisation of nitrogen might have been predominantly triggered by the decomposition of sward litter and the availability of labile organic carbon, which soil microbes could have accessed and used as an energy source (Reinsch et al., 2018b).

Also, the observed pulsed F_{N2O_R} might not have only been caused by accelerated decomposition rates but were likely associated with an increased general availability of N_r in the renewed paddock. Reactive soil nitrogen could have easily accumulated in the soil during previous grazing events prior to intervention and, thus, might have still been present for its subsequent reactivation and mineralisation following renewal-related soil disturbances. Between 18 March and 1 April, the rate of daily F_{N2O_RG} increased to a maximum of 91.3 g N_2O-N ha^{-1} d^{-1} and was likely related to a combined contributions of the before-mentioned factors, particularly when compared with the control site (15.1 g N_2O-N ha^{-1} d^{-1}).

Based on research conducted in the previous autumn season (2017), we knew that the daily rate of F_{N2O} at our site can be three to five times higher in autumn than in any other season (Liáng et al., 2018; Wecking et al., 2020b). In autumn, soil temperature

and WFPS tend to fluctuate around the optimal zone of soil N_2O production and favour the simultaneous occurrence of microbial nitrification and denitrification in the soil, ultimately, leading to N_2O losses (Firestone and Davidson, 1989; Coyne, 2018; Liu et al., 2018). We anticipated that fluctuations in natural drivers would add to the observed pulse F_{N2O_R} on P54, particularly, in the presence of readily available N_{min}. The overarching effect of natural drivers and their high variability also helped explain why pulsed F_{N2O_RF} were mainly observed around the ideal zone of soil N_2O production, i.e. a WFPS of 62–91% and higher soil temperatures (Fig. 4-5). Regarding temperature, the transformation of denitrified-nitrogen towards N_2O could have been promoted by accelerated enzymatic activity which is sensitive to temperature changes (Phillips et al., 2014; Liu et al., 2018). Mori and Hojito (2007) found that the temperature in the upper centimetres of a pasture soil after renewal was 2.7–3.0°C higher than at control sites due to higher inputs of solar radiation and, simultaneously, less insulation by plants.

Finally, understanding the effect of environmental drivers in relation to management interventions on the ever-changing pattern of soil F_{N2O} can be highly beneficial to plan management interventions and mitigation actions accordingly. Liáng et al. (2018), for instance, showed that the contribution of F_{N2O} pulses to total annual N_2O emissions at our site in the year before renewal intervention was around 40% of the total 6.5 kg N_2O-N ha^{-1} emitted. Currently, the significance of short-term N_2O pulse emissions for annual greenhouse gas budgets remains debated (Necpálová et al., 2013; Krol et al., 2016b; Buchen, 2017; Merbold et al., 2020). However, accounting for the effect of these pulsed F_{N2O} in farm emission budgets, even if short-term, might be urgently needed to identify potential off-setting mechanisms between the soil carbon and nitrogen cycle and, ultimately, to establish robust greenhouse gas accounting.

4.5.3 Rapid reseeding as a potential mitigation strategy

The rapid establishment of a new pasture sward is crucial to counterbalance the vulnerability of the soil to nutrient losses via leaching and gaseous emission by quickly reinforcing plant N_r uptake and carbon inputs via rhizodeposition (Necpálová et al., 2013; Reinsch, 2014; Krol et al., 2016b). In this study, we were interested whether shortening the time between conversion and seedling establishment would also decrease the impact of renewal intervention on these losses, i.e. could mitigate the renewal effect on N_2O emissions. At our farm site, this was previously demonstrated for the loss of SOC by Rutledge et al. (2017b) who found that the soil returned to being a carbon sink within 51–78 days after herbicide application and direct-drilling.

Based on this knowledge, the gap between herbicide application and direct-drilling was held intentionally short (four days) with seedling emergence first observed on day 13 after spraying (22 March 2018). However, when comparing the date of seedling emergence on P54 with pulse F_{N2O_R}, it became apparent that these were coinciding and seedling emergence did not initially prevent large F_{N2O_R}. Pulse F_{N2O_R} eased 21 days after herbicide application (1 April) when the photosynthetic activity of the young sward improved and the difference in daily NEP between P53 and P54 started to decrease. A second F_{N2O_R} pulse of similar magnitude was not observed on P54 apart from some higher than background F_{N2O_R} (> 0.6 nmol N_2O m^{-2} s^{-1}) occurring in response to occasional rain events throughout April and May (Fig. 4-2a). These F_{N2O_R} were likely caused by the short-term increase in soil moisture and the availability of NO_3^- fuelling microbial denitrification, but were still far from the magnitude of pulsed F_{N2O_R} observed during the first weeks after renewal intervention in March (Bouwman, 1996; Kim et al., 2013; Wecking et al., 2020b). Also, as control F_{N2O_C} from P53 showed a similar response to increases in WFPS, later pulsed F_{N2O_R} on P54 appeared to be predominantly driven by environmental factors rather than after-effects of the renewal intervention (Wallenstein et al., 2006; Butterbach-Bahl et al., 2013; Liáng et al., 2018).

Considering the short-term nature of this study, it was not clear if and how direct-drilling and rapid reseeding affected pasture productivity in the longer-term or to what degree it might have resulted in the loss of SOC. From Pronger et al. (unpublished) we know there might have been trade-offs between reducing nutrient losses by choosing a no-till approach and increasing disturbance such as ploughing. Some literature suggested that ploughing can increase the productivity of a new sward in the long-term with emerging seedlings benefiting from an excess release of nutrients after intervention (De Vliegher and Carlier, 2007; Reinsch et al., 2018b). In contrast, using no-till approaches might prevent access of the new sward to nitrogen released after renewal, hinder seedling emergence by leaving plant litter on the soil surface and favour emerging weeds (Helfrich et al., 2020). The latter effect was observed on P54, where the emergence of weeds concurrent with seedling germination and required an additional herbicide application on 7 April. Ideally, a no-till renewal technique should aim for a good establishment and long-lasting performance of the new sward (Davies et al., 2001; Thom et al., 2011; Reinsch, 2014; Pronger et al., unpublished).

4.5.4 Evaluation of footprint-splitting and associated gap-filling

In this study, we used a single EC system to allow for the direct comparison of F_{N2O} from adjacent, but differently managed, paddocks. This approach eliminated the spatial

separation between renewed and control paddocks and decreased the likelihood of differences in soil and site characteristics that influence F_{N2O}. Helfrich et al. (2020) and others (Buchen et al., 2017; Reinsch et al., 2018b) showed that differences between sites can have a much greater influence on N_2O emissions than differences between individual treatments depending on soil type, site management, and overall environmental conditions. Other advantages of the approach were: 1) the reduction of equipment costs; and 2) the avoidance of mixed signals (i.e. individual half-hours with F_{N2O} contributions across multiple paddocks), which is important for the performance and robustness of F_{N2O} measurements in intensively grazed systems (Wall et al., 2020b; Pronger et al., unpublished). However, it has to be considered that using a split-footprint approach decreases the data availability for each treatment/paddock (Cowan et al., 2016; Fuchs et al., 2018). This also applied to our study, where only 10.8% (P53) and 16.6% (P54) of all measured F_{N2O_F} remained at best quality after filtering and footprint-splitting. Having said this, we re-designed the paddock layout before renewal intervention to avoid additional biases in F_{N2O} data caused by the dependence of the flux footprint on the prevailing wind direction (Kormann and Meixner, 2001). A visual examination of half-hourly F_{N2O_RF} and F_{N2O_CF} showed that P54 and P53 footprints received a consistent flux contribution throughout the 66-day study period and any biasing from a disproportionate number and lengths of gaps, as reported by Cowan et al. (2016), was unlikely (Fig. 4-3).

Furthermore, the data coverage of F_{N2O_RF} and F_{N2O_CF} after filtering and footprint-splitting was still far greater than could have been achieved by static chambers (Krol et al., 2016b; Buchen et al., 2017; Reinsch et al., 2018b). Chamber measurements are usually conducted at once-daily to weekly or bi-weekly intervals to capture the best representative average of daily F_{N2O} but generally do not approach the temporal resolution of micrometeorological techniques (and the "when") necessary to identify short-term management effects on F_{N2O}, unless automated (Rochette and Eriksen-Hamel, 2008; Jones et al., 2011). In our study, we demonstrated that using filtered F_{N2O_RF} and F_{N2O_CF} would have been sufficient to determine that there was a short-term effect of pasture renewal on P54 (Fig. 4-6, Sec. 4.4.4).

However, the renewal effect became more apparent and better quantifiable when including the additional resolution of gap-filled F_{N2O_RG} and F_{N2O_CG}. Distinguishing these F_{N2O} on a paddock and treatment basis resulted in a total difference between P54 and P53 N_2O emissions of 1.22 kg N_2O-N ha^{-1} (Fig. 4-4). Previously, Wall et al. (2020b) suggested that reporting of cumulative flux data by individual paddocks rather than

aggregating across multiple fields can be very beneficial (even if all paddocks were under the same treatment). Our findings confirm that using the gap-filling approach by Goodrich et al. (2021) was able to distinguish management-induced differences in short-term F_{N2O} at paddock scales. Finally, using robust footprint-splitting and gap-filling will be of great relevance when evaluating the effect of any given mitigation strategy on N_2O emissions from adjacent paddocks in the future (Goodrich et al., 2021). This applies, in particular, to rotationally grazed dairy pastures, where the measurement of greenhouse gas emissions is challenged by day-to-day farm management (Wall et al., 2020b).

4.6 Conclusion

In this study, we used a single QCL EC system measuring across two adjacent paddocks to determine the short-term effect of pasture renewal on F_{N2O} in an intensively grazed dairy pasture. We found that F_{N2O} from the renewed paddock (P54) occurred in a distinct pulse from day eight after herbicide application onwards, however, weakened with increasing photosynthetic activity of the growing sward only 21 days after renewal intervention. The difference in paddock N_2O emissions for this short period was 1.14 kg N_2O-N ha^{-1}, i.e. equal to 93.4% of the total relative difference between the two paddocks within the 66-day study period. Utilising a rapid reseeding technique enabled seedling emergence eight days after sowing and likely contributed to mitigate the loss of N_2O in the longer term. However, the renewal effect on P54 was not only defined by anthropogenic disturbances made to the soil system via herbicide application and direct-drilling but also strongly controlled by environmental drivers, particularly WFPS. The effect of environmental drivers on F_{N2O} was persistent throughout the study period.

Overall, our findings showed that using footprint-splitting and advanced gap-filling allowed for the comparison of treatment effects on the soil N_2O exchange of adjacent paddocks using a single EC system. Previously, gap-filling micrometeorological F_{N2O} data has been a major constraint in producing defensible N_2O emission budgets at paddock scales and here we could highlight that applying a gap-filling approach based on machine learning tools can overcome this challenge, particularly, if preconditions, such as site selection and experimental design, are carefully considered. Gap-filled F_{N2O} datasets will help quantify greenhouse gas budgets in the future that include accounting for the effect of not only environmental drivers but also for trade-offs between different farm management/mitigation strategies and the associated nutrient loss from pastoral soil.

4.7 Acknowledgements

This research was funded by the New Zealand Agricultural Greenhouse Gas Research Centre (NZAGRC), AgResearch Ruakura, DairyNZ, and the University of Waikato. The authors like to acknowledge the fruitful cooperation with the farm owners, Sarah and Ben Troughton. Site maintenance work was gratefully received from Chris Morcom as was the continuous support from Aerodyne Research Ltd. We also like to point out the great network of MathWorks File Exchange providing free codes to the (research) community. Figures illustrated in this work were based in parts on MatLab functions provided by Pereira (2015) and Martínez-Cagigal (2020).

4.8 Author contributions

Author names: Anne R. Wecking (ARW), Aaron M. Wall (AW), Lìyǐn L. Liáng (LL), Louis A. Schipper (LS), Jordan P. Goodrich (JG), David I. Campbell (DC), Jack Pronger (JP), Jiafa Luo (JL).

ARW, AW, LL, and LS designed the experiment. ARW conducted the post-processing of F_{N2O} data using and developing MATLAB scripts based on the work from AW, LL, JG, and DC. JP made NEP data available. AW conducted the footprint-splitting. JG developed the gap-filling technique and provided this work with gap-filled F_{N2O} data. ARW made use of these data outputs, performed the result analysis, wrote and revised the manuscript with contributions from JG, AW, JP, DC, LL, JL, and LS.

Chapter Five

A Novel Injection Technique: Using a Field-based Quantum Cascade Laser for the Analysis of Gas Samples Derived from Static Chambers

5.1 Abstract

The development of fast-response analysers for the measurement of nitrous oxide (N_2O) has resulted in exciting opportunities for new experimental techniques beyond commonly used static chambers and gas chromatography (GC) analysis. For example, quantum cascade laser absorption spectrometers (QCL) are now being used with eddy covariance (EC) or automated chambers. However, using a field-based QCL EC system to also quantify N_2O concentrations in gas samples taken from static chambers has not yet been explored. Gas samples from static chambers are often analysed by GC, a method that requires labour and time-consuming procedures off-site. Here, we developed a novel field-based injection technique that allowed the use of a single QCL for 1) micrometeorological EC, and 2) immediate manual injection of headspace samples taken from static chambers. To test this approach across a range of low to high N_2O concentrations and fluxes, we applied ammonium nitrate (AN) at 0, 300, 600 and 900 kg N ha^{-1} (AN_0, AN_{300}, AN_{600}, AN_{900}) to plots on a pasture soil. After analysis, calculated N_2O fluxes from QCL (F_{N2O_QCL}) were compared with fluxes determined by a standard method, i.e. here laboratory-based GC (F_{N2O_GC}). Subsequently, the comparability of QCL and GC data was tested using orthogonal regression, Bland Altman and bioequivalence statistics. For AN treated plots, mean cumulative N_2O emissions across the seven-day campaign were 0.97 (AN_{300}), 1.26 (AN_{600}) and 2.00 (AN_{900}) kg N_2O-N ha^{-1} for F_{N2O_QCL}, and 0.99 (AN_{300}), 1.31 (AN_{600}) and 2.03 (AN_{900}) kg N_2O-N ha–1 for F_{N2O_GC}. These F_{N2O_QCL} and F_{N2O_GC} were highly correlated ($r = 0.996$, $n = 81$) based on orthogonal regression, in agreement following the Bland Altman approach (i.e. within ± 1.96 standard deviations of the mean difference) and shown to be for all intents and purposes the same (i.e. equivalent). The F_{N2O_QCL} and F_{N2O_GC} derived under near-zero flux conditions (AN_0) were weakly correlated ($r = 0.306$, $n = 27$) and not found to agree or to be equivalent.

This was likely caused by the calculation of small, but apparent positive and negative, F_{N2O} when in fact the actual flux was below the detection limit of static chambers. Our study demonstrated 1) that the capability of using one QCL to measure N_2O at different scales, including manual injections, offers a great potential to advance field measurements of N_2O (and other greenhouse gases) in the future; and 2) that suitable statistics have to be adopted when formally assessing the agreement and difference (not only the correlation) between two methods of measurement.

5.2 Introduction

Accurate measurements of nitrous oxide (N_2O) emissions from agricultural land are crucial to quantify the contribution of the gas's radiative forcing to climate warming (Thompson et al., 2019). Nitrous oxide is a long-lived greenhouse gas with a global warming potential 265-times higher than that of carbon dioxide (CO_2) over 100 years and is the largest contributor to the depletion of stratospheric ozone (Ravishankara et al., 2009; IPCC, 2013). Agricultural activities on intensively managed soils that receive high inputs of reactive nitrogen (N_r), mostly in the form of animal excreta and nitrogen fertiliser, are the main source of anthropogenic N_2O emissions (Reay et al., 2012). Reactive nitrogen facilitates microbial nitrification and denitrification in the soil with N_2O being an intermediate of these processes (Firestone and Davidson, 1989; Butterbach-Bahl et al., 2013). The production of N_2O in soils is controlled by a multitude of environmental and anthropogenic factors e.g., soil moisture, nitrogen input, and overall farm management, which often result in highly variable F_{N2O} (Flechard et al., 2007; Erisman et al., 2013; Rees et al., 2013). Adequate and precise flux measurements have, therefore, remained challenging (Rapson and Dacres, 2014; Cowan et al., 2020).

To date, the common method for measuring fluxes of N_2O (F_{N2O}) are closed, non-steady-state 'static chambers' (Lundegard, 1927; Hutchinson and Mosier, 1981); a method used for more than 95% of all field studies (Rochette and Eriksen-Hamel, 2008; Rochette, 2011; Lammirato et al., 2018). Static chambers are relatively cost-efficient and easy to deploy in the field (Velthof et al., 1996; de Klein et al., 2015). Gas samples are extracted from the chamber headspace during an up to 60-minute enclosure and injected into pre-evacuated glass vials (Rochette and Bertrand, 2003; Luo et al., 2007; van der Weerden et al., 2011). Subsequent analysis of the gas samples is commonly conducted off-site, using gas chromatography (GC) (Luo et al., 2008a; Parkin and Venterea, 2010). However, measurements using static chambers are discontinuous and labour-intensive with uncertainties in F_{N2O} caused by alterations

made to the soil environment after installation, pressure differences in the chamber headspace during sampling and the assumption of a linear increase/decrease in gas concentration with time (Denmead, 2008; Christiansen et al., 2011; Chadwick et al., 2014). Through time, different guidelines have been proposed to advance the standardisation of static chamber techniques (Rochette, 2011; de Klein et al., 2015; Pavelka et al., 2018); but essentially the basic method has remained unchanged for decades (Hutchinson and Mosier, 1981; Chadwick et al., 2014).

Alternative approaches to the static chamber method include the use of (semi-) automated chambers and micrometeorological techniques that allow F_{N2O} measurements at higher temporal frequency and resolution (Baldocchi, 2014; Rapson and Dacres, 2014; Pavelka et al., 2018). Recent developments in the technology of fast-response analysers have enabled e.g., tunable diode laser absorption spectrometers, Fourier transform infrared spectrometers, and in particular continuous-wave quantum cascade laser absorption spectrometers (QCL) to be coupled to automated chambers (Cowan et al., 2014; Savage et al., 2014; Brümmer et al., 2017) or eddy covariance (EC) systems (Nicolini et al., 2013; Nemitz et al., 2018). Despite these recent advances in analyser technology, our understanding of the micro and macro scale processes that lead to the emission of N_2O has yet remained limited. While chamber measurements help to examine the interaction between soil processes and F_{N2O} at point scale (Luo et al., 2017), EC promotes the understanding of diurnal, seasonal and annual F_{N2O} dynamics at field to ecosystem levels (Liáng et al., 2018; Cowan et al., 2020). Some studies have aligned chamber and EC measurements to determine the full range of processes that drive F_{N2O} dynamics across these different scales, but still these studies relied on the use of more than one analyser for measuring F_{N2O} (Jones et al., 2011; Tallec et al., 2019; Wecking et al., 2020a).

In this study, we tested whether a single field-deployed QCL could be used for manual injections of gas samples taken from static chambers to allow near-concurrent measurements of chamber N_2O samples alongside continuous EC. Field measurements using a QCL for both these purposes have, to our knowledge, not yet been conducted. Our objective was to examine whether chamber F_{N2O} determined by field-based QCL (F_{N2O_QCL}) were equivalent to F_{N2O} derived from laboratory GC (F_{N2O_GC}). An important component of this comparison was to demonstrate that manual injections into the QCL offer a robust method for the use in field environments. Our analysis, therefore, reached beyond the sole comparison of two analytic devices (QCL and GC) and also discussed the method real-world application.

Evidence of concept was provided by statistical tests to assess if the injection method would result in F_{N2O_QCL} equivalent to F_{N2O_GC}, these included: 1) orthogonal regression, 2) Bland Altman, and 3) bioequivalence analyses.

5.3 Methods

5.3.1 Study site

This study was conducted at Troughton Farm, a commercially operating 199 ha dairy farm in the Waikato region, 3 km east of Waharoa (37.78°S, 175.80°E, 54 m a.s.l.), North Island, Aotearoa New Zealand. The farm had been under long-term grazing for at least 80 years with micrometeorological measurements using a QCL EC system made since November 2016 (Liáng et al., 2018; Wecking et al., 2020a). Mean annual temperature and precipitation, recorded at a climate station 13 km to the south-west of the farm (1981–2010), were 13.3°C and 1249 mm, respectively (NIWA, 2018). The experimental site comprised three paddocks (P51, P53, P54) in the north of the farm with each sized about 2.8 ha. Soils were formed in rhyolitic and andesitic volcanic ash and rhyolitic alluvium. The dominant soil type based on the New Zealand soil taxonomy was a Mottled Orthic Allophanic soil (Te Puninga silt loam) (Hewitt, 2010). Plots used for the static chamber measurement of this study were located on P53 around 50 m to the south-west of the EC system. The physical distance between chamber plots and EC tower ensured that the EC footprint did not experience cross-contamination from any chamber F_{N2O} (Wall et al., 2020a).

5.3.2 Experiment design

One intensive field campaign was conducted between 10 and 16 September 2019. The campaign's primary purposes were to 1) manually collect gas samples from static chambers comprising potentially low to high N_2O concentrations (C_{N2O}); 2) analyse these samples on-site using QCL and off-site using GC; 3) quantify and compare resulting C_{N2O} and F_{N2O}. A thorough description of the QCL operating in EC mode has been provided by Liáng et al. (2018) and Wecking et al. (2020a).

5.3.2.1 Static chamber measurements

The static chamber trial comprised a randomised block design of circular treatment and control plots each of which included three replicates per treatment/control. Ammonium nitrate (AN) fertiliser was used as a treatment and applied at different rates to ensure production of a wide range of low to high C_{N2O} in the chamber headspace for subsequent measurements. The three application rates were 300 (AN_{300}),

600 (AN_{600}) and 900 kg N ha^{-1} (AN_{900}), while the control plots (AN_0) did not receive any AN. The rates of AN applied were to match nitrogen loading commonly found in cattle excreta patches, which is the main source of N_2O in grazed pastures (Selbie et al., 2015). Separate areas adjacent to the twelve chamber plots were established to collect soil samples for laboratory analyses of soil moisture and soil mineral nitrogen (N_{min}). Soil moisture and water-filled pore space (WFPS) were analysed and calculated using the methods described in Wecking et al. (2020a). Soil N_{min} was derived from field-moist soil samples extracted in 2M KCl (Mulvaney, 1996) and measured colourimetrically using a Skalar SAN++ flow analyser (Skalar Analytical B. V., Breda, Netherlands). Both, NH_4^+ and NO_3^-, were expressed in units kg ha^{-1} using a site-specific soil dry bulk density of 0.73 g cm^{-3} (Wecking et al., 2020a).

Chamber measurements were made on the day of treatment application and throughout the following six days with chamber gas samples collected on nine occasions (Table A3-1). The sampling followed a standardised chamber technique (de Klein et al., 2003; Luo et al., 2008b; de Klein et al., 2015) and was carried out daily at 10 AM (NZDT) (van der Weerden et al., 2013). Additional sampling was also conducted at noon on 12 and 15 September.

Before sampling, PVC lids were fitted to water-filled base channels that provided a gas-tight seal over the 10 L headspace of each chamber. Gas samples were taken from this headspace during a 45 min enclosure period at four times – t_0, t_{15}, t_{30} and t_{45} – per chamber (Pavelka et al., 2018). A sampling port served to extract air from the chamber headspace by using a 60 mL plastic syringe (Terumo Corp., Tokyo, Japan). After flushing the syringe three times with air from the chamber headspace, the following procedure was applied to ensure that GC and QCL analyses would receive identical headspace samples: 1) after flushing, 60 mL of sample air was extracted from the chamber headspace; 2) 10 mL of the sample was discarded to flush the syringe needle; 3) 15 mL was transferred into a pre-evacuated, septum-sealed, screw-capped 5.6 mL glass vial (Exetainer, Labco Ltd., High Wycombe, UK); 4) the syringe needle was flushed again by discarding a further 10 mL; 5) a second pre-evacuated glass vial was over-pressurised with 15 mL, and the remainder discarded. The procedure was repeated for each sample resulting in a total of 2 × 432 samples, i.e. two replicated sample batches for subsequent GC (1 × 432 samples) and QCL (1 × 432 samples) analyses. All samples remained in the septum-sealed Exetainers until analysis.

5.3.2.2 Laboratory gas chromatography

Gas chromatography was conducted on the first sample batch at the New Zealand National Centre for Nitrous Oxide Measurements (NZ-NCNM) at Lincoln University, New Zealand. Automated analysis (GX-271 Liquid Handler, Gilson Inc., Middleton, WI) was performed using a SRI 8610 GC (SRI Instruments, Torrance, CA, USA) and a Shimadzu GC-17a (Shimadzu Corp., Kyoto, Japan) equipped with a ^{63}Ni-electron capture detector. The analysis followed standard procedures described in detail by de Klein et al. (2015). Oxygen-free, ultra-high purity nitrogen (N_2) was used as the carrier gas (mobile phase) at a flow rate of 0.4 L min^{-1}. The measurement frequency was set to 1 Hz. Sample Exetainers experienced a storage time of up to two weeks before analysis which was due to transportation from the field site to the laboratory. The run time during GC analysis was about eight minutes per sample.

5.3.2.3 Field quantum cascade laser absorption spectrometry

The second batch of N_2O samples was collectively analysed on the day after the last chamber sampling, 17 September, by manual injection into a continuous-wave quantum cascade laser absorption spectrometer (CW-QCLAS, Aerodyne Research Inc., Billerica, MA, USA). Briefly, QCL uses infrared (IR) light energy which is passed through a 0.5 L multiple pass absorption cell with a pathlength of 76 m. Inside the cell, N_2O absorbs IR light energy which then is quantified as equivalent to the compositional N_2O concentration of the gas sample measured (Nelson et al., 2004).

For the purpose of our analysis, we switched the QCL from its continuous measurement (EC) mode to an 'injection mode'. The injection mode conversion took less than 30 minutes: a stainless steel three-way valve (Swagelok, Solon, OH, USA) mounted to the air inlet of the QCL allowed re-direction of the airflow from the primary inlet tube of the EC system into a second, 1 m long Bev-A-line tube (4 mm internal diameter). At its end, the tube was connected to a pressure regulator and a bottle of oxygen-free, industrial-grade N_2 carrier gas (BOC Ltd., NZ). Two stainless steel, T-junction connectors (Swagelok, Solon, OH, USA) were fitted to the sample tube allowing the overflow of excess carrier gas through a 0.45 µm PTFE membrane filter (ThermoFisher, Scientific, NZ) and sample injection through a septum-sealed port (Fig. 5-1). A dry scroll vacuum pump (XDS35i, Edwards, West Sussex, UK) was used for both EC measurements and manual injections to continuously draw either air or carrier gas through the QCL sample cell.

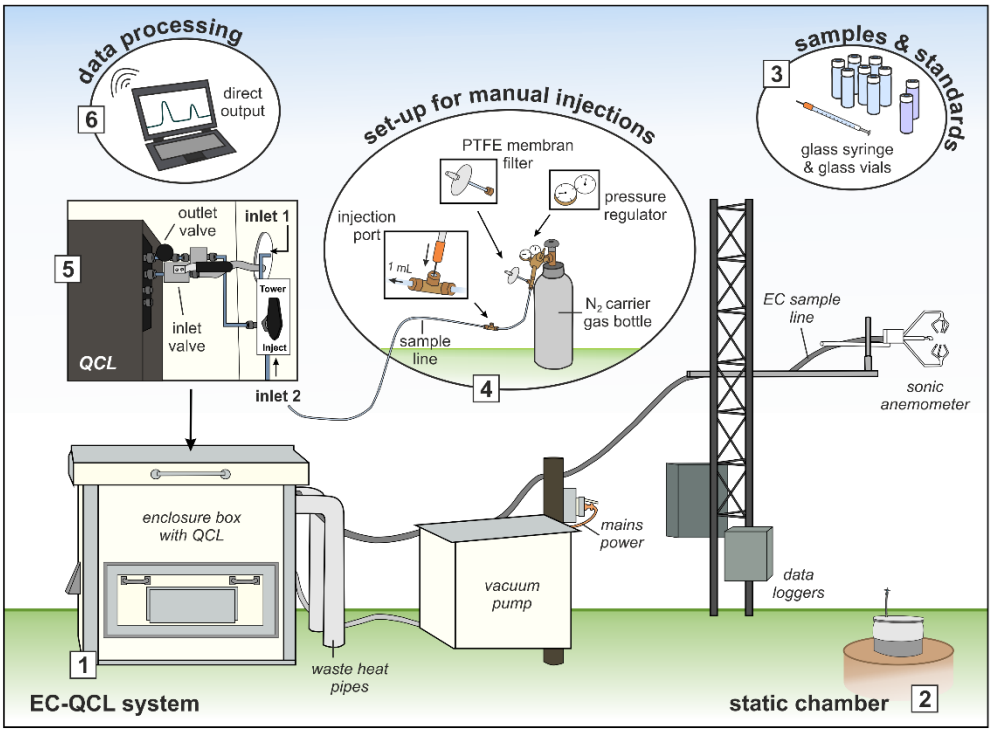

Figure 5-1 Schematic illustration of how to use a field-based QCL for EC measurements and manual injections. (1) shows the main components of the QCL EC system; (2) provides an example of a static chamber from which N_2O samples were taken and stored in (3) pre-evacuated glass vials. Once the set-up for manual injections (4) was assembled and the QCL air-inlet (5) adjusted from drawing ambient air through the EC sample line (inlet 1) to drawing air via the injection tube (inlet 2), the QCL was readily set-up for receiving injections of N_2O samples and associated standards through the injection port. The data output (6) was immediately allowing processing and data evaluation on the day of chamber sampling.

Once the injection line had been established, the flow rate was reduced from an initial 15 L min^{-1} used for EC to 1 L min^{-1} for manual injections based on Savage et al. (2014), Lebegue et al. (2016) and Brümmer et al. (2017). The reduction in flow was monitored using a RMA-SSV flow meter (Dwyer Instruments, PTY. Ltd., Michigan City, IN, USA) while setting the inlet control valve of the QCL to 2 Volt (using the TDLWintel software command) before manually adjusting inlet and outlet control valves of the QCL device further until the desired flow rate was achieved. Prior to sample injection, a minimum lag time of ten minutes was applied to let temperature and pressure of the QCL and its temperature-controlled enclosure box return to steady-state, i.e. 35 ± 0.5 Torr, 33.5°C laser temperature, and a QCL enclosure box temperature of 30 ± 0.1°C.

Standards of certified N_2O concentration (range 0.2 to 100 ppm) were injected before, during and after each sample run and complemented QCL analysis (Table A3-2). Ten out of the twelve N_2O standards were provided by the NZ-NCNM (except 0.321 and 0.401 ppm) and, therefore, identical to those used for GC. The QCL measurements were made at 10 Hz frequency with 1 mL of sample air extracted from each sample

Exetainer and manually injected into the flow of N_2 carrier gas by using a 1 mL glass syringe (SGE International PTY Ltd., VIC, Australia). The glass syringe was flushed with N_2 gas after each injection to avoid cross-contamination of samples and N_2O standards. The selection of syringe type, flow rate and the usage of N_2O standards were based on preliminary tests conducted in advance of the actual field campaign. Finally, it was important to keep a chronological record of the injected sample sequence to allow for re-identification of samples in the raw output data of the QCL.

5.3.3 Data processing

GC and QCL analyses resulted in the output of peak area data from the injected N_2O standards and chamber derived N_2O samples (Fig. A3-1). Data processing, therefore, first had to determine the relationship between peak area and (known) N_2O concentration (C_{N2O}) of the injected standards. To compute the final but initially unknown C_{N2O} of chamber N_2O samples, peak area data from N_2O standards were fitted to linear and quadratic (second-order-polynomial) models (van der Laan et al., 2009; de Klein et al., 2015). de Klein et al. (2015) recommended the use of quadratic curves models as the standard curve for C_{N2O} standards measured by GC analysis. However, we found that both linear and quadratic models adequately fitted C_{N2O} standards derived from QCL. Using a linear fit ultimately resulted in, on average, 3% smaller F_{N2O_QCL} (range -0.5 to -4.3%) than using a quadratic model. Nonetheless, since the quadratic fit suited lower C_{N2O} better than a linear fit, quadratic models were applied to represent the standard curves from injected standards of known C_{N2O} (Fig. A3-2). The quadratic model used to calculate final C_{N2O} was based on a selection of standards fitted to the expected minimum and maximum range of real sample C_{N2O}, which in our study ranged between 0.3–10 ppm (Fig. A3-1, Table A3-2). Output data from GC were processed in PeakSimple software (SRI Instruments, Torrance, CA, USA) and Excel (Microsoft Corp. Redmond, WA, USA). MatLab R2017a scripting (MathWorks Inc., Natick, MA, USA) served the processing of data derived from the QCL.

5.3.4 Flux calculation

The F_{N2O} in mg N_2O-N m^{-2} hr^{-1} was calculated for both data streams, GC (F_{N2O_GC}, n = 108) and QCL (F_{N2O_QCL}, n = 108), by applying a linear regression function to the increase in chamber headspace C_{N2O} between time t_0 and t_{45} following Eq. (5-1) (van der Weerden et al., 2011):

$$F_{N2O\_GC} \text{ and } F_{N2O\_QCL} = \frac{\Delta N_2O}{\Delta T} \times \frac{M}{Vm} \times \frac{V}{A} \qquad \text{(Eq. 5-1)}$$

where ΔN_2O is the increase in headspace C_{N2O} (µL N_2O L^{-1} (ppmv)) with time; ΔT is the enclosure period (in hours); M is the molar weight of nitrogen (44 g mol^{-1}) in N_2O; Vm is the molar volume of gas (L mol^{-1}) at the mean air temperature recorded at each sampling occasion; V is the chamber headspace volume (m^3); and A is the area covered by the chamber base, here 0.0415 m^2. All F_{N2O} were converted to units of nmol N_2O m^{-2} s^{-1} to allow for comparability between GC and QCL outputs. The integration of F_{N2O_GC} (n = 84) and F_{N2O_QCL} (n = 84) measured at 10 AM sampling was used to quantify the proportion of applied nitrogen emitted as N_2O (E_{N2O}) across the seven day trial in units kg N_2O-N ha^{-1} based on Luo et al. (2007) and Wecking et al. (2020a).

5.3.5 Statistical analyses

The statistical analysis for C_{N2O} data (C_{N2O_GC} and C_{N2O_QCL}, each n = 432) and resulting F_{N2O} (F_{N2O_GC} and F_{N2O_QCL}, each n = 108) was conducted in Genstat® (Version 19, VSN International, Hemel Hempstead, UK). After testing for normality using a Shapiro-Wilk test and homogeneity of variance by examining residual and fitted values, we applied three different statistical approaches to compare GC with QCL data: 1) orthogonal regression, 2) Bland Altman and 3) bioequivalence statistics.

Orthogonal regression analysis used *standardised* C_{N2O} and F_{N2O} following Eq. (5-2):

$$standardised\ C_{N2O}\ and\ F_{N2O} = \frac{(x - mean)}{standard\ deviation} \qquad \text{(Eq. 5-2)}$$

The core of this orthogonal regression was a principal component analysis which, in contrast to ordinary least square regression, allowed for measurements errors in the response and the predictor variable by minimising the squared residuals in a vertical and horizontal direction. While orthogonal regression returned a Pearson correlation coefficient r that provided information about the strength of the linear relationship between GC and QCL data, we found that r did not include any prediction about the level of agreement between the two methods (Bland and Altman, 1986; Giavarina, 2015). The degree to which GC and QCL data would agree was, for that reason, determined by using Bland Altman statistics that quantified the bias (i.e. the mean difference) and the limits of agreement between the two methods. The limits of agreement were calculated from the mean and the standard deviation (SD) of the difference between GC and QCL data. We defined that 95% of all data points had to be within ± 1.96 SD of the mean difference (Giavarina, 2015). The Bland Altman analysis was conducted for individual F_{N2O} as well as for mean F_{N2O} across replicates of the same treatment.

Still, testing for correlation and agreement did not determine whether GC and QCL data would effectively and for practical purposes be the same (termed 'equivalent'). We, therefore, used bioequivalence statistics to assess the biological and analytical relevance of the difference between the two methods. The first part of this analysis comprised a one-way analysis of variance (ANOVA) for F_{N2O} which was subset by treatment (AN_0, AN_{300}, AN_{600}, AN_{900}) and analytical device (GC, QCL). Results from this ANOVA determined the 90% confidence intervals (CI) of the mean difference between F_{N2O_QCL} and F_{N2O_GC}. In bioequivalence statistics, the 90% CI (at a standard power level of 80%) is generally preferred instead of using a 95% CI that often serves to establish a statistical difference between two methods or treatments rather than proving no difference. An important component of the analysis was to also define the equivalence range, i.e. the maximum acceptable difference, between the new (QCL) and the standard method (GC). Bioequivalence statistics acknowledge that two methods will never be exactly the same. Defining an acceptable equivalence range is, thus, an important precondition and might in some cases be even provided by a regulatory authority. Originating from pharmaceutical research (Bland and Altman, 1986; Giavarina, 2015; Patterson and Jones, 2006; Rani and Pargal, 2004), the concept of bioequivalence has not broadly been applied in environmental sciences. Therefore, an acceptable equivalence range for N_2O data based on the use of different analysers and methods has yet to be defined. We determined that the maximum acceptable difference of F_{N2O_QCL} had to be as small as possible and within ± 5% of the mean difference of the standard method (F_{N2O_GC}). The null hypothesis (F_{N2O_QCL} is different from F_{N2O_GC}) was rejected when the 90% CI of the difference (F_{N2O_QCL}-F_{N2O_GC}) was entirely within the predefined equivalence range at a significance level of 5%. Following the same principles, we conducted a bioequivalence analysis for C_{N2O_QCL} and C_{N2O_GC}.

5.4 Results and discussion

5.4.1 Environmental conditions and soil variables

Daily mean air temperatures during the seven-day chamber campaign ranged from 8.3 to 12.8°C. The WFPS of the soil within the chambers and associated plots did not fall below 73.9% with a mean of 79.5%. The cumulative rainfall in September 2019 was 119 mm of which only 2 mm occurred during the seven days of the campaign. As expected, soil NH_4^+ and NO_3^- levels increased with increasing application of AN fertiliser. The highest values of N_{min} measured at AN_{900} plots were 265 kg NH_4^+ ha^{-1} and 268 kg NO_3^- ha^{-1}. The mean background levels of soil NH_4^+ and NO_3^- were

around 2 kg ha^{-1}. At the end of the campaign, soil NH_4^+ levels for all treatments had decreased by less than half while the amount of soil NO_3^- remained similar to the initial level measured on the day of treatment application (Table A3-3).

5.4.2 Comparing GC and QCL derived data

5.4.2.1 Magnitude and general variability

Measurements resulted in a wide range of F_{N2O} but followed the same temporal and treatment-dependent patterns for both F_{N2O_GC} and F_{N2O_QCL}. The magnitude of individual fluxes was between -0.10 and 22.24 nmol N_2O m^{-2} s^{-1} for F_{N2O_GC} and -0.07 and 22.81 nmol N_2O m^{-2} s^{-1} for F_{N2O_QCL}. The mean F_{N2O} (n = 27) from chamber plots that received the highest application rate of AN fertiliser (AN_{900}) was 13.22 nmol N_2O m^{-2} s^{-1} ± 1.47 (± standard error of the mean, SEM) for F_{N2O_GC} and 13.27 nmol N_2O m^{-2} s^{-1} ± 1.43 for F_{N2O_QCL}. Similarly, the AN_{600} treatment had a mean F_{N2O} of 8.51 nmol N_2O m^{-2} s^{-1} ± 0.98 (F_{N2O_GC}) and 8.33 nmol N_2O m^{-2} s^{-1} ± 0.9 (F_{N2O_QCL}). The mean F_{N2O} for AN_{300} was 6.61 nmol N_2O m^{-2} s^{-1} ± 0.78 (F_{N2O_GC}) and 6.48 nmol N_2O m^{-2} s^{-1} ± 0.69 (F_{N2O_QCL}). At control plots, F_{N2O} were close to zero (Fig. 5-2, Table A3-3). We found that treatment F_{N2O} increased from a near-zero background flux to ≥ 8.5 nmol N_2O m^{-2} s^{-1} on the second day of the campaign.

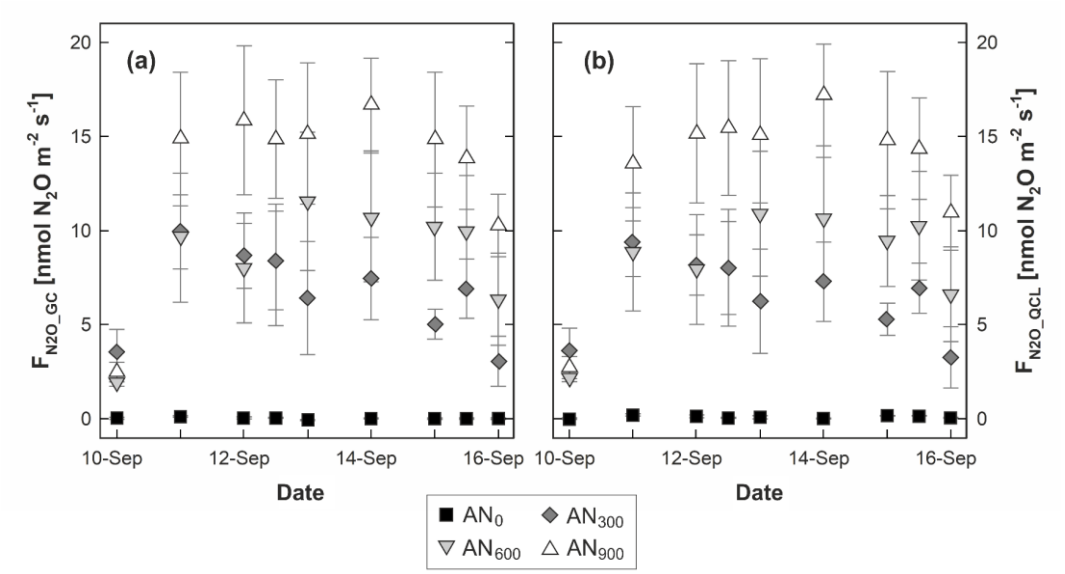

Figure 5-2 Fluxes of nitrous oxide (F_{N2O}) determined from (a) gas chromatography (F_{N2O_GC}) and (b) quantum cascade laser absorption spectrometry (F_{N2O_QCL}). Symbols depict mean F_{N2O} and marker shading displays the rate of ammonium nitrate (AN) applied: AN_0 (black squares), AN_{300} (dark grey diamonds), AN_{600} (light grey upside-down triangles) and AN_{900} (white triangles). Error bars illustrate the standard error of the mean (SEM) across the three replicates of the same treatment. Note that flux measurements on 12 and 15 September were conducted twice daily (10 AM and 12 PM) and that the time scale on the x-axis, therefore, is discrete. Soil water-filled pore space (WFPS) and mineral nitrogen (N_{min}) contents associated with flux measurements are provided in the supplementary material, Table A3-3.

From then, AN_{300} fluxes gradually decreased with time whereas F_{N2O} at AN_{600} and AN_{900} plots remained relatively elevated until the last day of the trial (Fig. 5-2). These temporal trends aligned with findings from Cowan et al. (2020) who observed N_2O emissions to peak within seven days after urea and AN fertiliser application and found that F_{N2O} returned to background levels after two or three weeks. Similarly, short-term responses of F_{N2O} to AN application were determined by others e.g., Bouwman et al. (2002), Jones et al. (2007), and Cardenas et al. (2019). However, for our study, AN treatment effects on F_{N2O} were of secondary interest. Different rates of AN fertiliser were only applied to result in a wide range of C_{N2O} and F_{N2O} and, thereby, allow to compare GC and QCL.

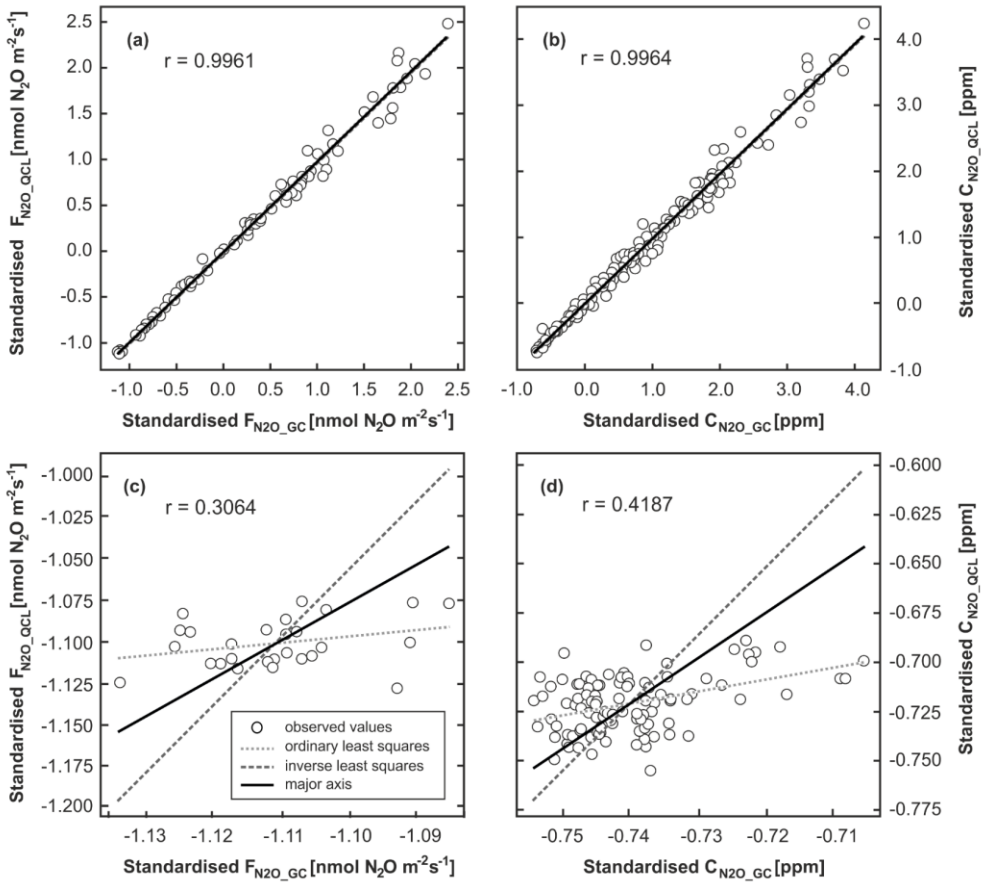

Figure 5-3 Orthogonal regression analysis of standardised N_2O concentrations (C_{N2O}) and fluxes (F_{N2O}). Data were distinguished by their analytic source of origin, i.e. GC (C_{N2O_GC}, F_{N2O_GC}) and QCL (C_{N2O_QCL}, F_{N2O_QCL}). The regression analysis included all C_{N2O} in (a) but only those C_{N2O} measured at control sites (AN_0) in panel (c). The orthogonal regression analysis was repeated for standardised F_{N2O} with (b) showing all F_{N2O_GC} and F_{N2O_QCL}, and (d) depicting the orthogonal regression for AN_0 fluxes only. Ordinary least squares (dotted light grey line) resulted from the regression of Y on X; inverse least squares from the regression of X on Y (long dotted dark grey line). The major axis (black line) based on orthogonal regression of Y and X using a principal component analysis. Here, the squared residuals perpendicular to the line are minimised. Note, for illustration, axes in panel (c) and (d) have different scales. Table A3-4 in the supplements provides further results.

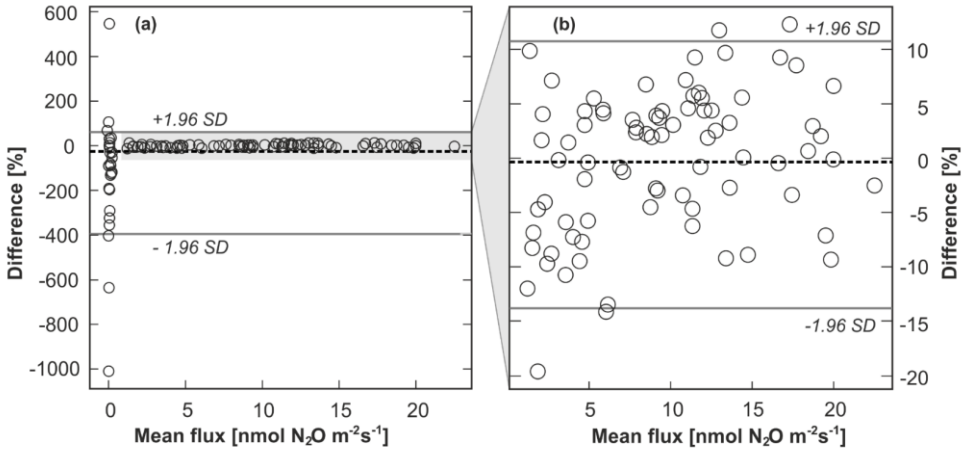

Figure 5-4 Bland Altman plots showing the difference between the GC and QCL method expressed as the percentage difference of the standard method A (F_{N2O_GC}) and the new method B (F_{N2O_QCL}) on the y-axis [((A-B)/mean)× 100] versus the mean of A and B on the x-axis. The limits of agreement are represented by continuous lines at ±1.96 standard deviation (SD) of the percentage difference. The inset (panel b) illustrates the same data but excludes F_{N2O_GC} and F_{N2O_QCL} from control (AN_0) sites. The percentage mean difference (bias) between F_{N2O_GC} and F_{N2O_QCL}, i.e. method A and B, is indicated by the gap between the dashed line (line of equality, which is not at zero) and an imaginary line parallel to the dashed line at y = 0. This figure is based on individual F_{N2O} (all treatment replicates). Results for mean F_{N2O} across replicates of the same treatment are provided in the supplements, see Table A3-5.

5.4.2.2 AN treatment flux and concentration data

The correlation between calculated F_{N2O_GC} and F_{N2O_QCL} and between C_{N2O_GC} and C_{N2O_QCL} across all treatments was high with an r value of 0.996 resulting from orthogonal regression (Fig. 5-3a, b). For both cases, major axis, ordinary and inverse least squares were nearly identical to a 1:1 line. All three regression models could therefore be used similarly well to predict the strength of the linear relationship between F_{N2O_GC} and F_{N2O_QCL} and C_{N2O_GC} and C_{N2O_QCL}, respectively (Table A3-4). The results of the orthogonal regression analysis suggested that QCL delivered equivalent data to the GC method. The Bland Altman statistic quantified a percentage difference between the two methods for F_{N2O} (i.e. F_{N2O_GC} and F_{N2O_QCL} treatment means) of not smaller than -11.2% and not greater than +9.2% (Table A3-5). The percentage difference between individual F_{N2O_GC} and F_{N2O_QCL} (not treatment means) was slightly greater but in only less than 3% of all cases exceeded +10% and -15%. This was likely due to the higher variability of F_{N2O} between individual replicates of the same treatment than across calculated means. For both cases, ≥ 95% of all data points were well within the pre-defined limits of agreement ± 1.96 SD (Fig. 5-4b). The overall mean difference (bias) between F_{N2O_GC} and F_{N2O_QCL} was 0.1 nmol N_2O m^{-2} s^{-1}. However, this small bias might be practically irrelevant when compared with the overall detection limit of static chambers and other method-associated uncertainties. Neftel et al. (2007)

quantified the detection limit of static chambers to be 0.23 nmol N_2O m^{-2} s^{-1}, and Parkin et al. (2012) reported 0.03 nmol N_2O m^{-2} s^{-1}. In contrast, Flechard et al. (2007) and others (e.g., Rochette and Eriksen-Hamel, 2008, Jones et al., 2011) showed that the uncertainty of integrated chamber F_{N2O} can be as high as 50% at the annual scale.

5.4.2.3 Control flux and concentration data

In contrast to the strong comparability of GC and QCL data at AN treatment sites, F_{N2O_GC} and F_{N2O_QCL} measured at control plots (AN_0) were only poorly correlated ($r = 0.3064$) (Fig. 5-3 c). The model-fit of the major axis, ordinary and inverse least squares indicated that the regression of F_{N2O_GC} on F_{N2O_QCL} (and vice versa) was not identical, i.e. differed in the minimisation of squared residuals in a vertical and horizontal direction. Likewise, this also applied to C_{N2O_GC} and C_{N2O_QCL} (Fig. 5-3d). Mean F_{N2O} ranged from a minimum of -0.05 to a maximum of only 0.21 nmol N_2O m^{-2} s^{-1} (Table A3-3). Consequently, Bland Altman statistics determined only small quantitative differences between F_{N2O_GC} and F_{N2O_QCL}. When computing the percentage difference between these F_{N2O_GC} and F_{N2O_QCL}, we found near-zero F_{N2O} from AN_0 plots were less consistent in relative terms than treatment F_{N2O} (Fig. 5-4). However, these inconsistencies were generally small and did not appear of great biological interest.

More generally, QCL analysis resulted in slightly higher C_{N2O} than GC, which explains why the calculated F_{N2O_QCL} at AN_0 plots were higher than F_{N2O_GC}. However, whether this finding was related to the potentially higher sensitivity of the QCL device or due to other variations in the sampling procedures was not resolved. Instead, we found that the disagreement between the GC and QCL method was likely related to ambient N_2O concentrations in the chamber headspace that remained between 300-400 ppb and showed a non-linear response with time, regardless of which analytic device was used. This might have resulted in the calculation of very small but apparent positive and negative F_{N2O}, when in fact the actual flux was zero (*Type I error* as defined by Parkin et al. (2012)). The integration of C_{N2O} with time to calculate F_{N2O}, therefore, likely included this error; rather than being caused by uncertainties associated with the measurement procedures or choice of analytic device (Kroon et al., 2008). The deviation between the control site (AN_0) and treatment F_{N2O} (AN_{300}, AN_{600}, AN_{900}) has to be taken into account when evaluating the above results and mathematical principles. Furthermore, since static chamber measurements often include near-ambient C_{N2O}, and likewise fluxes equal or near-zero, F_{N2O} from control plots were kept in the manuscript for completeness.

5.4.2.4 Cumulative nitrous oxide emissions

Cumulative N_2O emissions across the seven-day campaign were quantified slightly greater for the GC (E_{N2O_GC}) than the QCL (E_{N2O_QCL}) method. The mean difference between E_{N2O_GC} and E_{N2O_QCL} for the control (AN_0) and each treatment, AN_{300}, AN_{600} and AN_{900}, was -0.011, +0.0023, +0.050 and +0.028 kg N ha^{-1}, respectively. This was a difference of less than 4% in total N_2O emissions during deployment (Fig. 5-5).

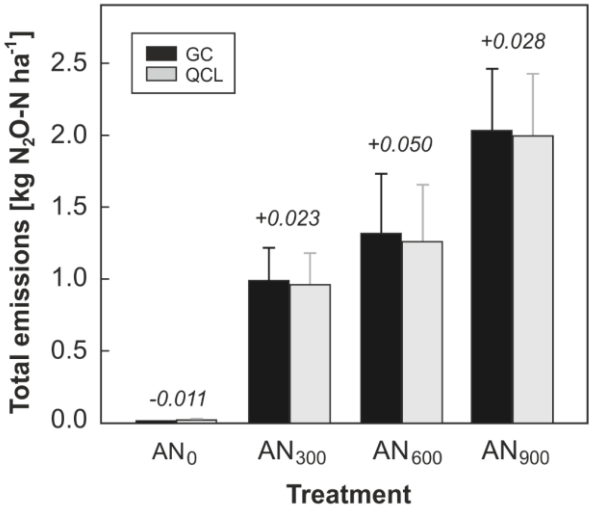

Figure 5-5 Cumulative N_2O emissions from each treatment (AN_{300}, AN_{600}, AN_{900}) and the control (AN_0) in kg N_2O-N ha^{-1} at the end of the campaign. Data are distinguished into GC (black bars) and QCL (grey bars) budgets. Error bars quantify the standard error of the mean (SEM). The absolute difference in kg N_2O-N ha^{-1} between the two budgets (GC-QCL) is highlighted by the number on the top of each bar-couple.

5.4.3 Measurement performance of QCL analysis

The measurement precision of QCL and, particularly, GC have been generally well-reviewed (Rapson and Dacres, 2014; de Klein et al., 2015; Lebegue et al., 2016). Gas chromatographs can be as precise as < 0.5 ppb (van der Laan et al., 2009; Rapson and Dacres, 2014) while the precision of a QCL is about 0.3 ppb for measurements made at 10 Hz, and 0.05 ppb for 1 Hz; but in some cases might be even higher (~1 ppt) (Curl et al., 2010; Rapson and Dacres, 2014; Savage et al., 2014). Zellweger et al. (2019), for instance, used laboratory QCL for the calibration of N_2O reference standards to inform the internationally accepted calibration scale of the Global Atmosphere Watch Programme of the World Meteorological Organisation. Similarly, Rosenstock et al. (2013) verified the accuracy and precision of different photoacoustic spectrometers based on laboratory QCL. However, the analytic precision can also depend on factors other than the technical performance of the analyser itself. Rannik et al. (2015) indicated that the performance (and thus the precision of F_{N2O}) of an analyser to measure gas samples from static chambers is likely more limited by the precision of

the chamber system than by errors related to the analysis or post-processing of the data. Imprecisions might be caused by several factors e.g., chamber type and dimension, experimental set-up, deployment time and preferred sampling method, all of which can affect the overall flux detection limit. In contrast, the sources of uncertainty in our study were most likely related to 1) insufficient evacuation of Exetainers leading to the sporadic dilution of gas samples and N_2O standards; and 2) variation of 1 mL sample volumes when injected into the QCL. In practice, these might not have always been equal to 1 mL and, thus, could have resulted in slight variations of output peak area. In agreement with our observations, de Klein et al. (2015) found that half the uncertainty of static chamber measurements could be explained by the variability of the sample volume in the Exetainers. The inclusion of a fixed volume sample loop might help to reduce this source of error in the future.

The QCL analysis of our study was conducted in a temperature- and pressure-controlled environment, where variations in these parameters were unlikely, and the variation in temperature expected to be less than 0.02 ppb $°C^{-1}$ (Lebegue et al., 2016). Nonetheless, we recommend a constant baseline flow of N_2 carrier gas at constant pressure (slightly higher than ambient) and temperature for manual injections made into the QCL device to avoid uncertainty affecting output peak areas. Depending on the QCL EC system, an initial lag time of 10 to 30 min before injections might be required to assemble the operational set-up (Section 5.3.2.3) and ensure sufficient stabilisation of pressure and temperature in the QCL sample cell. Given a flow rate of 1 L min^{-1}, rapid injections into the QCL should become possible shortly afterwards with a delay between single injections of 1 mL sample volumes of not more than 5 to 8 sec. Sample concentrations of the same volume but at N_2O concentrations > 20 ppm required a longer delay time between individual injections (> 20 sec) to ensure sufficient flushing of the QCL sample cell and avoid cross-contamination (Fig. A3-1). The identification of suitable delay times was straight forward in our case and could be easily accessed in real-time by visually examining the peak progression in TDLWintel. When observing the peak progression, for instance, it became noticeable that the injection of blanks (N_2 carrier gas) did not result in any changes in baseline flow. However, we did not determine the extent to which spontaneous but small variations in the flow rate of N_2 carrier gas would have affected our resulting output peak areas. Further uncertainties might have been associated with processing and curve-fitting procedures applied to the raw dataset in MatLab, and likely resulted in small underestimations of true output peak areas.

5.4.4 QCL injections

5.4.4.1 The concept of bioequivalence

Using the Pearson correlation coefficient and the coefficient of determination for comparing two or more quantitative methods is a generally preferred approach in the field of N_2O research. Comparisons of different methods for N_2O analysis made in the literature most commonly used orthogonal (Jones et al., 2011) and linear regression (Cowan et al., 2014; Brümmer et al., 2017; Tallec et al., 2019), Students t-tests (Christiansen et al., 2015) or were based on raw data (Savage et al., 2014). However, correlation studies as such have limitations when assessing the comparability between two methods since a correlation analysis only identifies the relationship between two variables, not the difference (Giavarina, 2015). Bland Altman and bioequivalence statistics overcome this limitation by assessing the degree of agreement between methods.

An important aspect of statistical hypothesis testing is that the null hypothesis is never accepted. But failure to reject the null hypothesis is not the same as proving no difference. A bioequivalence analysis allows the statistical assessment of whether two methods (e.g., measurement devices, drug treatment) are effectively the same. Central to a bioequivalence analysis is the "equivalence range" that defines the size of the acceptable difference for which the values are similar enough to be considered equivalent. This becomes important when considering that even with the most precise analytical design and the most tightly controlled experimental conditions, e.g., F_{N2O_GC} and F_{N2O_QCL} will never be exactly the same (Rani and Pargal, 2004). However, if the difference is sufficiently small for 'practical purposes', F_{N2O_GC} and F_{N2O_QCL} can be considered effectively the same. Here, accepted evidence of bioequivalence for F_{N2O_QCL} was that the 90% confidence interval of the difference F_{N2O_QCL}-F_{N2O_GC} (corresponding to a test with size 0.05) was within a ± 5% difference of F_{N2O_GC}. The equivalence range will vary depending on the objective of the research or guidelines provided by a regulatory authority but commonly does not exceed ± 20% (Westlake, 1988; Rani and Pargal, 2004; Ring et al., 2019). In our study, a small equivalence range of ± 5% was preferred to test the difference between F_{N2O_QCL} and F_{N2O_GC} since such recommendations did not exist. And given this precondition, our results showed that F_{N2O_GC} and F_{N2O_QCL} from AN_{300}, AN_{600} and AN_{900} plots provided evidence of bioequivalence. The 90% confidence intervals of the difference (F_{N2O_GC}-F_{N2O_QCL}) were quantified 0.127 (AN_{300}), 0.185 (AN_{600}) and -0.043 (AN_{900}) nmol N_2O m^{-2} s^{-1} and well within the pre-defined equivalence range of ± 5% (Fig. 5-6, Table A3-6).

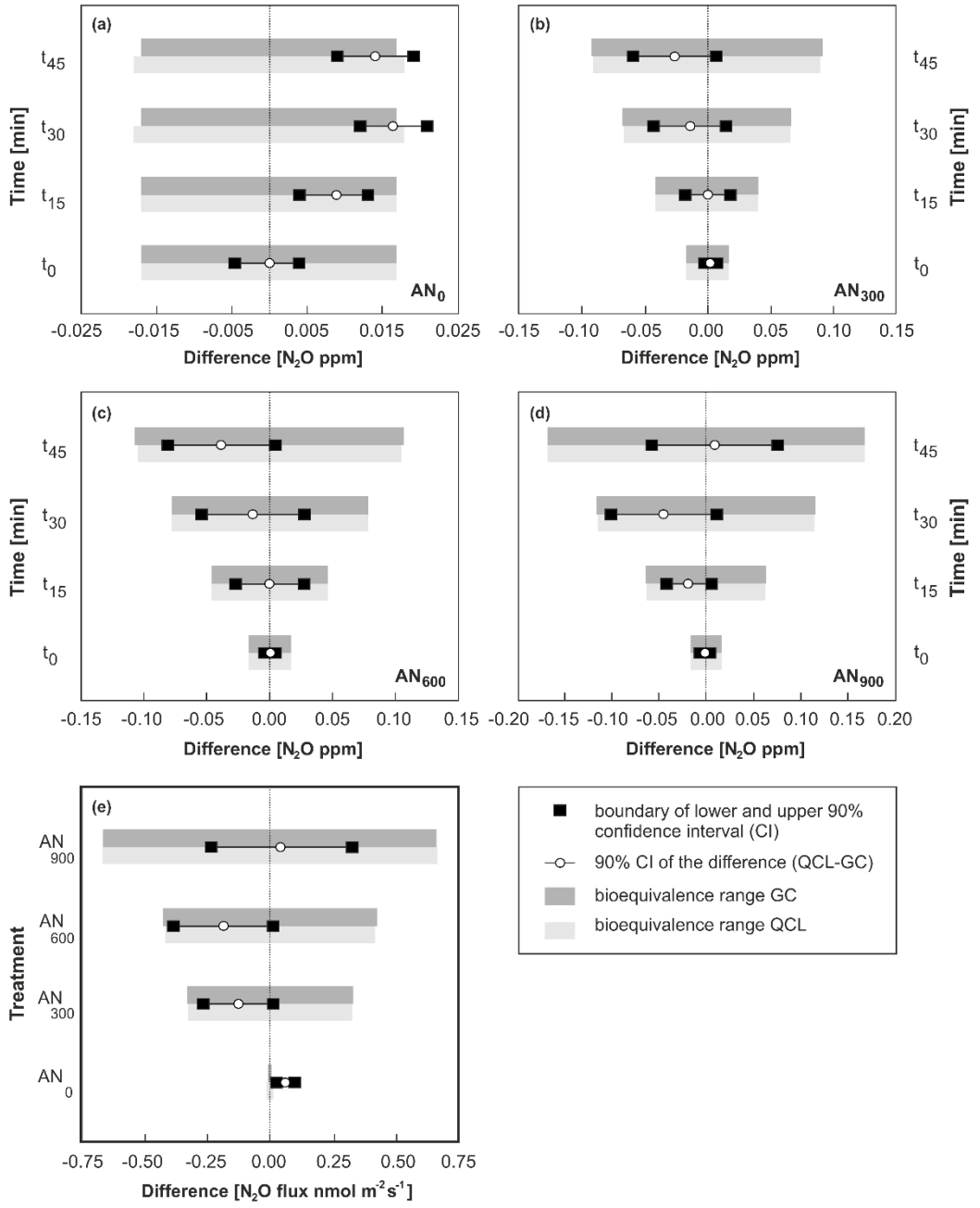

Figure 5-6 Bioequivalence analysis for N_2O concentrations (C_{N2O}) in (a-d) and N_2O fluxes (F_{N2O}) in (e) with GC defined as the standard method. C_{N2O} and F_{N2O} based on QCL analysis were considered bioequivalent when the 90% confidence interval (CI) of the difference between QCL and GC (x-axis) was within the predefined ± 5% bioequivalence range of the difference of the standard method. The bioequivalence analysis was distinguished for C_{N2O} by sampling interval (t_0, t_{15}, t_{30}, t_{45}) and treatment with panel (a) showing results for control sites (AN_0) and panels (b), (c) and (d) for AN_{300}, AN_{600} and AN_{900} treatment sites. Similarly, a bioequivalence analysis was conducted for F_{N2O} in panel (e) and distinguished by AN application rate on the y-axis (Table A3-6).

At control sites (AN_0), F_{N2O_GC} and F_{N2O_QCL} did not provide evidence for bioequivalence. However, the failure to establish equivalence for AN_0 sites was due to the overall limitation of the static chamber method to provide 'real' F_{N2O}, rather than based on a failure of the statistical principle (Section 5.4.2.3). On the contrary, when tested for C_{N2O} instead of F_{N2O}, equivalence was confirmed for t_0 and t_{15} but did not apply to t_{30} and t_{45} (Fig. 5-6a). Again, failure to establish equivalence was likely related to limitations of the static chamber method which, in this case, were indicated by the lower boundary of the 90% CI remaining outside the predefined equivalence ranges. Another possible reason for not accepting equivalence for GC and QCL derived data at AN_0 sites could have been the maximum acceptable difference between the two methods itself. We defined (Section 5.3.5) that this difference had to be within ± 5% of the mean difference of the standard method (i.e. GC). It has to be taken into consideration that the accepted evidence of bioequivalence would have led to different results if the percentage mean difference had been set to, for instance, ± 10%. Accepting a greater mean difference between the two methods would have consequently resulted in evidencing bioequivalence for C_{N2O_GC} and C_{N2O_QCL} even at ambient concentrations. More generally, we found that negative values of the 90% CI of the difference indicated that the difference between the two methods (QCL-GC) resulted in higher C_{N2O_GC} and F_{N2O_GC}. Positive values, instead, showed that the difference QCL-GC led C_{N2O_QCL} and F_{N2O_QCL} values to be greater than those from C_{N2O_GC} and F_{N2O_GC}. But in either case, the overall difference between the two methods did not exceed ± 0.1 ppm for C_{N2O} and ± 0.38 nmol N_2O m^{-2} s^{-1} for F_{N2O} (Fig. 5-6e).

To the best of our knowledge, bioequivalence has not broadly been applied in the greenhouse gas literature to identify and to discuss the range at which a difference in F_{N2O_GC} and F_{N2O_QCL} could be considered relevant when using different analytical methods. However, defining the magnitude of F_{N2O} (here in nmol N_2O m^{-2} s^{-1}) at which a unit difference would become relevant is important when using different methods to quantify, compare and, ultimately, upscale N_2O emissions. We, thus, recommend bioequivalence or other statistical approaches (e.g. Bland Altman) for more formally assessing the agreement between two methods in the future.

5.4.4.2 Strengths and weaknesses

The employment of a QCL analyser proposes an alternative approach for the injection of N_2O samples taken from static chambers, particularly as F_{N2O_QCL} were generally equivalent to F_{N2O_GC}.

Table 5-1 The GC and QCL methods in comparison: Details provided in the table relate to in this study and information provided were not generalised. NZD = New Zealand dollars.

	GC	**QCL**
Capital cost per device (NZD)	40,000	160,000
Labour effort for preparation and data processing of 100 samples (hours)	2 to 3	< 1
Transport of samples	required	not required
Storage of samples	required	optional
Analysis location	lab-based	field-based
Analysis time (days)	multiple days	immediate
Analysis cost per sample (NZD)	3.5	< 0.5
Possible injections (per hour)	7.5	~200
Lag time between injections (sec)	480	< 10
Injection procedure	manual/automated	manual
Injection of N_2O standards	required	required
Injection volume per sample (mL)	6	1
Carrier gas	N_2	N_2
Flow rate (L min^{-1})	0.4	1
Data output	post-analysis	immediate

Using a QCL for manual injections can be conducted without much disruption to other measurements (e.g., EC or automated chambers) and, therefore, helps justify the initially higher capital and general running costs involved with operating a QCL device. Additional labour effort and time associated with sample storage and transport necessary for laboratory GC do not necessarily apply for field-based injections into a QCL. Once established, a QCL system has relatively low maintenance and offers a straightforward application for manual injections in addition to EC or other measurement tasks. In our study, the assembly of the injection set-up required little equipment and was installed within 30 min. This allowed for a rapid analysis after chamber sampling without greatly interfering with other measurements, i.e. EC, that were offline during the time of injection into the QCL. To collectively inject a great number of samples turned out to be highly beneficial to minimise the downtime of the EC measurements, in our case, and also helped to reduce other interferences made to the QCL. For instance, we were able to inject a total of around 700, 1 mL samples (432 samples, 268 standards) within four hours (Table 5-1). Prior to QCL analysis, these samples had been kept in septum-sealed Exetainers that can store gas samples for up to 28 days at any temperature between -10 and 25°C (Faust and Liebig, 2018).

We acknowledge that a sporadic dilution of our samples might still have occurred due to storage in and potentially insufficient evacuation of Exetainers which, in turn, might have affected GC and QCL analyses (de Klein et al., 2015). Despite this potential

source of uncertainty, storing N_2O samples in Exetainers enabled repeated injections and allowed to postpone the analysis if EC measurements were of higher importance or if the weather conditions (e.g. precipitation) were unsuitable. Similar to GC, QCL injections required consumables (N_2 carrier gas, N_2O standards) but, in contrast, time and costs associated with laboratory work were substantially less (Table 5-1).

5.5 Conclusion

Previously, QCL had been used either in conjunction with EC or coupled to automated chambers. Here, we showed that one QCL device could be used as a practical tool for the analysis of static chamber derived N_2O samples without major disruption to these other measurement tasks. We found treatment N_2O concentrations (C_{N2O_QCL}) and fluxes (F_{N2O_QCL}) from QCL agreed with results based on laboratory GC (C_{N2O_GC}, F_{N2O_GC}). The percentage difference between treatment F_{N2O_GC} and F_{N2O_QCL} was not smaller than -11.2% and not greater than +9.2% with a mean difference between the two of only 0.1 nmol N_2O m^{-2} s^{-1}. A deviation between the GC and QCL methods was determined only for close to zero F_{N2O} at control plots where F_{N2O_GC} and F_{N2O_QCL} values were found outside the predefined equivalence range. However, this was likely due to the calculation of very small but apparent positive and negative F_{N2O} (when in fact the actual flux was zero), rather than due to uncertainties caused by a weakness of the GC or QCL analysis. Equivalence was evidenced for all other F_{N2O_GC} and F_{N2O_QCL} and confirmed that GC and QCL data were for practical purposes the same.

We found that using Bland Altman and bioequivalence statistics in addition to regression analysis served the comparison of GC and QCL particularly well. Yet, these two statistical approaches have not broadly been used in the field of greenhouse gas research to compare different analytical methods or to discuss the magnitude at which a difference in F_{N2O} would become relevant. Since correlation studies identify the relationship between two methods but not the difference, we recommend that bioequivalence or other suitable statistical approaches are used for more formally assessing the agreement between two methods. Finally, QCL offers great potential to interlink different methods of gas measurements across different temporal and spatial scales. In the future, this capability might not only be important for rapid field analysis of N_2O samples but equally also applies to the measurement of other gas species (e.g., CO_2, CH_4) and gas isotopomers of interest.

5.6 Acknowledgements

This research was supported by the New Zealand Agricultural Greenhouse Gas Research Centre (NZAGRC), AgResearch Ruakura, DairyNZ and the University of Waikato. The authors would like to recognise the farm owners, Sarah and Ben Troughton, for their cooperation. Chris Morcom is thanked for his help in the fields and Emily Huang from NZ-NCNM for her all-embracing support regarding gas chromatography. Training notes on the concept of bioequivalence were gratefully received from Neil Cox. We would like to further acknowledge the continuous support from Aerodyne Research Ltd. in maintaining and advancing our QCL EC systems. Finally, Cecile A. M. de Klein, Tom P. Moore, Jordan P. Goodrich and two anonymous reviewers are thanked for thoroughly revising the manuscript of this work.

5.7 Author contributions

Author names: Anne R. Wecking (ARW), Vanessa M. Cave (VC), Jiafa Luo (JL), Louis A. Schipper (LS), Aaron M. Wall (AW), David I. Campbell (DC), Lìyǐn L. Liáng (LL).

ARW, VC, JL and LS designed the experiment. ARW performed the fieldwork. ARW conducted the post-processing of GC and QCL data using MATLAB scripts, which based on the work from AW and DC. ARW performed the statistical analysis with inputs and contributions from VC. VC and LS commented on the results of the initial data analysis. ARW wrote and revised the manuscript with contributions from VC, AW, LL, JL, DC and LS.

Chapter Six

Synthesis and Conclusion

Agriculture has been the dominating human activity in the Anthropocene and its effect on the terrestrial biosphere has been modifying important planetary processes with time (Lal, 2020). At present, these modifications are becoming increasingly more apparent whether as alterations to the cycling of soil carbon and nitrogen, environmental degradation or atmospheric warming. Agriculture contributes about 10–12% to current global greenhouse gas emissions (CO_2, CH_4, N_2O) and most of these emissions result from livestock farming (Reisinger and Clark, 2018). Past research has made us aware that grassland soils are a major source of N_2O (Galloway et al., 2004; Fowler et al., 2013). However, a full understanding of the complexity of drivers and processes causing emissions of nitrous oxide from pastoral land has remained challenging (Butterbach-Bahl et al., 2013).

The main goal of this thesis was to add to the understanding of how N_2O is exchanged from pastoral soils that received high inputs of reactive nitrogen (N_r), primarily in the form of cattle excreta. Eddy covariance measurements formed the core of this work and were used to quantify annual emission budgets and compare to measurements from traditional static chambers (Chapter 3). The effect of farm management (business as usual versus renewal) was discussed in Chapter 4, where N_2O fluxes (F_{N2O}) from adjacent, but differently managed, paddocks were measured using a single EC system and processed by footprint-splitting and gap-filling techniques. Findings of Chapter 5 showed that the QCL analyser of the EC system also suited the manual injection of N_2O samples taken from static chambers. The following synthesis overviews the key findings of this thesis (Section 6.1). A broader discussion (Sections 6.2), including recommendations for future research, and some additional concluding remarks are provided at the end (Section 6.3).

6.1 Key findings

6.1.1 Overview of Chapter 3

The first thesis objective, addressed in Chapter 3 and published as Wecking et al. (2020b), was to reconcile and compare annual N_2O emission budgets based on two different measurement approaches. The exchange of N_2O was measured by 1) static chambers (three months), and 2) micrometeorological EC (one year).

Both these measurements were conducted at the same research site with annual emissions derived from site-specific EFs and the summation of half-hourly F_{N2O} from EC. Key findings of this comparison were:

- Annual N_2O emissions from EC (7.30 kg N_2O-N ha^{-1} yr^{-1}) were greater than estimates (3.82 kg N_2O-N ha^{-1} yr^{-1}) based on site-specific EFs obtained for cattle urine (1.53%), cattle dung (0.24%), and urea fertiliser (0.16%).
- This difference was likely because the EF approach used EFs values that did not take into account possible seasonal variations, the effect of supplementary feed on urinary nitrogen contents and background N_2O emissions (BNE).
- Estimating the contribution of these additional sources to the EF budget resulted in 0.92 kg N_2O-N ha^{-1} yr^{-1} from supplementary feed and 1.09 kg N_2O-N ha^{-1} yr^{-1} from BNE. It was suggested that the effect of seasonal variabilities partly contributed to the still remaining difference of 1.47 kg N_2O-N ha^{-1} yr^{-1} between the two budgets.

Comparing two annual emission budgets based on site-specific N_2O measurements allowed this thesis to evaluate the strengths and weaknesses of EF and the EC approach. Emission factors are commonly derived from point scale measurements using static chambers (de Klein et al., 2020), whereas EC is based on measuring F_{N2O} continuously at paddock scales and high temporal frequency (Nemitz et al., 2018). However, studies comparing EF and EC annual N_2O emission budgets are rare (if they exist at all), despite most present-day greenhouse gas inventories being founded on the use of EFs (Chadwick et al., 2018; IPCC, 2019; Voglmeier et al., 2019). In the light of this contradiction, our findings of Chapter 3 indicated that EFs did not seem to sufficiently account for the heterogeneity of processes driving the paddock scale exchange of N_2O. Using EFs resulted in estimated 3.48 kg N_2O-N ha^{-1} yr^{-1} (47.7%) lower annual emissions than determined by EC. This difference between the EF and EC budget was surprisingly distinct, particularly, when compared with the reported range of N_2O emissions (0.2–15.9 kg N_2O-N ha^{-1} yr^{-1}) from intensively grazed pastures in New Zealand (Luo et al., 2008a; de Klein et al., 2010; Luo et al., 2017).

Overall, it was found that the difference in annual N_2O budgets was likely due to EF estimates and EC measurements accounting differently for seasonal variations, the role of supplementary feed intake on cattle nitrogen excretion and BNE. The seasonal pattern present in the EC measurements e.g., the inherent interdependence between WFPS and F_{N2O}, was not well-described by site-specific EFs (Shang et al., 2020). Instead, it appeared that chamber F_{N2O} were only directly comparable to their EC

counterparts when measured at the same time and upscaled based on an area-weighted approach. The EF approach did not include that supplementary feed made up nearly 29.3% of the dairy cattle diet on-site in the year of measurement and, more generally, 20% in New Zealand (MPI, 2016; Ma et al., 2019). Supplements, such as maize silage, contain lower nitrogen contents than traditional perennial ryegrass-white clover pasture. Supplement intake can, therefore, reduce the excretion of urinary nitrogen but, on the other hand, includes the potential to also add to total nitrogen loads on farm (particularly when important from outside the farm boundary) (Luo et al., 2008c; Dijkstra et al., 2011; Gregorini et al., 2016).

A final factor leading to differences between the EF and EC emission budget were BNE; or rather that EFs only accounted for treatment effects but no other emissions that might have occurred continuously at low magnitude in the background of N_2O pulses. The literature has acknowledged BNE from agricultural land as a low and, more or less, constant positive F_{N2O} resulting from the mineralisation and cycling of residual soil N_r in response to soil management (Bouwman, 1996; Neftel et al., 2007; Aliyu et al., 2018). Our findings showed that 76% of F_{N2O} measured by EC occurred continuously at low magnitude throughout the year; while only 24% appeared in short bursts after grazing or management intervention and subsequent rainfall. Conversely, BNE are not commonly considered in EF derived estimates, which seems to conflict the potential significance of these low magnitude F_{N2O} in annual N_2O budgets quantified for grassland and agricultural soils (Kim et al., 2013; Aliyu et al., 2018).

The differences between EF estimates and EC measurements on the upscaling of N_2O emissions should, therefore, be thoroughly considered when quantifying N_2O budgets in the future. Particular attention is warranted for the inclusion of seasonal EFs along with the additional consideration of supplementary feed intake and the effect of BNE.

6.1.2 Overview of Chapter 4

The second thesis objective, as addressed in Chapter 4, was to investigate the effect of pasture renewal on F_{N2O}. Measurements were made across two adjacent, but differently managed, paddocks using a single EC system. Paddock 54 (P54) underwent pasture renewal using a no-till, direct-drill approach paired with rapid reseeding while the other paddock (P53) remained as a control under a ryegrass-white clover sward. The data analysis involved footprint-splitting and a new gap-filling approach. Key findings were:

- The total difference between P54 and P53 emissions during a 66-day period was 1.22 kg N_2O-N ha^{-1}; 93.4% of which were emitted in only two weeks.

- Reseeding four days after herbicide application to P54 led to the rapid establishment of a new pasture sward. Pulsed F_{N2O} subsided 21 days after herbicide application likely promoted by the increasing capacity for nitrogen uptake and photosynthetic strength of the emerging sward.
- The effect of renewal measured on P54 was apparent in both filtered and gap-filled flux data. Gap-filling supported a full quantification of the renewal effect and, therefore, allowed for a more defensible comparison of treatment effects on adjacent, but differently managed, paddocks than filtered F_{N2O} would have.

Highlighted by the findings of Chapter 4, pasture renewal on P54 led to distinct but short-term effects on F_{N2O}. We know from previous research that pulsed F_{N2O} after pasture renewal are often temporary with the majority of F_{N2O} accumulating immediately in the first days and months after intervention (Mori and Hojito, 2007; Velthof et al., 2010; MacDonald et al., 2011; Cowan et al., 2016; Krol et al., 2016b; Buchen, 2017). However, the degree to which the short-term nature of these renewal-related F_{N2O} needs to be accounted for in annual N_2O budgets and farm greenhouse gas balances has not yet been fully evaluated (Necpálová et al., 2013; Krol et al., 2016b; Buchen, 2017; Merbold et al., 2020).

However, the integration of these pulsed F_{N2O}, even if short-lived, into annual records could be very beneficial for N_2O budgeting and robustly accounting for potential trade-off between soil nitrogen (N_2O) and carbon (CO_2, CH_4) losses. Our findings suggested that F_{N2O} resulting from short-term management interventions should be included in full greenhouse gas accounting and IPCC Tier 2 and 3 datasets. Similarly, important for determining reliable and cost-efficient N_2O budgets will be the application of suitable data processing techniques. We used a single EC system to allow for the comparison of F_{N2O} from adjacent paddocks with our data processing based on utilising footprint-splitting and new gap-filling techniques. This approach enabled us to reduce the spatial separation between renewed and control paddocks and, in turn, minimised differences in soil and site characteristics that would also regulate F_{N2O}. Previous research has shown that differences between sites can have a much greater influence on N_2O emissions than differences between individual treatments depending on soil type, site management, and overall environmental conditions (Buchen et al., 2017; Reinsch et al., 2018b; Helfrich et al., 2020).

Hence, using a single EC system, coupled to robust footprint-splitting and gap-filling, will be very useful for evaluating the effect of farm management, including testing of different mitigation strategies, on N_2O emissions from adjacent paddocks in the future

(Goodrich et al., 2021). The approach applies particularly to rotationally grazed pastures, where greenhouse gas emissions vary with time, environmental conditions (e.g. precipitation) and day-to-day farm management decisions (Wall et al., 2020b).

6.1.3 Overview of Chapter 5

The third thesis objective, addressed in Chapter 5 and also presented as Wecking et al. (2020a), was to explore the ability of a quantum cascade laser (QCL) absorption spectrometer coupled to an EC system to analyse N_2O samples taken from static chambers. A novel injection technique was developed and the performance of the technique tested under field conditions by injecting samples of low to high N_2O concentration into the QCL device. Results from the QCL analysis were compared with measurements using gas chromatography (GC), which were conducted in an accredited laboratory of the New Zealand National Centre for Nitrous Oxide Measurements (NZ-NCNM). Key findings were:

- Sample N_2O concentrations (C_{N2O}) and calculated F_{N2O} from QCL analysis were equivalent to results from GC, i.e. for all intends and purposes the same.
- Missing equivalence between QCL and GC data was determined only for near-zero C_{N2O} and F_{N2O} and was likely caused by the calculation of small but apparent positive and negative F_{N2O} when in fact the actual flux was zero.
- Bland Altman and bioequivalence analyses were a valuable statistical tool in addition to orthogonal regression and not only determined the correlation between QCL and GC data but allowed to formally assess method agreement.
- Manual injections into the QCL were conducted at a rate of around 170 samples per hour and only included a short downtime of EC measurements.

The development of fast-response analysers for the measurement of N_2O has resulted in exciting opportunities for new experimental techniques beyond commonly used static chambers and GC analysis (Rannik et al., 2015; Brümmer et al., 2017; Zellweger et al., 2019). We showed that a fast-response analyser (QCL) for measuring N_2O can be used not only in its EC mode or connected to auto-chambers but also for the analysis of N_2O samples taken from static chambers via manual injection. Results from these manual injections compared well with results from laboratory GC, i.e. meaning that QCL analysis provided equivalent data while avoiding additional labour effort and time associated with sample storage and transport necessary for GC. The QCL analysis, therefore, provided an alternative and overall very practicable approach for rapidly analysing N_2O samples in the field. A strength of the technique was that it did not

greatly interfere with other measurements that were offline during the time of sample analysis. Storing N_2O samples in septum-sealed Exetainers enabled sample injection at suitable times e.g., postponing analysis if EC measurements were of higher importance. The use of a single QCL analyser thereby enabled the cost-efficient analysis of N_2O samples from static chambers alongside and near-concurrent to EC.

Overall, it was demonstrated that suitable statistical methods have to be adopted when formally assessing the agreement and difference (not only the correlation) between two quantitative methods of measurement, in this case, QCL and GC. Previous comparisons made in the literature commonly based on orthogonal (Jones et al., 2011) and linear regression (Cowan et al., 2014a; Brümmer et al., 2017; Tallec et al., 2019), Students t-tests (Christiansen et al., 2015) or raw data (Savage et al., 2014); but to assess the comparability of a standard and a new method, agreement and bioequivalence statistics are recommended in addition to these other approaches.

6.2 Broader implications

The work presented in this thesis highlights the suitability of the EC technique for the measurement of F_{N2O} at paddock scales. The need for more comprehensive measurements matching these larger scales was emphasised in the literature review (Chapter 2) where it became clear that most of our current understanding of the soil N_2O exchange process is based on the use of point scale static chambers (Rochette and Eriksen-Hamel, 2008; Rochette, 2011). Building on the need for F_{N2O} measurements at larger than point scales, the results of Chapter 3 and Chapter 4 revealed how EC can be used under real farm conditions (Fuchs et al., 2018; Liáng et al., 2018). We further showed (Chapter 5) how utilising a single QCL EC system for the injection of chamber N_2O samples can become possible near concurrent to EC. This thesis shall now be concluded by discussing the broader implications of the above findings. Recommendations for future research are suggested at the end of this section.

6.2.1 The impact of heterogeneity on measured nitrous oxide fluxes

Measurements to date are struggling to precisely represent the spatio-temporal heterogeneity of N_2O emissions from soil (Butterbach-Bahl et al., 2013). A primary reason for the variable nature of the soil N_2O exchange is that the microbial production of N_2O mostly occurs within small discrete volumes of soil that can undergo rapid physical and chemical changes (Kravchenko et al., 2017). The production of N_2O via denitrification accelerates under increased soil moisture and available NO_3^-, whereas only a slight shift in these conditions can favour nitrification, instead (Firestone and

Davidson, 1989). Also, it is likely that microbial nitrification and denitrification occur simultaneously in different microsites of the same pedon (Kool et al., 2011; Butterbach-Bahl et al., 2013; Smith et al., 2018). This means, firstly, that F_{N2O} are episodic in dependence on e.g., changes in soil moisture and, secondly, implies that measurements do not always describe these variations realistically. The smaller or larger the scale of a given measurement, the smaller or greater will be the spatio-temporal variability of measured F_{N2O}. Measurements using static chambers, for instance, are based on area points of generally much less than 1 m^2 from where F_{N2O} and derived EFs are upscaled to hectares or even feed into national inventories (Rochette and Eriksen-Hamel, 2008). In New Zealand, for instance, static chambers commonly cover an area of 0.0415 m^2. The variability between individual chambers of the same treatment and underlying soil conditions can lead to large coefficients of variation in resulting mean F_{N2O} e.g., 13–57% (Yamulki et al., 1995), 60–81% (Khalil et al., 2007) and 8–108% (Chadwick et al., 2014), where the scale of the actual measurement (area points) deviated from the desired output (upscaled F_{N2O} to represent N_2O emissions at the field scale).

The discrepancy between scales was explicitly discussed in our comparison of static chamber derived EF and EC annual N_2O emission budgets (Chapter 3). Findings showed that annual emissions from EC (7.30 kg N_2O-N ha^{-1} yr^{-1}) were greater than EF estimates (3.82 kg N_2O-N ha^{-1} yr^{-1}). The difference (3.48 kg N_2O-N ha^{-1} yr^{-1}) between these two budgets exemplified how the spatio-temporal scale of a measurement technique and its ability to represent that scale can affect the desired output data (Chadwick et al., 2018; Aliyu et al., 2019; Voglmeier et al., 2019; de Klein et al.; van der Weerden et al., 2020). In our study, the EF approach did not fully account for the complexity of processes that drive pasture N_2O exchange and this was mainly due to not including the effect of seasonal variability and pulse emission drivers e.g., WFPS (Liáng et al., 2018), the effect of supplementary feed intake on cattle nitrogen excretion (Selbie et al., 2015; Gibbs, 2018a) and BNE (Bouwman, 1996) – among other factors or even potentially cumulative effects. Our findings therefore stressed the importance of aligning field research as best as possible with measurement techniques suitable to represent the heterogeneity of the underlying N_2O exchange (Cowan et al., 2015; Shi et al., 2019; Shang et al., 2020).

Advances in analyser technology made in the last decade now allow the use of micrometeorological techniques to measure F_{N2O} at ecosystem scales (Wilkerson et al., 2019; Cowan et al., 2020; Merbold et al., 2020). One of these new analysers (QCL) was

used in this thesis with findings not only adding to a relatively small pool of literature but demonstrating the great ability of QCL EC to operate under realistic management conditions in the field (Jones et al., 2011; Wang et al., 2013a; Lucas-Moffat et al., 2018). An important contribution in this regard was made by developing a novel injection technique (Chapter 5), which allows using QCL for the analysis of chamber N_2O samples via manual injections and near-concurrent to EC. This ability of QCL analysers is of great interest for researchers because it offers to interlink point and paddock scale measurements, i.e. chambers and EC. Simultaneously utilising a QCL for both these purposes can provide data for understanding microbial processes (at point/chamber scales) and paddock F_{N2O} required for upscaling (Butterbach-Bahl et al., 2013). We recommend that studies aimed at measuring F_{N2O} consider and account for the impact of spatial and temporal heterogeneity on measured F_{N2O}. This can be done by selecting measurement techniques that suit the overall intention of the research objectives (Fig. 6-1).

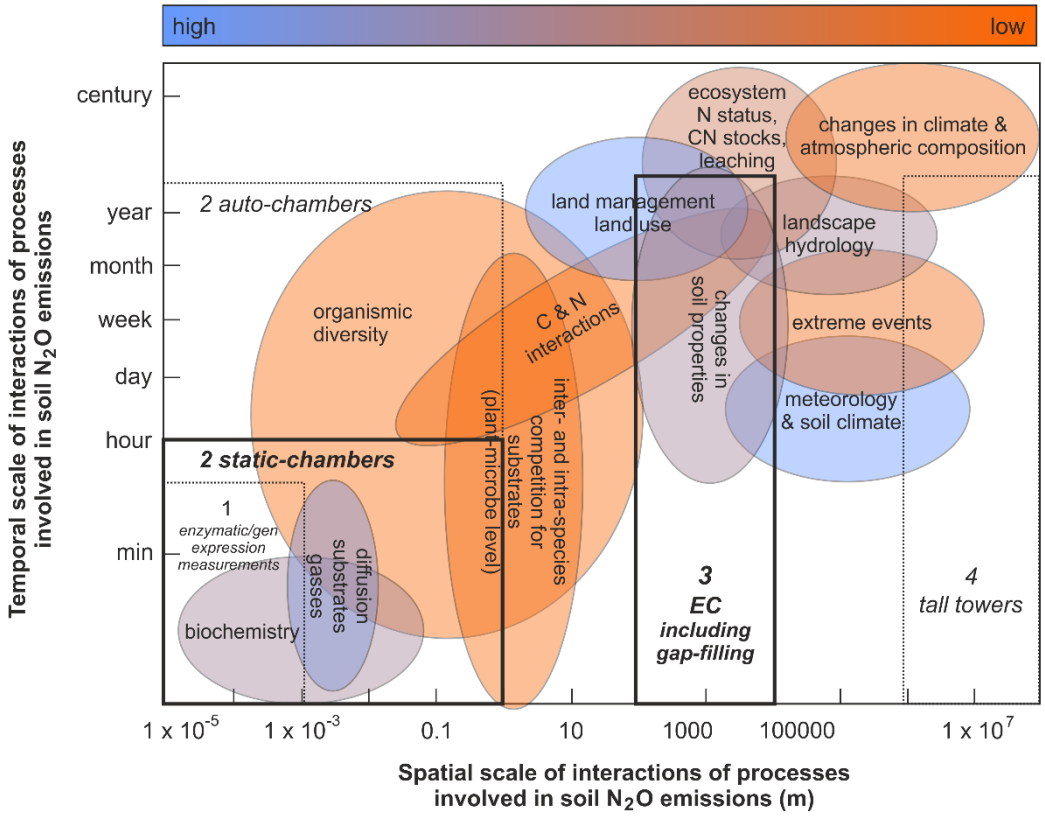

Figure 6-1 Drivers and processes of soil F_{N2O} across different temporal and spatial scales. The colour range (blue to orange) indicates the current level of understanding. Boxes (No. 1–4) show different techniques commonly used for measuring the soil N_2O exchange. Boxes No. 2 and 3 (in bold) distinguish the two measurement approaches (chambers and EC) used in this thesis. The figure was adapted and modified from Butterbach-Bahl et al. (2013).

6.2.2 The impact of farm management on nitrous oxide exchange

A major effect of grazing is the decoupling of the soil carbon and nitrogen cycles, where carbon is respired to the atmosphere (CO_2, CH_4) while N_r is returned to the soil, mostly in form of animal excreta, and eventually emitted as N_2O (Soussana and Lemaire, 2014; Pereira et al., 2018). Farm management practices can influence the magnitude of these (carbon and nitrogen) losses and, thus, dictate the associated environmental consequences (Aguirre-Villegas et al., 2017). In rotationally grazed systems, for instance, grazing intensity and time between grazing events control sward recovery after plant defoliation. This means that decisions regarding grazing intensity will also define the response of the plant-soil system after grazing (Lestienne et al., 2006; Pereira et al., 2018). Management practices, therefore, are likely to act as anthropogenic drivers of the soil N_2O exchange in addition to natural controls e.g., rainfall. The interdependence of anthropogenic N_r inputs and F_{N2O} has been well established (Luo et al., 1999; Müller et al., 2004; Shi et al., 2019) but, to date, not been fully investigated at larger than point scales.

The paddock scale EC measurements presented in this thesis showed a clear pattern of half-hourly F_{N2O} in response to animal grazing and the control of humans and environmental factors. Pulses of F_{N2O} generally occurred in response to changes in WFPS during and after grazing and, particularly, in autumn when the WFPS varied around the optimal zone of soil N_2O production (60–80%). It was found that pulsed F_{N2O} often remained discrete from regularly occurring F_{N2O} of lower magnitude, i.e. ≤ 0.6 nmol N_2O-N m^{-2} s^{-1} (Liáng et al., 2018), and, interestingly, these low F_{N2O} contributed an overall 76% to annual N_2O emission (Chapter 3). Low F_{N2O} were recognised as continuous fluxes that likely resulted from soil compaction through animal treading and the mineralisation of N_r bound to SOM and might as well have been a consequence of repeated inputs of N_r to the soil due to farm management and land-use history.

Our data also showed that low F_{N2O} made a substantial contribution to annual paddock N_2O emissions. However, the importance of low F_{N2O} occurring in the background of flux pulses was not acknowledged in the EF-based budget which was based on treatment effects only and did not per se consider any F_{N2O} of low magnitude or BNE (Bouwman, 1996; Kim et al., 2013; Aliyu et al., 2018). We suggested, therefore, that the quantification of annual N_2O budgets would benefit from including BNE and other factors (seasonal variations, animal diet) to realistically account for the effect of farm management on paddock N_2O exchange.

Day-to-day management decisions can have a major influence on the emission of N_2O but quantifying the effect of these short-term interventions has remained difficult in practice, particularly, when using static chambers (Fuchs et al., 2018; Ammann et al., 2020; De Rosa et al., 2020). We demonstrated in Chapter 4 that determining the effect of farm management, i.e. direct-drill pasture renewal, can be measured when using EC. Our findings showed that 93.4% of the difference in N_2O emissions between a renewed (P54) and a control (P53) site was emitted in bursts within a two weeks' period of the first 21 days after renewal intervention. Data processing and derived results were based on an advanced footprint-splitting (Wall et al., 2020b) and gap-filling (Goodrich et al., 2021) approach. To our knowledge, this approach had not been used by others before and, thus, is a major advance on existing approaches for comparing F_{N2O} from different management strategies (Fuchs et al., 2018; Liáng et al., 2018; Nemitz et al., 2018; Lognoul et al., 2019; Cowan et al., 2020). Our approach enables researchers to now evaluate farm management effects on N_2O emissions more robustly and particularly in rotationally grazed systems where F_{N2O} are notoriously variable.

6.3 Recommendations and concluding remarks

The investigations presented in this thesis illustrated the potential of technological advances to contribute to the measurement of F_{N2O} from intensively grazed dairy pastures. Overall, it was recommended to increase the number of multi-year N_2O studies to enable further comparisons between existing datasets and F_{N2O} data resulting from some of these new technologies (Voglmeier et al., 2019; Merbold et al., 2020; Shang et al., 2020; van der Weerden et al., 2020). An increasing number of studies and comparisons could then be used to help refine present and future N_2O inventories and potentially also influence the behaviour of farmers, stakeholders, and policymakers towards sustainability (Röös et al., 2017; Berners-Lee et al., 2018). The findings of this work support the view that science and technology have advanced to a point where the practical implementation of knowledge about soil N_2O exchange processes into applied farm management strategies should be eagerly pursued (Jantke et al., 2020; Kanter et al., 2020; Ogle et al., 2020).

Working in the field of greenhouse gas research for the past years, I experienced first-hand how some of the advancing state of knowledge was implemented. Emission factors, for instance, have become more refined in the New Zealand national N_2O inventory (Section 2.4.1) (MfE, 2020; van der Weerden et al., 2020). And, at the thesis scale, I demonstrated myself how to improve and use the QCL EC technique for continuous F_{N2O} measurements on intensively grazed land (Liáng et al., 2018; Wall et

al., 2020b; Goodrich et al., 2021). However, this thesis would not have been possible without the willing cooperation of the farm owners, who recorded essential farm management data and were highly interested in whether my findings could be applied in practice. Based on this experience, I believe that further research should strive to include precise farm management data as well as consider the farmers' knowledge, perspective, and attitude towards greenhouse gas emissions and sustainability (Jantke et al., 2020). My work highlighted that accounting for N_2O emissions from agricultural land has to reach beyond looking into single drivers and individual EFs alone. Much further work is needed to evaluate the interactive response of multiple factors and controls on soil N_2O exchange (Luo et al., 2008d; Zhu et al., 2016; Li et al., 2020). For the days yet to come, we have to bear in mind that a major remaining question (and challenge alike) will always be to evaluate whether the level of our understanding and technological advance will be used to a degree sufficient enough to keep pace with a rapidly changing climate?

In light of the findings of this thesis, I recommend future research to address some of the following points:

- Continuation of the measurements at Troughton farm to add to the long-term record of site-specific F_{N2O}. The current dataset comprises about four years (2016–2020) with selected parts being presented in this thesis (Liáng et al., 2018; Goodrich et al., 2021). Since EC measurements beyond the five-year scale are rare, both in New Zealand and elsewhere (Ammann et al., 2020; Cowan et al., 2020; Merbold et al., 2020), F_{N2O} data from Troughton farm are of great value for the research community, particularly, for the development of process-based models (Fuchs et al., 2020).

- The number of EC studies from intensively managed grasslands is increasing, but measurements from intensively grazed pastures, except for Liáng et al. (2018), are underrepresented. Therefore, building up the numbers of high-frequency measurements on these lands would be very beneficial to examine how differences between sites, inter-annual variabilities, and farm management would affect soil N_2O exchange.

- Increasing the number of micrometeorological F_{N2O} measurements could be achieved by coupling suitable N_2O analysers (e.g., QCL) to existing flux towers or greenhouse gas observation systems as provided by global flux measurement initiatives (e.g. the Integrated Carbon Observation System, ICOS). Combining

F_{N2O} with the measurement of other greenhouse gases (CO_2, CH_4) would foster the understanding of linkages between soil carbon and nitrogen cycles, and also help to account for the effect of trade-offs on greenhouse gas balances, especially, when evaluating mitigation practices. Future flux measurements would ideally be complemented by measurements of soil nutrient stocks to disentangle fluxes and flows of the nutrient (carbon, nitrogen) cycling network.

- An interesting area of research are manipulative studies to observe the effect of extreme events on N_2O emissions (Li et al., 2020). These could include chamber and/or micrometeorological methods to examine and model how a change in plant community, species diversity or weather severity would affect the soil N_2O exchange. Changes to the frequency and magnitude of extreme events are likely consequences of climate change and, therefore, understanding their impacts on soil functioning will be important (Jentsch et al., 2007; Reyer et al., 2013). Likewise, testing the effect of diverse swards on N_2O emissions might be useful to develop sustainable management practices and greenhouse gas mitigation strategies (Box et al., 2017; Gardiner et al., 2018). [4]

To conclude, this thesis used the EC technique to measure F_{N2O} from an intensively grazed dairy pasture in New Zealand that received high inputs of excreta nitrogen. Findings emphasised the ability of EC measurement to provide an alternative approach to traditional static chambers and, thereby, added to an advancing but yet still confined pool of research. Long-term, high frequency measurements of N_2O from intensively grazed pastures are rare and, as such, EC measurements from New Zealand grasslands have much to contribute to the global understanding of how the exchange of N_2O from intensively farmed land works.

[4] We are aware that the content of this thesis was focused on the production side of the food system. However, the above recommendations do not intend to prioritise research efforts regarding this side. Amendments on the consumption side, e.g. reducing food waste, consumer behaviour and rebalancing the human diet, will be equally important for creating a sustainable future (Röös et al., 2017).

References

Abdalla, M., Jones, M., Smith, P., Williams, M., 2009. Nitrous oxide fluxes and denitrification sensitivity to temperature in Irish pasture soils. Soil Use Manage. 25, 4, 376-388.

Acevedo, O.C., Moraes, O.L.L., Degrazia, G.A., Fitzjarrald, D.R., Manzi, A.O., Campos, J.G., 2009. Is friction velocity the most appropriate scale for correcting nocturnal carbon dioxide fluxes? Agric. For. Meteorol. 149, 1, 1-10.

Aguirre-Villegas, H.A., Passos-Fonseca, T.H., Reinemann, D.J., Larson, R., 2017. Grazing intensity affects the environmental impact of dairy systems. J. Dairy Sci. 100, 8, 6804-6821.

Aliyu, G., Sanz-Cobena, A., Müller, C., Zaman, M., Luo, J., Liu, D., Yuan, J., Chen, Z., Niu, Y., Arowolo, A., Ding, W., 2018. A meta-analysis of soil background N_2O emissions from croplands in China shows variation among climatic zones. Agric. Ecosyst. Environ. 267, 63-73.

Aliyu, G., Luo, J., Di, H.J., Lindsey, S., Liu, D., Yuan, J., Chen, Z., Lin, Y., He, T., Zaman, M., Ding, W., 2019. Nitrous oxide emissions from China's croplands based on regional and crop-specific emission factors deviate from IPCC 2006 estimates. Sci. Total Environ., 669, 547-558.

Allan, J.D., Coe, H., Cohen, R.C., Fried, A., F., H.J., Heard, E.E., Hofzumahaus, A., Lewis, A.C., Plane, J.M.C., Richter, D., Lopez-Saiz , A., J., W.A., Williams, J., Wood, E.C., 2006. Analytical Techniques for Atmospheric Measurement, Heard, D.E. (Ed.). Blackwell Publishing, Oxford, UK, Iowa, USA, Victoria, Australia. 501p.

Allard, V., Soussana, J.F., Falcimagne, R., Berbigier, P., Bonnefond, J.M., Ceschia, E., D'hour, P., Hénault, C., Laville, P., Martin, C., Pinarès-Patino, C., 2007. The role of grazing management for the net biome productivity and greenhouse gas budget (CO_2, N_2O and CH_4) of semi-natural grassland. Agric. Ecosyst. Environ. 121, 1, 47-58.

Ammann, C., Spirig, C., Leifeld, J., Neftel, A., 2009. Assessment of the nitrogen and carbon budget of two managed temperate grassland fields. Agric. Ecosyst. Environ. 133, 3, 150-162.

Ammann, C., Neftel, A., Jocher, M., Fuhrer, J., Leifeld, J., 2020. Effect of management and weather variations on the greenhouse gas budget of two grasslands during a 10-year experiment. Agric. Ecosyst. Environ. 292, 1-14.

Amon, B., Kryvoruchko, V., Amon, T., Zechmeister-Boltenstern, S., 2006. Methane, nitrous oxide and ammonia emissions during storage and after application of dairy cattle slurry and influence of slurry treatment. Agric. Ecosyst. Environ. 112, 2-3, 153-162.

Arp, D.J., Stein, L.Y., 2003. Metabolism of inorganic N compounds by ammonia-oxidizing bacteria. Crit. Rev. Biochem. Mol. Biol. 38, 471-495.

Aubinet, M., Grelle, A., Ibrom, A., Rannik, Ü., Moncrieff, J., Foken, T., Kowalski, A.S., Martin, P.H., Berbigier, P., Bernhofer, C., Clement, R., Elbers, J., Granier, A.,

Grünwald, T., Morgenstern, K., Pilegaard, K., Rebmann, C., Snijders, W., Valentini, R., Vesala, T., 1999. Estimates of the Annual Net Carbon and Water Exchange of Forests: The EUROFLUX Methodology. In: Fitter, A.H. ,Raffaelli, D.G. (Eds.), Adv. Ecol. Res. Academic Press, pp. 113-175.

Aubinet, M., Vesala, T., Papale, D., 2012. Eddy covariance: a practical guide to measurement and data analysis. Springer, Dordrecht, London. 722p.

Austin, W.M.D., 1788. Experiments of the formation of volatile alkali, and on the affinities of the phlogisticated and light inflamable airs. Philos. Trans. R. Soc. Lond. 78, 379-387.

Baggs, E.M., Rees, R.M., Smith, K.A., Vinten, A.J.A., 2000. Nitrous oxide emission from soils after incorporating crop residues. Soil Use Manage. 16, 2, 82-87.

Balaine, N., Clough, T.J., Beare, M.H., Thomas, S.M., Meenken, E.D., Ross, J.G., 2013. Changes in relative gas diffusivity explain soil nitrous oxide flux dynamics. Soil Sci. Soc. Am. J. 77, 5, 1496-1505.

Baldocchi, D., Falge, E., Gu, L., Olson, R., Hollinger, D.Y., Running, S., Anthoni, P., Bernhofer, C., Davis, K., Evans, R., Fuentes, J., Goldstein, A., Katul, G., Law, B., Lee, X., Malhi, Y., Meyers, T.P., Munger, J.W., Oechel, W., Paw, K.T., Pilegaard, K., Schmid, H.P., Valentini, R., Verma, S., Vesala, T., Wilson, K., Wofsy, S.C., 2001. FLUXNET: A New Tool to Study the Temporal and Spatial Variability of Ecosystem–Scale Carbon Dioxide, Water Vapor, and Energy Flux Densities. Bull. Am. Meteorol. Soc. 82, 11, 2415-2434.

Baldocchi, D., 2014. Measuring fluxes of trace gases and energy between ecosystems and the atmosphere – the state and future of the eddy covariance method. Global Change Biol. 20, 12, 3600-3609.

Baldocchi, D.D., Hincks, B.B., Meyers, T.P., 1988. Measuring Biosphere-Atmosphere Exchanges of Biologically Related Gases with Micrometeorological Methods. Ecology. 69, 5, 1331-1340.

Baldocchi, D.D., 2003. Assessing the eddy covariance technique for evaluating carbon dioxide exchange rates of ecosystems: past, present and future. Global Change Biol. 9, 4, 479-492.

Baldocchi, D.D., 2019. How eddy covariance flux measurements have contributed to our understanding of Global Change Biology. Global Change Biol. 0, 1-19.

Balesdent, J., Chenu, C., Balabane, M., 2000. Relationship of soil organic matter dynamics to physical protection and tillage. Soil Tillage Res. 53, 3, 215-230.

Ball, B.C., Scott, A., Parker, J.P., 1999. Field N_2O, CO_2 and CH_4 fluxes in relation to tillage, compaction and soil quality in Scotland. Soil Tillage Res. 53, 1, 29-39.

Ball, B.C., 2013. Soil structure and greenhouse gas emissions: a synthesis of 20 years of experimentation. Eur. J. Soil Sci. 64, 3, 357-373.

Barnard, R., Leadley, P.W., Hungate, B.A., 2005. Global change, nitrification, and denitrification: A review. Global Biogeochem. Cycles. 19, 1, 1-13.

Barrow, N.J., Lambourne, L.J., 1962. Partition of excreted nitrogen, sulphur, and phosphorus between the faeces and urine of sheep being fed pasture. Aust. J. Agric. Res. 13, 3, 461-471.

Beck, M., Hofstetter, D., Aellen, T., Faist, J., Oesterle, U., Ilegems, M., Gini, E., Melchior, H., 2002. Continuous Wave Operation of a Mid-Infrared Semiconductor Laser at Room Temperature. Science. 295, 5553, 301-305.

Bergamaschi, P., Corazza, M., Karstens, U., Athanassiadou, M., Thompson, R., Pison, I., Manning, A., Segers, A.J., Vermeulen, A., Janssens-Maenhout, G., Schmidt, M., Ramonet, M., Meinhardt, F., Aalto, T., Haszpra, L., Moncrieff, J., Popa, E., Lowry, D., Dlugokencky, E., 2014. Top-down estimates of European CH_4 and N_2O emissions based on four different inverse models. Atmos. Chem. Phys. Discuss. 14, 15683-15734.

Berners-Lee, M., Kennelly, C., Watson, R., N. Hewitt, C., 2018. Current global food production is sufficient to meet human nutritional needs in 2050 provided there is radical societal adaptation. Elem. Sci. Anth. 6, 52, 1-14.

Beukes, P.C., Gregorini, P., Romera, A.J., Levy, G., Waghorn, G.C., 2010. Improving production efficiency as a strategy to mitigate greenhouse gas emissions on pastoral dairy farms in New Zealand. Agric. Ecosyst. Environ. 136, 3, 358-365.

Bidaux, Y., Bismuto, A., Patimisco, P., Sampaolo, A., Gresch, T., Strubi, G., Blaser, S., Tittel, F.K., Spagnolo, V., Muller, A., Faist, J., 2016. Mid infrared quantum cascade laser operating in pure amplitude modulation for background-free trace gas spectroscopy. Opt. Express. 24, 23, 26464-26471.

Blume, H.P., Brümmer, G.W., Scheffer, F., Horn, R., Kandeler, E., Schachtschabel, P., Kögel-Knabner, I., Welp, G., Kretzschmar, R., Thiele-Bruhn, S., 2009. Scheffer/Schachtschabel: Lehrbuch der Bodenkunde, 16 ed. Spektrum Akademischer Verlag. 584p.

Bol, R., Dunn, R.M., Pilgrim, E.S., 2011. Managing C and N in grassland systems: the adaptive cycle theory perspective. In: Lemaire, G., Hodgson, J.G. ,Chabbi, A. (Eds.), Grassland Productivity and Ecosystem Services. CAB International, Wallingford, UK, pp. 73-82.

Bolan, N.S., Saggar, S., Luo, J., Bhandral, R., Singh, J., 2004. Gaseous Emissions of Nitrogen from Grazed Pastures: Processes, Measurements and Modelling, Environmental Implications, and Mitigation. Adv. Agron. 84, 37-120.

Bolin, B., Rodhe, H., 1973. A note on the concepts of age distribution and transit time in natural reservoirs. Tellus. 25, 1, 58-62.

Bouwman, A.F., 1996. Direct emission of nitrous oxide from agricultural soils. Nutr. Cycling Agroecosyst. 46, 53-70.

Bouwman, L., Goldewijk, K.K., Van Der Hoek, K.W., Beusen, A.H.W., Van Vuuren, D.P., Willems, J., Rufino, M.C., Stehfest, E., 2013. Exploring global changes in nitrogen and phosphorus cycles in agriculture induced by livestock production over the 1900–2050 period. PNAS. 110, 52, 20882-20887.

Bowatte, S., Hoogendoorn, C.J., Newton, P.C.D., Liu, Y., Brock, S., Theobald, P., 2015. Pasture species and cultivar effects on N_2O emissons after cattle urine

application. Report prepared for New Zealand Agricultural Greenhouse Gas Research Centre: Milestone 6.1.5. AgResearch. 22p.

Box, L.A., Edwards, G.R., Bryant, R.H., 2017. Milk production and urinary nitrogen excretion of dairy cows grazing plantain in early and late lactation. N.Z. J. Agric. Res. 60, 4, 470-482.

Box, L.A., Edwards, G.R., Bryant, R.H., 2018. Seasonal and diurnal changes in aucubin, catalpol and acteoside concentration of plantain herbage grown at high and low N fertiliser inputs. N.Z. J. Agric. Res., 1-11.

Braker, G., Conrad, R., 2011. Diversity, Structure, and Size of N_2O-Producing Microbial Communities in Soils—What Matters for Their Functioning? Adv. Appl. Microbiol. 75, 33-70.

Brümmer, C., Lyshede, B., Lempio, D., Delorme, J.-P., Rüffer, J.J., Fuß, R., Moffat, A.M., Hurkuck, M., Ibrom, A., Ambus, P., Flessa, H., Kutsch, W.L., 2017. Gas chromatography vs. quantum cascade laser-based N_2O flux measurements using a novel chamber design. Biogeosciences. 14, 6, 1365-1381.

Buchen, C. 2017. The fate of nitrogen after grassland renewal and grassland conversion to maize cropping – An investigation of N_2O processes and mineral N dynamics at the field scale. thesis, Technischen Universität Carolo-Wilhelmina zu Braunschweig, Braunschweig.

Buchen, C., Well, R., Helfrich, M., Fuß, R., Kayser, M., Gensior, A., Benke, M., Flessa, H., 2017. Soil mineral N dynamics and N_2O emissions following grassland renewal. Agric. Ecosyst. Environ. 246, 325-342.

Bureau, J., Grossel, A., Loubet, B., Laville, P., Massad, R., Haas, E., Butterbach-Bahl, K., Guimbaud, C., Hénault, C., 2017. Evaluation of new flux attribution methods for mapping N_2O emissions at the landscape scale. Agric. Ecosyst. Environ. 247, 9-22.

Burgin, A.J., Yang, W.H., Hamilton, S.K., Silver, W.L., 2011. Beyond carbon and nitrogen: how the microbial energy economy couples elemental cycles in diverse ecosystems. Front. Ecol. Environ. 9, 1, 44-52.

Butterbach-Bahl, K., Gundersen, P., Ambus, P., Augustin, J., Beier, C., Boeckx, P., Dannenmann, M., Gimeno, B.S., Ibrom, A., Kiese, R., Kitzler, B., Rees, R.M., Smith, K.A., Stevens, C., Vesala, T., Zechmeister-Boltenstern, S., 2011. Nitrogen processes in terrestrial ecosystems. In: Bleeker, A., Grizzetti, B., Howard, C.M., Billen, G., van Grinsven, H., Erisman, J.W., Sutton, M.A. ,Grennfelt, P. (Eds.), The European Nitrogen Assessment: Sources, Effects and Policy Perspectives. Cambridge University Press, Cambridge, pp. 99-125.

Butterbach-Bahl, K., Baggs, E.M., Dannenmann, M., Kiese, R., Zechmeister-Boltenstern, S., 2013. Nitrous oxide emissions from soils: how well do we understand the processes and their controls? Philos. Trans. R. Soc. Lond. B. Biol. Sci. 368, 1621, 1-13.

Cai, Y., Akiyama, H., 2016. Nitrogen loss factors of nitrogen trace gas emissions and leaching from excreta patches in grassland ecosystems: A summary of available data. Sci. Total Environ. 572, 185-195.

Cai, Y., Golub, A.A., Hertel, T.W., 2017a. Agricultural research spending must increase in light of future uncertainties. Food Policy. 70, 71-83.

Cai, Y.J., Chang, S.X., Cheng, Y., 2017b. Greenhouse gas emissions from excreta patches of grazing animals and their mitigation strategies. Earth-Sci. Rev. 171, 44-57.

Carran, R.A., Theobald, P.W., Evans, J.P., 1995. Emission of Nitrous Oxide from some Grazed Pasture Soils in New Zealand. Aust. J. Soil Res. 33, 341-352.

Casciotti, K.L., Ward, B.B., 2001. Dissimilatory Nitrite Reductase Genes from Autotrophic Ammonia-Oxidizing Bacteria. Appl. Environ. Microbiol. 67, 5, 2213-2221.

Castillo, A., Kebreab, E., Beever, D., Barbi, J., 2001. The effect of protein supplementation on nitrogen utilization in lactating dairy cows fed grass silage diets. J. Anim. Sci. 79, 1, 247-53.

Chadwick, D.R., Cardenas, L., Misselbrook, T.H., Smith, K.A., Rees, R.M., Watson, C.J., McGeough, K.L., Williams, J.R., Cloy, J.M., Thorman, R.E., Dhanoa, M.S., 2014. Optimizing chamber methods for measuring nitrous oxide emissions from plot-based agricultural experiments. Eur. J. Soil Sci. 65, 2, 295-307.

Chadwick, D.R., Cardenas, L.M., Dhanoa, M.S., Donovan, N., Misselbrook, T., Williams, J.R., Thorman, R.E., McGeough, K.L., Watson, C.J., Bell, M., Anthony, S.G., Rees, R.M., 2018. The contribution of cattle urine and dung to nitrous oxide emissions: Quantification of country specific emission factors and implications for national inventories. Sci. Total Environ. 635, 607-617.

Chapuis-Lardy, L., Wrage, N., Metay, A., Chotte, J.L., Bernoux, M., 2007. Soils, a sink for N_2O? A review. Global Change Biol. 13, 1-17.

Chen, H., Williams, D., Walker, J.T., Shi, W., 2016. Probing the biological sources of soil N_2O emissions by quantum cascade laser-based ^{15}N isotopocule analysis. Soil Biol. Biochem. 100, 175-181.

Christiansen, J.R., Korhonen, J.F.J., Juszczak, R., Giebels, M., Pihlatie, M., 2011. Assessing the effects of chamber placement, manual sampling and headspace mixing on CH_4 fluxes in a laboratory experiment. Plant Soil. 343, 1, 171-185.

Christiansen, J.R., Outhwaite, J., Smukler, S.M., 2015. Comparison of CO_2, CH_4 and N_2O soil-atmosphere exchange measured in static chambers with cavity ring-down spectroscopy and gas chromatography. Agric. For. Meteorol. 211-212, 48-57.

Cicerone, R., 1989. Analysis of sources and sinks of atmospheric nitrous oxide (N_2O). J. Geophys. Res. 94, 18265-18721.

Cofman Anderson, I., Levine, J.S., 1986. Relative rates of nitric oxide and nitrous oxide production by nitrifiers, denitrifiers, and nitrate respirers. Appl. Environ. Microbiol. 51, 938-945.

Conant, R.T., Paustian, K., Elliott, E.T., 2001. Grassland management and conversion into grassland: Effects on soil carbon. Ecol. Appl. 11, 2, 343-355.

Conrad, R., 1996. Soil microorganisms as controllers of atmospheric trace gases (H_2, CO, CH_4, OCS, N_2O, and NO). Microbiol. Rev. 60, 4, 609-640.

Cowan, N., Levy, P., Maire, J., Coyle, M., Leeson, S.R., Famulari, D., Carozzi, M., Nemitz, E., Skiba, U., 2020. An evaluation of four years of nitrous oxide fluxes after application of ammonium nitrate and urea fertilisers measured using the eddy covariance method. Agric. For. Meteorol. 280, 107812.

Cowan, N.J., Famulari, D., Levy, P.E., Anderson, M., Bell, M.J., Rees, R.M., Reay, D.S., Skiba, U.M., 2014a. An improved method for measuring soil N_2O fluxes using a quantum cascade laser with a dynamic chamber. Eur. J. Soil Sci. 65, 5, 643-652.

Cowan, N.J., Famulari, D., Levy, P.E., Anderson, M., Reay, D.S., Skiba, U.M., 2014b. Investigating uptake of N_2O in agricultural soils using a high-precision dynamic chamber method. Atmos. Meas. Tech. 7, 12, 4455-4462.

Cowan, N.J., Norman, P., Famulari, D., Levy, P.E., Reay, D.S., Skiba, U.M., 2015. Spatial variability and hotspots of soil N_2O fluxes from intensively grazed grassland. Biogeosciences. 12, 5, 1585-1596.

Cowan, N.J., Levy, P.E., Famulari, D., Anderson, M., Drewer, J., Carozzi, M., Reay, D.S., Skiba, U.M., 2016. The influence of tillage on N_2O fluxes from an intensively managed grazed grassland in Scotland. Biogeosciences. 13, 16, 4811-4821.

Coyne, M.S., 2018. Denitrification in Soil. In: Bobby, A.S. ,Rattan, L. (Eds.), Soil Nitrogen Uses and Environmental Impacts, 1 ed. CRC Press, Boca Raton, pp. 95-139, Chapter 5.

Crutzen, P.J., 1970. The influence of nitrogen oxides on the atmospheric ozone content. Q. J. R. Meteorolog. Soc. 96, 408, 320-325.

Crutzen, P.J., Mosier, A.R., Smith, K.A., Winiwarter, W., 2008. N_2O release from agro-biofuel production negates global warming reduction by replacing fossil fuels. Atmos. Chem. Phys. 8, 2, 389-395.

Curl, R.F., Capasso, F., Gmachl, C., Kosterev, A.A., McManus, B., Lewicki, R., Pusharsky, M., Wysocki, G., Tittel, F.K., 2010. Quantum cascade lasers in chemical physics. Chem. Phys. Lett. 487, 1, 1-18.

Daniel, J.S., Velders, G.J.M., Solomon, S., McFarland, M., Montzka, S.A., 2007. Present and future sources and emissions of halocarbons: Toward new constraints. J. Geophys. Res. Atmos. 112, D02301, 1-11.

Danielson, R.E., Sutherland, P.L., 1986. Porosity. In: Klute, A. (Ed.), Methods of soil analysis. Part 1 - physical and mineralogical methods. Soil Science Society America Publications, Madison, WI, pp. 443-461.

Davidson, E.A., 1991. Fluxes of nitrous oxide and nitric oxide from terrestrial eocsystems. In: Rogers, J.E. ,Whitman, W.B. (Eds.), Microbial production and consumption of greenhouse gases: methane, nitrogen oxides, and halomethanes. ASM Press, American Society for Microbiology, Washington, D. C., pp. 219-235.

Davidson, E.A., 2009. The contribution of manure and fertilizer nitrogen to atmospheric nitrous oxide since 1860. Nat. Geosci. 2, 9, 659.

Davidson, E.A., Kanter, D., 2014. Inventories and scenarios of nitrous oxide emissions. Environ. Res. Lett. 9, 105012, 1-12.

Davies, Smith, Vinten, 2001. The mineralisation and fate of nitrogen following ploughing of grass and grass-clover swards. Biol. Fertil. Soils. 33, 5, 423-434.

de Klein, C.A.M., Sherlock, R.R., Ledgard, S.F., Barton, L., Kelliher, F.M., Walcroft, A.S., Rys, G., 2002. Nitrous oxide emissions from New Zealand agriculture: research to refine the national inventory. In: VanHam, J., Baede, A.P.M., Guicherit, R. ,Williams Jacobse, J.G.F.M. (Eds.), Non-CO2 greenhouse gases: scientific understanding, control options and policy aspects. Proceedings of the Third International Symposium, 21-23 January 2002. Millpress Science Publishers, Maastricht, Netherlands, pp. 275-280.

de Klein, C.A.M., Barton, L., Sherlock, R.R., Li, Z., Littlejohn, R.P., 2003. Estimating a nitrous oxide emission factor for animal urine from some New Zealand pastoral soils. Aust. J. Soil Res. 41, 381-399.

de Klein, C.A.M., Novoa, R.S.A., Ogle, S., Smith, K.A., Rochette, P., Wirth, T.C., McConkey, B.G., Mosier, A., Rypdal, K., 2006a. N_2O emissions from managed soils, and CO_2 emissions from lime and urea application. In: Gytarsky, M., Higarashi, T., Irving, W., Krug, T. ,Penman, J. (Eds.), 2006 IPCC Guidelines for National Greenhouse Gas Inventories. Intergovernmental Panel on Climate Change, Geneva, Switzerland, pp. 11.1-11.54.

de Klein, C.A.M., Smith, L.C., Monaghan, R.M., 2006b. Restricted autumn grazing to reduce nitrous oxide emissions from dairy pastures in Southland, New Zealand. Agric. Ecosyst. Environ. 112, 2, 192-199.

de Klein, C.A.M., Eckard, R.J., 2008. Targeted technologies for nitrous oxide abatement from animal agriculture. Australian Journal of Experimental Agriculture. 48, 2, 14-20.

de Klein, C.A.M., Eckhard, R., van der Weerden, T., 2010. Nitrous Oxide Emissions from the Nitrogen Cycle in Livestock Agriculture: Estimation and Mitigation. In: Smith, K.A. (Ed.), Nitrous oxide and climate change. Earthscan, London, pp. 107-142.

de Klein, C.A.M., Harvey, M.J., Clough, T., Rochette, P., Kelliher, F., Venetera, R., Alfaro, M., Chadwick, D., 2015. Nitrous Oxide Chamber Methodology Guidelines. Version 1.1. Ministry of Primary Industries, Wellington. 146p.

de Klein, C.A.M., Alfaro, M.A., Giltrap, D., Topp, C.F.E., Simon, P.L., Noble, A., van der Weerden, T.J., 2020. Global research alliance N_2O chamber methodology guidelines: Statistical considerations, emission factor calculation, and data reporting. J. Environ. Qual. n/a, 1-12.

De Rosa, D., Rowlings, D., Fulkerson, B., Scheer, C., Friedl, J., Labadz, M., Grace, P., 2020. Field-scale management and environmental drivers of N_2O emissions from pasture-based dairy systems. Nutr. Cycling Agroecosyst. 117, 299-315.

De Vliegher, A., Carlier, L., 2007. The effect of the age of grassland on yield, botanical composition and nitrate content in the soil under grazing conditions. In: De Vliegher, A. ,Carlier, L. (Eds.), Grassl. Sci. Europ, pp. 51-54, Chapter 12.

Decock, C., Lee, J., Necpalova, M., Pereira, E.I.P., Tendall, D.M., Six, J., 2015. Mitigating N_2O emissions from soil: from patching leaks to transformative action. Soil. 1, 2, 687-694.

Del Grosso, S.J., Wirth, T., Ogle, S.M., Parton, W.J., 2008. Estimating Agricultural Nitrous Oxide Emissions. Eos, Transactions American Geophysical Union. 89, 51, 529-529.

Denmead, O., 2008. Approaches to measuring fluxes of methane and nitrous oxide between landscapes and the atmosphere. Plant Soil. 309, 1-2, 5-24.

Dennis, S.J. 2009. Nitrate leaching and nitrous oxide emission from grazed grassland: upscaling from lysimeters to farm. thesis, Lincoln Universit, New Zealand.

Dietz, M., Machill, S., Hoffmann, H., Schmidtke, K., 2013. Inhibitory effects of Plantago lanceolata L. on soil N mineralization. Plant Soil. 368, 1, 445-458.

Dijkstra, J., Oenema, O., Bannink, A., 2011. Dietary strategies to reducing N excretion from cattle: Implications for methane emissions. Curr. Opin. Environ. Sustain. 3, 5, 414-422.

Drewer, J., Anderson, M., Levy, P.E., Scholtes, B., Helfter, C., Parker, J., Rees, R.M., Skiba, U.M., 2016. The impact of ploughing intensively managed temperate grasslands on N_2O, CH_4 and CO_2 fluxes. Plant Soil. 411, 1-2, 193-208.

Dumortier, P., Aubinet, M., Lebeau, F., Naiken, A., Heinesch, B., 2019. Point source emission estimation using eddy covariance: Validation using an artificial source experiment. Agric. For. Meteorol. 266-267, 148-156.

Dungait, J.A.J., Hopkins, D.W., Gregory, A.S., Whitmore, A.P., 2012. Soil organic matter turnover is governed by accessibility not recalcitrance. Global Change Biol. 18, 6, 1781-1796.

Ehhalt, D., Prather, M., Dentener, F., Derwent, R.G., Dlugokencky, E., Holland, E.A., Isaksen, I.S.A., Katima, J., Kirchhoff, V., Matson, P.A., Midgley, P.W., M., 2001. Atmospheric Chemistry and Greenhouse Gases. In: Joos, F. ,McFarland, M. (Eds.), Climate Change 2001: The Scientific Basis, Third Assessment Report. IPCC: Working Group I of the Intergovernmental Panel on Climate Change. IPCC, Geneva, Switzerland, pp. 239-287, Chapter 4.

Elmerich, C., Newton, W.E., 2007. Associative and endophytic nitrogen-fixing bacteria and cyanobacterial associations, Newton, W.E. (Ed.). Springers, Heidelberg, Gemany.

Epstein, H.E., Burke, I.C., Mosier, A.R., 2001. Plant effects on nitrogen retention in shortgrass steppe 2 years after 15N addition. Oecologia. 128, 3, 422-430.

Eriksen, J., Jensen, L.S., 2001. Soil respiration, nitrogen mineralization and uptake in barley following cultivation of grazed grasslands. Biol. Fertil. Soils. 33, 2, 139-145.

Erisman, J.W., Bleeker, A., Galloway, J., Sutton, M.S., 2007. Reduced nitrogen in ecology and the environment. Environ. Pollut. 150, 1, 140-149.

Erisman, J.W., Sutton, M.A., Galloway, J., Klimont, Z., Winiwarter, W., 2008. How a century of ammonia synthesis changed the world. Nat. Geosci. 1, 636.

Erisman, J.W., Galloway, J.N., Seitzinger, S., Bleeker, A., Dise, N.B., Petrescu, A.M.R., Leach, A.M., de Vries, W., 2013. Consequences of human modification of the global nitrogen cycle. Philos. Trans. R. Soc. Lond. B. Biol. Sci. 368, 1621, 1-9.

Eugster, W., Zeyer, K., Zeeman, M., Michna, P., Zingg, A., Buchmann, N., Emmenegger, L., 2007. Methodical study of nitrous oxide eddy covariance measurements using quantum cascade laser spectrometery over a Swiss forest. Biogeosciences. 4, 5, 927-939.

Eugster, W., Merbold, L., 2015. Eddy covariance for quantifying trace gas fluxes from soils. Soil. 1, 1, 187-205.

Faist, J., Capasso, F., Sivco, D.L., Sirtori, C., Hutchinson, A.L., Cho, A.Y., 1994. Quantum cascade laser. Science. 264, 5158, 553-556.

Faist, J., Capasso, F., Sivco, D.L., Hutchinson, A.L., Sirtori, C., Cho, A.Y., 1995. Quantum cascade laser: A new optical source in the mid-infrared. Infrared Phys. Technol. 36, 1, 99-103.

FAO, 2020. Grasslands, Rangelands and Forage Crops. http://www.fao.org/agriculture/crops/thematic-sitemap/theme/spi/grasslands-rangelands-and-forage-crops/en/ (accessed 09/06/2020).

Felber, R., Münger, A., Neftel, A., Ammann, C., 2015. Eddy covariance methane flux measurements over a grazed pasture: effect of cows as moving point sources. Biogeosciences. 12, 12, 3925-3940.

Fenchel, T., Blackburn, H., King, G.M., 2012. Bacterial Biogeochemistry. The Ecophysiology of Mineral Cycling, 3 ed. Academic Press, London, UK. Waltham, MA, USA. San Diego, CA, USA. 312p.

Firestone, M.K., Firestone, R.B., Tiedje, J.M., 1980. Nitrous Oxide from Soil Denitrification: Factors Controlling Its Biological Production. Science. 208, 4445, 749-751.

Firestone, M.K., Davidson, E.A., 1989. Microbiological Basis of NO and N_2O Production and Consumption in Soil. In: Andreae, M.O., Schmimmel, D. S. (Ed.), Exchange of Trace Gases between Terrestrial Ecosystems and the Atmosphere. John Wiley & Sons Ltd, Berlin, Chichester, pp. 7-21.

Flechard, C.R., Ambus, P., Skiba, U., Rees, R.M., Hensen, A., van Amstel, A., van Den Pol-van Dasselaar, A., Soussana, J.F., Jones, M., Clifton-Brown, J., Raschi, A., Horvath, L., Neftel, A., Jocher, M., Ammann, C., Leifeld, J., Fuhrer, J., Calanca, P., Thalman, E., Pilegaard, K., Di Marco, C., Campbell, C., Nemitz, E., Hargreaves, K.J., Levy, P.E., Ball, B.C., Jones, S.K., van de Bulk, W.C.M., Groot, T., Blom, M., Domingues, R., Kasper, G., Allard, V., Ceschia, E., Cellier, P., Laville, P., Henault, C., Bizouard, F., Abdalla, M., Williams, M., Baronti, S., Berretti, F., Grosz, B., 2007. Effects of climate and management intensity on

nitrous oxide emissions in grassland systems across Europe. Agric. Ecosyst. Environ. 121, 1, 135-152.

Flückiger, J., Monnin, E., Stauffer, B., Schwander, J., Stocker, T.F., Chappellaz, J., Raynaud, D., Barnola, J.-M., 2002. High-resolution Holocene N_2O ice core record and its relationship with CH_4 and CO_2. Global Biogeochem. Cycles. 16, 1, 10-1-10-8.

Forster, P., Ramaswamy, V., Artaxo, P., Berntsen, T., Betts, R., Fahey, Haywood, J., Lean, J., Lowe, D.C., Myhre, G., Nganga, J., Prinn, R., Raga, G., M., S., Van Dorland, R., 2007. Changes in Atmospheric Constituents and in Radiative In: Solomon, S., Qin, D., Manning, M., Chen, Z., Marquis, M., Averyt, K.B., Tignor, M. ,Miller, H.L. (Eds.), Climate Change 2007: The Physical Science Basis. Contribution of Working Group I to the Fourth Assessment Report of the Intergovernmental Panel on Climate Change, Cambridge, New York, pp. 131-234.

Fowler, D., Coyle, M., Skiba, U., Sutton, M.A., Cape, J.N., Reis, S., Sheppard, L.J., Jenkins, A., Grizzetti, B., Galloway, J.N., Vitousek, P.M., Leach, A.M., Bouwman, A.F., Butterbach-Bahl, K., Dentener, F., Stevenson, D., Amann, M., Voss, M., 2013. The global nitrogen cycle in the twenty-first century. Philos. Trans. R. Soc. Lond. B. Biol. Sci. 368, 1621, 1-13.

Fratini, G., Ibrom, A., Arriga, N., Burba, G., Papale, D., 2012. Relative humidity effects on water vapour fluxes measured with closed-path eddy-covariance systems with short sampling lines. Agric. For. Meteorol. 165, 53-63.

Fuchs, K., Hörtnagl, L., Buchmann, N., Eugster, W., Snow, V., Merbold, L., 2018. Management matters: Testing a mitigation strategy for nitrous oxide emissions on intensively managed grassland. Biogeosciences. 15, 5519-5543.

Fuchs, K., Merbold, L., Buchmann, N., Bretscher, D., Brilli, L., Fitton, N., Topp, C.F.E., Klumpp, K., Lieffering, M., Martin, R.E., Newton, P.C.D., Rees, R.M., Rolinski, S., Smith, P., Snow, V., 2020. Multimodel Evaluation of Nitrous Oxide Emissions From an Intensively Managed Grassland. J. Geophys. Res. Biogeosci. 125, 1, e2019JG005261.

Galloway, j.N., Aber, J.D., Erisman, J.W., Seitzinger, S.P., Howarth, R.W., Cowling, E.B., Cosby, B.J., 2003. The Nitrogen Cascade. BioScience. 53, 4, 341-356.

Galloway, J.N., Dentener, F.J., Capone, D.G., Boyer, E.W., Howarth, R.W., Seitzinger, S.P., Asner, G.P., Cleveland, C.C., Green, P.A., Holland, E.A., Karl, D.M., Michaels, A.F., Porter, J.H., Townsend, A.R., Vöosmarty, C.J., 2004. Nitrogen Cycles: Past, Present, and Future. Biogeochemistry. 70, 2, 153-226.

Galloway, J.N., Leach, A.M., Bleeker, A., Erisman, J.W., 2013. A chronology of human understanding of the nitrogen cycle. Philos. Trans. R. Soc. Lond. B. Biol. Sci. 368, 1621, 1-11.

Gardiner, C.A., Clough, T.J., Cameron, K.C., Di, H.J., Edwards, G.R., de Klein, C.A.M., 2016. Potential for forage diet manipulation in New Zealand pasture ecosystems to mitigate ruminant urine derived N_2O emissions: a review. N.Z. J. Agric. Res. 59, 3, 301-317.

Gardiner, C.A., Clough, T.J., Cameron, K.C., Di, H.J., Edwards, G.R., de Klein, C.A.M., 2018. Potential inhibition of urine patch nitrous oxide emissions by Plantago lanceolata and its metabolite aucubin. N.Z. J. Agric. Res. 61, 4, 495-503.

Gawel, E., Grzelak, M., 2020. Influence of grassland renovation methods on dry matter and protein yields and nutritive value. Appl. Ecol. Environ. Res. 18, 1, 1661-1677.

Gayon, U., Dupetit, G., 1886. Recherches sur la reduction des nitrates par les infiniment petits. Mem. Sot. Sci. Phys. Nat. Bordeaux Ser. 3. 2, 201-307.

Gibbs, J. (2018a). The role of supplementary feed in the NZ GHG inventory. Personal Communication. Ministry of Primary Industries: New Zealand.

Gibbs, J. (2018b). Calculating New Zealand's agricultural greenhouse gas emissions. Version 4.0 (208 p). Ministry for Primary Industries (MPI): Wellington.

Giltrap, D., Godfrey, A., 2016. The effects of spatial variability of nitrous oxide emissions from grazed pastures on the sampling distribution of chamber measurements. J. Agric. Sci. 154, 2, 223-241.

Giltrap, D., Yeluripati, J., Smith, P., Fitton, N., Smith, W., Grant, B., Dorich, C.D., Deng, J., Topp, C.F.E., Abdalla, M., Liáng, L.L., Snow, V., 2020. Global research alliance N_2O chamber methodology guidelines: Summary of modelling approaches. J. Environ. Qual. 49, 5, 1168-1185.

Giltrap, D.L., Berben, P., Palmada, T., Saggar, S., 2014. Understanding and analysing spatial variability of nitrous oxide emissions from a grazed pasture. Agric. Ecosyst. Environ. 186, 1-10.

Glassey, C.B., Roach, C.G., Lee, J.M., Clark, D.A., 2013. The impact of farming without nitrogen fertiliser for ten years on pasture yield and composition, milksolids production and profitability; a rsearch farmlet comparison. Proc. N. Z. Grassl. Assoc. 75, 71-78.

Goodrich, J.P., Wall, A.M., Campbell, D.I., Fletcher, D., Wecking, A.R., Schipper, L.A., 2021. Improved gap filling approach and uncertainty estimation for eddy covariance N_2O fluxes. Agric. For. Meteorol. 297, 108280, 1-9.

Goulden, M.L., Munger, J.W., Fan, S.-M., Daube, B.C., Wofsy, S.C., 1996. Measurements of carbon sequestration by long-term eddy covariance: methods and a critical evaluation of accuracy. Global Change Biol. 2, 3, 169-182.

Grandy, A.S., Robertson, G.P., 2006. Initial cultivation of a temperate-region soil immediately accelerates aggregate turnover and CO_2 and N_2O fluxes. Global Change Biol. 12, 8, 1507-1520.

Gregorini, P., Beukes, P., Bryant, R., Romera, A., 2010. A brief overview and simulation of the effects of some feeding strategies on nitrogen excretion and enteric methane emission from grazing dairy cows. Proceedings of the 4th Australasian Dairy Science Symposium, 29-43.

Gregorini, P., Beukes, P.C., Dalley, D., Romera, A.J., 2016. Screening for diets that reduce urinary nitrogen excretion and methane emissions while maintaining or increasing production by dairy cows. Sci. Total Environ. 551-552, 32-41.

Griebel, A., Bennett, L.T., Metzen, D., Cleverly, J., Burba, G., Arndt, S.K., 2016. Effects of inhomogeneities within the flux footprint on the interpretation of seasonal, annual, and interannual ecosystem carbon exchange. Agric. For. Meteorol. 221, 50-60.

Groffman, P.M., 1985. Nitrification and Denitrification in Conventional and No-Tillage Soils. Soil Sci. Soc. Am. J. 49, 2, 329-334.

Groffman, P.M., Altabet, M.A., Böhlke, J.K., Butterbach - Bahl, K., David, M.B., Firestone, M.K., Giblin, A.E., Kana, T.M., Nielsen, L.P., Voytek, M.A., 2006. Methods for measuring denitrification: diverse approaches to a difficult problem. Ecol. Appl. 16, 6, 2091-2122.

Groffman, P.M., Butterbach-Bahl, K., Fulweiler, R., Gold, A., Morse, J., Stander, E., Tague, C., Tonitto, C., Vidon, P., 2009. Challenges to incorporating spatially and temporally explicit phenomena (hotspots and hot moments) in denitrification models. Biogeochemistry. 93, 1, 49-77.

Gu, J., Zheng, X., Zhang, W., 2009. Background nitrous oxide emissions from croplands in China in the year 2000. Plant Soil. 320, 1, 307-320.

Gundersen, P., Christiansen, J.R., Alberti, G., Brueggemann, N., Castaldi, S., Gasche, R., Kitzler, B., Klemedtsson, L., Lobo-do-Vale, R., Moldan, F., Ruetting, T., Schleppi, P., Weslien, P., Zechmeister-Boltenstern, S., 2012. The response of methane and nitrous oxide fluxes to forest change in Europe. Biogeosciences. 9, 3999-4012.

Haber, F., 2002. The synthesis of ammonia from its elements Nobel Lecture, June 2, 1920. Resonance. 7, 9, 86-94.

Harpole, W.S., Potts, D.L., Suding, K.N., 2007. Ecosystem responses to water and nitrogen amendment in a California grassland. Global Change Biol. 13, 11, 2341-2348.

Haynes, R.J., Williams, P.H., 1993. Nutrient cycling and soil fertility in the grazed pasture ecosystem. Adv. Agron. 49, 119-199.

Heggie, K., Savage, C., 2009. Nitrogen yields from New Zealand coastal catchments to receiving estuaries. N.Z. J. Mar. Freshwater Res. 43, 5, 1039-1052.

Helfrich, M., Nicolay, G., Well, R., Buchen-Tschiskale, C., Dechow, R., Fuß, R., Gensior, A., Paulsen, H., Berendonk, C., Flessa, H., 2020. Effect of chemical and mechanical grassland conversion to cropland on soil mineral N dynamics and N_2O emission. Agric. Ecosyst. Environ. 298, 1-13.

Henry, B., Eckard, R.J., 2009. Greenhouse gas emissions in livestock production systems. Trop. Grassl.-Forrajes Trop. 43, Article number: TRGRB 232-238.

Henry, S., Baudoin, E., Lopez-Gutierrez, J.C., Martin-Laurent, F., Baumann, A., Philippot, L., 2004. Quantification of denitrifying bacteria in soils by nirK gene targeted real-time PCR. J. Microbiol. Meth. 59, 3, 327-335.

Herrero, M., Gerber, P., Vellinga, T., Garnett, T., Leip, A., Opio, C., Westhoek, H.J., Thornton, P.K., Olesen, J., Hutchings, N., Montgomery, H., Soussana, J.F., Steinfeld, H., McAllister, T.A., 2011. Livestock and greenhouse gas emissions: The importance of getting the numbers right. Anim. Feed Sci. Technol. 166-167, 779-782.

Herridge, D.F., Peoples, M.B., Boddey, R.M., 2008. Global inputs of biological nitrogen fixation in agricultural systems. Plant Soil. 311, 1, 1-18.

Hertel, O., Reis, S., Skjøth, C.A., Bleeker, A., Harrison, R., Cape, J.N., Fowler, D., Skiba, U., Simpson, D., Jickells, T., Baker, A.R., Kulmala, M., Gyldenkærne, S., Sørensen, L.L., Erisman, J.W., 2011. Nitrogen processes in the atmosphere. In: Bleeker, A., Grizzetti, B., Howard, C.M., Billen, G., van Grinsven, H., Erisman, J.W., Sutton, M.A. ,Grennfelt, P. (Eds.), The European Nitrogen Assessment: Sources, Effects and Policy Perspectives. Cambridge University Press, Cambridge, pp. 177-208.

Hewitt, A.E., 2010. New Zealand Soil Classification. 2nd edition. Manaaki Whenua Press, Lincoln. 136p.

Hirsch, A.I., Michalak, A.M., Bruhwiler, L.M., Peters, W., Dlugokencky, E.J., Tans, P.P., 2006. Inverse modeling estimates of the global nitrous oxide surface flux from 1998–2001. Global Biogeochem. Cycles. 20, GB1008, 1-17.

Hopkins, A., Gilbey, J., Dibb, C., Bowling, P.J., Murray, P.J., 1990. Response of permanent and reseeded grassland to fertilizer nitrogen. 1. Herbage production and herbage quality. Grass Forage Sci. 45, 1, 43-55.

Hopkins, A., Murray, P.J., Bowling, P.J., Rook, A.J., Johnson, J., 1995. Productivity and nitrogen uptake of ageing and newly sown swards of perennial ryegrass (Lolium perenne L.) at different sites and with different nitrogen fertilizer treatments. Eur. J. Agron. 4, 1, 65-75.

Horst, T., Lenschow, D., 2009. Attenuation of Scalar Fluxes Measured with Spatially-displaced Sensors. Boundary Layer Meteorol. 130, 2, 275-300.

Horst, T.W., Weil, J.C., 1994. How Far is Far Enough?: The Fetch Requirements for Micrometeorological Measurement of Surface Fluxes. J. Atmos. Oceanic Technol. 11, 4, 1018-1025.

Hörtnagl, L., Wohlfahrt, G., 2014. Methane and nitrous oxide exchange over a managed hay meadow. Biogeosciences. 11, 24, 7219-7236.

Hörtnagl, L., Barthel, M., Buchmann, N., Eugster, W., Butterbach-Bahl, K., Díaz-Pinés, E., Zeeman, M., Klumpp, K., Kiese, R., Bahn, M., Hammerle, A., Lu, H., Ladreiter-Knauss, T., Burri, S., Merbold, L., 2018. Greenhouse gas fluxes over managed grasslands in Central Europe. Global Change Biol. 24, 1843–1872.

Huang, H., Wang, J., Hui, D., Miller, D.R., Bhattarai, S., Dennis, S., Smart, D., Sammis, T., Reddy, K.C., 2014. Nitrous oxide emissions from a commercial cornfield (Zea mays) measured using the eddy covariance technique. Atmos. Chem. Phys. 14, 23, 12839-12854.

Huang, J., Golombek, A., Prinn, R., Weiss, R., Fraser, P., Simmonds, P., Dlugokencky, E.J., Hall, B., Elkins, J., Steele, P., Langenfelds, R., Krummel, P., Dutton, G.,

Porter, L., 2008. Estimation of regional emissions of nitrous oxide from 1997 to 2005 using multinetwork measurements, a chemical transport model, and an inverse method. J. Geophys. Res. Atmos. 113, D17313, 1-19.

Huang, Y., Zou, J., Zheng, X., Wang, Y., Xu, X., 2004. Nitrous oxide emissions as influenced by amendment of plant residues with different C:N ratios. Soil Biol. Biochem. 36, 6, 973-981.

Hüppi, R., Felber, R., Krauss, M., Six, J., Leifeld, J., Fuß, R., 2018. Restricting the nonlinearity parameter in soil greenhouse gas flux calculation for more reliable flux estimates. PLoS One. 13, 7, 1-17.

Hutchinson, G.L., Mosier, A.R., 1981. Improved Soil Cover Method for Field Measurement of Nitrous Oxide Fluxes1. Soil Sci. Soc. Am. J. 45, 2, 311-316.

IFA, 2011. Fertilizer - use statistics. International Fertilizer Association. https://www.ifastat.org/ (accessed 27/09/2020).

Imer, D., Merbold, L., Eugster, W., Buchmann, N., 2013. Temporal and spatial variations of CO_2, CH_4 and N_2O fluxes at three differently managed grasslands. Biogeosciences Discuss. 10, 2, 2635-2673.

IPCC, 1996. Revised 1996 IPCC Guidelines for National Greenhouse Gas Inventories: Workbook. Volume 2, Agriculture. In: IPCC (Ed.), Revised 1996 IPCC Guidelines for National Greenhouse Gas Inventories, pp. 4.1-4.20.

IPCC, 2006a. Guidelines for National Greenhouse Gas Inventories, National Greenhouse Gas Inventories Programme, IGES. IPCC, Hayama, Japan.

IPCC, 2006b. N_2O emissions from managed soils, and CO_2 emissions from lime and urea application. In: De Klein, C.A.M., Novoa, R.S.A., Ogle, S., Smith, K.A., Rochette, P., Wirth, T.C., McConkey, B.G., Mosier, A. ,Rypdal, K. (Eds.), 2006 IPCC Guidelines for National Greenhouse Gas Inventories. IGES, Japan, pp. 11.1-11.54, Chapter 11.

IPCC, 2013. Anthropogenic and Natural Radiative Forcing. In: Myhre, G., Shindell, D., Breon, F.-M., Collins, W., Fuglestvedt, J., Huang, J., Koch, D., Lamarque, J.-F., Lee, D., Mendoza, B., Nakajima, T., Robock, A., Stephens, G., Takemura, T., Zhang, H., Jacob, D., Ravishankara, A.R. ,Shine, K.P. (Eds.), Climate Change 2013: The Physical Science Basis. Contribution of Working Group I to the Fifth Assessment Report of the Intergovenmental Panel on Climate Change., Cambidge UK and New York, NY, USA, pp. 659-740, Chapter 8.

IPCC, 2013, 2014. 2013 Supplement to the 2006 IPCC Guidelines for National Greenhouse Gas Inventories: Wetlands., Hiraishi, T., Krug, T., Tanabe, K., Srivastava, N., Baasansuren, J., Fukuda, M. ,Troxler, T.G. (Eds.). IPCC, Switzerland. 354p.

IPCC, 2019. N_2O emissions from managed soils, and CO_2 emissions from lime and urea application. . In: Hergoulac'h, K., Akiyama, H., Bernoux, M., Chirinda, N., Del Prado, A., Kasimir, Å., MacDonald, J.D., Ogle, S.M., Regina, K. ,van der Weerden, T.J. (Eds.), Refinement to the 2006 IPCC Guidelines for National Greenhouse Gas Inventories, pp. 11.1-11.48, Chapter 11.

Jantke, K., Hartmann, M.J., Rasche, L., Blanz, B., Schneider, U.A., 2020. Agricultural Greenhouse Gas Emissions: Knowledge and Positions of German Farmers. Land. 9, 130, 1-13.

Jarvis, S.C., Scholefield, D., Pain, B.F., 1995. Nitrogen cycling in grazing systems. In: Bacon, P. (Ed.), Nitrogen Fertilization in the Environment. Dekker Inc, New York, pp. 381-419.

Jarvis, S.C., Yamulki, S., Brown, L., 2001. Sources of nitrous oxide emissions in intensive grassland managements. Phyton. 41, 107-118.

Jentsch, A., Kreyling, J., Beierkuhnlein, C., 2007. A new generation of climate-change experiments: events, not trends. Front. Ecol. Environ. 5, 7, 365-374.

Johnson, J.M.F., Franzluebbers, A.J., Weyers, S.L., Reicosky, D.C., 2007. Agricultural opportunities to mitigate greenhouse gas emissions. Environ. Pollut. 150, 1, 107-124.

Johnston, A.E., Poulton, P.R., Coleman, K., 2009. Soil Organic Matter: Importance in Sustainable Agriculture and Carbon Dioxide Fluxes. In: Sparks, D.L. (Ed.), Adv. Agron. Academic Press, pp. 1-57, Chapter 1.

Johnston, H., 1971. Reduction of Stratospheric Ozone by Nitrogen Oxide Catalysts from Supersonic Transport Exhaust. Science. 173, 3996, 517-522.

Joly, L., Robert, C., Parvitte, B., Catoire, V., Durry, G., Richard, G., Nicoullaud, B., Zéninari, V., 2008. Development of a spectrometer using a continuous wave distributed feedback quantum cascade laser operating at room temperature for the simultaneous analysis of N_2O and CH_4 in the Earth's atmosphere. Appl. Opt. 47, 9, 1206-1214.

Jones, S., Famulari, D., Marco, C., Nemitz, E., Skiba, U., Rees, R., Sutton, M., 2011. Nitrous oxide emissions from managed grassland: a comparison of eddy covariance and static chamber measurements. Atmos. Meas. Tech. 4, 10, 2179-2194.

Jones, S.K., Rees, R.M., Skiba, U.M., Ball, B.C., 2007. Influence of organic and mineral N fertiliser on N_2O fluxes from a temperate grassland. Agric. Ecosyst. Environ. 121, 1, 74-83.

Jones, S.K., Helfter, C., Anderson, M., Coyle, M., Campbell, C., Famulari, D., Di Marco, C., van Dijk, N., Tang, Y.S., Topp, C.F.E., Kiese, R., Kindler, R., Siemens, J., Schrumpf, M., Kaiser, K., Nemitz, E., Levy, P.r.E., Rees, R.M., Sutton, M.A., Skiba, U.M., 2017. The nitrogen, carbon and greenhouse gas budget of a grazed, cut and fertilised temperate grassland. Biogeosciences. 14, 8, 2069-2088.

Kanter, D.R., Ogle, S.M., Winiwarter, W., 2020. Building on Paris: integrating nitrous oxide mitigation into future climate policy. Curr. Opin. Environ. Sustain. 47, 7-12.

Kayser, M., Müller, J., Isselstein, J., 2018. Grassland renovation has important consequences for C and N cycling and losses. Food and Energy Secur. 7:e00146, 1-12.

Kelliher, F., Li, Z., Nobel, A., 2014a. Nitrogen application rate and nitrous oxide flux from a pastoral soil. N.Z. J. Agric. Res. 57, 4, 1-7.

Kelliher, F.M., Cox, N., van Der Weerden, T.J., de Klein, C.A.M., Luo, J., Cameron, K.C., Di, H.J., Giltrap, D., Rys, G., 2014b. Statistical analysis of nitrous oxide emission factors from pastoral agriculture field trials conducted in New Zealand. Environ. Pollut. 186, 63-66.

Kelliher, F.M., Henderson, H.V., Cox, N.R., 2017. The uncertainty of nitrous oxide emissions from grazed grasslands: A New Zealand case study. Atmos. Environ. 148, 329-336.

Khalil, M.I., Van Cleemput, O., Rosenani, A.B., Schmidhalter, U., 2007. Daytime, Temporal, and Seasonal Variations of N_2O Emissions in an Upland Cropping System of the Humid Tropics. Commun. Soil Sci. Plant Anal. 38, 1-2, 189-204.

Kim, D.-G., Giltrap, D., Hernandez-Ramirez, G., 2013. Background nitrous oxide emissions in agricultural and natural lands: a meta-analysis. Plant Soil. 373, 1, 17-30.

Kim, D.-G., Giltrap, D., 2017. Determining optimum nitrogen input rate and optimum yield-scaled nitrous oxide emissions: Theory, field observations, usage, and limitations. Agric. Ecosyst. Environ. 247, 371-378.

Kim, D.G., Hernandez-Ramirez, G., Giltrap, D., 2012. Linear and nonlinear dependency of direct nitrous oxide emissions on fertilizer nitrogen input: A meta-analysis. Agric. Ecosyst. Environ. 168, 53–65.

Kong, A.Y.Y., Fonte, S.J., van Kessel, C., Six, J., 2009. Transitioning from standard to minimum tillage: Trade-offs between soil organic matter stabilization, nitrous oxide emissions, and N availability in irrigated cropping systems. Soil Tillage Res. 104, 2, 256-262.

Kool, D.M., Dolfing, J., Wrage, N., Van Groenigen, J.W., 2011. Nitrifier denitrification as a distinct and significant source of nitrous oxide from soil. Soil Biol. Biochem. 43, 1, 174-178.

Kormann, R., Meixner, F.X., 2001. An Analytical Footprint Model For Non-Neutral Stratification. Boundary Layer Meteorol. 99, 2, 207-224.

Kravchenko, A.N., Toosi, E.R., Guber, A.K., Ostrom, N.E., Yu, J., Azeem, K., Rivers, M.L., Robertson, G.P., 2017. Hotspots of soil N_2O emission enhanced through water absorption by plant residue. Nat. Geosci. 10, 7, 496-500.

Kroeze, C., Mosier, A., Bouwman, L., 1999. Closing the global N_2O budget: A retrospective analysis 1500–1994. Global Biogeochem. Cycles. 13, 1, 1-8.

Krol, D.J., Carolan, R., Minet, E., McGeough, K.L., Watson, C.J., Forrestal, P.J., Lanigan, G.J., Richards, K.G., 2016a. Improving and disaggregating N_2O emission factors for ruminant excreta on temperate pasture soils. Sci. Total Environ. 568, Supplement C, 327-338.

Krol, D.J., Jones, M.B., Williams, M., Richards, K.G., Bourdin, F., Lanigan, G.J., 2016b. The effect of renovation of long-term temperate grassland on N_2O emissions and N leaching from contrasting soils. Sci. Total Environ. 560-561, 233-240.

Kroon, P., Hensen, A., Bulk, W., Jongejan, P., Vermeulen, A., 2008. The importance of reducing the systematic error due to non-linearity in N_2O flux measurements by static chambers. Nutr. Cycling Agroecosyst. 82, 2, 175-186.

Kroon, P.S., Hensen, A., Jonker, H.J.J., Zahniser, M.S., Van't Veen, W.H., Vermeiden, A.T., 2007. Suitability of quantum cascade laser spectroscopy for CH_4 and N_2O eddy covariance flux measurements. Biogeosciences. 4, 5, 715-728.

Kroon, P.S., Hensen, A., Jonker, H.J.J., Ouwersloot, H.G., Vermeulen, A.T., Bosveld, F.C., 2010a. Uncertainties in eddy covariance flux measurements assessed from CH_4 and N_2O observations. Agric. For. Meteorol. 150, 6, 806-816.

Kroon, P.S., Schrier-Uijl, A.P., Hensen, A., Veenendaal, E.M., Jonker, H.J.J., 2010b. Annual balances of CH_4 and N_2O from a managed fen meadow using eddy covariance flux measurements. Eur. J. Soil Sci. 61, 5, 773-784.

Kutsch, W.L., Brümmer, C., Lyshede, B., Fuß, R., Smith, J., Delorme, J.-P., 2013. Comparison of two chamber methods and eddy covariance measurements for N_2O for low flux conditions. EGU General Assembly 2013. Geophys. Res. Abstr. 15, EGU2013-12714.

Kuypers, M.M.M., Marchant, H.K., Kartal, B., 2018. The microbial nitrogen-cycling network. Nat. Rev. Microbiol. 16, 5, 263-276.

Lal, R., 2020. Managing soils for negative feedback to climate change and positive impact on food and nutritional security. Soil Sci. Plant Nutr. 66, 1, 1-9.

Lammirato, C., Lebender, U., Tierling, J., Lammel, J., 2018. Analysis of uncertainty for N_2O fluxes measured with the closed-chamber method under field conditions: Calculation method, detection limit, and spatial variability. J. Plant Nutr. Soil Sci. 181, 1, 78-89.

Lary, D.J., 1997. Catalytic destruction of stratospheric ozone. J. Geophys. Res. Atmos. 102, D17, 21515-21526.

Lassaletta, L., Billen, G., Grizzetti, B., Garnier, J., Leach, A.M., Galloway, J.N., 2014. Food and feed trade as a driver in the global nitrogen cycle: 50-year trends. Biogeochemistry. 118, 1, 225-241.

Lebegue, B., Schmidt, M., Ramonet, M., Wastine, B., Yver Kwok, C., Laurent, O., Belviso, S., Guemri, A., Philippon, C., Smith, J., Conil, S., 2016. Comparison of N_2O analyzers for high-precision measurements of atmospheric mole fractions. Atmos. Meas. Tech. 9, 3, 1221-1238.

Ledgard, S., Schils, R., Erikson, J., Luo, J., 2009. Environmental impacts of grazed clover/grass pastures. Ir. J. Agric. Food Res. 48, 209-226.

Ledgard, S.F., Jarvis, S.C., Hatch, D.J., 1998. Short-term nitrogen fluxes in grassland soils under different long-term nitrogen management regimes. Soil Biol. Biochem. 30, 10, 1233-1241.

Lesschen, J.P., Velthof, G.L., de Vries, W., Kros, J., 2011. Differentiation of nitrous oxide emission factors for agricultural soils. Environ. Pollut. 159, 11, 3215-3222.

Lestienne, F., Thornton, B., Gastal, F., 2006. Impact of defoliation intensity and frequency on N uptake and mobilization in Lolium perenne. J. Exp. Bot. 57, 4, 997-1006.

Leuning, R., Moncrieff, J., 1990. Eddy-covariance CO_2 flux measurements using open- and closed-path CO_2 analysers: Corrections for analyser water vapour sensitivity and damping of fluctuations in air sampling tubes. Boundary Layer Meteorol. 53, 1, 63-76.

Levy, P.E., Gray, A., Leeson, S.R., Gaiawyn, J., Kelly, M.P.C., Cooper, M.D.A., Dinsmore, K.J., Jones, S.K., Sheppard, L.J., 2011. Quantification of uncertainty in trace gas fluxes measured by the static chamber method. Eur. J. Soil Sci. 62, 6, 811-821.

Li, D., Lanigan, G., Humphreys, J., 2011. Measured and simulated nitrous oxide emissions from ryegrass- and ryegrass/white clover-based grasslands in moist temperate climate. PLoS One. 6, 10, 1-9.

Li, J., Parchatka, U., Königstedt, R., Fischer, H., 2012. Real-time measurements of atmospheric CO using a continuous-wave room temperature quantum cascade laser based spectrometer. Opt. Express. 20, 7, 7590-7601.

Li, J., Parchatka, U., Fischer, H., 2013a. Development of field-deployable QCL sensor for simultaneous detection of ambient N_2O and CO. Sens. Actuators, B. 182, 659-667.

Li, J.S., Chen, W., Fischer, H., 2013b. Quantum Cascade Laser Spectrometry Techniques: A New Trend in Atmospheric Chemistry. Appl. Spectrosc. Rev. 48, 7, 523-559.

Li, L., Zheng, Z., Wang, W., Biederman, J.A., Xu, X., Ran, Q., Qian, R., Xu, C.-Y., Zhang, B., Wang, F., Zhou, S., Cui, L., Che, R., Hao, Y., Cui, X., Xu, Z., Wang, Y., 2020. Terrestrial N_2O emissions and related functional genes under climate change: A global meta-analysis. Global Change Biol. 26, 2, 931-943.

Liáng, L.L., Campbell, D.I., Wall, A.M., Schipper, L.A., 2018. Nitrous oxide fluxes determined by continuous eddy covariance measurements from intensively grazed pastures: Temporal patterns and environmental controls. Agric. Ecosyst. Environ. 268, 171-180.

Liáng, L.L., Kirschbaum, M.U.F., Giltrap, D.L., Wall, A.M., Campbell, D.I., 2020. Modelling the effects of pasture renewal on the carbon balance of grazed pastures. Sci. Total Environ. 715, 136917, 1-12.

Linn, D.M., Doran, J.W., 1984. Effect of Water-Filled Pore Space on Carbon Dioxide and Nitrous Oxide Production in Tilled and Nontilled Soils. Soil Sci. Soc. Am. J. 48, 1267-1272.

Liu, Y., He, N., Wen, X., Xu, L., Sun, X.Z., Yu, G., Liang, L.L., Schipper, L., 2018. The optimum temperature of soil microbial respiration: Patterns and controls. Soil Biol. Biochem. 121, 35-42.

Livingston, G.P., Hutchinson, G.I., 1995. Enclosure-based measurement of trace gas exchange: applications and sources of error. In: Matson, P.A., Harriss, R. C.

(Ed.), Biogenic Trace Gases: Measuring Emissions from Soil and Water. Blackwell Science, Cambridge, pp. 14-50, Chapter 2.

Loescher, H.W., Law, B.E., Mahrt, L., Hollinger, D.Y., Campbell, J., Wofsy, S.C., 2006. Uncertainties in, and interpretation of, carbon flux estimates using the eddy covariance technique. J. Geophys. Res. Atmos. 111, D21S90, 1-19.

Lognoul, M., Debacq, A., De Ligne, A., Dumont, B., Manise, T., Bodson, B., Heinesch, B., Aubinet, M., 2019. N_2O flux short-term response to temperature and topsoil disturbance in a fertilized crop: An eddy covariance campaign. Agric. For. Meteorol. 271, 193-206.

López-Aizpún, M., Horrocks, C.A., Charteris, A.F., Marsden, K.A., Ciganda, V.S., Evans, J.R., Chadwick, D.R., Cárdenas, L.M., 2019. Meta-analysis of global livestock urine-derived nitrous oxide emissions from agricultural soils. Global Change Biol. 00:1, 1-12.

Lucas-Moffat, A.M., Huth, V., Augustin, J., Brümmer, C., Herbst, M., Kutsch, W.L., 2018. Towards pairing plot and field scale measurements in managed ecosystems: Using eddy covariance to cross-validate CO_2 fluxes modeled from manual chamber campaigns. Agric. For. Meteorol. 256-257, 362-378.

Luo, J., Tillman, R.W., Ball, P.R., 1999. Grazing effects on denitrification in a soil under pasture during two contrasting seasons. Soil Biol. Biochem. 31, 6, 903-912.

Luo, J., Ledgard, S.F., Lindsey, S.B., 2007. Nitrous oxide emissions from application of urea on New Zealand pasture. N.Z. J. Agric. Res. 50, 1, 1-11.

Luo, J., Ledgard, S., Klein, C., Lindsey, S., Kear, M., 2008a. Effects of dairy farming intensification on nitrous oxide emissions. Plant Soil. 309, 1, 227-237.

Luo, J., Lindsey, S., Ledgard, S., 2008b. Nitrous oxide emissions from animal urine application on a New Zealand pasture. Biol. Fertil. Soils. 44, 3, 463-470.

Luo, J., Saggar, S., Bhandral, R., Bolan, N.S., Ledgard, S., Lindsey, S., Sun, W., 2008c. Effects of irrigating dairy-grazed grassland with farm dairy effluent on nitrous oxide emissions. Plant Soil. 309, 1-2, 119-130.

Luo, J., van der Weerden, T.J., Hoogendoorn, C.J., de Klein, C.A.M., 2009. Determination of the N_2O Emission Factor for Animal Dung Applied in Spring in Three Regions of New Zealand. MAF Technical Paper No: 2011/30, Report prepared for the Ministry of Agriculture and Forestry by AgResearch. Ministry of Agriculture and Forestry, Wellington. 41p.

Luo, J., Hoogendoorn, C.J., van Der Weerden, T., Saggar, S., de Klein, C.A.M., Giltrap, D., Rollo, M., Rys, G., 2013a. Nitrous oxide emissions from grazed hill land in New Zealand. Agric. Ecosyst. Environ. 181, 58-68.

Luo, J., Ledgard, S.F., Lindsey, S.B., 2013b. Nitrous oxide and greenhouse gas emissions from grazed pastures as affected by use of nitrification inhibitor and restricted grazing regime. Sci. Total Environ. 465, 107-114.

Luo, J., Kelliher, F., 2014. Partitioning of animal excreta N into urine and dung and developing the N_2O inventory. MPI Technical Paper No: 2014/05, Report prepared by AgResearch. Ministry for Primary Industries, Wellington. 21p.

Luo, J., Sun, X.Z., Pacheco, D., Ledgard, S.F., Lindsey, S.B., Hoogendoorn, C.J., Wise, B., Watkins, N.L., 2015. Nitrous oxide emission factors for urine and dung from sheep fed either fresh forage rape (Brassica napus L.) or fresh perennial ryegrass (Lolium perenne L.). Animal. 9, 3, 534-543.

Luo, J., Wyatt, J., van der Weerden, T.J., Thomas, S.M., de Klein, C.A.M., Li, Y., Rollo, M., Lindsey, S., Ledgard, S.F., Li, J., Ding, W., Qin, S., Zhang, N., Bolan, N.S., Kirkham, M.B., Bai, Z., Ma, L., Zhang, X., Wang, H., Liu, H., Rys, G., 2017. Potential Hotspot Areas of Nitrous Oxide Emissions From Grazed Pastoral Dairy Farm Systems. Adv. Agron. 145, 205-268.

Luo, J., Saggar, S., van der Weerden, T., de Klein, C.A.M., 2019. Quantification of nitrous oxide emissions and emission factors from beef and dairy cattle excreta deposited on grazed pastoral hill lands. Agric. Ecosyst. Environ. 270-271, 103-113.

Luo, Y., Gerten, D., Le Maire, G., Parton, W.J., Weng, E., Zhou, X., Keough, C., Beier, C., Ciais, P., Cramer, W., Dukes, J.S., Emmett, B.A., Hanson, P.J., Knapp, A., Linder, S., Nepstad, D.C., Rustad, L., 2008d. Modeled interactive effects of precipitation, temperature, and [CO_2] on ecosystem carbon and water dynamics in different climatic zones. Global Change Biol. 14, 9, 1986-1999.

Ma, W., Bicknell, K., Renwick, A., 2019. Feed use intensification and technical efficiency of dairy farms in New Zealand. Aust. J. Agric. Resour. Econ. 63, 1, 20-38.

MacDonald, J.D., Rochette, P., Chantigny, M.H., Angers, D.A., Royer, I., Gasser, M.-O., 2011. Ploughing a poorly drained grassland reduced N_2O emissions compared to chemical fallow. Soil Tillage Res. 111, 2, 123-132.

MacFarling Meure, C., Etheridge, D., Trudinger, C., Steele, P., Langenfelds, R., van Ommen, T., Smith, A., Elkins, J., 2006. Law Dome CO_2, CH_4 and N_2O ice core records extended to 2000 years BP. Geophys. Res. Lett. 33, L14810, 1-4.

Makowski, D., 2019. N_2O increasing faster than expected. Nat. Clim. Change. 9, 12, 909-910.

Martínez-Cagigal, V., 2020. Custom Colormap. MATLAB Central File Exchange. https://www.mathworks.com/matlabcentral/fileexchange/69470-custom-colormap (accessed 30/07/2020).

Massman, W.J., Lee, X., 2002. Eddy covariance flux corrections and uncertainties in long-term studies of carbon and energy exchanges. Agric. For. Meteorol. 113, 1, 121-144.

Matthews, R.A., Chadwick, D.R., Retter, A.L., Blackwell, M.S.A., Yamulki, S., 2010. Nitrous oxide emissions from small-scale farmland features of UK livestock farming systems. Agric. Ecosyst. Environ. 136, 3, 192-198.

Mauder, M., Foken, T., 2006. Impact of post-field data processing on eddy covariance flux estimates and energy balance closure. Meteorol Z. 15, 597-609.

McCosh, F.W.J., 1984. Boussingault: Chemist and Agriculturist. D. Reidel Publishing Company, Springer, Dordrecht, Holland. 298p.

McLeod, M., 1992. Soils of part northern Matamata County, North Island, New Zealand. DSIR Land Resources, Lower Hut. 96p.

Merbold, L., Eugster, W., Stieger, J., Zahniser, M., Nelson, D., Buchmann, N., 2014. Greenhouse gas budget (CO_2, CH_4 and N_2O) of intensively managed grassland following restoration. Global Change Biol. 20, 6, 1913-28.

Merbold, L., Decock, C., Eugster, W., Fuchs, K., Wolf, B., Buchmann, N., Hörtnagl, L., 2020. Memory effects on greenhouse gas emissions (CO_2, N_2O and CH_4) following grassland restoration? Biogeosciences Discuss. 2020, 1-38.

MfE, 2012. Land Cover Database. Area of land cover classes by year. http://archive.stats.govt.nz/browse_for_stats/environment/environmental-reporting-series/environmental-indicators/Home/Land/land-cover.aspx (accessed 22/01/2018).

MfE, 2018. New Zealand's Greenhouse Gas Inventory. 1990-2016. Fulfilling reporting requirements under the United national Fraework convention on Climate Change and the Kyoto Protocol. Ministry for the Environment (MfE), Wellington. 497p.

MfE, 2019. New Zealand's Greenhouse Gas Inventory 1990-2017. Fulfilling reporting requirements under the United Nations Framework Convention on Climate Change and the Kyoto Protocol. Volume 1, Chapters 1-15. Ministry for the Environment (MfE), Wellington. 459p.

MfE, 2020. New Zealand's Greenhouse Gas Inventory 1990-2018. Fulfilling reporting requirements under the United Nations Framework Convention on Climate Change and the Kyoto Protocol. Volume 1, Chapters 1-15. Ministry for the Environment (MfE), Wellington. 486p.

Miller, M.N., Zebarth, B.J., Dandie, C.E., Burton, D.L., Goyer, C., Trevors, J.T., 2008. Crop residue influence on denitrification, N_2O emissions and denitrifier community abundance in soil. Soil Biol. Biochem. 40, 10, 2553-2562.

Ming, T., de Richter, R., Shen, S., Caillol, S., 2016. Fighting global warming by greenhouse gas removal: destroying atmospheric nitrous oxide thanks to synergies between two breakthrough technologies. Environmental Science and Pollution Research. 23, 7, 6119-6138.

Mishurov, M., Kiely, G., 2011. Gap-filling techniques for the annual sums of nitrous oxide fluxes. Agric. For. Meteorol. 151, 12, 1763-1767.

Moir, J.L., Cameron, K.C., Di, H.J., Fertsak, U., 2011. The spatial coverage of dairy cattle urine patches in an intensively grazed pasture system. J. Agric. Sci. 149, 4, 473-485.

Molodovskaya, M., Warland, J., Richards, B.K., Öberg, G., Steenhuis, T.S., 2011. Nitrous oxide from heterogeneous agricultural landscapes: Source contribution analysis by eddy covariance and chambers. Soil Sci. Soc. Am. J. 75, 5, 1829-1838.

Moncrieff, J.B., Massheder, J.M., de Bruin, H., Elbers, J., Friborg, T., Heusinkveld, B., Kabat, P., Scott, S., Soegaard, H., Verhoef, A., 1997. A system to measure

surface fluxes of momentum, sensible heat, water vapour and carbon dioxide. J. Hydrol. 188-189, 589-611.

Mori, A., Hojito, M., 2007. Grassland renovation increases N_2O emission from a volcanic grassland soil in Nasu, Japan. Soil Sci. Plant Nutr. 53, 6, 812-818.

Mori, A., 2020. Greenhouse gas emissions from cut grasslands renovated with full inversion tillage, shallow tillage, and use of a tine drill in Nasu, Japan. Agriculture. 10, 31, 1-16.

Mosier, A.R., Duxbury, J.M., Freney, J.R., Heinemeyer, O., Minami, K., 1996. Nitrous oxide emissions from agricultural fields: Assessment, measurement and mitigation. Plant Soil. 181, 1, 95-108.

Mottet, A., de Haan, C., Falcucci, A., Tempio, G., Opio, C., Gerber, P., 2017. Livestock: On our plates or eating at our table? A new analysis of the feed/food debate. Glob. Food Sec. 14, 1-8.

MPI, 2016. Feed Use in the NZ Dairy Industry. MPI Technical Paper 2017/53. Ministry for Primary Industries, Wellington. 66p.

Mueller, C., Sherlock, R.R., Williams, P.H., 1995. Direct field measurements of nitrous oxide emissions from urine-affected and urine-unaffected pasture in Canterbury. Massey University, Palmerston North. 234-243p.

Muller, C., Sherlock, R.R., Williams, P.H., 1995. Direct field measurements of nitrous oxide emissions from urine-affected and urine-unaffected pasture in Canterbury. Massey University, Palmerston North. 243-247p.

Müller, C., Stevens, R.J., Laughlin, R.J., Jäger, H.J., 2004. Microbial processes and the site of N_2O production in a temperate grassland soil. Soil Biol. Biochem. 36, 3, 453-461.

Mulvaney, R.L., 1996. Extraction of exchangeable ammonium, nitrate and nitrite. In: Sparks, D.L., Page, A.L., Helmke, P.A. ,Loeppert, R.H. (Eds.), Methods of soil analysis Part 3: chemical methods. Soil Science Society of America, American Society of Agronomy, Madison, WI, pp. 1129-1131.

Mumford, M.T., Rowlings, D.W., Scheer, C., De Rosa, D., Grace, P.R., 2019. Effect of irrigation scheduling on nitrous oxide emissions in intensively managed pastures. Agric. Ecosyst. Environ. 272, 126-134.

Myrold, D.D., 2005. Transformations of Nitrogen. In: Sylvia, D.M., Hartel, P.G., Fuhrmann, J.J. ,Zuberer, D.A. (Eds.), Principles and applications of soil microbiology, 2 ed. Pearson Education LTD, Singapore, Canada, Japan, Australia, North Asia, Mexico, Malaysia, pp. 333-372, Chapter 14.

Nakicenovic, N., Swart, R., 2000. Special report on emissions scenarios: a special report of Working Group III of the Intergovernmental Panel on Climate Change. IPCC, Cambridge. 599p.

Necpálová, M., Casey, I., Humphreys, J., 2013. Effect of ploughing and reseeding of permanent grassland on soil N, N leaching and nitrous oxide emissions from a clay-loam soil. Nutr. Cycling Agroecosyst. 95, 3, 305-317.

Neftel, A., Flechard, C., Ammann, C., Conen, F., Emmenegger, L., Zeyer, K., 2007. Experimental assessment of N_2O background fluxes in grassland systems. Tellus B Chem. Phys. Meteorol. 59, 3, 470-482.

Neftel, A., Ammann, C., Fischer, C., Spirig, C., Conen, F., Emmenegger, L., Tuzson, B., Wahlen, S., 2010. N_2O exchange over managed grassland: Application of a quantum cascade laser spectrometer for micrometeorological flux measurements. Agric. For. Meteorol. 150, 6, 775-785.

Nelson, D.D., McManus, B., Urbanski, S., Herndon, S., Zahniser, M.S., 2004. High precision measurements of atmospheric nitrous oxide and methane using thermoelectrically cooled mid-infrared quantum cascade lasers and detectors. Spectrochim. Acta, Part A. 60, 14, 3325-3335.

Nemitz, E., Mammarella, I., Ibrom, A., Aurela, M., Burba, G., Dengel, S., Gielen, B., Grelle, A., Heinesch, B., Herbst, M., Hörtnagl, L., Klemedtsson, L., Lindroth, A., Lohila, A., McDermitt, K.D., Meier, P., Merbold, L., Nelson, D., Nicolini, G., Zahniser, M., 2018. Standardisation of eddy-covariance flux measurements of methane and nitrous oxide. Int. Agrophys. 32, 517-549.

Nevison, C., 2000. Review of the IPCC methodology for estimating nitrous oxide emissions associated with agricultural leaching and runoff. Chemosphere: Global Change Sci. 2, 3-4, 493-500.

Nicolini, G., Castaldi, S., Fratini, G., Valentini, R., 2013. A literature overview of micrometeorological CH_4 and N_2O flux measurements in terrestrial ecosystems. Atmos. Environ. 81, 311-319.

Niu, S., Wu, M., Han, Y.I., Xia, J., Zhang, Z.H.E., Yang, H., Wan, S., 2010. Nitrogen effects on net ecosystem carbon exchange in a temperate steppe. Global Change Biol. 16, 1, 144-155.

NIWA, 2015. National Climate Database. National Institute of Water and Atmospheric Research. http://cliflo.niwa.co.nz (accessed 27/09/2020).

NIWA, 2018. National Climate Database. National Institute of Water and Atmospheric Research. http://cliflo.niwa.co.nz (accessed 27/09/2020).

Nömmik, H., 1956. Investigations on Denitrification in Soil. Acta Agric. Scand. Sect B. 6, 2, 195-228.

Oenema, O., Velthof, G.L., Yamulki, S., Jarvis, S.C., 1997. Nitrous oxide emissions from grazed grassland. Soil Use Manage. 13, 4, 288-295.

Oenema, O., Wrage, N., Velthof, G., Groenigen, J.W., Dolfing, J., Kuikman, P., 2005. Trends in Global Nitrous Oxide Emissions from Animal Production Systems. Nutr. Cycling Agroecosyst. 72, 1, 51-65.

Ogle, S., Butterbach-Bahl, K., Cardenas, L., Skiba, M., Scheer, C., 2020. From research to policy: optimizing the design of a national monitoring system to mitigate soil nitrous oxide emissions. Curr. Opin. Environ. Sustain. 47, 28-36.

Otte, J.M., Blackwell, N., Ruser, R., Kappler, A., Kleindienst, S., Schmidt, C., 2019. N_2O formation by nitrite-induced (chemo)denitrification in coastal marine sediment. Sci. Rep. 9, 10691, 1-12.

Parfitt, R.L., Stevenson, B.A., Dymond, J.R., Schipper, L.A., Baisden, W.T., Ballantine, D.J., 2012. Nitrogen inputs and outputs for New Zealand from 1990 to 2010 at national and regional scales. N.Z. J. Agric. Res. 55, 3, 241-262.

Parkin, T.B., 1993. Spatial variability of microbial processes in soil - a review. Soil Sci. Soc. Am. J. 51, 1194-1199.

Parkin, T.B., Venetera, R.T., 2010. USDA-ARS GRACEnet Project Protocols Sampling Protocols. Chamber-Based Trace Gas Flux Measurements. In: Follett, R.F. (Ed.), Sampling Protocols. U.S. Department of Agriculture, Agricultural Research Service, National Laboratory for Agriculture & the Environment, Ames, IA; St. Paul, MN, pp. 3.1-3.39, Chapter 3.

Parkin, T.B., Venterea, R.T., Hargreaves, S.K., 2012. Calculating the Detection Limits of Chamber-based Soil Greenhouse Gas Flux Measurements. J. Environ. Qual. 41, 3, 705-715.

Paustian, K., Lehmann, J., Ogle, S., Reay, D.S., Robertson, G.P., Smith, P., 2016. Climate-smart soils. Nature. 532, 49-57.

Pavelka, M., Acosta, M., Kiese, R., Altimir, N., Bruemmer, C., Crill, P., Darenova, E., Fuß, R., Gielen, B., Graf, A., Klemedtsson, L., Lohila, A., Longdoz, B., Lindroth, A., Nilsson, M., Marañón-Jiménez, S., Merbold, L., Montagnani, L., Peichl, M., Kutsch, W.L., 2018. Standardisation of chamber technique for CO_2, N_2O and CH_4 fluxes measurements from terrestrial ecosystems. Int. Agrophys. 32, 569-587.

Payne, W.J., 1986. Centenary of the isolation of denitrifying bacteria. ASM News. 52, 627-629.

Pereira, D., 2015. WindRose for Matlab. MATLAB Central File Exchange. https://au.mathworks.com/matlabcentral/fileexchange/47248-wind-rose (accessed 11/09/2020).

Pereira, L., Silva, S., Matthew, C., López, I., Sbrissia, A., 2018. Grazing management for sustainable grazing systems. In: Marshall, A. ,Collins, R. (Eds.), Improving grassland and pasture management in temperate agriculture. Burleigh Dodds Science Publishing, Cambridge, UK, pp. 79-122, Chapter 4.

Petrakis, S., Seyfferth, A., Kan, J., Inamdar, S., Vargas, R., 2017. Influence of experimental extreme water pulses on greenhouse gas emissions from soils. Biogeochemistry. 133, 2, 147-164.

Philippot, L., Hallin, S., Börjesson, G., Baggs, E.M., 2009. Biochemical cycling in the rhizosphere having an impact on global change. Plant Soil. 321, 1-2, 61-81.

Phillips, F.A., Leuning, R., Baigent, R., Kelly, K.B., Denmead, O.T., 2007. Nitrous oxide flux measurements from an intensively managed irrigated pasture using micrometeorological techniques. Agric. For. Meteorol. 143, 1, 92-105.

Phillips, R.L., McMillan, A.M.L., Palmada, T., Dando, J., Giltrap, D., 2014. Temperature effects on N_2O and N_2 denitrification end-products for a New Zealand pasture soil. N.Z. J. Agric. Res. 58, 1, 89-95.

Pihlatie, M. 2007. Nitrous oxide emissions from selected natural and managed northern ecosystems. thesis, University of Helsinki, Helsinki.

Piñeiro, G., Paruelo, J.M., Jobbágy, E.G., Jackson, R.B., Oesterheld, M., 2009. Grazing effects on belowground C and N stocks along a network of cattle exclosures in temperate and subtropical grasslands of South America. Global Biogeochem. Cycles. 23, GB2003, 1-14.

Pinto, M., Merino, P., del Prado, A., Estavillo, J.M., Yamulki, S., Gebauer, G., Piertzak, S., Lauf, J., Oenema, O., 2004. Increased emissions of nitric oxide and nitrous oxide following tillage of a perennial pasture. Nutr. Cycling Agroecosyst. 70, 1, 13-22.

Poeplau, C., Don, A., Vesterdal, L., Leifeld, J., Van Wesenmael, B., Schumacher, J., Gensior, A., 2011. Temporal dynamics of soil organic carbon after land-use change in the temperate zone – carbon response functions as a model approach. Global Change Biol. 17, 7, 2415-2427.

Portmann, R.W., Daniel, J.S., Ravishankara, A.R., 2012. Stratospheric ozone depletion due to nitrous oxide: influences of other gases. Philos. Trans. R. Soc. Lond. B. Biol. Sci. 367, 1593, 1256-64.

Poth, M., Focht, D.D., 1985. N^{-15} Kinetic analysis of N_2O production by Nitrosomonas europaea: an examination of nitrifier denitrification. Appl. Environ. Microbiol. 49, 5, 1134-1141.

Powell, A.M., Kemp, P.D., Jaya, I.D., Osborne, M.A., 2007. Establishment, growth and development of plantain and chicory under grazing. Proc. N. Z. Grassl. Assoc. 69, 41-45.

Prather, M.J., Holmes, C.D., Hsu, J., 2012. Reactive greenhouse gas scenarios: Systematic exploration of uncertainties and the role of atmospheric chemistry. Geophys. Res. Lett. 39, L09803, 1-5.

Pronger, J., Campbell, D.I., Clearwater, M.J., Rutledge, S., Wall, A.M., Schipper, L.A., 2016. Low spatial and inter-annual variability of evaporation from a year-round intensively grazed temperate pasture system. Agric. Ecosyst. Environ. 232, 46-58.

Pronger, J., Campbell, D.I., Clearwater, M.J., Mudge, P.L., Rutledge, S., Wall, A.M., Schipper, L.A., 2019. Toward optimisation of water use efficiency in dryland pastures using carbon isotope discrimination as a tool to select plant species mixtures. Sci. Total Environ. 665, 698-708.

Pronger, J., Wall, A.M., Campbell, D.I., Mudge, P.L., Schipper, L.A. (unpublished). Short pasture renewal period minimises soil carbon losses, but poor pasture establishment leads to annual scale soil carbon losses. Manaaki Whenua Landcare Research, University of Waikato.

Pumpanen, J., Kolari, P., Ilvesniemi, H., Minkkinen, K., Vesala, T., Niinistö, S., Lohila, A., Larmola, T., Morero, M., Pihlatie, M., Janssens, I.A., Yuste, J.C., Grünzweig, J.M., Reth, S., Subke, J.-A., Savage, K., Kutsch, W., Østreng, G., Ziegler, W., Anthoni, P., Lindroth, A., Hari, P., 2004. Comparison of different chamber techniques for measuring soil CO_2 efflux. Agric. For. Meteorol. 123, 3, 159-176.

Rabot, E., Hénault, C., Cousin, I., 2016. Effect of the soil water dynamics on nitrous oxide emissions. Geoderma. 280, 38-46.

Rafique, R., Hennessy, D., Kiely, G., 2011. Nitrous Oxide Emission from Grazed Grassland Under Different Management Systems. Ecosystems. 14, 4, 563-582.

Rannik, Ü., Haapanala, S., Shurpali, N.J., Mammarella, I., Lind, S., Hyvönen, N., Peltola, O., Zahniser, M., Martikainen, P.J., Vesala, T., 2015. Intercomparison of fast response commercial gas analysers for nitrous oxide flux measurements under field conditions. Biogeosciences. 12, 2, 415-432.

Rapson, T.D., Dacres, H., 2014. Analytical techniques for measuring nitrous oxide. Trends Anal. Chem. 54, 65-74.

Ravishankara, J.S., Daniel, R.W., Portmann, R.W., 2009. Nitrous oxide (N_2O): The dominant ozone-depleting substance emitted in the 21st century. Science. 326, 5949, 123-125.

Reay, D.S., Davidson, E.A., Smith, K.A., Smith, P., Melillo, J.M., Dentener, F., Crutzen, P.J., 2012. Global agriculture and nitrous oxide emissions. Nat. Clim. Change. 2, 410-416.

Rees, R., Augustin, J., Alberti, G., Ball, B., Boeckx, P., Cantarel, A., Castaldi, S., Chirinda, N., Chojnicki, B., Giebels, M., Gordon, H., Grosz, B., Horvath, L., Juszczak, R., Klemedtsson, Å., Klemedtsson, L., Medinets, S., Machon, A., Mapanda, F., Nyamangara, J., Olesen, J., Reay, D., Sanchez, L., Cobena, A., Smith, K., Sowerby, A., Sommer, M., Soussana, J., Stenberg, M., Topp, C., van Cleemput, O., Vallejo, A., Watson, C., Wuta, M., 2013. Nitrous oxide emissions from European agriculture - an analysis of variability and drivers of emissions from field experiments. Biogeosciences. 10, 2671-2682.

Reinsch, T. 2014. Grünlandumbruch und Neuansaat: kurz- und langfristige Effekte auf Treibhausgasemissionen und Ertragsleistungen von Grünlandbeständen. thesis, Christian-Albrechts-Universität zu Kiel, Kiel.

Reinsch, T., Loges, R., Kluß, C., Taube, F., 2018a. Effect of grassland ploughing and reseeding on CO_2 emissions and soil carbon stocks. Agric. Ecosyst. Environ. 265, 374-383.

Reinsch, T., Loges, R., Kluß, C., Taube, F., 2018b. Renovation and conversion of permanent grass-clover swards to pasture or crops: Effects on annual N_2O emissions in the year after ploughing. Soil Tillage Res. 175, 119-129.

Reisinger, A., Clark, H., 2018. How much do direct livestock emissions actually contribute to global warming? Global Change Biol. 24, 4, 1749-1761.

Rennenberg, H., Dannenmann, M., Gessler, A., Kreuzwieser, J., Simon, J., Papen, H., 2009. Nitrogen balance in forest soils: nutritional limitation of plants under climate change stresses. Plant Biol. 11, s1, 4-23.

Reyer, C.P.O., Leuzinger, S., Rammig, A., Wolf, A., Bartholomeus, R.P., Bonfante, A., de Lorenzi, R., Dury, M., Gloning, P., Abou Jaoudé, R., Klein, T., Kuster, T.M., Martins, M., Niedrist, G., Riccardi, M., Wohlfahrt, G., de Angelis, P., de Dato, G., François, L., Menzel, A., Pereira, M., 2013. A plant's perspective of

extremes: terrestrial plant responses to changing climatic variability. Global Change Biol. 19, 1, 75-89.

Robertson, G., 1989. Nitrification and denitrification in humid tropical ecosystems: potential controls on nitrogen retention In: Proctor, J. (Ed.), Mineral Nutrients in Tropical Forest and Savanna Ecosystems. Blackwell Scientific, Cambridge, pp. 55-69.

Rochette, P., Bertrand, N., 2003. Soil air sample storage and handling using polypropylene syringes and glass vials. Can. J. Soil Sci. 83, 5, 631-637.

Rochette, P., Bertrand, N., 2007. Soil-Surface Gas Emissions. In: Carter, M.S. ,Gregorich, E.G. (Eds.), Soil Sampling and Methods of Analysis, 2 ed. CRC Press, Boca Raton, FL, USA, pp. 851-861, Chapter 6.

Rochette, P., Eriksen-Hamel, N., 2008. Chamber Measurements of Soil Nitrous Oxide Flux: Are Absolute Values Reliable? Soil Sci. Soc. Am. J. 72, 2, 331-342.

Rochette, P., 2011. Towards a standard non-steady-state chamber methodology for measuring soil N_2O emissions. Anim. Feed Sci. Technol. 166, 141-146.

Röös, E., Bajželj, B., Smith, P., Patel, M., Little, D., Garnett, T., 2017. Greedy or needy? Land use and climate impacts of food in 2050 under different livestock futures. Global Environ. Change. 47, 1-12.

Rowlings, D.W., Grace, P.R., Scheer, C., Liu, S., 2015. Rainfall variability drives interannual variation in N_2O emissions from a humid, subtropical pasture. Sci. Total Environ. 512-513, 8-18.

Ruser, R., Flessa, H., Russow, R., G., S., Buegger, F., Munch, J.C., 2006. Emission of N_2O, N_2 and CO_2 from soil fertilized with nitrate: effect of compaction, soil moisture and rewetting. Soil Biol. Biochem. 38, 263-274.

Rutledge, S., Wall, A.M., Mudge, P.L., Troughton, B., Campbell, D.I., Pronger, J., Joshi, C., Schipper, L.A., 2017a. The carbon balance of temperate grasslands part I: The impact of increased species diversity. Agric. Ecosyst. Environ. 239, 310-323.

Rutledge, S., Wall, A.M., Mudge, P.L., Troughton, B., Campbell, D.I., Pronger, J., Joshi, C., Schipper, L.A., 2017b. The carbon balance of temperate grasslands part II: The impact of pasture renewal via direct drilling. Agric. Ecosyst. Environ. 239, 132-142.

Saarijarvi, K., Virkajarvi, P., 2009. Nitrogen dynamics of cattle dung and urine patches on intensively managed boreal pasture. J. Agric. Sci. 147, 4, 479-491.

Saggar, S., Luo, J., Kim, D.-G., Jha, N., 2011. Intensification in Pastoral Farming: Impacts on Soil Attributes and Gaseous Emissions. In: Singh, B., Cowie, A., Chan, K. (Ed.), Soil Health and Climate Change. Springer, Berlin, Heidelberg, pp. 207-236, Chapter 10.

Saggar, S., Jha, N., Deslippe, J., Bolan, N.S., Luo, J., Giltrap, D.L., Kim, D.G., Zaman, M., Tillman, R.W., 2013. Denitrification and N_2O:N_2 production in temperate grasslands: processes, measurements, modelling and mitigating negative impacts. Sci. Total Environ. 465, 173-95.

Savage, K., Phillips, R., Davidson, E., 2014. High temporal frequency measurements of greenhouse gas emissions from soils. Biogeosciences. 11, 10, 2709-2720.

Scanlon, T.M., Kiely, G., 2003. Ecosystem-scale measurements of nitrous oxide fluxes for an intensely grazed, fertilized grassland. Geophys. Res. Lett. 30, 16, 1-4.

Schaufler, G., Kitzler, B., Schindlbacher, A., Skiba, U., Sutton, M.A., Zechmeister-Boltenstern, S., 2010. Greenhouse gas emissions from European soils under different land use: effects of soil moisture and temperature. Eur. J. Soil Sci. 61, 5, 683-696.

Schils, R., Verhagen, A., Aarts, H., Šebek, L., 2005. A farm level approach to define successful mitigation strategies for GHG emissions from ruminant livestock systems. Nutr. Cycling Agroecosyst. 71, 2, 163-175.

Schilt, A., Baumgartner, M., Eicher, O., Chappellaz, J., Schwander, J., Fischer, H., Stocker, T.F., 2013. The response of atmospheric nitrous oxide to climate variations during the last glacial period. Geophys. Res. Lett. 40, 9, 1888-1893.

Schimel, J., Holland, E.A., 2005. Global Gases. In: Sylvia, D.M., Hartel, P.G.F., J. J. ,Zuberer, D.A. (Eds.), Principles and applications of soil microbiology. Pearson, New Jersey, pp. 491-509, Chapter 19.

Schindlbacher, A., Zechmeister-Boltenstern, S., Butterbach-Bahl, K., 2004. Effects of soil moisture and temperature on NO, NO_2, and N_2O emissions from European forest soils. J. Geophys. Res. Atmos. 109, DI17302, 1-12.

Schipper, L.A., Percival, H.J., Sparling, G.P., 2004. An approach for estimating when soils will reach maximum nitrogen storage. Soil Use Manage. 20, 3, 281-286.

Schipper, L.A., Baisden, W.T., Parfitt, R.L., Ross, C., Arnold, J.J., Claydon, G., Baisden, G., 2007. Large losses of soil C and N from soil profiles under pasture in New Zealand during the past 20 years. Global Change Biol. 13, 6, 1138-1144.

Schipper, L.A., Parfitt, R.L., Fraser, S., Littler, R.A., Baisden, W.T., Ross, C., 2014. Soil order and grazing management effects on changes in soil C and N in New Zealand pastures. Agric. Ecosyst. Environ. 184, 67-75.

Schloesing, T., Muentz, A., 1877. Sur la nitrification par les ferments organises. C. R. Hebd. Seances Acad. Sci 84, 301-303.

Schmid, H.P., 1994. Source areas for scalars and scalar fluxes. Boundary Layer Meteorol. 67, 3, 293-318.

Schmidt, I., van Spanning, R.J.M., Jetten, M.S.M., 2004. Denitrification and ammonia oxidation by Nitrosomonas europaea wild-type, and NirK- and NorB-deficient mutants. Microbiology. 150, 12, 4107-4114.

Schuepp, P.H., Leclerc, M.Y., MacPherson, J.I., Desjardins, R.L., 1990. Footprint prediction of scalar fluxes from analytical solutions of the diffusion equation. Boundary Layer Meteorol. 50, 1-4, 355-373.

Seinfeld, J.H., 2006. Atmospheric chemistry and physics : from air pollution to climate change, Pandis, S.N. (Ed.), 2 ed. John Wiley & Sons, Hoboken, N.J. 1232p.

Seitzinger, S., Harrison, J.A., Böhlke, J.K., Bouwman, A.F., Lowrance, R., Peterson, B., Tobias, C., Drecht, G.V., 2006. Denitrification across landscapes and waterscapes: a synthesis. Ecol. Appl. 16, 6, 2064-2090.

Selbie, D.R., Buckthought, L.E., Shepherd, M.A., 2015. Chapter Four - The Challenge of the Urine Patch for Managing Nitrogen in Grazed Pasture Systems. Adv. Agron. 129, 229-292.

Shang, Z., Abdalla, M., Kuhnert, M., Albanito, F., Zhou, F., Xia, L., Smith, P., 2020. Measurement of N_2O emissions over the whole year is necessary for estimating reliable emission factors. Environ. Pollut. 259, 113864, 1-8.

Shcherbak, I., Millar, N., Robertson, G.P., 2014. Global metaanalysis of the nonlinear response of soil nitrous oxide (N_2O) emissions to fertilizer nitrogen. PNAS. 111, 25, 9199-9204.

Shepherd, M.A., Hatch, D.J., Jarvis, S.C., Bhogal, A., 2001. Nitrate leaching from reseeded pasture. Soil Use Manage. 17, 2, 97-105.

Shi, B., Xu, W., Zhu, Y.G., Wang, C., Loik, M.E., Sun, W., 2019. Heterogeneity of grassland soil respiration: Antagonistic effects of grazing and nitrogen addition. Agric. For. Meteorol. 268, 215-223.

Shine, K.P., Derwent, R.G., Wuebbles, D.J., Morcrette, J.J., 1990. Radiative forcing of climate. In: Houghton, J.T. (Ed.), Climate change the IPCC scientific assessment. Cambridge University Press, Cambridge, pp. 41-68, Chapter 2.

Signor, D., Cerri, C.E.P., 2013. Nitrous oxide emissions in agricultural soils: a review. Pesq. Agropec. Trop. 43, 3, 322-338.

Šimek, M., 2008. Nitrous oxide emissions from grazed grasslands: Key sources and abatement strategies (case study-overwintering areas in the Czech Republic, Central Europe). In: Schroeder, H.G. (Ed.), Grassl.: Ecol. Manag. Restor. Nova Science Publishers, Incorporated pp. 235-250, Chapter 10.

Simon, P., de Klein, C.A.M., Worth, W., Rutherford, A.J., Dieckow, J., 2019. The efficacy of Plantago lanceolata for mitigating nitrous oxide emissions from cattle urine patches. Sci. Total Environ. 691, 430-441.

Skiba, U., Van Dijk, S., Ball, B.C., 2002. The influence of tillage on NO and N_2O fluxes under spring and winter barley. Soil Use Manage. 18, 4, 340-345.

Smith, K.A., Dobbie, K.E., 2001. The impact of sampling frequency and sampling times on chamber-based measurements of N_2O emissions from fertilized soils. Global Change Biol. 7, 8, 933-945.

Smith, K.A., Mosier, A.R., Crutzen, P.J., Winiwarter, W., 2012. The role of N_2O derived from crop-based biofuels, and from agriculture in general, in Earth's climate. Philos. Trans. R. Soc. Lond. B. Biol. Sci. 367, 1593, 1169-1174.

Smith, K.A., Ball, T., Conen, F., Dobbie, K.E., Massheder, J., Rey, A., 2018. Exchange of greenhouse gases between soil and atmosphere: interactions of soil physical factors and biological processes. Eur. J. Soil Sci. 69, 1, 10-20.

Smith, P., Martino, D., Cai, Z., Gwary, D., Janzen, H., Kumar, P., McCarl, B., Ogle, S., O'Mara, F., Rice, C., Scholes, B., Sirotenko, O., Howden, M., McAllister, T., Pan, G., Romanenkov, V., Schneider, U., Towprayoon, S., Wattenbach, M., Smith, J., 2008. Greenhouse gas mitigation in agriculture. Philos. Trans. R. Soc. Lond. B. Biol. Sci. 363, 1492, 789-813.

Sonthi, R.K. 2010. Gaseous emissions (NH_3, N_2O and CH_4) following manure or urea application to soil as influenced by ammendments. thesis, The University of Waikato, Hamilton.

Soussana, J.F., Allard, V., Pilegaard, K., Ambus, P., Amman, C., Campbell, C., Ceschia, E., Clifton-Brown, J., Czobel, S., Domingues, R., Flechard, C., Fuhrer, J., Hensen, A., Horvath, L., Jones, M., Kasper, G., Martin, C., Nagy, Z., Neftel, A., Raschi, A., Baronti, S., Rees, R.M., Skiba, U., Stefani, P., Manca, G., Sutton, M., Tuba, Z., Valentini, R., 2007. Full accounting of the greenhouse gas (CO_2, N_2O, CH_4) budget of nine European grassland sites. Agric. Ecosyst. Environ. 121, 1-2, 121-134.

Soussana, J.F., Lemaire, G., 2014. Coupling carbon and nitrogen cycles for environmentally sustainable intensification of grasslands and crop-livestock systems. Agric. Ecosyst. Environ. 190, 9-17.

Sparling, G., Chibnall, E., Pronger, J., Rutledge, S., Wall, A., Campbell, D., Schipper, L., 2016. Estimates of annual leaching losses of dissolved organic carbon from pastures on Allophanic Soils grazed by dairy cattle, Waikato, New Zealand. N.Z. J. Agric. Res., 1-18.

Stevenson, F.J., 1982. Nitrogen in agricultural soils. American Society of Agronomy, Madison, Wis. 940p.

Stewart, A.A., Little, S.M., Ominski, K.H., Wittenberg, K.M., Janzen, H.H., 2009. Evaluating greenhouse gas mitigation practices in livestock systems: an illustration of a whole-farm approach. J. Agric. Sci. 147, 4, 367-382.

Stüeken, E.E., Kipp, M.A., Koehler, M.C., Buick, R., 2016. The evolution of Earth's biogeochemical nitrogen cycle. Earth-Sci. Rev. 160, 220-239.

Subbarao, G.V., Ito, O., Sahrawat, K.L., Berry, W.L., Nakahara, K., Ishikawa, T., Watanabe, T., Suenaga, K., Rondon, M., Rao, I.M., 2006. Scope and Strategies for Regulation of Nitrification in Agricultural Systems - Challenges and Opportunities. Crit. Rev. Plant Sci. 25, 4, 303-335.

Suttie, J.M., Reynolds, S.G., Batello, C., 2005. Grasslands of the World. Plant Production and Protection Series, No. 34. Food and Agricultural Organisation (FAO), Rome. 513p.

Sutton, M.A., Skiba, U.M., Davidson, E.A., Kanter, D., van Grinsven, H.J.M., Oenema, O., Maas, R., Pathak, H., 2013. Drawing-down N_2O To Protect Climate and the Ozone Layer. A UNEP Synthesis Report. United Nations Environmental Programme (UNEP), Nairobi. 57p.

Syakila, A., Kroeze, C., Slomp, C.P., 2010. Neglecting sinks for N_2O at the earth's surface: does it matter? J. Integr. Environ. Sci. 7, sup1, 79-87.

Syakila, A., Kroeze, C., 2011. The global nitrous oxide budget revisited. Greenhouse Gas Meas. Manage. 1, 1, 17-26.

Sylvia, D.M., Fuhrmann, J.J., Hartel, P.G., Fuhrmann, J.J., 2005. Principles and applications of soil microbiology, 2 ed. Pearson Prentice Hall, Upper Saddle River, N.J. 672p.

Tallec, T., Brut, A., Joly, L., Dumelié, N., Serça, D., Mordelet, P., Claverie, N., Legain, D., Barrié, J., Decarpenterie, T., Cousin, J., Zawilski, B., Ceschia, E., Guérin, F., Le Dantec, V., 2019. N_2O flux measurements over an irrigated maize crop: A comparison of three methods. Agric. For. Meteorol. 264, 56-72.

Tate, K.R., Wilde, R.H., Giltrap, D.J., Baisden, W.T., Saggar, S., Trustrum, N.A., Scott, N.A., Barton, J.P., 2005. Soil organic carbon stocks and flows in New Zealand: System development, measurement and modelling. Can. J. Soil Sci. 85, 4, 481-489.

Taylor, A.M., Amiro, B.D., Tenuta, M., Gervais, M., 2017. Direct whole-farm greenhouse gas flux measurements for a beef cattle operation. Agric. Ecosyst. Environ. 239, 65-79.

Teh, Y.A., Silver, W.L., Sonnentag, O., Detto, M., Kelly, M.P.C., Baldocchi, D.D., 2011. Large Greenhouse Gas Emissions from a Temperate Peatland Pasture. Ecosystems. 14, 2, 311-325.

Thom, E.R., Fraser, T.J., Hume, D.E., 2011. Sowing methods for successful pasture establishment - a review. Pasture Persistence - Grassland Research and Practice Series. 15, 31-38.

Thomas, S., Wallance, D., Beare, M., 2014. Pasture renewal activity data and factors for New Zealand. A report prepared for: Ministry of Primary Industries. Plant & Food Research Client Report No. 16806. Plant and Food Research. 65p.

Thompson, R., Lassaletta, L., Patra, P., Wilson, C., Wells, K., Gressent, A., Koffi, E., Chipperfield, M., Winiwarter, W., Davidson, E., Tian, H., Canadell, J., 2019. Acceleration of global N_2O emissions seen from two decades of atmospheric inversion. Nat. Clim. Change. 9, 1-6.

Thompson, R.L., Chevallier, F., Crotwell, A.M., Dutton, G., Langenfelds, R.L., Prinn, R.G., Weiss, R.F., Tohjima, Y., Nakazawa, T., Krummel, P.B., Steele, L.P., Fraser, P., O'Doherty, S., Ishijima, K., Aoki, S., 2014. Nitrous oxide emissions 1999 to 2009 from a global atmospheric inversion. Atmos. Chem. Phys. 14, 4, 1801-1817.

Tian, H., Lu, C., Ciais, P., Michalak, A.M., Canadell, J.G., Saikawa, E., Huntzinger, D.N., Gurney, K.R., Sitch, S., Zhang, B., Yang, J., Bousquet, P., Bruhwiler, L., Chen, G., Dlugokencky, E., Friedlingstein, P., Melillo, J., Pan, S., Poulter, B., Prinn, R., Saunois, M., Schwalm, C.R., Wofsy, S.C., 2016. The terrestrial biosphere as a net source of greenhouse gases to the atmosphere. Nature. 531, 7593, 225.

Tian, H., Yang, J., Xu, R., Lu, C., Canadell, J.G., Davidson, E.A., Jackson, R.B., Arneth, A., Chang, J., Ciais, P., Gerber, S., Ito, A., Joos, F., Lienert, S., Messina, P., Olin, S., Pan, S., Peng, C., Saikawa, E., Thompson, R.L., Vuichard, N., Winiwarter, W., Zaehle, S., Zhang, B., 2019. Global soil nitrous oxide

emissions since the preindustrial era estimated by an ensemble of terrestrial biosphere models: Magnitude, attribution, and uncertainty. Global Change Biol. 25, 2, 640-659.

Tian, H., Xu, R., Canadell, J.G., Thompson, R.L., Winiwarter, W., Suntharalingam, P., Davidson, E.A., Ciais, P., Jackson, R.B., Janssens-Maenhout, G., Prather, M.J., Regnier, P., Pan, N., Pan, S., Peters, G.P., Shi, H., Tubiello, F.N., Zaehle, S., Zhou, F., Arneth, A., Battaglia, G., Berthet, S., Bopp, L., Bouwman, A.F., Buitenhuis, E.T., Chang, J., Chipperfield, M.P., Dangal, S.R.S., Dlugokencky, E., Elkins, J.W., Eyre, B.D., Fu, B., Hall, B., Ito, A., Joos, F., Krummel, P.B., Landolfi, A., Laruelle, G.G., Lauerwald, R., Li, W., Lienert, S., Maavara, T., MacLeod, M., Millet, D.B., Olin, S., Patra, P.K., Prinn, R.G., Raymond, P.A., Ruiz, D.J., van der Werf, G.R., Vuichard, N., Wang, J., Weiss, R.F., Wells, K.C., Wilson, C., Yang, J., Yao, Y., 2020. A comprehensive quantification of global nitrous oxide sources and sinks. Nature. 586, 7828, 248-256.

Tiedje, J.M., 1988. Ecology of denitrification and the dissimilatory nitrate reduction to ammonium. In: Zehnder, A.J.B. (Ed.), Biology of anaerobic microorganisms. John Wiley & Sons Inc, New York, pp. 179-244.

Tisdall, J.M., Oades, J.M., 1982. Organic matter and water-stable aggregates in soils. J. Soil Sci. 33, 2, 141-163.

Uchida, Y., Clough, T.J., 2015. Nitrous oxide emissions from pastures during wet and cold seasons. Grassl. Sci. . 61, 61-74.

Ussiri, D., Rattan, L., 2012. Soil Emission of Nitrous Oxide and its Mitigation. Springer, Dordrecht, Netherlands 378p.

van der Weerden, T., Beukes, P., de Klein, C.A.M., Hutchinson, K., Farrell, L., Stormink, T., Romera, A., Dalley, D.E., Monaghan, R.M., Chapman, D., Macdonald, K., Dynes, R., 2018. The Effects of System Changes in Grazed Dairy Farmlet Trials on Greenhouse Gas Emissions, Vol. 8.

van der Weerden, T., Noble, A., Luo, J., De Klein, C.A.M., Saggar, S., Giltrap, D., Gibbs, J., Rys, G., 2020. Meta-analysis of New Zealand's nitrous oxide emission factors for ruminant excreta supports disaggregation based on excreta form, livestock type and slope class. Sci. Total Environ. 732, 139235, 1-12.

van der Weerden, T.J., Luo, J., de Klein, C.A.M., Hoogendoorn, C.J., Littlejohn, R.P., Rys, G.J., 2011. Disaggregating nitrous oxide emission factors for ruminant urine and dung deposited onto pastoral soils. Agric. Ecosyst. Environ. 141, 3, 426-436.

van der Weerden, T.J., Clough, T.J., Styles, T.M., 2013. Using near-continuous measurements of N_2O emission from urine-affected soil to guide manual gas sampling regimes. N.Z. J. Agric. Res. 56, 1, 60-76.

van der Weerden, T.J., Manderson, A., Kelliher, F.M., de Klein, C.A.M., 2014. Spatial and temporal nitrous oxide emissions from dairy cattle urine deposited onto grazed pastures across New Zealand based on soil water balance modelling. Agric. Ecosyst. Environ. 189, 92-100.

van der Weerden, T.J., Cox, N., Luo, J., Di, H.J., Podolyan, A., Phillips, R.L., Saggar, S., de Klein, C.A.M., Ettema, P., Rys, G., 2016. Refining the New Zealand

nitrous oxide emission factor for urea fertiliser and farm dairy effluent. Agric. Ecosyst. Environ. 222, 133-137.

van der Weerden, T.J., Laurenson, S., Vogeler, I., Beukes, P.C., Thomas, S.M., Rees, R.M., Topp, C.F.E., Lanigan, G., de Klein, C.A.M., 2017a. Mitigating nitrous oxide and manure-derived methane emissions by removing cows in response to wet soil conditions. Agric. Syst. 156, 126-138.

van der Weerden, T.J., Noble, A., Kelliher, F., Luo, J., de Klein, C.A.M., Rollo, M., Giltrap, D., 2017b. Review of summer values for nitrous oxide emissions - final report. MPI technical Paper 2017/56. Ministry for Primary Industries (MPI), Wellington. 52p.

Van Drecht, G., Bouwman, A.F., Knoop, J.M., Beusen, A.H.W., Meinardi, C.R., 2003. Global modeling of the fate of nitrogen from point and nonpoint sources in soils, groundwater, and surface water. Global Biogeochem. Cycles. 17, 4, 20.

van Groenigen, K.J., Osenberg, C.W., Hungate, B.A., 2011. Increased soil emissions of potent greenhouse gases under increased atmospheric CO_2. Nature. 475, 214-218.

Velthof, G.L., Oenema, O., 1995. Nitrous oxide fluxes from grassland in the Netherlands: II. Effects of soil type, nitrogen fertilizer application and grazing. Eur. J. Soil Sci. 46, 4, 541-549.

Velthof, G.L., Jarvis, S.C., Stein, A., Allen, A.G., Oenema, O., 1996. Spatial variability of nitrous oxide fluxes in mown and grazed grasslands on a poorly drained clay soil. Soil Biol. Biochem. 28, 9, 1215-1225.

Velthof, G.L., Oenema, O., 1997. Nitrous oxide emission from dairy farming systems in the Netherlands. Neth. J. Agric. Sci. 45, 3, 347-360.

Velthof, G.L., Hoving, I.E., Dolfing, J., Smit, A., Kuikman, P.J., Oenema, O., 2010. Method and timing of grassland renovation affects herbage yield, nitrate leaching, and nitrous oxide emission in intensively managed grasslands. Nutr. Cycling Agroecosyst. 86, 3, 401-412.

Venterea, R.T., Baker, J.M., 2008. Effects of Soil Physical Nonuniformity on Chamber-Based Gas Flux Estimates. Soil Sci. Soc. Am. J. 72, 5, 1410-1417.

Venterea, R.T., 2010. Simplified Method for Quantifying Theoretical Underestimation of Chamber-Based Trace Gas Fluxes. J. Environ. Qual. 39, 1, 126-135.

Verchot, L.V., Davidson, E.A., Cattânio, J.H., Ackerman, I.L., Erickson, H.E., Keller, M., 1999. Land-use change and biogeochemical controls of nitrogen oxide emissions from soils in eastern Amazonia. Global Biogeochem. Cycles. 13, 31-46.

Vertes, F., Hatch, D.J., Velthof, G.L., Taube, F., Laurent, F., Loiseau, P., Recous, S., 2007. Short-term and cumulative effects of grassland cultivation on nitrogen and carbon cycling in ley-arable rotations. Grassl. Sci. Europ. 12, 227-246.

Vickers, D., Mahrt, L., 1997. Quality control and flux sampling problems for tower and aircraft data. J. Atmos. Oceanic Technol. 14, 3, 512-526.

Vitousek, P.M., Howarth, R.W., 1991. Nitrogen limitation on land and in the sea: How can it occur? Biogeochemistry. 13, 2, 87-115.

Vitousek, P.M., Menge, D.N.L., Reed, S.C., Cleveland, C.C., 2013. Biological nitrogen fixation: rates, patterns and ecological controls in terrestrial ecosystems. Philos. Trans. R. Soc. Lond. B. Biol. Sci. 368, 1621, 1-9.

Voglmeier, K. 2018. Hot spots and more: multi-scale measurements for a better understanding of gaseous emissions from grazing systems. thesis, ETH Zurich, Zurich.

Voglmeier, K., Six, J., Jocher, M., Ammann, C., 2019. Grazing-related nitrous oxide emissions: from patch scale to field scale. Biogeosciences. 16, 8, 1685-1703.

Vuuren, D.P.v., Bouwman, L.F., Smith, S.J., Dentener, F., 2011. Global projections for anthropogenic reactive nitrogen emissions to the atmosphere: an assessment of scenarios in the scientific literature. Curr. Opin. Environ. Sustain. 3, 5, 359-369.

Wall, A.M., Campbell, D.I., Schipper, L.A., 2017. Split Footprint Approach for Eddy Covariance Studies in Grazed Pastoral Systems. ERI report number 99. Prepared for the New Zealand Agricultural Greenhouse Gas Research Centre. Environmental Research Institute, Faculty of Science and Engineering, The University of Waikato, Hamilton. 26p.

Wall, A.M., Campbell, D.I., Mudge, P.L., Rutledge, S., Schipper, L.A., 2019. Carbon budget of an intensively grazed temperate grassland with large quantities of imported supplemental feed. Agric. Ecosyst. Environ. 281, 1-15.

Wall, A.M., Campbell, D.I., Morcom, C.P., Mudge, P.L., Schipper, L.A., 2020a. Quantifying carbon losses from periodic maize silage cropping of permanent temperate pastures. Agric. Ecosyst. Environ. 301, 1-11.

Wall, A.M., Campbell, D.I., Mudge, P.L., Schipper, L.A., 2020b. Temperate grazed grassland carbon balances for two adjacent paddocks determined separately from one eddy covariance system. Agric. For. Meteorol. 287, 1-14.

Wallenstein, M.D., Myrold, D.D., Firestone, M.K., Voytek, M., 2006. Environmental controls on denitrifying communities and denitrification rates: insights from molecular methods. Ecol. Appl. 16, 6, 2143-2152.

Wang, K., Liu, C., Zheng, X., Pihlatie, M., Li, B., Haapanala, S., Vesala, T., Liu, H., Wang, Y., Liu, G., Hu, F., 2013a. Comparison between eddy covariance and automatic chamber techniques for measuring net ecosystem exchange of carbon dioxide in cotton and wheat fields. Biogeosciences. 10, 6865-6877.

Wang, K., Zheng, X., Pihlatie, M., Vesala, T., Liu, C., Haapanala, S., Mammarella, I., Rannik, Ü., Liu, H., 2013b. Comparison between static chamber and tunable diode laser-based eddy covariance techniques for measuring nitrous oxide fluxes from a cotton field. Agric. For. Meteorol. 171-172, 9-19.

Watson, C.J., Jordan, C., Kilpatrick, D., McCarney, B., Stewart, R., 2007. Impact of grazed grassland management on total N accumulation in soil receiving different levels of N inputs. Soil Use Manage. 23, 2, 121-128.

Wayne, R.P., 2000. Chemistry of atmospheres: an introduction to the chemistry of the atmospheres of earth, the planets, and their satellites, 3 ed. Oxford University Press, Oxford, New York. 808p.

Wecking, A.R., Cave, V.M., Liáng, L.L., Wall, A.M., Luo, J., Campbell, D.I., Schipper, L.A., 2020a. A novel injection technique: using a field-based quantum cascade laser for the analysis of gas samples derived from static chambers. Atmos. Meas. Tech. 13, 5763-5777.

Wecking, A.R., Wall, A.M., Liáng, L.L., Lindsey, S.B., Luo, J., Campbell, D.I., Schipper, L.A., 2020b. Reconciling annual nitrous oxide emissions of an intensively grazed dairy pasture determined by eddy covariance and emission factors. Agric. Ecosyst. Environ. 287, 1-14.

White, S.L., Sheffield, R.E., Washburn, S.P., King, L.D., Green J.T, Jr., 2001. Spatial and time distribution of dairy cattle excreta in an intensive pasture system. J. Environ. Qual. 30, 6, 2180-2187.

Whitehead, D., Schipper, L.A., Pronger, J., Moinet, G.Y.K., Mudge, P.L., Calvelo Pereira, R., Kirschbaum, M.U.F., McNally, S.R., Beare, M.H., Camps-Arbestain, M., 2018. Management practices to reduce losses or increase soil carbon stocks in temperate grazed grasslands: New Zealand as a case study. Agric. Ecosyst. Environ. 265, 432-443.

Whitehead, D.C., Bristow, A.W., Lockyer, D.R., 1990. Organic matter and nitrogen in the unharvested fractions of grass swards in relation to the potential for nitrate leaching after ploughing. Plant Soil. 123, 1, 39-49.

Whitehead, D.C., 2000. Nutrient elements in grassland soil-plant-animal relationships. CABI Pub., Wallingford. 369p.

Wichtl, M., 2004. Herbal Drugs and Phytopharmaceuticals, 3 ed. CRC Press, Boca Raton. 704p.

Wilkerson, J., Dobosy, R., Sayres, D.S., Healy, C., Dumas, E., Baker, B., Anderson, J.G., 2019. Permafrost nitrous oxide emissions observed on a landscape scale using the airborne eddy-covariance method. Atmos. Chem. Phys. 19, 7, 4257-4268.

Wilkinson, S., Lowrey, R.W., 1973. Cycling of mineral nutrients in pasture ecosystems. In: Butler, G.W. ,Bailey, R.W. (Eds.), Chemistry and Biochemistry of Herbage. Academic Press, New York, pp. 247-315.

WMO, 2017a. Statement on the State of the Global Climate in 2016. WMO Report, No. 1189. World Meteorological Organization, Geneva, Switzerland. 28p.

WMO, 2017b. WMO Greenhouse Gas Bulletin No. 13. The State of Greenhouse Gases in the Atmosphere Based on Global Observations through 2016. https://public.wmo.int/en/resources/library/wmo-greenhouse-gas-bulletin (accessed 27/09/2020).

WMO, 2018. WMO Greenhouse Gas Bulletin No. 14. The State of Greenhouse Gases in the Atmosphere Based on Global Observations through 2017. https://public.wmo.int/en/resources/library/wmo-greenhouse-gas-bulletin (accessed 27/09/2020).

Wold, S., Geladi, P., Esbensen, K., Öhman, J., 1987. Multi-way principal components-and PLS-analysis. J. Chemom. 1, 1, 41-56.

Wood, P.M., 1986. Nitrification as an energy source. In: Prosser, J.I. (Ed.), Nitrification. IRL Press, Oxford, pp. 39-62.

Woodwell, G.M., Whittaker, R.H., 1968. Primary production in terrestrial ecosystems. Am. Zoologist. 8, 19-30.

Xia, J., Niu, S., Wan, S., 2009. Response of ecosystem carbon exchange to warming and nitrogen addition during two hydrologically contrasting growing seasons in a temperate steppe. Global Change Biol. 15, 6, 1544-1556.

Yamulki, S., Goulding, K.W.T., Webster, C.P., Harrison, R.M., 1995. Studies on no and N20 fluxes from a wheat field. Atmos. Environ. 29, 14, 1627-1635.

Yamulki, S., Jarvis, S., 2002. Short-term effects of tillage and compaction on nitrous oxide, nitric oxide, nitrogen dioxide, methane and carbon dioxide fluxes from grassland. Biol. Fertil. Soils. 36, 3, 224-231.

Zahniser, M.S., Nelson, D.D., McManus, B., Kebabian, P.L., Lloyd, D., Fowler, D., Jenkinson, D.S., Monteith, J.L., Unsworth, M.H., 1995. Measurement of trace gas fluxes using tunable diode laser spectroscopy. Philos. Trans. Phys. Sci. Eng. 351, 1696, 371-382.

Zellweger, C., Steinbrecher, R., Laurent, O., Lee, H., Kim, S., Emmenegger, L., Steinbacher, M., Buchmann, B., 2019. Recent advances in measurement techniques for atmospheric carbon monoxide and nitrous oxide observations. Atmos. Meas. Tech. 12, 11, 5863-5878.

Zheng, X., Han, S., Huang, Y., Wang, Y., Wang, M., 2004. Re-quantifying the emission factors based on field measurements and estimating the direct N_2O emission from Chinese croplands. Global Biogeochem. Cycles. 18, 2, 1-19.

Zhou, M., Zhu, B., Wang, S., Zhu, X., Vereecken, H., Brüggemann, N., 2017. Stimulation of N_2O emission by manure application to agricultural soils may largely offset carbon benefits: a global meta-analysis. Global Change Biol. 23, 10, 4068-4083.

Zhu, K., Chiariello, N.R., Tobeck, T., Fukami, T., Field, C.B., 2016. Nonlinear, interacting responses to climate limit grassland production under global change. PNAS. 113, 38, 10589-10594.

Zöll, U., Brümmer, C., Schrader, F., Ammann, C., Ibrom, A., Flechard, C.R., Nelson, D.D., Zahniser, M., Kutsch, W.L., 2016. Surface–atmosphere exchange of ammonia over peatland using QCL-based eddy-covariance measurements and inferential modeling. Atmos. Chem. Phys. 16, 17, 11283-11299.

Zumft, W.G., 1997. Cell biology and molecular basis of denitrification. Microbiol. Mol. Biol. Rev. 61, 4, 533.

Appendices

A1 – Scientific abstract in German

Vom Menschen genutzte Böden sind Emittenten klimawirksamer Treibhausgase. Je nach Nutzung kann ein Boden dabei große Mengen an Kohlenstoffdioxid (CO_2), Methan (CH_4) und Distickstoffmonoxid (N_2O), umgangssprachlich auch bekannt als Lachgas, ausstoßen. Auf N_2O bezogen, trifft dies insbesondere zu, wenn sich der Boden unter intensiv bewirtschaftetem und beweidetem Land befindet und damit einhergehend oft hohen Mengen an reaktiven Stickstoffverbindungen ausgesetzt ist.

Reaktiver Stickstoff gelangt meist in Form von Tierexkrementen und/oder Düngern in den Boden, kann aber auch biologisch aus atmosphärischen Quellen dort fixiert werden. Geschätzt tragen agrarwirtschaftlich genutzte Böden derzeit zu etwa 60% zum globalen N_2O-Emissionsbudget bei. In manchen Fällen liegt der Anteil allerdings wesentlich höher, so z.B. in Neuseeland, wo N_2O von Weideböden 94% des nationalen N_2O-Emissionsbudgets ausmacht. Der Emissionsprozess von N_2O aus dem Boden in die Atmosphäre wird von einer Vielfalt von Faktoren kontrolliert (mikrobielle Aktivität, Umweltbedingungen, Bodenmanagement etc.) und ist zeitlich wie räumlich äußerst variabel, was die Quantifizierung des daraus emittierten N_2O erschwert. Eine zuverlässige Quantifizierung jedoch ist unersetzlich, nicht nur, um Rückschlüsse auf biogeochemische Prozessgefüge zu ziehen, sondern auch, um aussagekräftige Treibhausgasinventare berechnen und die Wirkung von Maßnahmen zur Schadstoffminderung ermessen zu können. Die Entwicklung neuer Analyseinstrumente und -methoden ermöglicht es seit ungefähr einem Jahrzehnt, kontinuierliche Messungen von N_2O-Flüssen auf Feldebene durchzuführen.

Die Messungen sind mikrometeorologischer Natur und bieten den Vorteil, die raum-zeitliche Variabilität von N_2O-Emissionen genauer zu erfassen. Die Anwendung dieser Methoden, z.B. mikrometeorologische eddy covariance (EC) Messungen, ist derzeit allerdings auf ausgewählte Bodentypen, Landnutzungen, Agrarmanagement- und Mitigationsszenarien beschränkt. Auch ist weitestgehend unklar, ob und inwiefern sich die Ergebnisse von EC-Messungen mit traditionellen Ansätzen wie Kammer-messungen und Emissionsfaktoren (EF) vergleichen lassen oder wie die Ergebnisse der neuen Messansätze auf der Inventarebene verwendet werden können.

Das Ziel dieser Studie war folglich, einige der bestehenden Wissenslücken in der Anwendung von EC aufzuarbeiten, sowie mehrjährige EC-Messungen auf einer intensiv beweideten Farm durchzuführen. Flussmessungen wurden dabei zunächst auf drei Weiden über dem natürlichen Grass-Klee-Bestand durchgeführt, bevor ein Teil der Messfläche erneuert und anschließend mit Spitzwegerich (*Plantago lanceolata*), ausdauerndem Weidegras (*Lolium perenne*), weißem und rotem Klee (*Trifolium pratense*) bepflanzt wurde. Die EC-Messungen wurden durch Messkampagnen unter der Verwendung sogenannter Kammern (static chambers) ergänzt, um (1) die Unterschiedlichkeit beider Messmethoden zu quantifizieren und (2) eine neue Analysemethode zu entwickeln, welche eine direkte Injektion der Kammerproben in den Quantumkaskadenlaser (QCL) des EC-Systems erlauben würde.

Die Ergebnisse des Vergleichs (1) zeigten, dass die Verwendung von Messkammern und feldspezifischen EF zu einer deutlichen Unterbewertung der jährlichen N_2O-Emissionen führte. Während EF kumulierte Jahresemissionen von 3.82 kg N_2O-N ha^{-1} yr^{-1} quantifizierten, bezifferte EC eine Summe von 7.30 kg N_2O-N ha^{-1} yr^{-1}. Die Differenz der Budgets konnte auf Abweichungen im EF-Ansatz zurückgeführt werden, welcher weder Unterschiede in der Futtergrundlage der Kühe, noch saisonale Variabilität oder Hintergrundemissionen miteinschloss. Es zeigte sich, dass die von diesen Faktoren gesteuerten N_2O-Emissionen ausschließlich in den EC-Daten enthalten waren und dass dem EF-basierten Emissionsbudget daher durchaus kritisch zu begegnen war. Die Verwendung von EF zur Erstellung von Emissionsbudgets wird künftig einer Betrachtung bedürfen, die weit über das vereinfachte Hochskalieren von räumlich begrenzten Messpunkten auf die nationale Ebene hinausreicht.

Ein weiteres Anliegen dieser Studie war es, zu untersuchen, wie sich eine Erneuerung der Weidefläche auf die direkten N_2O-Flüsse aus dem Boden auswirken würde. Dazu wurden die N_2O-Flüsse der erneuerten Weidefläche mit denen einer Kontrollfläche verglichen. Die Erfassung der Gasflüsse basierte dabei auf den simultanen Messungen eines einzelnen EC-Systems (in einem sogenannten *split-footprint*) und wurde durch Anwendung einer neuen Technik zum Schließen vorhandener Datenlücken (*gap-filling*) ermöglicht, welche eine robuste Quantifizierung des Erneuerungseffektes erlaubte. Die Differenz zwischen den N_2O-Emissionen von der erneuerten und der unveränderten Weidefläche lag bei 1.2 kg N_2O-N ha^{-1}. Emissionsstöße traten lediglich innerhalb eines sehr begrenzten Zeitraums von 14 Tagen nach Weideumbruch auf (93.4% der Gesamtdifferenz) und wurden von der sich rasch einstellenden Photosyntheseleistung des Jungpflanzenwachstums limitiert. Insgesamt zeigte sich, dass

langanhaltende Nährstoffverluste durch die Emission von N_2O-Stickstoff abgemildert werden können, wenn die zeitliche Verzögerung zwischen Weideumbruch und Einsaat der Samen möglichst kurz gehalten wird. Für eine aussagekräftige Quantifizierung verschiedener Mitigationsstrategien und die finale Berechnung von N_2O-Budgets ist zudem zu empfehlen, diese mit geeigneten Methoden (footprint-splitting, gap-filling) zu unterfüttern. Erst dann wird eine Bewertung von N_2O-Flüssen und den damit assoziierten Treibhausgasemissionen möglich.

Wie in dem letzten Forschungskapitel dieser Arbeit (2) deutlich wird, bot die Verwendung eines QCL-basierten EC-Systems auch den Vorteil, Gasproben aus Kammermessungen annähernd simultan zu den Messungen des EC-Systems zu analysieren. Um dies zu ermöglichen, wurde eine neue Injektionstechnik entwickelt, welche sich die Analysestärke und Schnelligkeit des QCL zu Nutzen gemacht hat und es erlaubte, die N_2O-Konzentration der Kammerproben mittels Absorptions-spektrometrie direkt im Gelände zu bestimmen. Ein Vergleich der vom QCL analysierten N_2O-Konzentrationen und -Flüsse mit den Ergebnissen identischer Proben aus gaschromatographischen Analysen im Labor ergab keinen signifikanten Unterschied. Entscheidende Vorteile der neuentwickelten Injektionstechnik waren ihre Analyseschnelligkeit und praktische Anwendung im Gelände, insbesondere aber auch das Vermögen, die Leistungsfähigkeit des QCLs optimal auszunutzen und so differenzierte Aussagen über N_2O-Flüsse auf verschiedenen räumlichen (und zeitlichen) Skalenebenen treffen zu können. Die Ergebnisse komplementieren den eigentlichen, auf die EC-Technik ausgelegten Fokus dieser Doktorarbeit, verdeutlichen sie doch, dass Messkammern ihre Daseinsberechtigung haben, beispielsweise um die Wirkung von Einzelfaktoren auf den N_2O-Fluss bewerten zu können. Je nach Forschungsziel, kann eine Kopplung von Kammermessungen mit EC-QCL auf der Feldebene sehr vorteilhaft sein.

A2 – Supplementary material from Chapter 4

Figure A2-1 Webcam photography of the EC site with time during and after pasture renewal: (a) herbicide application on P54, 10-Mar-2018; (b) direct drilling of new seed into the soil, 14-Mar-2018; (c) bare died-off pasture, 20-Mar; (d), (e) seedling emergence in early April; (f) grazing of the control paddock P53, 17-Apr; (g) and (h) on-going sward establishment on the renewal site till 14-May, one day before P54 experienced the first post-renewal grazing.

A3 – Supplementary material from Chapter 5

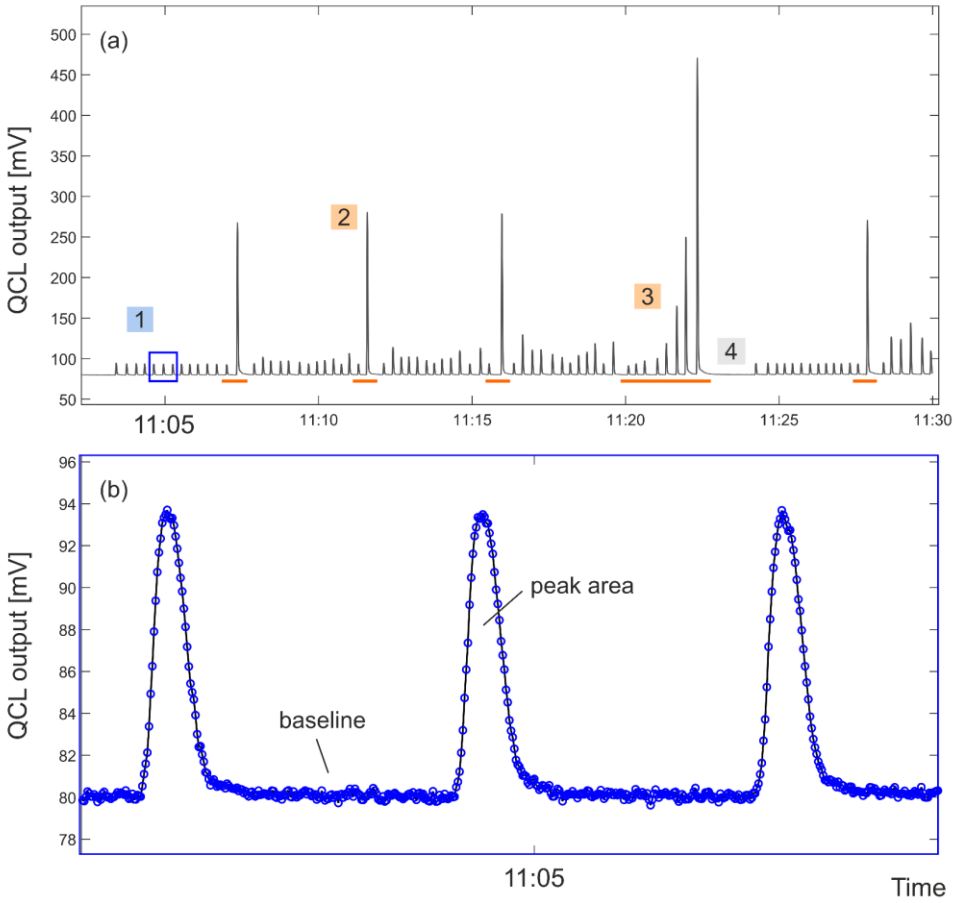

Figure A3-1 Example of QCL output data depicting how a one half-hourly peak progression sequence looked like. Panel (a) shows the full sequence for injected N_2O samples and standards in a given half-hour from 11–11:30 AM, 17 September 2020. Panel (b) captures three individual peaks from within this period (1) (blue rectangle). Single measurement points are depicted by blue dots with the black line showing an interpolated curvature. Orange bars underneath individual peaks in panel (a) distinguish injected N_2O standards of known from N_2O samples of unknown concentration; (2) identifies 1 ppm and 5 ppm standards injected after every 12 samples, here serving as a running control; (3) shows an example of an injected standard line of known N_2O concentration (range: 0.2–10 ppm); and (4) illustrates the lag time that was required to ensure sufficient flushing of the QCL sample cell after injecting a sample or standard (here 10 ppm) of higher N_2O concentration. The QCL output unit is millivolt.

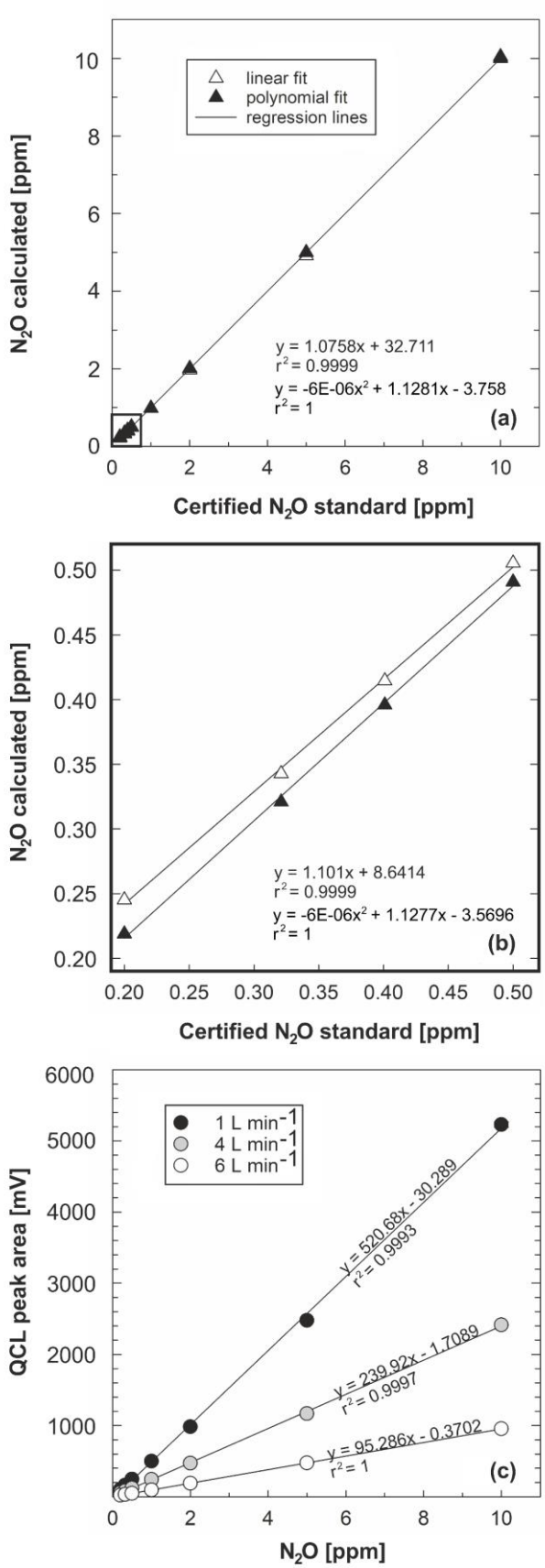

Figure A3-2 Tests conducted prior to the main study showing the calculated normal linear relationship between output peak area and N_2O concentration (C_{N2O}) for different scenarios and ranges of N_2O standards injected: (a) from 0.2–10 ppm and (b) from 0.2–0.5 ppm; (c) demonstrates the effect of flow rate in L min^{-1} on the slope of the associated regression lines, output peak area and measured N_2O concentration in ppm.

Table A3-1 Chronology of experimental activities.

Date	Activity
15-Aug-19	Trial site fenced off Preliminary injections: testing different syringe types
20-Aug-19	Installation of chamber collars
30-Aug-19	Preliminary injections into QCL: testing different flow rates
10-Sep-19	Treatment application to chamber and soil plots Gas and soil sampling – run 1
11-Sep-19	Gas and soil sampling – run 2
12-Sep-19	Gas and soil sampling – run 3 & 4
13-Sep-19	Gas and soil sampling – run 5
14-Sep-19	Gas and soil sampling – run 6
15-Sep-19	Gas and soil sampling – run 7 & 8
16-Sep-19	Gas and soil sampling – run 9
17-Sep-19	Sample injection into QCL

Table A3-2 Certified N_2O standards used in this study and associated uncertainty levels. Standards printed in bolt fond were used in quadratic curve models to calculate final N_2O concentration of the samples taken from static chambers.

N_2O [µL L^{-1}] [ppmv]	**Uncertainty** [alpha/beta] [%]	**Background** (gas)	**Company** (name)
0.200	± 0.01	Nitrogen	BOC Ltd.
0.321	± 0.1–0.9%	Cryogenic UltraPure Air	Praxair, Inc.
0.3252	± 0.01	Air	NIWA
0.401	± 0.1–0.9%	Cryogenic UltraPure Air	Praxair, Inc.
0.500	± 0.01	Nitrogen	BOC Ltd.
1.00	± 0.01	Nitrogen	BOC Ltd.
2.00	± 0.02	Nitrogen	BOC Ltd.
5.00	± 0.1	Nitrogen	BOC Ltd.
10.00	± 0.2	Nitrogen	BOC Ltd.
20.00	± 0.2	Nitrogen	BOC Ltd.
50.00	± 1.0	Nitrogen	BOC Ltd.
100.00	± 1.0	Nitrogen	BOC Ltd.

Table A3-3 This table presents the measured values of nitrous oxide fluxes (F_{N2O}) analysed by GC and QCL, soil water-filled pore space (WFPS), soil ammonium (NH_4^+) and nitrate (NO_3^-) content of the control (AN_0) and across the different treatments of ammonium-nitrate (AN_{300}, AN_{600}, AN_{900}). The associated standard error of the mean (SEM) is provided at the right-hand side of each control/treatment column.

date	AN_0	SEM	AN_{300}	SEM	AN_{600}	SEM	AN_{900}	SEM
	GC nitrous oxide flux [F_{N2O_GC} in nmol N_2O m^{-2} s^{-1}]							
10-Sep-2019	0.04	0.05	3.56	1.20	1.95	0.19	2.49	0.52
11-Sep-2019	0.13	0.04	9.93	1.97	9.63	3.44	14.88	3.55
12-Sep-2019*	0.06	0.05	8.67	1.73	8.02	2.92	15.87	3.96
12-Sep-2019*	0.06	0.01	8.42	2.62	8.19	3.23	14.87	3.15
13-Sep-2019	-0.05	0.03	6.43	3.00	11.57	3.68	15.16	3.76
14-Sep-2019	0.03	0.01	7.46	2.19	10.71	3.43	16.71	2.46
15-Sep-2019*	0.02	0.03	5.03	0.80	10.21	2.84	14.85	3.58
15-Sep-2019*	0.03	0.03	6.92	1.57	9.98	2.96	13.88	2.75
16-Sep-2019	0.02	0.04	3.06	1.33	6.37	2.45	10.29	1.67
	QCL nitrous oxide flux [F_{N2O_QCL} in nmol N_2O m^{-2} s^{-1}]							
10-Sep-2019	0.00	0.03	3.65	1.18	2.17	0.19	2.74	0.60
11-Sep-2019	0.21	0.05	9.40	1.83	8.88	3.14	13.57	3.04
12-Sep-2019*	0.14	0.07	8.19	1.60	7.94	2.92	15.17	3.71
12-Sep-2019*	0.06	0.02	8.02	2.47	8.04	3.11	15.46	3.57
13-Sep-2019	0.09	0.08	6.25	2.77	10.91	3.33	15.09	4.05
14-Sep-2019	0.03	0.02	7.30	2.10	10.66	3.24	17.22	2.71
15-Sep-2019*	0.17	0.01	5.30	0.86	9.46	2.42	14.81	3.65
15-Sep-2019*	0.18	0.03	6.95	1.33	10.27	2.89	14.36	2.69
16-Sep-2019	0.06	0.01	3.28	1.63	6.63	2.51	10.97	1.99
	Water filled pore space of the soil [%]							
10-Sep-2019	79.43	0.48	78.66	1.82	78.06	1.40	82.30	2.35
11-Sep-2019	81.64	0.59	84.97	1.68	80.16	0.53	82.13	1.79
12-Sep-2019	82.18	1.12	80.63	1.23	79.35	1.05	79.20	1.00
13-Sep-2019	79.62	0.95	79.72	1.87	76.62	2.08	78.13	1.76
14-Sep-2019	79.43	0.56	80.60	2.00	78.37	1.74	77.78	1.19
15-Sep-2019	79.79	0.50	81.70	2.65	77.17	1.49	76.81	0.37
16-Sep-2019	77.92	1.06	81.05	1.98	73.93	1.60	77.41	1.80
	Soil ammonium [kg NH_4^+ ha^{-1}]							
10-Sep-2019	1.82	0.50	81.73	5.20	89.36	2.72	264.63	17.19
11-Sep-2019	0.81	0.11	52.26	7.18	141.51	11.08	233.63	33.62
12-Sep-2019	2.15	0.57	44.61	6.52	109.37	6.77	213.76	3.41
13-Sep-2019	2.21	0.33	36.88	6.75	124.48	9.36	194.76	18.88
14-Sep-2019	3.71	0.09	20.31	5.07	59.88	6.05	188.70	18.05
15-Sep-2019	1.84	0.64	9.58	0.99	78.98	12.30	155.84	18.49
16-Sep-2019	1.80	0.29	13.21	3.23	38.50	4.59	124.38	7.64
	Soil nitrate [kg NO_3^- ha^{-1}]							
10-Sep-2019	2.99	0.37	83.67	3.87	104.95	1.33	267.77	15.17
11-Sep-2019	2.46	0.18	69.08	6.54	149.95	8.62	248.89	33.69
12-Sep-2019	2.29	0.07	79.41	6.57	142.52	8.61	230.94	7.36
13-Sep-2019	1.64	0.20	82.21	7.92	149.85	6.25	232.40	13.77
14-Sep-2019	1.84	0.35	73.37	12.71	114.20	8.41	237.77	8.96
15-Sep-2019	2.47	0.31	78.91	1.51	162.60	8.72	231.51	16.94
16-Sep-2019	1.85	0.22	92.49	16.22	134.38	7.60	211.88	18.92

* flux measurements conducted twice daily at 10 AM and 12 PM
SEM = standard error of the mean

Table A3-4 Results from the linear functional relationship analysis (orthogonal regression). Columns labelled C_{N2O} show the results of the regression analysis when using standardised N_2O concentrations. Columns labelled F_{N2O} provide results based on standardised N_2O fluxes. Part of the regression analysis was to characterise both data streams by treatment and control, i.e. first including all data (AN_0, AN_{300}, AN_{600}, AN_{900}) in the analysis and then, separately, only the control (AN_0).

	C_{N2O} all AN	**C_{N2O}** AN_0 only	**F_{N2O}** all AN	**F_{N2O}** AN_0 only
Number of observations	432	108	108	27
Response mean	-0.003164	0.3272	-0.004008	0.3776
Explanatory mean	0.003164	-0.3272	0.004008	-0.3776
Response variance	0.9811	1.238	0.9860	1.139
Explanatory variance	1.021	0.5551	1.023	0.6029
r^2 value	0.9928	0.1753	0.9922	0.0939
r value	0.9964	0.4187	0.9961	0.3064
Angle between Y on X and X on Y	0.2068	42.32	0.2229	54.59
Major eigenvalue	1.999	1.384	2.005	1.241
Minor eigenvalue	0.003606	0.4096	0.003901	0.5017
Bootstrap resampling	200	200	200	200
Ordinary least squares:				
Constant	-0.006253	0.532	-0.007926	0.537
Standard error	0.003914	0.1038	0.007861	0.26
Lower	-0.01331	0.3101	-0.02204	-0.02
Upper	0.001710	0.734	0.006998	1.030
Slope	0.9766	0.625	0.9778	0.421
Inverse least squares:				
Constant	-0.006276	1.49	-0.007957	2.072
Standard error	0.003902	0.6585	0.007902	82.46
Lower	-0.01369	0.9211	-0.02246	-44.95
Upper	0.001786	3.478	0.007118	18.732
Slope	0.9837	3.567	0.9854	4.486
Major axis:				
Constant	-0.006264	1.108	-0.007941	1.326
Standard error	0.003904	0.44	0.007872	40.17
Lower	-0.01349	0.7105	-0.02217	-19.84
Upper	0.001610	2.484	0.006920	9.937
Slope	0.9801	2.387	0.9815	2.511

Table A3-5 Bland-Altman analysis for F_{N2O_GC} and F_{N2O_QCL} distinguished by treatment in units nmol m^{-2} s^{-1}, if not specified otherwise. This table provides a summary based on mean F_{N2O_GC} and F_{N2O_QCL} across replicates of the same treatment. Figure 5-4, instead, illustrates the results of individual F_{N2O_GC} and F_{N2O_QCL} (not depicted in the below table) for each replicate and each treatment as the percentage mean difference between the two methods, i.e. GC (A) and QCL (B).

Sampling	**Treatment**	**GC (A)**	**QCL (B)**	**Mean**	**Difference**	**Difference (%)**
[No.]	[kg N ha^{-1}]	F_{N2O_GC}	F_{N2O_QCL}	(A+B)/2	(A-B)	((A-B)/mean)*100
1	0	0.04	0.00	0.02	0.04	182.48
1	300	3.56	3.65	3.61	-0.09	-2.59
1	600	1.95	2.17	2.06	-0.23	-11.11
1	900	2.49	2.74	2.61	-0.24	-9.24
2	0	0.13	0.21	0.17	-0.08	-44.70
2	300	9.93	9.40	9.67	0.53	5.51
2	600	9.63	8.88	9.26	0.75	8.11
2	900	14.88	13.57	14.22	1.31	9.20
3	0	0.06	0.14	0.10	-0.08	-78.52
3	300	8.67	8.19	8.43	0.48	5.69
3	600	8.02	7.94	7.98	0.08	0.98
3	900	15.87	15.17	15.52	0.70	4.51
4	0	0.06	0.06	0.06	0.00	1.93
4	300	8.42	8.02	8.22	0.39	4.79
4	600	8.19	8.04	8.11	0.15	1.82
4	900	14.87	15.46	15.16	-0.59	-3.89
5	0	-0.05	0.09	0.02	-0.14	-595.36
5	300	6.43	6.25	6.34	0.18	2.88
5	600	11.57	10.91	11.24	0.66	5.88
5	900	15.16	15.09	15.13	0.07	0.49
6	0	0.03	0.03	0.03	0.00	4.14
6	300	7.46	7.30	7.38	0.16	2.19
6	600	10.71	10.66	10.68	0.05	0.47
6	900	16.71	17.22	16.96	-0.51	-3.02
7	0	0.02	0.17	0.09	-0.15	-157.04
7	300	5.03	5.30	5.17	-0.27	-5.22
7	600	10.21	9.46	9.84	0.75	7.67
7	900	14.85	14.81	14.83	0.03	0.22
8	0	0.03	0.18	0.10	-0.15	-149.70
8	300	6.92	6.95	6.94	-0.02	-0.34
8	600	9.98	10.27	10.13	-0.29	-2.86
8	900	13.88	14.36	14.12	-0.48	-3.39
9	0	0.02	0.06	0.04	-0.04	-105.26
9	300	3.06	3.28	3.17	-0.22	-6.86
9	600	6.37	6.63	6.50	-0.26	-4.02
9	900	10.29	10.97	10.63	-0.68	-6.39

Table A3-6 Bioequivalence analysis for N_2O concentrations (C_{N2O}) and associated fluxes (F_{N2O} in bottom panel of the table). C_{N2O_QCL} and F_{N2O_QCL} were considered bioequivalent when the 90% confidence interval of the difference was completely within the predefined ± 5% bioequivalence range of difference to C_{N2O_GC} and F_{N2O_GC} (corresponding to a test with size 0.05). rep. = replicates, d.f = degrees of freedom, s.e.d = standard error of the difference, LSD = least significant difference

Time/ Treatment	**Mean**		**Standard error of the difference of the mean**			**LSD**	**90% confidence interval**			**Bioequivalence range**			
AN_0	**C_{N2O_GC}** [ppm]	**C_{N2O_QCL}** [ppm]	rep.	d.f.	s.e.d	s.e.d.	difference (QCL-GC)	lower	upper	GC lower	GC upper	QCL lower	QCL upper
t0	0.333	0.332	27	26	0.0027	0.0046	0.000	-0.005	0.004	-0.017	0.017	-0.017	0.017
t15	0.333	0.342	27	26	0.0028	0.0048	0.009	0.004	0.013	-0.017	0.017	-0.017	0.017
t30	0.335	0.352	27	26	0.0029	0.0049	0.016	0.012	0.021	-0.017	0.017	-0.018	0.018
t45	0.340	0.354	27	26	0.0027	0.0046	0.014	0.009	0.019	-0.017	0.017	-0.018	0.018
AN_{300}													
t0	0.333	0.336	27	26	0.0028	0.0048	0.003	-0.002	0.007	-0.017	0.017	-0.017	0.017
t15	0.822	0.821	27	26	0.1090	0.0186	-0.001	-0.020	0.017	-0.041	0.041	-0.041	0.041
t30	1.341	1.327	27	26	0.0168	0.0286	-0.014	-0.042	0.015	-0.067	0.067	-0.066	0.066
t45	1.831	1.804	27	26	0.0192	0.0327	-0.026	-0.059	0.007	-0.092	0.092	-0.090	0.090
AN_{600}													
t0	0.336	0.335	27	26	0.0023	0.0042	-0.001	-0.005	0.003	-0.017	0.017	-0.017	0.017
t15	0.912	0.912	27	26	0.0160	0.0273	0.000	-0.027	0.027	-0.046	0.046	-0.046	0.046
t30	1.563	1.550	27	26	0.0242	0.0412	-0.013	-0.054	0.028	-0.078	0.078	-0.078	0.078
t45	2.143	2.104	27	26	0.0250	0.0427	-0.039	-0.082	0.004	-0.107	0.107	-0.105	0.105
AN_{900}													
t0	0.338	0.337	27	26	0.0028	0.0319	-0.001	-0.005	0.004	-0.017	0.017	-0.017	0.017
t15	1.285	1.268	27	26	0.0136	0.1380	-0.017	-0.041	0.006	-0.064	0.064	-0.063	0.063
t30	2.338	2.294	27	26	0.0325	0.1959	-0.044	-0.100	0.012	-0.117	0.117	-0.115	0.115
t45	3.370	3.379	27	26	0.3900	0.2850	0.009	-0.058	0.076	-0.169	0.169	-0.169	0.169
Treatment	**F_{N2O_GC}** [nmol N_2O m^{-2} s^{-1}]	**F_{N2O_QCL}**											
AN_0	0.039	0.105	27	26	0.0187	0.0319	0.066	0.034	0.098	-0.002	0.002	-0.005	0.005
AN_{300}	6.610	6.483	27	26	0.0809	0.1380	-0.127	-0.265	0.011	-0.331	0.331	-0.324	0.324
AN_{600}	8.514	8.329	27	26	0.1149	0.1959	-0.185	-0.381	0.011	-0.426	0.426	-0.416	0.416
AN_{900}	13.222	13.265	27	26	0.1671	0.2850	0.043	-0.242	0.328	-0.661	0.661	-0.663	0.663

Curriculum Vitae

Personal Details

Name	Anne Roswitha Wecking
Date of birth	24th December 1990
Nationality	German

Education

2017 – 2020 **University of Waikato**, Hamilton, New Zealand
Doctoral studies, School of Science and Engineering,
Thesis: *Paddock scale nitrous oxide emissions from grazed pastures: quantification and mitigation*

2014 – 2017 **Leibniz University Hanover**, Germany
Master of Science in Soil Science and Landscape Science
Thesis: *Managing forest ecosystems in Mongolia – the crucial role of soil*

2013 – 2014 **University of Salford**, United Kingdom
Abroad studies focused on glacial and fluvial systems, student under the European Community Action Scheme for the Mobility of University Students

2010 – 2014 **Leibniz University Hanover**, Germany
Bachelor of Science in Physical Geography and Landscape Science
Thesis: *Pedogenesis and pedodynamics on anthropogenically built sediment bodies – exemplified on coal mining waste heap Haniel*

2010 – 2013 **Institut zur Förderung publizistischen Nachwuchses**, Munich, Germany
Journalistic apprenticeship, print and broadcasting media

2001 – 2010 **St. Ursula Gymnasium Dorsten**, Germany
Secondary education

List of Publications

Wecking, A.R., Wall, A.M., Liáng, L.L., Lindsey, S.B., Luo, J., Campbell, D.I., Schipper, L.A., 2020. Reconciling annual nitrous oxide emissions of an intensively grazed dairy pasture determined by eddy covariance and emission factors. Agric. Ecosyst. Environ. 287, 1-14.

Wecking, A.R., Cave, V.M., Liáng, L.L., Wall, A.M., Luo, J., Campbell, D.I., Schipper, L.A., 2020. A novel injection technique: using a field-based quantum cascade laser for the analysis of gas samples derived from static chambers. Atmos. Meas. Tech. 13, 5763-5777.

Goodrich, J.P., Wall, A.M., Campbell, D.I., Fletcher, D., Wecking, A.R., Schipper, L.A., 2021. Improved gap filling approach and uncertainty estimation for eddy covariance N_2O fluxes. Agric. For. Meteorol. 297, 108280, 1-9.

Conference Talks (selected)

Wecking, A.R., Wall, A.M., Liáng, L.L., Lindsey, S.B., Luo, J., Campbell, D.I., Schipper, L.A., 2019. A never ending story? What continuous measurements of nitrous oxide emissions in the Waikato tell us. WaiBoP Soils Biennial Conference, Hamilton, New Zealand, 29/11/2019.

Wecking, A.R., Wall, A.M., Liáng, L.L., Lindsey, S.B., Luo, J., Campbell, D.I., Schipper, L.A., 2019. Bottom-up meets top-down: Quantification of direct N_2O emissions from intensively grazed pasture measured by static chambers and eddy covariance. MPI Agriculture Greenhouse Gas Inventory Conference, Palmerston North, New Zealand, 11/04/2019.

Wecking, A.R., Wall, A.M., Liáng, L.L., Lindsey, S.B., Luo, J., Campbell, D.I., Schipper, L.A., 2018. Bottom-up or top-down? Paddock-scale nitrous oxide budgets using static chamber and eddy covariance data. "Diverse Soils – Productive Landscapes" NZSSS Soil Science Conference, Napier, New Zealand, 03–06/12/2018.

Wecking, A.R., Wall, A.M., Liáng, L.L., Lindsey, S.B., Luo, J., Campbell, D.I., Schipper, L.A., 2018. Eddy covariance measurements of N_2O emissions under intensive grazing before, during and after pasture renewal. International Conference on Agricultural GHG Emissions and Food Security – Connecting research to policy and practice, Berlin, Germany, 10–13/09/2018.

Wecking, A.R., Wall, A.M., Liáng, L.L., Lindsey, S.B., Luo, J., Campbell, D.I., Schipper, L.A., 2018. From points to paddocks: measuring N_2O fluxes by static chambers and eddy covariance. MPI Agriculture Greenhouse Gas Inventory Conference, Wellington, New Zealand, 21–22/03/2018.

Wecking, A.R., Wall, A.M., Liáng, L.L., Lindsey, S.B., Luo, J., Campbell, D.I., Schipper, L.A., 2017. Across scales: Employment of a quantum cascade laser to detect static chamber derived N_2O emissions. WaiBoP Soils Biennial Conference, Hamilton, New Zealand, 05/12/2017.

Conference Posters

Wecking, A.R., Guggenberger, G., 2018. Managing forest ecosystems in Mongolia: the crucial role of soil. "Diverse Soils – Productive Landscapes" NZSSS Soil Science Conference, Napier, New Zealand, 03–06/12/2018.

Wecking, A.R., Mackay, A., Manderson, A. K., Dominati, E., Palmer, A. S., Parfitt, R. L., 2018. Anthropedogenesis – the future of land development?. "Soil Science for Future Generations" NZSSS Soil Science Conference, Hamilton, New Zealand, 01–04/12/2014.

Conference Convening

Lowe, D., Wecking, A. R., 2019. WaiBoP Soils Biennial Conference 2019. Hamilton, New Zealand, 29/11/2019.

…

The End

Die Erkenntnis der Stunde:

Bodenkundler schauen sich schon zu Lebzeiten die Radieschen von unten an.

…

Statutory Declaration

I declare that I have authored this PhD thesis *'Paddock Scale Nitrous Oxide Emissions from Grazed Pastures: Quantification and Mitigation'* independently, that I have not used any other than the declared sources, and that I have explicitly marked all material, which has been quoted either literally or by content from the referenced sources.

In order to challenge plagiarism, I accept inspection on this issue by software and third-party review.

Hamilton, New Zealand, 30th September 2020

Anne Wedding